Investigating the role of vesicle trafficking in chemotactic invasion of breast cancer cells

by

Laura Mutch

A thesis submitted to
The University of Birmingham
for the degree of
DOCTOR OF PHILOSOPHY

School of Biosciences
The University of Birmingham
September 2014

Parts of Chapters 1 to 5 inclusive of this thesis contain material that has been published as a multi-author paper (Mutch et al. Traffic. 2014 Jun;15(6):648-64). The sections of that work presented here are my own work with negligible contribution from the other authors, unless otherwise stated.

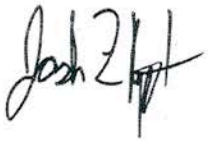

20th September, 2014

Joshua Z. Rappoport PhD

Director of the Center for Advanced Microscopy and the Nikon Imaging Center at Northwestern University
Northwestern University Feinberg School of Medicine
303 E. Chicago Avenue
Chicago, IL 60611
(312) 503-4140

Laura Mutch.

20/09/14.

Abstract

Cell migration towards a chemical cue (chemotaxis) underlies a variety of physiological processes, including embryonic development and the immune response. This mode of migration is also hijacked by metastatic cancer cells that use this process to enter blood or lymphatic vessels to enable growth of secondary tumours at other sites within the body. Using a novel cell migration assay we sought to determine the molecular mechanisms by which vesicle trafficking regulates chemotactic invasion. In particular we focused upon the inter-dependency of growth factor receptor signalling and trafficking.

We use this assay to show that the large GTPase dynamin is necessary for epidermal-growth factor (EGF)-dependent migration in the breast cancer cell line MDA-MB-231 and a pancreatic cancer cell line PDAC. By following this result with RNAi studies we found clathrin-mediated endocytosis, but not caveolar endocytosis, to be necessary for migration in MDA-MB-231 cells.

Inhibiting dynamin in MDA-MB-231 cells not only inhibited migration but resulted in an elongated phenotype of the cells. This and the current literature led us to investigate whether focal adhesion disassembly during chemotactic invasion occurred through endocytosis of integrins. Using total internal reflection fluorescence (TIRF) microscopy we found no significant colocalisation of focal adhesion markers with markers of endocytosis and found inhibiting endocytosis to have no effect on the number or localisation of focal adhesions.

We next investigated colocalisation between the EGF receptor (EGFR) and markers of endocytosis in migrating cells and found a high degree of colocalisation with clathrin, but not with caveolin. Inhibiting endocytosis led to a build-up of receptor at the front of the cell and time-lapse imaging revealed that events of clathrin-mediated endocytosis are polarised to the front of migrating cells. Thus during EGF-directed chemotactic invasion of human breast cancer derived cells, EGFR endocytosis is polarised to the front of migrating cells and occurs via clathrin-mediated endocytosis.

We then went on to analyse the exocytic trafficking of EGFR during chemotactic invasion, and observed polarisation of EGFR exocytosis events towards the front of migrating cells. We also found significant colocalisation of EGFR with Rab11, a marker of the long-loop recycling pathway, whereas only a small amount of colocalisation was seen with NPY, a marker for the biosynthetic secretory pathway.

Finally we use fluorescent lifetime imaging-fluorescence resonance energy transfer (FLIM-FRET) microscopy to show that cells migrating in an EGF-dependent manner have

increased signalling of Scr and Akt Biosensors, compared to those not in an EGF environment. We also observed that this signalling was further increased upon inhibition of endocytosis. These experiments begin to investigate the link between endocytosis and signalling, an area not yet very well studied.

Acknowledgements

Firstly, it goes without saying that I would like to thank my supervisor, Josh, for his help throughout this PhD. Thanks for the opportunity to work in this awesome lab and thanks for your continued advice and guidance over my five years here. We may not always see eye to eye but the good times and the bad have helped shape my experience here and I wouldn't change any of it. I'll treasure all the mugs you bought me to remind me of my time here!

I am also grateful for the tragically short time that Carina was a co-supervisor of mine too. From her first days here you could tell that she was a force to be reckoned with, one of those scarily intelligent people who I could never dream of keeping up with. But she'd always give me very positive feedback after a meeting or a lab presentation, which meant so much coming from her. She truly will not be forgotten by those who knew her here.

I want to thank previous lab members who helped me out when I started. Sarah was always there to help with just about anything, and Nat was my microscope guru who can also possibly talk for longer than I can! Eric was always good for a laugh (whether with or at!). Thank you Jeni for fun times at gigs and vintage fairs and for being my coffee-buddy!

Thanks to all the current lab members who have made this an entertaining place to work over the years. Ju, I will never cease to find your crazy French ways funny and will always tell you where I got my outfit (even if it was Primark!). Abs you have been great to work with and are always able to distract me with a funny video or something to keep me in a good mood. Thank you, Phil, for being as crazy as you are, the lab wouldn't be the same without you. Jez, I'm hoping to still see you in Staff House sometime because drunk Jez is hilarious. Gym-buddy Emily, thank you for all our very necessary coffee breaks, and I'll always have deodorant for you to borrow when you need it!

Thanks also to the Tomlinson lab for the help and fun times throughout the years. I'm glad I'm leaving knowing that we finally beat you in a pub quiz. Mike, you have been a great source of knowledge on just about any topic throughout my PhD, from Western blotting to the power of energy gels during a half marathon. Jing was always around to help when I needed it, and mostly to aid me in stealing Tomlinson lab reagents. Lizzie was always available for in-depth discussions about Grey's Anatomy and other such vital topics. Beccy you've been a great friend to me all the way from Undergrad and kept me sane since being here with our tea breaks and wedding-based discussions.

Thank you also to all of the students I've worked with over the years. In particular Rob, Jake, Emma and Bobby.

Thanks to my wonderful parents for always being supportive of me and for encouraging me in whatever I've wanted to do. Finally, thank you to my wonderful husband-to-be, Jack. Thank you for patiently listening to every lab meeting or presentation rehearsal, being an ear to listen when experiments were going wrong or microscopes weren't behaving and for proofreading this thesis!

Contents

List of Figures

List of abbreviations

AP	Adaptor protein
ARH	Autosomal recessive hypercholesterolemia protein
Arp2/3	Actin-related protein 2/3
ATP	Adenosine triphosphate
BAR	Bin-Amphiphysin-Rvs
BSE	Bundle signalling element
cAMP	Cyclic adenosine monophosphate
CDR	Circular dorsal ruffles
CHC	Clathrin heavy chain
CLC	Clathrin light chain
CTx555	Cholera toxin Subunit B Alexa Fluor® 555 conjugate
Dab2	Disabled protein 2
DMEM	Dulbecco's modified eagle medium
DMSO	Dimethy sulphoxide
ECM	Extra-cellular matrix
EGF	Epidermal growth factor
EGFR	Epidermal growth factor receptor
EMT	Epithelial-mesenchymal transition
ENTH	Epsin N-terminal homology
Eps15	EGFR pathway substrate 1
ER	Endoplasmic reticulum
ERK	Extracellular signal-regulated kinase
FAK	Focal adhesion kinase
FCHO1/2	Fer/Cip4 homology domain-only proteins 1 and 2
FCS	Fetal calf serum
FLIM	Fluorescence lifetime imaging
FRET	Fluorescence resonance energy transfer
GEFs	Guanine nucleotide exchange proteins
GAPs	GTPase activating proteins
GFP	Green fluorescent protein
GPCRs	G-protein coupled receptors
GTP	Guanosine-5'-triphosphate
GUV	Giant unilamellar vesicle
HSC70	Heat shock cognate protein 70
JAK	Janus kinase

LDL	Low density lipoprotein
MAPK	Mitogen-activated protein kinase
MDA-MB-231	M.D. Anderson - metastatic breast number 231
MLC	Myosin light chain
MTOC	Microtubule organising centre
NPY	Neuropeptide Y
NPF	Nucleation promoting factor
NSC	Non-silencing control
PAK1	p21-activated kinase1
PBS	Phosphate-buffered saline
PDAC	Pancreatic ductal andeocarcinoma
PFA	Paraformaldehyde
PH	Pleckstrin homology
PI3K	Phosphoinositide-3 kinase
$PI(3,4)P_2$	Phosphatidylinositol-(3,4)-bisphosphate
PIP_3	Phosphatidylinositol-(3,4,5)-trisphosphate
PKC	Protein kinase C
PKD	Protein kinase D
PNRC	Perinuclear recycling compartment
PRD	Proline-rich domain
PTB	Phospho-tyrosine binding
PTEN	Phosphatase and tensin homologue
RCP	Rab-coupling protein
RFP	Red fluorescent protein
RhoGDIs	Rho guanine nucleotide dissociation inhibitors
RTK	Receptor tyrosine kinase
SEM	Standard error of the mean
siRNA	Small interfering RNA
SFM	Serum-free media
SNX9	Sorting nexin 9
SH2	Src-homology 2 SH3 Src-homology 3
STATs	Signal transducers and activators of transcription
SUPER	Supported bilayers with excess membrane reservoir
SV40	Simian virus 40
Tf568	Transferrin Alexa Fluor® 568 conjugate
TGF	transforming growth factor
TIRF	Total internal reflection fluorescence
VEGF	Vascular endothelial growth factor
WASP	Wiskott–Aldrich syndrome protein
WAVE	WASP-family verprolin-homologous protein

Chapter 1

Introduction

1.1 Metastasis

The spread of cancer cells from a primary tumour to other locations within the body is known as metastasis. This process is strongly associated with a poor prognosis and chance of survival; as such the prevention of metastasis is a key target for therapeutic intervention (Sporn, 1997).

Prior to the onset of metastasis tumour cells undergo epithelial-mesenchymal transition (EMT). A complex set of morphological and phenotypic changes occur which ultimately lead to the loss of adherens junctions, an increased expression of proteases and increased migratory ability (Hanahan and Weinberg, 2011). These newly acquired characteristics are key to the process of metastasis, for which a tumour cell must first detach itself from surrounding cells through the disruption of adhesions. The second stage is termed intravasation and involves degradation of the extracellular matrix (ECM), through the production of matrix metalloproteinases, and migration of the tumour cell into a nearby blood or lymphatic vessel (Coussens and Werb, 1996; Wyckoff et al., 2000). Extravasation occurs when a tumour cell exits the blood stream in order to form a secondary tumour site; cells must then seek to colonise the new site in order for metastasis to be successful (Figure 1.1; Hanahan and Weinberg 2011).

Particular primary tumours often have a higher likelihood to metastasize to a specific site, for example tumours of the colon have a higher propensity of metastasizing to

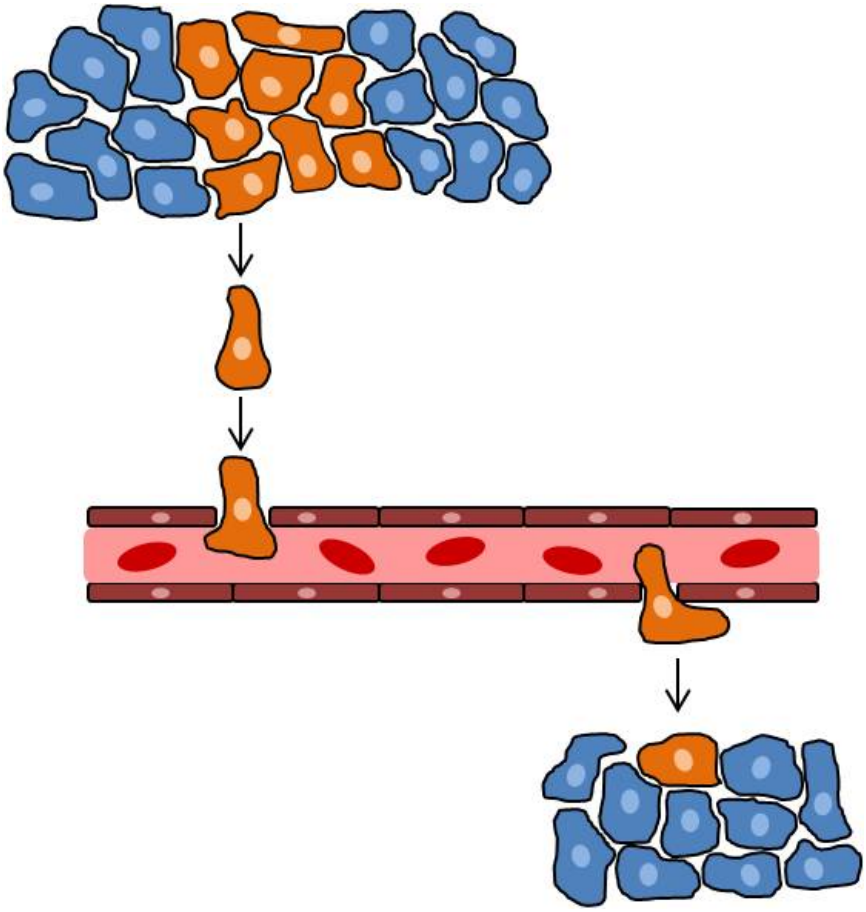

Figure 1.1: Model of metastasis. Firstly, cells separate from the primary tumour before secreting proteases to degrade the ECM and vessel wall of a nearby blood or lymphatic vessel. Tumour cells then migrate towards the blood or lymphatic vessel before entering, in a process termed intravasation. Tumour cells leave the circulation by extravasation and form secondary tumour sites elsewhere in the body.

the liver rather than any other organ (Pathak et al., 2010). Primary breast cancer tumours are most likely to metastasize to the lung, liver or bones but metastasis has been observed in many other organs as well as multiple organs at once (Weigelt et al., 2005). Chemotactic cues play a role in the homing of tumour cells to particular sites of secondary tumour formation (Hiratsuka et al., 2006).

The process of directed cell migration to a source of chemoattractant is known as chemotaxis and is vital to the intravasation and extravasation stages of metastasis. Consequently a thorough understanding of this process is needed to provide novel targets for anti-metastatic therapies (Condeelis et al., 2005).

1.2 Chemotaxis

Chemotaxis is triggered by the binding of chemoattractant molecules to cell surface receptors (e.g. epidermal growth factor (EGF) binding to its receptor (EGFR; Bagorda et al. 2006). Activation of such receptors results in a complex signalling cascade that leads to polarisation of the cell in the direction of migration, increased contractility and subsequent directed motility (Bagorda and Parent, 2008). Chemotaxis is vital during embryonic development and the immune response but is also utilised by tumour cells to enable metastasis of the primary tumour to other areas of the body. A large number of studies on the chemotactic process focus on the amoebae *Dictyostelium discoideum* that is able to chemotactically respond to a gradient of cyclic adenosine monophosphate (cAMP) of less than 2% different across the length of its body (Mato et al., 1975). Amazingly, the chemotactic mechanisms of this single-celled organism are remarkably similar to those of mammalian leukocytes that diverged from *Dictyostelium* during evolution approximately one billion years ago (Pollard and Borisy, 2003). This serves to demonstrate how fundamental the process is to all living systems and also allows research in model organisms such as *Dictyostelium* to be translated to that of mammalian cells. The present report serves to introduce the process of chemotaxis as has been elucidated

in various cell types using a number of experimental systems.

1.2.1 Membrane organisation during chemotaxis

The initial response upon the sensing of a chemoattractant is for the cell to polarize and to extend protrusions in the direction of migration (Lauffenburger and Horwitz, 1995). Such protrusions can be large, sheet-like extensions called lamellipodia or the more spike-like filopodia (Figure 1.2). The polymerisation of actin provides the driving force for these protrusions (Welch and Mullins, 2002). Actin can either be monomeric (G actin) or filamentous (F actin). Polymerisation of monomers leads to formation of actin filaments which grow largely from their barbed ends (Welch and Mullins, 2002). The driving force for this polymerisation comes from the actin-related protein 2/3 (Arp2/3) complex, a 7 subunit complex able to polymerise actin by binding to existing filaments and nucleating new filaments at a 70° angle to the exisiting filament (Machesky et al., 1994). The Arp2/3 complex is in turn activated by a set of proteins called nucleation promoting factors (NPFs; Machesky et al. 1994). These NPFs are a highly diverse set of proteins and as such may serve to differentially regulate the function of Arp2/3 depending on the upstream factors at the time (Welch and Mullins, 2002). The organisation of actin is different within these two types of membrane extension; this difference may allow the extensions to have distinct roles in migration. Lamellipodia are broad in width but usually quite thin structures and contain highly cross-linked dendritic actin filaments. The Rho family GTPase Rac is involved in actin nucleation in lamellipodia and is thought to be acted on upstream by the NPF WAVE (WASP-family verprolin-homologous protein; Miki et al. 1998; Welch and Mullins 2002). As stated, filopodia are thinner spike-like structures and contain tightly packed bundles of parallel actin. The regulation of filopodia appears to be by an interaction between Cdc42 and WASP (Wiskott–Aldrich syndrome protein)/N-WASP leading to the activation of Arp2/3 which in turn causes actin nucleation (Kim et al., 2000; Welch and Mullins, 2002). Another difference noted between lamellipodia and fliopodia is the turnover of

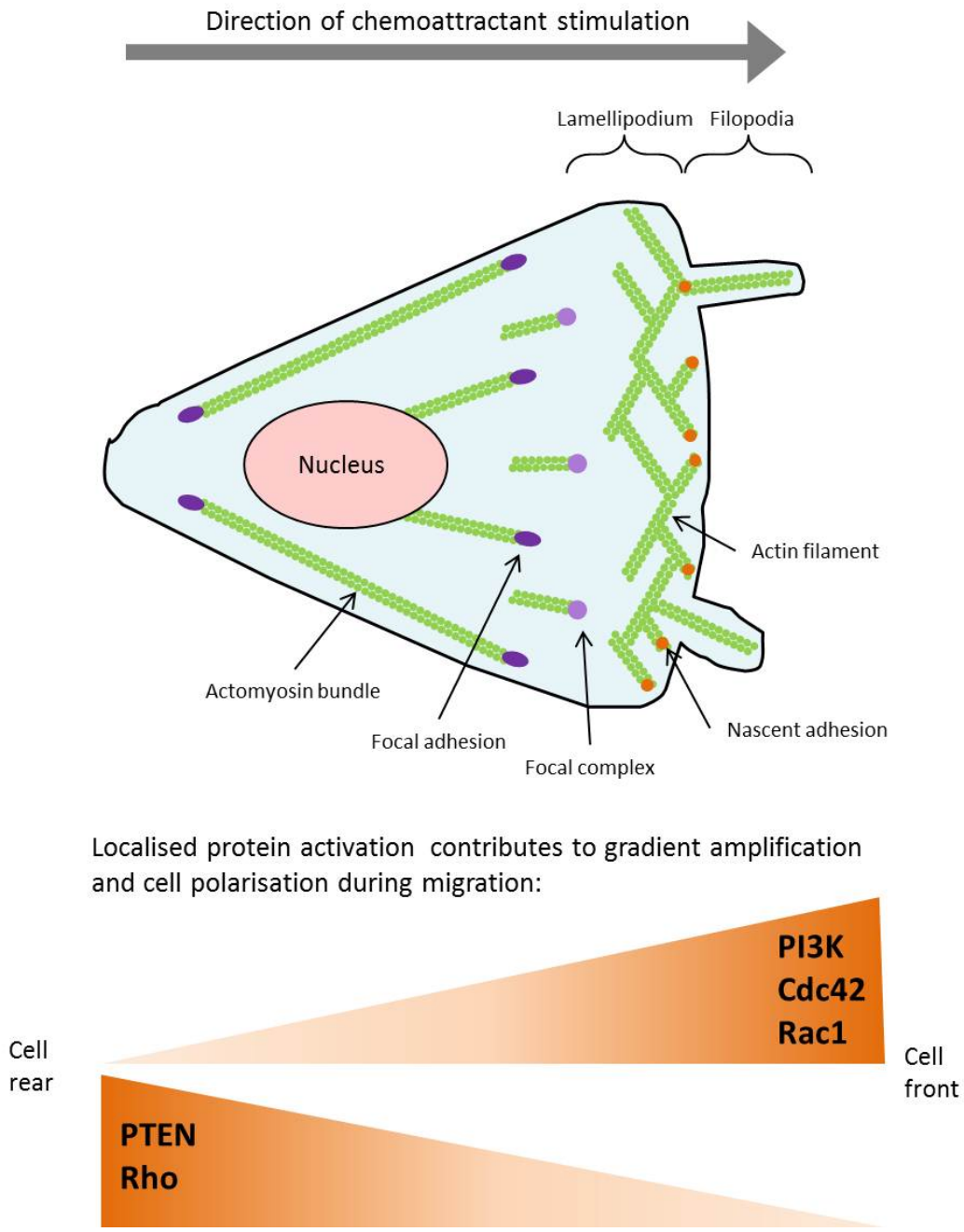

Figure 1.2: Model of a chemotaxing cell. After sensing an extracellular cue by receptors on the cell surface, membrane extensions form in the direction of the chemotactic gradient. Nascent adhesions form in the region of the lamellipodium and are either disassembled or mature first to focal complexes and then mature further into focal adhesions. Focal adhesions form the site of contact between the ECM and actomyosin bundles and, as such, are the region of traction force generation to enable the cell to migrate. Small Rho GTPases and other signalling molecules are polarised during migration in order to localise migration specific activities to particular regions of the cell. Figure inspired by Parsons et al. 2010, Figure 1.

actin within the structures: actin filaments within lamellipodia appear to be undergoing constant turnover compared to that within filopodia which appear much more stable (Mallavarapu and Mitchison, 1999).

1.2.2 Amplifying the gradient

Cells have the ability to respond to very shallow gradients of chemoattractant and in order to do this the gradient needs to be amplified by the cell (Ridley et al., 2003). This amplification involves phosphoinositide-3 kinase (PI3K) and phosphatase and tensin homologue (PTEN), and cells with altered activity of these molecules are unable to migrate directionally along a gradient (Devreotes and Janetopoulos, 2003). PI3K is involved in the production of phosphatidylinositol-(3,4,5)-trisphosphate (PIP_3) and phosphatidylinositol-(3,4)-bisphosphate ($PI(3,4)P_2$); PTEN is involved in the breakdown of these two phospholipids. In non-migrating cells PI3K is found in the cytosol whereas PTEN is located at the plasma membrane. Upon application of a chemoattractant a rearrangement occurs which sees PI3K polarise to the front of the migrating cell and PTEN more to the sides and the posterior of the cell (Funamoto et al., 2002). Such strict localisation of these two proteins following addition of chemoattractant results in PIP_3 quickly becoming polarised at the front of the cell providing a method for amplification of small chemoattractant gradients (Devreotes and Janetopoulos, 2003).

There is evidence to suggest that PIP_3 has a role in regulating sites of actin protrusion in the migrating cell (Funamoto et al., 2002). Experiments abrogating PI3K activity prevent such actin structures from properly forming, conversely inhibiting PTEN causes excess and unwanted actin polymerisation within the cell (Devreotes and Janetopoulos, 2003; Iijima and Devreotes, 2002).

1.2.3 Rho proteins in cell migration

The Rho family of GTPases have a variety of important roles in cell migration, particularly in the formation and regulation of lamellipodia and filopodia, as already men-

tioned, and also in the establishment of cell polarity (Machesky and Hall, 1997; Welch and Mullins, 2002; Ridley et al., 2003). Rho GTPases cycle between active GTP-bound and inactive GDP-bound states by the action of guanine nucleotide exchange proteins (GEFs) and GTPase activating proteins (GAPs), Rho guanine nucleotide dissociation inhibitors (RhoGDIs) also add another level of complexity to their regulation. In GTP-bound active states Rho GTPases interact with a number of effectors including activators of the Arp2/3 complex, which, as mentioned previously, is crucial for the initiation of actin polymerisation (Etienne-Manneville and Hall, 2002). Rho proteins with particular importance to the formation of lamellipodia and filopodia are RhoG, Cdc42 and Rac1 (Ridley et al., 2003; Murali and Rajalingam, 2013). The role of RhoG in the process of lamellipodia formation appears to be upstream of Rac; it has been shown to activate RacGEFs thereby indirectly leading to Rac activation (Katoh et al., 2006). Following its activation Rac1 is able to activate WAVE leading to actin polymerisation through the action of the Arp2/3 complex (Eden et al., 2002).

Cdc42 is involved in the formation of filopodia through interaction with WASP (Welch and Mullins, 2002). While this claim is backed up by studies including those in Cdc42-null mouse embryonic fibroblasts which are unable to form filopodia (Yang et al., 2006), conflicting evidence has been found in other migratory models such as a study in Cdc42-null embryonic stem cells derived from fibroblastoid cells which were able to form filopodia as normal (Czuchra et al., 2005). More work therefore needs to be done to fully elucidate the role of Cdc42 in filopodia formation; perhaps other small GTPases of the Cdc42 family or wider Rho family are involved in the process in certain cases.

A polarized phenotype needs to be maintained in order to achieve directed migration. Cdc42 plays an important role in the creation and maintenance of such polarity (Ridley et al., 2003). Work showing the involvement of Cdc42 in the process includes experiments in macrophages using a dominant-negative form of the protein. In this case cells were still able to migrate and form an axis of polarity; however the axis was not oriented in the direction of the chemotactic gradient (Allen et al., 1997). This points to an im-

portant role for Cdc42 in interpreting external cues as to the direction of the gradient and hence controlling polarity of the cell. Cdc42 is active towards the leading edge of migrating cells (Itoh et al., 2005) and is involved in determining where protrusions form at the front of the cell (Srinivasan et al., 2003). Is has also been shown to have an effect on localisation of the Golgi and the microtubule organising centre (MTOC) towards the front of the cell, thereby influencing traffic and microtubule formation in this area (Palazzo et al., 2001). Positive feedback loops have been suggested to be involved in the activation of Cdc42 towards the front of migrating cells, including one involving the kinase p21-activated kinase1 (PAK1), which is also a downstream target of Cdc42. G-protein coupled receptors (GPCRs) at the cell surface can be activated by the binding of chemoattractants, this in turn activates PAK1 which can cause Cdc42 activation, providing a mechanism for increased Cdc42 activation at the leading edge (Li et al., 2003).

The Rho GTPase Rac also has wider roles in the activation and maintenance of actin polymerisation at the leading edge of migrating cells, many of these mechanisms appear to involve feedback loops (Eden et al., 2002). As with Cdc42, activation of Rac1 is localised to the front of the cell, this is likely to be due to the production of PIP_3 in this area by the highly localised activation of PI3K; PIP_3 in turn leads to localised activation of a number of Rac GEFs (Welch et al., 2003). One positive feedback loop stems from further activation of PI3K by Rac at the plasma membrane, thereby ensuring its own sustained activation in this area (Welch et al., 2003). A second positive feedback loop occurs from the activation of Rac by microtubules and in return the stabilisation of microtubules by Rac (Waterman-Storer et al., 1999; Rodriguez et al., 2003). A third mechanism of localised Rac activation comes from activation of Rac by integrins, thereby ensuring Rac activation at the leading edge which in turn enables clustering of integrins to the lamellipodia completing a third feedback loop (Kiosses et al., 2001; Burridge and Wennerberg, 2004).

The role of defining the 'tail' area of a migrating cell appears to be mediated by Rho. Rho and Rac inhibit each other's activity meaning that suppression of Rho would occur

at the front of the cell where Rac is activated (Sander et al., 1999). Similarly, Rho would inhibit Rac activity at the back of the migrating cell therefore preventing lamellipodia formation in this area of the cell (Worthylake and Burridge, 2003; Sander et al., 1999). Rho activity in the lagging edge of cells is thought to stabilise microtubules which in turn enables focal adhesion turnover at the back of the cell, again keeping processes at the front of the cell distinct from those at the back (Rodriguez et al., 2003).

1.2.4 Integrins and adhesions in cell migration

Integrins are key to the process of cell migration; they are the anchors that allow the stabilisation of protrusions by linking them to the ECM. Integrins also have valuable roles when it comes to signalling, with the ability to participate in outside-in as well as inside-out signalling (Hynes, 2002). More details will be presented about integrin trafficking at later stages of this report, for now focus will be on their direct role in the mechanics of migration.

Integrins are transmembrane proteins that bind to ligands in the ECM, such as collagen and fibronectin. The outdated view of adhesion formation was that ligand binding caused conformational changes within the integrins which leads to clustering and ultimately to the formation of larger adhesion complexes (Ridley et al., 2003). A more recent standpoint is that the process of their formation depends largely on actin, and in fact inhibiting actin polymerisation prevents the formation of new adhesions (Choi et al., 2008; Vicente-Manzanares et al., 2009). An updated view consists of nascent adhesions containing a small number of adhesion proteins forming in the protruding lamellipodium in a manner dependent on polymerised actin, this complex can then either undergo quick turnover or can become stabilised by integrins and go on to form a larger adhesion complexes (Figure 1.2; Parsons et al. 2010; Vicente-Manzanares et al. 2009). Such larger complexes, termed focal adhesions, contain a complex array of proteins including integrins, paxillin, talin, focal adhesion kinase (FAK) and α-actinin, amongst others (Parsons et al., 2010), and in fact more than 150 proteins have been

found to be adhesion-associated in some way (Huttenlocher and Horwitz, 2011). The large number of proteins involved serves to highlight the complexity and multifaceted role of focal adhesions within cells.

Focal adhesions serve as an important signalling hub, transferring information between the ECM and the internal actin-based protrusions. This signalling can also aid in polarisation of the cell, since focal adhesions form at the front of migrating cells. In fact, integrin specific activation of protein kinase A at the leading edge of migrating cells has been shown to be an important early factor in the migratory process (Lim et al., 2008).

Focal adhesions act as sites for traction enabling cell movement. The traction force is provided by the interaction of myosin II and actin with the ECM via the intermediate proteins of the adhesion complex, including talin and α-actinin. In this way the adhesions are seen as the 'molecular clutch' of the cell (Vicente-Manzanares et al., 2009; Huttenlocher and Horwitz, 2011). The activity of myosin II is regulated by phosphorylation of myosin light chain (MLC) by either MLC kinase or Rho kinase and this activation of myosin II results in cell contractility and the application of tension at focal adhesion sites (Ridley et al., 2003; Riento and Ridley, 2003) .

Disassembly of adhesions can occur both at the front and the rear of migrating cells. At the front focal complexes which do not mature into focal adhesions are disassembled as new adhesion complexes form at the leading edge (Broussard et al., 2008). A complex interaction between focal adhesion kinase (FAK) and Src as well as regulators of Rac appears to underlie adhesion turnover at the front (Ridley et al., 2003). At the rear of the cell myosin II may be involved in the disassembly of the mature focal adhesions and many of the proteins necessary for disassembly at the front also appear to be required for disassembly at the rear of migrating cells (Ridley et al., 2003). There also seems to be a role for intracellular calcium levels, perhaps in the activation of calpain, a protease which is involved in cleavage of focal adhesion components (Glading et al., 2002).

1.2.5 Vesicle trafficking in chemotaxis

In order to control the directionality and magnitude of migration the availability of chemoattractant receptors and cell adhesion molecules on the cell surface must be carefully regulated. The availability of these molecules depends heavily upon the process of vesicle trafficking, meaning that in order to fully understand chemotaxis, vesicle trafficking must be taken into account (Fletcher and Rappoport, 2010).

Three main vesicle trafficking pathways control the composition of the plasma membrane; endocytosis, endosomal recycling and exocytosis. The interplay between these pathways is pivotal to the process of chemotaxis in order to control the protein and lipid composition of the cell surface. Endocytosis is important for the down-regulation of receptor signalling by internalisation of such receptors (Doherty and McMahon, 2009). Recycling and exocytosis are needed to provide the correct amount and cell surface localisation of receptors and cell adhesion molecules for the control of cell motility. For each of these cellular trafficking pathways there are a number of routes, some of which are cargo- or cell-type specific. Endocytosis includes the well-characterised clathrin-mediated endocytosis pathway, but also less well understood but nevertheless important pathways such as caveolar endocytosis (Hommelgaard et al., 2005; Doherty and McMahon, 2009). Endosomal recycling includes immediate return of proteins to the cell surface following endocytosis (short-loop recycling), and the long-loop recycling pathway via the perinuclear recycling compartment (PNRC; van der Sluijs et al. 1992; Ullrich et al. 1996).

Polarised vesicle trafficking has been suggested as important for the promotion of cell migration, however this area has many conflicting ideas and it is not yet clear which vesicle trafficking pathways are involved (Sheetz et al., 1999). Using a wound healing system it has been suggested that in migrating cells clathrin-mediated endocytosis takes place in the middle-to-front area of the cell (Fletcher and Rappoport, 2010). Conversely, caveolar endocytosis is polarised towards the rear of the cell and endocytic recycling appears polarised to the leading edge of migrating cells (Fletcher and Rappoport, 2010).

This polarisation, however, may differ in different cell types and experimental systems.

1.2.6 Model for chemotaxis

Piecing together the above information and findings allows a picture to be built of what we currently know about migration and chemotaxis. Firstly environmental chemoattractants bind to cell surface receptors initiating a signalling cascade; these can be through GPCRs or growth factor receptors (Bagorda et al., 2006). The signalling cascade results in the localised activation of GEFs for Rho GTPases. The activation of Rac and Cdc42 by their GEFs results in the activation of WASP/WAVE proteins, which in turn leads to activation of the Arp2/3 complex (Miki et al., 1998; Kim et al., 2000; Welch and Mullins, 2002). Arp2/3 initiates branched actin polymerisation, stimulating the formation of membrane protrusions in the direction of migration (Burridge and Wennerberg, 2004). Cdc42 is also involved in the activation of PI3Ks that serve to concentrate the amount of PIP_3 to the leading edge of the cell where it acts to amplify the gradient (Devreotes and Janetopoulos, 2003). An axis of polarity exists in the migrating cell controlled by Cdc42. This protein serves a number of functions related to cell polarity including orientation of the Golgi and MTOC (Ridley et al., 2003; Palazzo et al., 2001). Activities of Rac and Rho are also polarised in the migrating cell whereby Rac's activation at the front inhibits Rho and the converse occurs at the rear (Worthylake and Burridge, 2003; Sander et al., 1999). Stabilisation of protrusions occurs via interaction with focal complexes that link them to the ECM. These focal complexes/adhesions also serve as traction points over which the cell moves (Huttenlocher and Horwitz, 2011).

1.3 Endocytosis

As mentioned above, for correct migration, cells need to be able to control the composition of the plasma membrane. Endocytosis is the process of internalising plasma membrane lipids and proteins (Doherty and McMahon, 2009). This internalisation takes place in vesicles that bud from the membrane and, once inside the cell, are trafficked to

intracellular compartments for sorting. For growth factor receptors at the plasma membrane endocytosis can have opposing effects: endocytosis can lead to down-regulation by degradation, or can lead to the maintenance of signalling by delivering the receptor to a compartment where the ligand is detached and the receptor recycled (Doherty and McMahon, 2009). Endocytosis has been found to be a route of cellular entry for certain viruses and so is a focal point for studies hoping to prevent spread of these viruses (Doherty and McMahon, 2009; Thorley et al., 2010). There are many mechanisms of endocytosis involving the action of a large array of proteins, however this introduction will concentrate on the two most highly studied methods of endocytosis: clathrin-mediated endocytosis and caveolar endocytosis.

1.3.1 Clathrin-mediated endocytosis

First observations of clathrin-mediated endocytosis date back 50 years to the study of yolk protein uptake by insect oocytes (Roth and Porter, 1964), although at the time of this study researchers did not know the identity of the coat protein. Since this study the coat protein has been identified as clathrin and the process of clathrin-mediated endocytosis has been studied in numerous cell types (Pearse, 1976). Clathrin-mediated endocytosis is now widely established as the main route for internalisation in eukaryotic cells.

Clathrin

In clathrin-mediated endocytosis the internalising vesicle is surrounded by a lattice of clathrin. The lattice is made up of clathrin triskelia, which each contain three clathrin heavy chains (CHCs), in an arrangement with their legs radiating out from a central hub, shown in Figure 1.3 (Kirchhausen and Harrison, 1981). Each CHC unit consists of eight repeats of a clathrin heavy chain repeat (CHCR0-8), these make up the regions known as the ankle, distal leg, knee and proximal leg of the structure (Ybe et al., 1999; Brodsky, 2012). Connected to CHCR0 by a linker region is the terminal domain

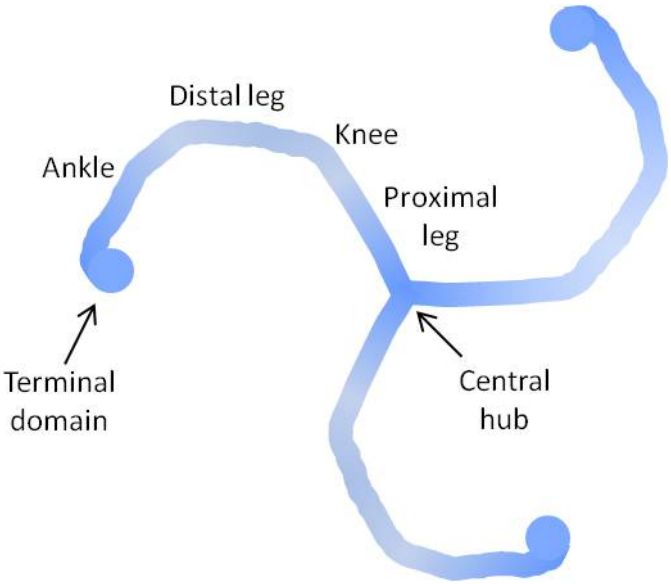

Figure 1.3: Diagram showing the domain structure of a clathrin triskelion

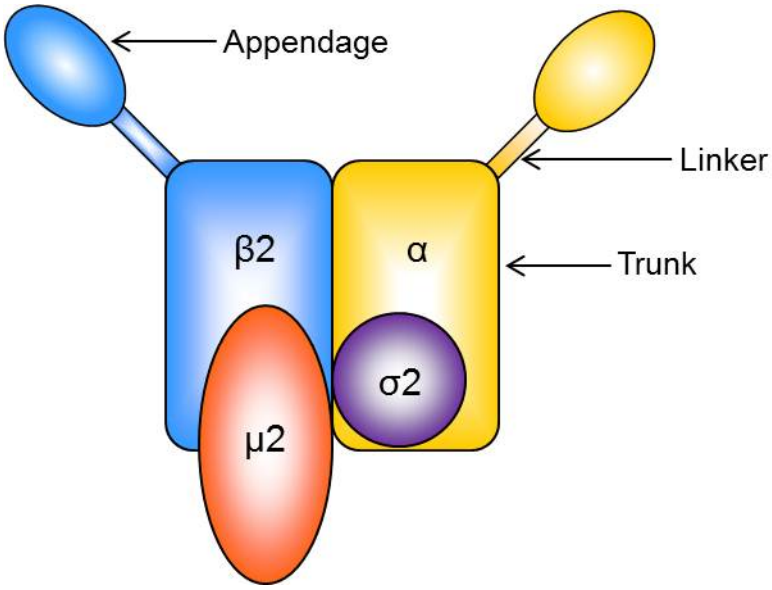

Figure 1.4: Diagram showing the four subunits of AP2. Subunits the α and β have both a trunk domain and flexible linker. Approximate positioning of the medium and small subunits are also shown.

(TD; Wilbur et al. 2005). The TD can bind to a number of different adaptor/accessory proteins via four interaction sites contained within its sequence (Ter Haar et al., 2000; Miele et al., 2004; Lemmon and Traub, 2012). A further adaptor protein binding site has been mapped to the region in the ankle domain between CHCR1 and CHCR2 (Knuehl et al., 2006). Each CHC is associated with a clathrin light chain (CLC; Kirchhausen and Harrison 1981). This interaction is mediated by three tryptophan residues in the CLCs (Chen et al., 2002). The functions of the central hub include aiding CLC binding, trimerisation and lattice formation (Blank and Brodsky, 1986, 1987; Näthke et al., 1992).

The diameter of the clathrin lattice ranges from 60 – 200 nm but can vary greatly depending on species and the cargo being transported (Crowther et al., 1976; McMahon and Boucrot, 2011). Clathrin coat assembly occurs by crosslinking of triskelia, a process facilitated by the action of adaptor protein (AP) complexes. Clathrin triskelia lie approximately 20 nm away from the vesicle contained within the coat, the link between the two being formed of interactions between the CHCs and AP complexes (Kirchhausen, 2000).

Adaptor protein 2

Adaptor protein 2 (AP2) is a tetrameric complex thought to function as the main adaptor protein for clathrin-mediated endocytosis. It is analogous to AP1 and AP3 which have functions in vesicle formation from sites other than the plasma membrane. The 200 kDa AP2 complex is made up of four subunits as shown in Figure 1.4: two large subunits, α and $\beta 2$, which each contain a trunk joined by a flexible linker to an appendage, a medium subunit ($\mu 2$) and a small subunit ($\sigma 2$; Kirchhausen 1999). The roles of AP2 in clathrin-mediated endocytosis include the initial binding to the plasma membrane and recruitment of clathrin, binding to and incorporation of cargo into the vesicle and recruitment of other proteins necessary for the endocytic process (Collins et al., 2002).

Targetting of AP2 to the plasma membrane occurs by its binding to membrane lipids, especially PIP_2 (Gaidarov et al., 1996). This interaction requires phosphorylation of

the Thr-156 residue on the $\mu 2$ subunit of AP2 which causes a conformational change within AP2 revealing an additional site for PIP_2 binding and cargo molecule binding sites, increasing interactions between the adaptor complex and the membrane (Olusanya et al., 2001; Collins et al., 2002). AP2 is able to bind clathrin through interaction with its $\beta 2$ appendage domain and also a clathrin box motif in the hinge region of its $\beta 2$ subunit (Ter Haar et al., 2000; Owen and Evans, 1998). AP2 predominantly binds cargo proteins with specific motifs: those containing tyrosine-based motifs (Yxxϕ), which it binds via the C-terminal of its $\mu 2$ domain, and those containing dileucine motifs (D/ExxxLL) which it binds via its $\mu 2$ or $\beta 2$ subunits (Ohno et al., 1995; Rodionov and Bakke, 1998; Rapoport et al., 1997).

There is a large array of proteins involved in clathrin-mediated endocytosis. To discuss fully the function of the key players it becomes necessary to discuss clathrin-mediated endocytosis in terms of the five stages which make up the process, those are: initiation, cargo incorportation, membrane bending, scission and uncoating. Figure 1.5 also shows these stages in the form of a diagram.

Coated pit initiation

The longstanding view of coated pit initiation begins with AP2 binding to PIP_2 at the plasma membrane, from here it can bind to cargo molecules, recruit more AP2 and also recruit clathrin (Doherty and McMahon, 2009). This view was challenged recently by Henne and colleagues who published that a protein complex including Fer/Cip4 homology domain-only (FCHO) proteins 1 and 2, EGFR pathway substrate 15 (Eps15) and intersectin was responsible for coated pit initiation in clathrin-mediated endocytosis (Henne et al., 2010). Using spinning disk confocal microscopy they showed that FCHO1/2 could be detected at sites of coated pit formation prior to the recruitment of clathrin or AP2 and that coated pit formation failed when the FCHO1/2 proteins were knocked-down by RNA interference (RNAi). They also showed that the number of clathrin-coated pits which formed on the plasma membrane correlated with the number

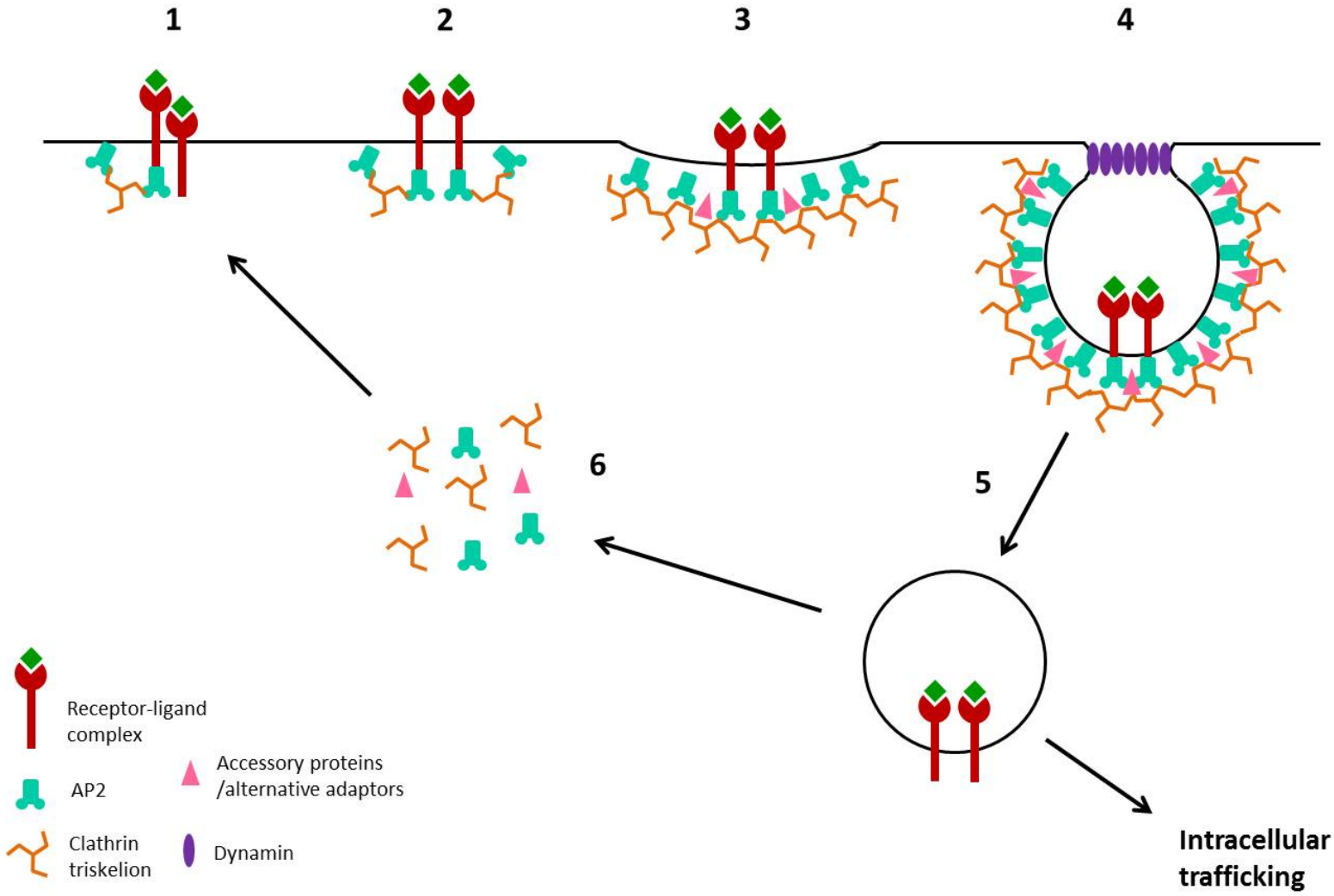

Figure 1.5: Diagram to demonstrate the stages of clathrin-mediated endocytosis. Coated pit formation is initiated and cargo incorporated by the binding of AP2 and clathrin (1 and 2). Membrane bending and further binding of AP2, clathrin and accessory/alternative adaptor proteins occurs (3). The vesicle is pinched off the membrane by the action of dynamin (4). Once internalised the vesicle is uncoated (5) and can be trafficked to other regions of the cell; coat and accessory proteins are recycled for use in more internalisation events (6).

of FCHO1/2 molecules present in the cell. From this they concluded that FCHO1/2, in complex with intersectins and Eps15 was the initiator of clathrin-coated pit formation (Henne et al., 2010).

Data from other groups has, however, conflicted with this viewpoint (Cocucci et al., 2012; Umasankar et al., 2012). Cocucci and colleagues were able to recapitulate some of Henne et al.'s results using the same methods of experimental design and image acquisition. However, when they used a highly sensitive total internal reflection fluorescence (TIRF) microscopy method with single fluorophore sensitivity they found that in FCHO1/2 knock-down cells AP2-containing pits were forming but were mostly short-lived (<10 s) and abortive (Cocucci et al., 2012). From this they concluded that FCHO1/2 proteins are necessary for clathrin-mediated endocytosis but are not involved in initiation of the pit, rather they are necessary for its stabilisation (Cocucci et al., 2012). In the study by Umasankar et al. they used a genetics approach with zebrafish predicting that if FCHO1/2's function was vital to pit formation interfering with FCHO1/2 expression would give a similar phenotype to interfering with AP2 expression (Umasankar et al., 2012). Results showed that knock-down of AP2 in the developing embryos was lethal at later stages of embryogenesis, however this was not the case with knock-down of FCHO1 which showed embryos with more developed dorsal regions and under developed ventral regions. This, along with other results, led the group to conclude that FCHO proteins could not be directly responsible for pit formation, although they must have some role in the endocytic process (Umasankar et al., 2012).

The aforementioned study by Cocucci et al. also involved detailed imaging of fluorescent clathrin and AP2 at early stages of endocytosis, they then used modelling software to come up with predictions about the stoichiometries of these molecules during endocytosis (Cocucci et al., 2012). They found that one event corresponding to the arrival of clathrin and AP2 is followed very quickly by another such event and that in each case the most likely stoichiometry was one clathrin to two AP2 molecules. They discussed that if AP2 were to bind alone the dwell time would most likely not be long enough

for any further interactions to take place, similarly short-lived interactions would occur if only a single AP2-clathrin complex interacted with the plasma membrane. However, the binding of two AP2 molecules and clathrin to the plasma membrane creates a much stronger contact due to the increased number of AP2-PIP_2 interactions and AP2-cargo interactions, leading to a longer dwell time at the plasma membrane, therefore increasing the likelihood of interaction with more clathrin and AP2 (Cocucci et al., 2012). As mentioned previously PIP_2 is indispensible for the initial binding of AP2 molecules to the plasma membrane as shown by a number of studies (Boucrot et al., 2006; Zoncu et al., 2007; Antonescu et al., 2011).

Cargo incorporation

AP2 is the main protein known to be involved in cargo sorting into clathrin-coated vesicles. AP2 binds to cargo such as receptor tyrosine kinases (RTKs) in the plasma membrane containing either tyrosine-based or dileucine motifs, as mentioned previously (Ohno et al., 1995; Rodionov and Bakke, 1998; Collins et al., 2002). In addition to AP2 other adaptor proteins exist which regulate incorporation of specific cargo proteins. There has been much controversy over whether these proteins act independently of AP2 or whether AP2 is still necessary for clathrin-mediated endocytosis in these cases. Examples of such include arrestins for the internalisation of GPCRs; Disabled protein 2 (Dab2) and Autosomal recessive hypercholesterolemia protein (ARH) for low density lipoprotein receptor (LDLR) endocytosis; and epsin as an adaptor for ubiquitinated cargo, amongst others (Benmerah et al., 1996; Traub, 2003).

The evidence that AP2 was not needed to form clathrin-coated pits in all cases comes largely from RNAi experiments looking into the effect knock-down of one or more subunits of AP2 had on endocytosis (Motley et al., 2003; Keyel et al., 2006; Maurer and Cooper, 2006; Hinrichsen et al., 2003). Such experiments showed that knock-down of AP2 subunits was able to prevent transferrin endocytosis but was unable to completely halt endocytosis of LDLR or EGFR. However, a more recent study by Boucrot et al.

sought to identify whether these results could be substantiated or were likely an artefact of experimental procedure. Boucrot and colleagues pointed out that in most cases of AP2 subunit knock-down there was still some AP2 left in the cells and investigated the theory that while there was clearly a massive reduction in the number of forming clathrin-coated vesicles perhaps those that were still forming contain this residual AP2 and were therefore sites of clathrin-mediated endocytosis (Boucrot et al., 2010). Through their own experiments they showed that only a small number of clathrin spots remained on the cell surface following RNAi against AP2, but importantly all AP2 spots contained clathrin and all clathrin spots contained AP2 (Boucrot et al., 2010). Another point the Boucrot et al. study sought to test was whether LDLR internalisation could occur following AP2 knock-down as had been shown in previous studies (Motley et al., 2003; Keyel et al., 2006; Maurer and Cooper, 2006). Experimental procedures in some of the previous studies had allowed cells to cool to 4°C which would prevent endocytosis while ligand binding to the surface receptors was still able to occur, before warming to 37°C to allow endocytosis (Motley et al., 2003; Keyel et al., 2006). When this experiment was repeated by Boucrot and colleagues at physiological temperature of 37°C throughout the experiment LDLR internalisation was inhibited in a way comparable to transferrin uptake (Boucrot et al., 2010). Consolidating all these results led the group to postulate that AP2 is necessary for clathrin-coat formation in all cases and that taking experimental procedure into account when analysing results is very important. These results corroborate with others such as Huang and colleagues who undertook internalisation experiments at a physiological 37°C to show a role for AP2 in endocytosis of EGFR, thereby showing how valuable correct experimental procedure is in such studies (Huang et al., 2004).

The necessity for AP2 in the process of clathrin-mediated endocytosis is backed up by other more recent studies (Aguet et al., 2013; Cocucci et al., 2012). The current view is that alternative adaptor proteins bind to AP2 and therefore work cooperatively with AP2. Alternative adaptors are likely to be necessary for tissue specificity of the en-

docytic process, for example since the liver needs to take up large amount of LDLR, ARH is present in hepatocytes to facilitate its incorporation into vesicles (Traub, 2003; Doherty and McMahon, 2009).

Membrane bending

Clathrin polymerisation itself is able to allow membrane deformation but calculations previously showed this was unlikely to be enough to cause vesicle formation (Nossal, 2001). Various proteins known to be recruited to sites of clathrin-coated pit formation are thought to be involved in the bending of the membrane. The protein epsin has been identified as being involved in membrane deformation during clathrin-coated pit formation, as well as a possible role as an adaptor protein (Ford et al., 2002). The epsin N-terminal homology (ENTH) domain allows epsin to bind PIP_2, and therefore be recruited to the plasma membrane. Once bound an amphipathic helix (known as helix 0) contained within the protein's N-terminal reverts to an ordered state allowing its insertion into the cytosolic side of the plasma membrane (Ford et al., 2002). This act causes membrane deformation by the pushing apart of lipid head-groups within the plasma membrane.

Another set of proteins with importance in membrane deformation during endocytosis are the Bin-Amphiphysin-Rvs (BAR) domain containing proteins which work by creating or stabilising membrane curvature (Mim and Unger, 2012). Endcoytosis of the transferrin receptor has been shown to be dependent on this class of proteins and they have been shown to cause tubulation of liposomes *in vitro* (Itoh et al., 2005). Recruitment of these proteins mainly occurs by binding to phospholipids in the plasma membrane (Daumke et al., 2014). The BAR domain of these proteins contains a three helix coiled-coil which enables dimerisation of the protein; dimerisation can be either homo- or hetero-dimerisation (Mim and Unger, 2012). The dimerised complex has a so-called 'banana shape' structure that aids the hypothesis that these proteins allow invagination simply by imposing their shape onto the membrane. These proteins also

have a high density of positively charged residues along their length which likely assist in binding and shaping of the negatively charged membrane (Peter et al., 2004). BAR domain containing proteins can be split up into several classes which differ in the extent of curvature they can mediate, whether this curvature is positive or negative and also in the stage they are recruited to the forming clathrin-coated pit (Mim and Unger, 2012). The aforementioned FCHO1/2 proteins contain F-BAR domains; these are recruited early in clathrin-coated pit formation and are known to induce positive but only shallow membrane curvature (Henne et al., 2010; Daumke et al., 2014).

Amphiphysin, endophilin and sorting nexin 9 (SNX9) are examples of BAR domain containing proteins recruited to late stages of clathrin-coated vesicle formation (Doherty and McMahon, 2009). In addition to their N-terminal BAR domains they have Src-homology 3 (SH3) domains in their C-terminal which are important for interaction with dynamin at the site of vesicle formation and therefore aid in targeting the protein to the plasma membrane (Itoh et al., 2005). As well as the roles of inducing and/or stabilising membrane curvature BAR domain containing proteins are predicted to have other important roles in clathrin-mediated endocytosis including acting as scaffolds involved in the wider organisation of proteins involved in the internalisation process and recruitment of actin polymerising proteins (Mim and Unger, 2012).

More recent studies have proposed alternate and conflicting mechanisms for how membranes are deformed during endocytosis (Dannhauser and Ungewickell, 2012; Stachowiak et al., 2012). The first study conflicts with the idea presented earlier, that clathrin is not sufficient, by itself, to cause membrane deformation during endocytosis. The researchers used a system containing lyposomes where they were able to control the composition of each experimental system. Using this system they showed that when only clathrin and a truncated version of epsin, only able to bind clathrin and the membrane (ie. not able to bend membranes), were added to the liposome solution clathrin-coated vesicles were able to form (Dannhauser and Ungewickell, 2012). The authors conclude that clathrin is able to bend membranes to the necessary degree for vesicle formation. It is, how-

ever, unknown whether such a mechanism would be sufficient for this process *in vivo*. A second study, again conflicting with earlier ideas, proposed that membrane bending could occur without the insertion of any proteins into the membrane, simply by over-crowding of proteins in a particular region (Stachowiak et al., 2012). Giant unilamellar vesicles (GUVs) were used in this study along with only the membrane binding portions of epsin or AP180 (another molecule proposed to play a role in vesicle formation) to allow membrane binding but not insertion into the membrane (Stachowiak et al., 2012). Tubulation of the GUVs was evident in both cases and the group used it to conclude that such 'membrane crowding' could aid membrane invagination (Stachowiak et al., 2012). Once again, however, it is uncertain whether this so called 'membrane crowding' would be enough to cause membrane invagination *in vivo* and it is noted that the concentrations of proteins in both of these above mentioned studies is too high to be physiologically relevant (Kirchhausen, 2012).

Until some of these processes are tested in live cells and *in vivo* systems we cannot know for sure the method of membrane curvature formation during clathrin-coat assembly. Perhaps clathrin is sufficient to begin membrane curvature but curvature-sensing proteins are necessary for later stages of pit formation to stabilise the curved region and recruit membrane scission factors.

Vesicle scission

Dynamin is a large GTPase responsible for the scission event in clathrin-mediated endocytosis. Mammals have three dynamin isoforms but in non-neuronal cells the ubiquitously expressed dynamin2 isoform has been shown to be the major isoform necessary for clathrin-mediated endocytosis, hence this will be the main focus of discussion here (Liu et al., 2008). Dynamin's first appearance on clathrin-coated pits appears to be during early stages of formation, however only a small amount is present at this time (Aguet et al., 2013). Research suggests that early dynamin recruitment may be necessary in order to pass a regulatory checkpoint; vesicles devoid of dynamin were found to

be abortive at early stages, whereas dynamin-positive vesicles had lifetimes > 40 s, consistent with a completed endocytic event (Aguet et al., 2013). Later in vesicle formation there is a characteristic burst in dynamin activity consistent with its role in fission of the vesicle from the membrane (Taylor et al., 2011).

Dynamin has five main domains in its structure: a proline-rich domain (PRD) in its C-terminal for binding to SH3-containing proteins, a GTPase domain, a bundle signalling element (BSE), a stalk and finally a pleckstrin homology (PH) domain for binding phospholipids (Daumke et al., 2014). The stalk domain is able to self-assemble in a criss-cross fashion via a hydrophobic interface to create an extended dimer (Faelber et al., 2011). A second hydrophobic interface allows additional oligomer assembly. The BSE interacts with the GTPase domain of the same dynamin molecule forming a flexible hinge region. The stalk region also forms an interface with the PH domain and this is thought to regulate oligomerisation in some way (Faelber et al., 2011). Oligomerised dynamin assembles in a helix around the neck of a forming vesicle, whereas dimerisation occurs between GTPase domains on adjacent rungs (Ferguson and De Camilli, 2012).

The actual mechanism of vesicle fission by dynamin remains to be fully explained. The hydrolysis of GTP appears to be the essential factor (Marks et al., 2001). The constricted arrangement of dynamin creates high curvature and stress at the neck of the vesicle and interaction of the PH domain with acidic phospholipids in the plasma membrane helps to stabilise the reaction (Bashkirov et al., 2008b; Ramachandran et al., 2009). One mechanism suggests that GTP hydrolysis by a GTPase domain dimer leads to movement of the BSE in such a way as to cause rotational sliding of the dynamin helix rungs leading to constriction of the vesicle neck (Chappie et al., 2011). The reaction is likely to be more complex than this and other studies have implicated longitudinal tension, actin polymerisation and insertion of amphipathic helixes into the membrane as other key factors in the process as well as pointing out that dynamin may respond in different ways depending on the curvature of the membrane lipids (Bashkirov et al., 2008a; Boucrot et al., 2012; Daumke et al., 2014).

As eluded to earlier there is a high degree of co-operativity between dynamin and BAR domain proteins. The SH3 domains of amphiphysin and endophilin have been implicated in the recruitment of dynamin by binding to its PRD. Endophilin has been shown to be reciprocally involved in dynamin recruitment, whereby depletion of endophilin leads to decreased dynamin recruitment and vice versa. Recent studies proposed conflicting views on how the interaction between BAR domain proteins and dynamin affects fission (Meinecke et al., 2013; Neumann and Schmid, 2013). Neumann et al. used supported bilayers with excess membrane reservoir (SUPER) templates to show that N-BAR domain containing proteins, such as amphiphysin and endophilin acted to increase efficiency of the fission reaction but that this was not dependent on SH3-PRD interactions and that these were in fact inhibitory to the fission process (Neumann and Schmid, 2013). They further hypothesised that the positive effect of N-BAR associated membrane bending balanced with negative regulation by the SH3-PRD interaction allowed these proteins to intimately regulate dynamin efficiency and vesicle fission (Neumann and Schmid, 2013). Another study from 2013 used GUVs to test the relationship between BAR domain proteins and dynamin (Meinecke et al., 2013). They found that dynamin and GTP had to be present in addition to amphphysin or endophilin in order for tubulation of the GUVs to occur, and that, in contrast to results from Neumann et al., this was highly dependent on the interaction between the BAR domain protein and dynamin (Meinecke et al., 2013; Neumann and Schmid, 2013). To fully appreciate the extent to which these, and other, results mirror the physiological process more live cell studies are needed.

Vesicle uncoating

After a clathrin-coated vesicle has been internalised the clathrin coat must be removed to allow the vesicle to fuse with intracellular membranes. The uncoating process requires the proteins heat shock cognate protein 70 (Hsc70) and auxilin (McMahon and Boucrot, 2011). Following vesicle internalisation auxilin is recruited to the TD and ankle regions of clathrin triskelia, allowing it to localise to the hub region of a neighbouring triskelion (Fotin et al., 2004). Auxillin enables Hsc70 to bind via its J-domain (Ungewickell et al.,

1995). For maximal disassembly the ratio of auxillin to Hsc70 appears to be one auxillin and three Hsc70 per triskelion (Böcking et al., 2011). Disassembly of the coat occurs from energy obtained through ATP hydrolysis by the ATPase activity of Hsc70 (Ungewickell et al., 1995). Clathrin, along with accessory and adaptor proteins, is recycled for use in further clathrin-mediated endocytosis, and the vesicle is now free to fuse with other organelles within the cell (Young, 2007).

1.3.2 Caveolar endocytosis

Caveolae were first identified in mammalian cells as flask-shaped invaginations, 55 - 65 nm diameter in size, connected to the plasma membrane (Yamada, 1955). Since their discovery caveolae have been shown to have a role in a number of cellular processes including lipid regulation in adipocytes, signalling and mechanosensing (Parton and Simons, 2007; Bastiani and Parton, 2010). These functions of caveolae are out of the scope of this discussion and the focus will be on the role of caveolae in endocytosis.

Caveolin

The protein caveolin has been found to be indispensible for caveolae formation (Razani et al., 2001). Caveolin has three family members: caveolin1 and caveolin2 are found in non-muscle cells as well as smooth muscle, caveolin3 is expressed in skeletal muscle, cardiac muscle and some smooth muscle (Drab et al., 2001; Way and Parton, 1996). In their respective tissues caveolin1 and caveolin3 function similarly and are required for caveolae formation, shown by loss of these isoforms leading to a loss of caveolae formation (Drab et al., 2001; Galbiati et al., 2001). Caveolin2 is not thought to be necessary for caveolae formation, although it often co-associates with caveolin1 (Razani et al., 2002). Caveolin1 is able to oligomerise, and this appears necessary for caveolar formation. The C-terminal of caveolin1 is palmitoylated, with three possible sites for this palmitoylation identified, however this was found not to be necessary for the plasma membrane localisation of caveolin1 (Dietzen et al., 1995; Monier et al., 1995). At the plasma membrane

caveolin1 forms a hairpin structure and inserts into the plasma membrane, its N- and C-terminals protrude into the cytoplasm. In particular cell types caveolae have been observed to make up a third of the plasma membrane (Parton and Richards, 2003).

Requirements for caveolae

It has been estimated that 144 caveolin molecules are required to form one caveolae (Pelkmans and Zerial, 2005). Regions of the plasma membrane enriched in caveolae also contain higher than normal levels of glycosphingolipids, sphingomyelin and cholesterol (Örtegren et al., 2004; Parton and Simons, 2007). Cholesterol has been reported to be very important for caveolae structure and cholesterol depletion leads to flattening of caveolae (Rothberg et al., 1992). Caveolae on the plasma membrane are found to be highly stable structures and budding only occurs under particular stimuli (Pelkmans et al., 2004). An interesting model for how caveolae form has become apparent (Parton and Simons, 2007; Bastiani and Parton, 2010). Caveolin proteins are first synthesised in the endoplasmic reticulum (ER) where they also undergo an initial stage of oligomerisation (Monier et al., 1995). Transport to the Golgi occurs and exit from the Golgi takes place along with further oligomerisation and association with lipid-raft domains enriched with cholesterol and glycosphingolipids (Parton and Simons, 2007). These 'mature' caveolae can then fuse with the plasma membrane. The formation of these mature structures and exit from the Golgi is dependent on cholesterol (Pol et al., 2005). The ganglioside GM1 has also been shown to be important for caveolae maintenance at the plasma membrane (Singh et al., 2010).

In endothelial cells dynamin has been shown to be important for endocytosis by caveolae; as in clathrin-mediated endocytosis it appears to localise to the neck of caveolar vesicles (Oh et al., 1998; Nabi and Le, 2003). Additionally dynamin has been shown to be important for caveolae internalisation in various cell types (Lamaze et al., 2001; Puri et al., 2001; Nabi and Le, 2003). Phosphorylation of caveolin at residue Tyr-14 is also important for caveolar endocytosis and likely occurs by action of the kinase Src

(Cao et al., 2002; del Pozo et al., 2005b; Hill et al., 2007). Other factors that appear to be important for caveolar endocytosis include Src kinases, protein kinase C (PKC) and actin (Bastiani and Parton, 2010). Imaging of Simian virus 40 (SV40) internalisation showed recruitment of dynamin as well as a burst of actin polymerisation as the vesicle internalised (Pelkmans et al., 2002).

Fairly recently another set of proteins, called cavins, were found to be necessary for caveolae stabilization at the plasma membrane (Liu and Pilch, 2008). Interaction of the four cavin family members into a 60-80 molecule complex is known as the 'cavin complex' (Bastiani and Parton, 2010). Depletion of cavin-1 negatively impacts caveolae formation and results in a flat plasma membrane, it also lead to degradation of caveolin1 (Hill et al., 2008). Caveolin recruits the cavin complex to the plasma membrane in a cavin-1-dependent manner (Bastiani et al., 2009). The role of these proteins isn't known in detail but it appears they have some function in the stabilisation of caveolae at the plasma membrane (Bastiani and Parton, 2010).

Roles for caveolar endocytosis

Controversy exists over the role of caveolar endocytosis in mammalian cells and many studies have given conflicting results. Caveolar endocytosis has been noted as the internalisation route for glycosphingolipids and integrins as well as various pathogens (Bastiani and Parton, 2010). The stimulation of caveolar endocytosis by glycosphingolipids has been shown to cause clustering of β1-integrin and subsequent internalisation of the adhesion protein (Sharma et al., 2004, 2005). Another interesting link between caveolar endocytosis and integrins is that in adherent cells caveolin is found to be present in focal adhesions, this serves sequester the caveolin in these structures preventing them from forming caveolae at the plasma membrane (del Pozo et al., 2005a). When these cells detatch from the ECM caveolin is free to promote caveolae formation at the cell surface and mediate endocytosis (del Pozo et al., 2005a). Once internalised caveolae appear to fuse with early endosomes in a manner dependent on Rab5 (Parton and Simons, 2007;

Hayer et al., 2010). Interestingly, it has been shown that internalisation by the caveolar route can lead to a different fate than internalisation of the same molecule by clathrin-mediated endocytosis; transforming growth factor beta (TGFβ) receptor can enter cell by both of these internalisation routes however entry by clathrin-mediated endocytosis leads to sustained signalling whereas internalisation by caveolae leads to degradation of the receptor (Di Guglielmo et al., 2003).

Some bacterial toxins and viruses have been shown to enter cells by caveolar endocytosis, and as such derivatives of these molecules are often used to study the process. Fluorescent or gold-tagged cholera toxin is often used, however under some circumstances this molecule has been shown to enter cells by methods others than caveolar endocytosis, making its use for the study of this process questionable (Torgersen et al., 2001). Another maker often used is SV40, which has been shown to internalise via caveolae; however, as with cholera toxin, SV40 has been shown to enter cells lacking caveolae, yet again questioning its use as a marker for the caveolar endocytic pathway (Damm et al., 2005; Ewers et al., 2010). Another caveat to using such markers for the study of caveolar endocytosis is that antibodies and toxins are known to cluster receptors at the sites of their binding which can lead to the formation of caveolae, or caveolae-like transport intermediates, however this unlikely to represent the endogenous mechanism for internalisation of these receptors (Rothberg et al., 1992).

There are clear links between the caveolar endocytic pathway and other raft-dependent internalisation routes that require neither caveolin nor dynamin; for example the internalisation of SV40 can occur by either of these types of internalisation process (Pelkmans et al., 2002; Damm et al., 2005). However, SV40 uptake is in fact decreased in cells containing caveolae, thus caveolar endocytosis may represent a method of regulating uptake of particular molecules (Damm et al., 2005). It seems like the presence of caveolin and dynamin in the caveolar endocytic pathway is a method of adding regulation to raft-dependent endocytosis.

There is conflicting evidence about the role caveolar endocytosis plays in migration, with groups many reporting opposing results. One group used caveolin1-deficient fibroblasts to show that a lack of caveolin1 abrogated cell polarisation and directional persistency, thereby pointing to the necessity of caveolin1 in these processes (Grande-García et al., 2007). In a similar vein, Shatz et al. were able to show that inhibition of caveolin1 by expressing dominant-negative versions of the protein lead to decreased cell migration and invasion (Shatz et al., 2010). These results point to a possible tumour promoting role for caveolin1. In contrast to this one group have shown that expression of caveolin1 inhibited lamellipodia formation in a breast cancer cell line (Zhang et al., 2000). Bonucchelli and colleagues also point to a role for caveolin1 in tumour supression by showing that a mutant version of caveolin1 is able to promote tumour cell migration and invasion (Bonuccelli et al., 2009). It is clear from just these studies that the role for caveolin1 in cell migration and therefore metastasis is complex and more streamlined research is needed before its role is fully elucidated.

1.4 Endosomal recycling and exocytosis

Endosomal recycling and exocytosis are integral to the process of cell migration (Figure 1.6 shows a simplified version of cargo trafficking through the endosomal system). They are necessary to provide correct surface localisation of chemoattractant receptors and adhesion molecules, as well as lipid membrane for membrane extension (Bretscher, 1996). Once internalised vesicles fuse with early endosomes which have a pH of approximately 6.0 (Maxfield and Yamashiro, 1991), this causes some (but not all) ligand-receptor complexes to dissociate (French et al., 1995). Endosomes and other membrane structures within the cell are given identity by specific Rab GTPases and phosphoinositides; the early endosome is marked by Rab5, and phosphatidylinositol-3-phosphate (Grant and Donaldson, 2009). Over time the early endosome matures into a late endosome which contains acid hydrolases, has a lower pH (5.0-6.0) and is marked by the loss of Rab5 and

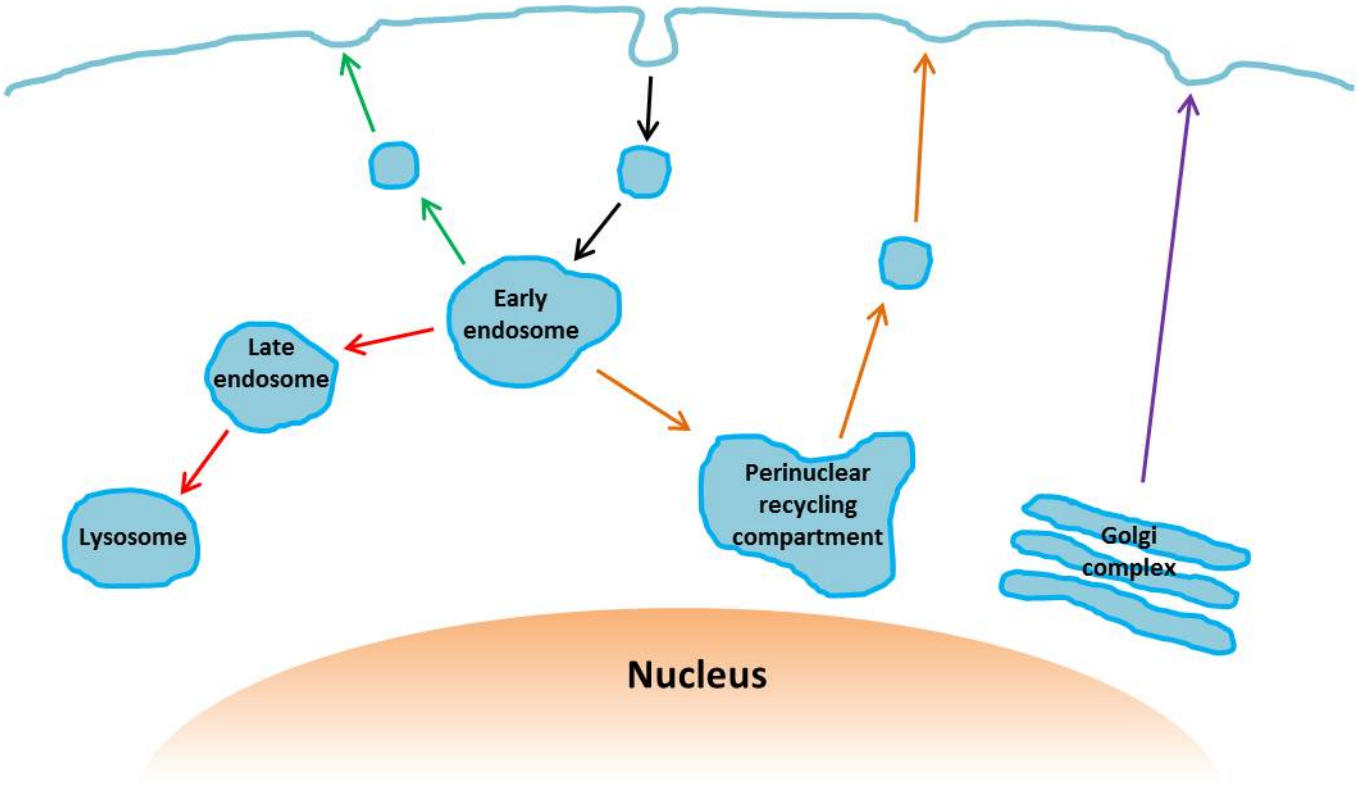

Figure 1.6: A simplified diagram of the endosomal system. After internalisation vesicles fuse with early endosomes (black arrows) from where they can be recycled by the short-loop recycling pathway (green arrows) or by the long-loop recycling pathway via the PNRC (orange arrows). Alternatively cargo can be transported for degradation via the late endosome (red arrows). Newly synthesised cargo can be trafficked from the Golgi complex to the plasma membrane (purple arrows).

addition of Rab7 (Li et al., 2013; Poteryaev et al., 2010). Even further in the maturation process late endosomes mature into lysosomes or fuse with pre-existing lysosomes which have a lower internal pH of 4.5-5.0; cargo degradation occurs here (Mindell, 2012; Li et al., 2013).

For cargo to avoid transport along the degradation route it must be re-routed before it reaches the lysosome. Taking the transferrin receptor as an example, over 95% of it leaves the early endosome before maturation occurs, pointing to the default route for this receptor to involve recycling (Dunn et al., 1989; Maxfield and McGraw, 2004). Recycling occurs either directly from the early endosome in a 'short-loop' recycling route, or via the PNRC in a 'long-loop' recycling route (Grant and Donaldson, 2009; Maxfield and McGraw, 2004). The short-loop recycling pathway is the route for the transferrin receptor and various integrins (Jones et al., 2006). This pathway is dependent on Rab4 which appears to be involved in cargo sorting in this pathway (Daro et al., 1996; van der Sluijs et al., 1992). When Rab4 is inhibited short-loop specific cargo ends up in juxtanuclear compartments, consistent with a re-routing of cargo via the long-loop pathway (McCaffrey et al., 2001). The PNRC is a tubular structure localised in a juxtanuclear region, transport to this compartment requires the proteins EDH4 and also the Rab11 effector Rab11FIP5 (Sharma et al., 2008; Schonteich et al., 2008). Recycling back to the plasma membrane from the PNCR is dependent on Rab11 and Arf1 and/or 6 (Ullrich et al., 1996; Mohrmann and van der Sluijs, 1999; Jones et al., 2006).

Both recycling pathways are important for cell migration and chemotaxis. Integrins internalised from adhesion complexes at the leading edge have been observed to route to a juxtanuclear recycling compartment, and recycling vesicles are shown to transport from this compartment to the front of cells (Jones et al., 2006). A role for the Rab4-dependent route of recycling in migration is indicated by a decrease in directional migration and $\alpha v\beta 3$ integrin recycling in NIH 3T3 fibroblasts following expression of dominant-negative Rab4, suggesting a role for the short-loop pathway in the polarized trafficking of this integrin to the leading edge of migrating cells (Woods et al., 2004;

White et al., 2007). The Rab11-dependent long-loop recycling pathway also has a noted role in cell migration. Expression of a dominant-negative Rab11 impairs random migration of MDCK cells and wound healing in the PtK1 epithelial cell type (Mammoto et al., 1999; Prigozhina and Waterman-Storer, 2006). Interestingly, in the latter system, the speed of migration appeared increased but the directionality was seriously reduced using this inhibitor. As with the short-loop pathway, there is also evidence that the long-loop pathway is involved in polarized trafficking of specific integrins (Caswell and Norman, 2006). A third member of the Rab11 family, known as Rab25 or Rab11c, has been found in epithelial cells (Goldenring et al., 1993). Overexpression of this Rab protein correlates with increased invasiveness and aggressiveness of some ovarian and breast cancers, presenting a possible role for Rab25 in epithelial cell migration (Cheng et al., 2004), however the situation remains controversial as Rab25 has also been reported to act as a tumour suppressor in some cases (Cheng et al., 2006, 2010).

The importance of the trafficking of newly synthesised cargo has come to light in recent years, particularly following the finding that the Golgi reorientates between the nucleus and the leading edge in migrating cells of some cell types (Gotlieb et al., 1981; Yadav et al., 2009). Disrupting post-Golgi secretion with Brefeldin A, which prevents transport of newly synthesised protein from the ER, inhibits the formation of a polarised phenotype and cell migration in Swiss 3T3 fibroblasts (Bershadsky and Futerman, 1994). However, non-specific effects caused by this inhibitor mean it is not ideal to use to directly study post-Golgi transport. PKD is a protein found to be necessary for fission of cargo from the Golgi (Liljedahl et al., 2001), this therefore provides a more specific target for study of transport from this organelle. Abrogation of the pathway by use of dominant-negative PKD in Swiss 3T3 fibroblasts showed decreased migration and suppression of lamellipodia formation, highlighting the necessity of this pathway in cell migration (Prigozhina and Waterman-Storer, 2004).

1.5 Integrins and their trafficking

Integrins are adhesion molecules that make up a family of transmembrane proteins that serve to connect cells to the ECM or other cells (Margadant et al., 2011). In this way they are important mediators of signalling from the extracellular environment to intracellular regions and vice versa. In mammals there are 18 integrin α subunits and eight integrin β subunits that are arranged into 24 different heterodimers (Hynes, 2002). Roles for integrins have been found in cell migration, proliferation and apoptosis amongst others and deregulation of integrins has been observed in many cancers (Caswell and Norman, 2006). The polarisation of integrins is vital to enable directionality of migration pointing to a key role for vesicle trafficking in the regulation of integrins during this process (Jones et al., 2006). Integrin heterodimers typically have two conformations: a bent (or 'inactive') conformation and an open (or 'active') conformation (Bridgewater et al., 2012). Factors that influence whether integrins are in the active or inactive conformation include the binding of extracellular ligands such as fibronectin and collagen in a process known as 'outside-in' signalling (Humphries et al., 2006), or the influence of intracellular factors such as the binding of the proteins talin or kindlins in a process known as 'inside-out' signalling (Legate et al., 2009).

The trafficking of integrins greatly influences their function in cells. Integrins in adhesion complexes have been reported to be internalised by both clathrin-dependent and clathrin-independent routes (Caswell et al., 2009). One integrin, αvβ5, has been seen to bind directly to clathrin and therefore its internalisation by clathrin-mediated endocytosis is proposed (De Deyne et al., 1998). β integrin subunits contain NxxY motifs in their cytoplasmic tails and so are predicted to bind clathrin adaptor proteins for entry into the cell. The alternative adaptors Numb and Dab2 have been proposed to aid entry of certain integrins via clathrin-mediated endocytosis and indeed Numb has been shown to bind β1 and β3 integrins, with Dab2 known to associate and aid internalisation of β1 (Calderwood et al., 2003). Dab2 and AP2 have also been shown to localise at or near to sites of focal adhesions at the time of their disassembly (Margadant et al., 2011). A cave-

olar internalisation route has been proposed for some integrins. $\alpha 2\beta 1$ has been shown to internalise by a route dependent on caveolin which may also involve interaction of the $\beta 1$ tail with PKC (Upla et al., 2004). Other integrins have been shown to colocalise to caveolae in certain cell types and some integrins, such as $\alpha v\beta 3$ and $\alpha 5\beta 1$, are also reported to enter cells by more than one endocytic route (Caswell et al., 2009). Evidence against a direct role of integrin endocytosis as a method of focal adhesion disassembly also exists (Gu et al., 2011; Fletcher et al., 2012).

Once internalised, integrins are trafficked in a Rab5-dependent manner to early endosomes (Caswell et al., 2009). The vast majority of integrins are quickly recycled; however some do traffic to the lysosome for degradation (Margadant et al., 2011). Integrins not destined for degradation are recycled either by the Rab4-dependent short-loop recycling pathway or via the PNRC in a Rab11- and/or Arf6-dependent manner in a long-loop recycling pathway (Jones et al., 2006). The Rab4-dependent recycling of $\alpha v\beta 3$ integrin back to the cell surface requires direct interaction with PKD1 to enable correct polarisation for cell migration and abrogation of this contact decreases persistency and directionality of migrating fibroblasts (Woods et al., 2004; White et al., 2007). The activation of Rab4-dependent short-loop recycling appears to be mediated by growth factor signalling meaning that signalling from the extracellular environment plays a large role in the control of recycling and hence, function of integrins. There is also evidence that the Rab11-dependent long-loop recycling process requires certain signalling pathways to confer selectivity (Caswell and Norman, 2006). Particular roles for PKCε, Akt and Arf6 have been have been found in the regulation of integrin traffic via the Rab11-dependent pathway (Ivaska et al., 2002; Powelka et al., 2004; Roberts et al., 2004). The recycling of $\beta 1$ integrins by this pathway has been found to involve the phosphorylation of an Arf6GAP which then physically associates with $\beta 1$ integrins to promote their recycling from the PNRC (Li et al., 2005).

Polarisation of integrin internalisation and recycling has been proposed to occur during migration. Much evidence exists to show that focal adhesion disassembly, and there-

fore presumably integrin internalisation, occurs at the rear of migrating cells (Bretscher and Aguado-Velasco, 1998; Laukaitis et al., 2001; Webb et al., 2004; Broussard et al., 2008). This would likely allow retraction of the cell rear and trafficking of integrins to the leading edge for use in more adhesion complexes. However, in some cases it has been observed that rather than internalise the integrins are left bound to the substratum (Regen and Horwitz, 1992). Some evidence also suggests integrin endocytosis actually occurs at the front of cells in the region behind the lamellipodia and evidence for this includes visualisation of polarised endocytosis in this region and localisation of sorting endosomes towards the leading edge (Rappoport and Simon, 2003; Caswell et al., 2009). Although this is not direct evidence for polarised endocytosis of integrins at the leading edge visualisation of one particular integrin, $\alpha 5$, has mapped its internalisation to this region (Laukaitis et al., 2001). Perhaps integrin endocytosis can take place at different regions of the cell depending on cell type and migratory system. Recycling via the PNRC appears to take place at the rear of the cell where it then travels back to the cell front along a similar route to newly synthesised material from the Golgi (Laukaitis et al., 2001; Schmoranzer et al., 2003). Numerous studies have shown that inhibiting integrin recycling blocks cell migration providing evidence that their trafficking is involved in the migratory process (Powelka et al., 2004; Yoon et al., 2005; Fan et al., 2004; Caswell and Norman, 2006). These recycling processes most likely contribute to the polarisation of integrins in migrating cells; indeed disruption of recycling by inhibition of Rab4 or PKD1 prevents localisation of $\alpha v \beta 3$ integrin to the leading edge of fibroblasts (Woods et al., 2004). This requirement for PKD1 suggests that vesicles involved in integrin recycling may be regulated in a similar way to vesicles derived from the Golgi, since this process also requires PKD1 (Caswell and Norman, 2006).

As mentioned previously integrins are the link between the ECM and the actin cytoskeleton and therefore are the regions of traction force generation during cell migration. Another role for integrins during migration has emerged in the control of Rho signalling (Caswell et al., 2009). It has been shown that high levels of $\alpha v \beta 3$ integrin and low $\alpha 5 \beta 1$

supports active Rac at the front of cells leading to a stable lamellipodium and persistent directional migration (Danen et al., 2005; White et al., 2007). Switching the expression of these two integrins increases Rho signalling and leads to random migration. In cells such as NIH3T3 fibroblasts that express both these integrin heterodimers differences in their trafficking is used to control the balance of Rho and Rac during migration (White et al., 2007).

A role for integrins in the trafficking of RTKs has become apparent. It was discovered that $\alpha v\beta 3$ integrin inhibition could lead to a decrease in cell migration and angiogenesis *in vitro* and so this integrin was targeted for anti-cancer therapies (Nisato et al., 2003; Maubant et al., 2006). Unfortunately the inhibitors appeared to have little effect in more physiological studies and it was subsequently shown that inhibiting $\alpha v\beta 3$ was stimulating a Rab4-dependet recycling route for the VEGFR2 which led to its trafficking back to the plasma membrane, whereas under non-inhibitory conditions this receptor was usually degraded in a ligand-dependent manner (Reynolds et al., 2009). Another effect inhibiting this particular integrin has is to recruit Rab-coupling protein (RCP) to the cytoplasmic tail of integrin $\beta 1$. This interaction in turn leads to association of RCP with EGFR promoting the recycling of both $\alpha 5\beta 1$ intergin and EGFR to the plasma membrane, increasing EGFR signalling to Akt, thereby increasing tumour cell invasiveness (Caswell and Norman, 2008). We can therefore see that certain integrins play an important role in preventing tumour cell invasion by preventing trafficking processes that would drive invasion.

1.6 The EGFR family

EGFR is of particular importance to this report as all chemotaxis research undertaken in this project has utilised EGF as the chemoattractant. The EGFR family of tyrosine kinase receptors has roles in many vital and varied processes within the cell. These processes range from cell differentiation and proliferation to the regulation of metabolism

and cell motility (Arkhipov et al., 2013). The EGF receptor family of tyrosine kinase receptors consists of four members: EGFR (also known as ErbB1), ErbB2 (also known as Her2/Neu), ErbB3 and ErbB4. EGF was discovered when it was shown to be a regulator of mouse eyelid opening and to cause growth of cultured human cells (Cohen, 1997, 2004). Previous to this EGF had already been shown to be important for breast development, and subsequent studies showed that EGFR mutations led to impaired breast development in mice (Cohen, 1997). Research following these studies led to the discovery of the first receptor of the family, EGFR. Structurally, the EGFR family of receptors consist of a ligand binding extracellular region (containing four distinct domains), a single transmembrane region and a C-terminal region containing the kinase activity of the receptor and a long regulatory tail region (Arkhipov et al., 2013).

The EGFR family functional unit is as a dimer, which can be either heterodimeric or homodimeric (Lemmon et al., 1997; Schlessinger, 2002). ErbB2 is the preferred partner for all other family members as it contains a larger interaction loop than the other members which readily enables dimerisation (Eccles, 2011). Including splice varients, there are 13 known ligands for members of the EGFR family, of which EGF and TGFα are the main ligands that bind EGFR (Harris et al., 2004; Eccles, 2011).

Following ligand binding to an EGFR family member conformational changes occur to expose interaction regions of the receptor. These changes are sufficient to allow receptor dimerisation to occur to form either a homodimer or a heterodimer (Schlessinger, 2002). Dimerisation allows the kinase domain of one monomer to be stabilised by the cytoplasmic region of the other monomer, enabling the kinase domain to achieve an active conformation. The active kinase domain is subsequently able to access tyrosine residues on the other monomer resulting in receptor transphosphorylation (Riese et al., 2007; Foley et al., 2010). These phosphorylation sites serve to create docking regions for the binding of proteins containing either Src-homology 2 (SH2) or phospho-tyrosine binding (PTB) domains which includes many proteins involved in both signalling and receptor internalisation (Normanno et al., 2006). The binding of particular proteins and

the affinity to which they bind is influenced by which particular receptors are present in the dimer (Schulze et al., 2005). The signalling cascade following receptor activation can lead to activation of a multitude of proteins including Akt, extracellular signal-regulated kinase (ERK) and Janus kinase/signal transducers and activators of transcription (JAK/STATs) (Figure 1.7 shows some of the signalling pathways EGFR is known to act through). The receptor is therefore linked to many vital cellular processes such as cell survival, proliferation, differentiation and migration (Yarden et al., 2001).

1.6.1 EGFR in breast cancer

All four members of the EGFR family have been reported to be overexpressed to some degree in breast cancer (Eccles, 2011). The term 'triple-negative' is used to describe breast tumours lacking the oestrogen receptorα, the progesterone receptor and ErbB2 (Korsching et al., 2008). These tumours are generally associated with a high degree of metastasis and poor prognosis, and a high level of them (50-70%) are found to be EGFR expressing (Burness et al., 2010). Recent transcriptome analysis has found oestrogen receptorα-negative breast cancers to contain increased levels of EGFR family ligands including TGFα and NRG2β as well as proteins necessary for ligand maturation, when compared to oestrogen receptorα-positive breast cancers (Foley et al., 2010). This observation points to a potential role for autocrine EGFR signalling in the potency of these tumours. EGFR expression has also been shown to be higher in patients where distant and nodal metastases are found (Foley et al., 2010).

For tumours to metastasise they first need to stimulate the growth of blood vessels by angiogenesis. The most potent pro-angiogenic factor is VEGF. One mechanism for the production of this growth factor is via EGFR/ErbB2 signalling resulting in Akt signalling and subsequently upregulation of VEGF (Eccles, 2011). In this way overexpression/overactivation of EGFR can be seen to promote angiogenesis leading to increased tumour survival.

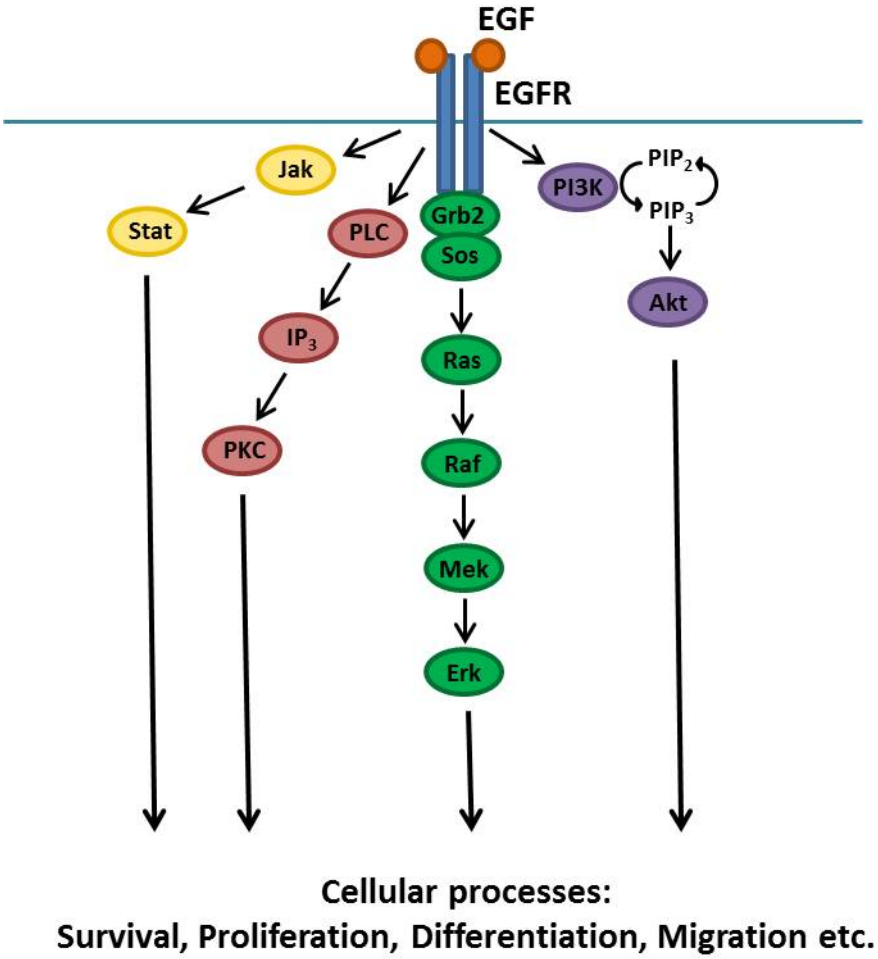

Figure 1.7: Ligand binding to EGFR can activate a multitude of signalling pathways leading to a number of different cellular responses including cell migration. Pathways here are simplified and in reality include cross talk between pathways, positive and negative feedback and other proteins not included in this diagram.

EGFR and ErbB2 are seen as key players in the process of tumour cell migration. Identification of disseminated tumour cells from the blood and bone marrow are an indication of poor prognosis; a high proportion of the time these cells also express EGFR/ErbB2, even if the primary tumour does not (Braun et al., 2001; Eccles, 2011). This observation points to a major role for the EGFR signalling pathway in the metastatic process. The bone presents a major site for breast cancer metastases to appear. A positive feedback loop has been described whereby breast tumour cells promote bone destruction and this in turn aids tumour growth (Guise et al., 1996). EGFR signalling has been implicated in this cycle; breast tumour cells that reach the bone release EGF which acts on EGFR-expressing osteoclasts acting to disrupt the balance of RANKL and osteoprotegerin (which regulate osteoclast activity; Gilmore et al. 2008; Foley et al. 2010). This disruption enhances osteoclast-mediated destruction of bone which, in turn, leads to a release of growth factors that stimulate tumour growth and invasion.

1.6.2 Therapeutic targeting of EGFR

Multiple approaches have been taken in the targeting of EGFR family members as a treatment for breast cancer; these include antibody-based therapies, gene therapy, RNAi and even vaccines (Eccles, 2011). Many of the therapeutics in current clinical trials are used to target tumours with ErbB2 amplification by preventing receptor dimerisation – trastuzumab and pertuzumab fall under this category (Baselga and Swain, 2010; Eccles, 2011). Antibodies directed specifically to EGFR include cetuximab and panitumumab, but neither has yet been shown to be an ideal treatment against EGFR-positive breast cancer (Burness et al., 2010). Inhibitors of the kinase activity of EGFRs have also been trialled with varying success. Selective inhibitors of EGFR kinase activity, erlotinib and gefitinib, have little effect when used alone, but are currently being trialled in combination with other cytotoxic agents (Eccles, 2011). Neratinib, a compound shown to bind and prevent the kinase activity of EGFR, ErbB2 and ErbB3, is showing some positive results in trials, alone and in combination with other drugs (Colombo et al., 2010). As

well as therapies targeted directly to the receptors, components of the downstream signalling pathways also represent targets for anti-cancer therapies for tumours using the signalling pathways for survival and growth (Eccles, 2011).

1.6.3 EGFR internalisation and trafficking

There is conflicting evidence over which route of internalisation EGFR takes and what its fate is following internalisation. In particular, there is evidence for both clathrin-dependent and clathrin-independent routes of internalisation which are in dispute by many groups (Sorkina et al., 2002; Motley et al., 2003; Hinrichsen et al., 2003; Huang et al., 2004; Sigismund et al., 2005; Johannessen et al., 2006; Orlichenko et al., 2006; Rappoport and Simon, 2009). Using RNAi Huang et al. showed that knocking down CHC reduced the amount of EGFR endocytosis to 25% of that of control cells (Huang et al., 2004). Two papers previously published conflicted with these new results by showing that knocking-down components of AP2 has very little effect on EGFR endocytosis (Motley et al., 2003; Hinrichsen et al., 2003); this therefore points to a clathrin-independent pathway for EGFR entry, or at least a clathrin-dependent AP2-independent pathway. However, as discussed earlier, the ligand binding stage of this internalisation assay was conducted at 4°C and likely does not represent the physiological situation (Motley et al., 2003; Keyel et al., 2006; Huang et al., 2004; Boucrot et al., 2010). In 2009 Rappoport and Simon demonstrated the necessity of clathrin and AP2 in EGFR endocytosis (Rappoport and Simon, 2009). Firstly, they imaged plasma membrane localised EGFR in conjunction with fluorescently labelled clathrin or caveolin1 to show a much higher colocalisation of EGFR with clathrin than with cavelolin1, they also showed that EGFR was recruited to pre-formed clathrin spots rather than stimulating the formation of new clathrin clusters. Secondly, they depleted AP2 using RNAi and found a decrease in the amount of EGFR internalisation taking place (Rappoport and Simon, 2009). Like the Huang and Boucrot studies, internalisation assays in this paper were conducted at a more physiological 37°C (Huang et al., 2004; Rappoport and Simon, 2009; Boucrot

et al., 2010).

More conflicting evidence comes from work by Orlichenko et al. and Sigismund et al. (Sigismund et al., 2005; Orlichenko et al., 2006; Sigismund et al., 2008). Orlichenko and colleagues show evidence that EGFR signalling is responsible for the phosphorylation of caveolin1 and leads to an increase in the number of caveolae present on the cell surface (Orlichenko et al., 2006). However, viewing these results in context with other work led the authors to postulate a situation where the EGFR is sequestered in caveolae until EGF stimulation where it becomes exchanged into clathrin-coated pits (Orlichenko et al., 2006). In 2005 Sigismund et al. concluded that at low concentrations of EGF, EGFR is exclusively internalised by clathrin-mediated endocytosis whereas at higher (but still physiologically relevant) concentrations a raft-dependent route, possibly caveolae, is involved in the receptor's internalisation (Sigismund et al., 2005). They state that at the higher concentrations ubiquitination of the receptor becomes more substantial and may be the switch between the two internalisation routes. In 2008 the group furthered these results by suggesting that clathrin-mediated endocytosis of the EGFR leads solely to its recycling back to the cell surface, and hence sustains the signalling capabilities of the cell (Sigismund et al., 2008). They propose that this sustained signalling due to clathrin-mediated endocytosis is pivotal to some highly important cellular processes such as DNA synthesis. The clathrin-independent pathway of internalisation was shown to lead to degradation of the receptor instead of recycling and was also shown at this point to not be caveolae-dependent, as was thought by a number of groups citing this paper (Sigismund et al., 2008).

The classic view of the role of internalisation of growth factor receptors was that it led to attenuation of signalling via degradation of the receptor. However, a growing body of evidence says that EGFR continues to signal for some time from endosomes (Miaczynska et al., 2004; von Zastrow and Sorkin, 2007; Murphy et al., 2009). There is also evidence that particular signalling pathways can be activated by EGFR signalling from endosomes, making this type of signalling distinct from that which occurs at the cell

surface (von Zastrow and Sorkin, 2007). Early studies showed that particular components of EGFR signalling cascades, such as Grb2, Shc and Sos, could be found located to endosomes following EGFR activation by EGF (Di Guglielmo et al., 1994). Another group showed that using a dominant-negative form of dynamin to inhibit endocytosis of the receptor led to decreased signalling of the MAPK signalling proteins ERK and p85 (a subunit of PI3K), pointing to the necessity of internalisation for certain signalling pathways to occur (Vieira et al., 1996).

One role for endosomal signalling might be to provide some temporal regulation of signalling, for example TGFα quickly dissociates from EGFR once the complex has reached early endosomes due to high sensitivity to changes in pH, whereas EGF does not dissociate so readily and can therefore increase the duration of signalling (French et al., 1995). Another role for such signalling is likely to be in spatially arranging molecules such that particular signalling cascades can be driven while unwanted events are prevented (Miaczynska et al., 2004). A more recent study took advantage of two systems, one to specifically stimulate plasma membrane EGFR signalling and one to specifically stimulate endosomal EGFR signalling (Wu et al., 2012). Their results showed that EGFR signalling from the plasma membrane led to a gradual and lasting activation of ERK in the nucleus, whereas endosomal EGFR signalling led to fast and short-lived ERK activation (Wu et al., 2012). The consequence of this was phosphorylation of the transcription factor c-fos only following plasma membrane activation of EGFR but not following endosomal EGFR activation. Another recent study conflicts with those that have shown roles for endosomal signalling of EGFR (Sousa et al., 2012). By using dynamin-deficient fibroblasts they were able to show that plasma membrane localised active EGFR was able to stimulate normal MAPK activation as well as increased phosphorylation of Shc and sustained Akt activation (Sousa et al., 2012).

A role for late endosomes in EGFR signalling has also become apparent. Taub and colleagues were able to manipulate cells so as to relocalise late endosomes from their usual juxtanuclear location to two different localisations: the periphery of the cell or clus-

tered very close to the nucleus (Taub et al., 2007). The first manipulation didn't affect transport of the activated receptor to late endosomes but did slow down the degradation process and in this way promoted prolonged activation of ERK and another MAPK, p38 (Taub et al., 2007). The manipulation that led to late endosomes clustered close to the nucleus resulted in slow transport of active EGFR from early endosomes to late endosomes causing prolonged activation of the receptor, however the delayed traffic appeared to decrease ERK activation (Taub et al., 2007). Taken together these results show that the spatial regulation of receptor location is of importance to signalling and that late endosomes, as well as early, also have a role to play in EGFR signalling.

The studies mentioned above use a wide variety of experimental procedure and investigate EGFR internalisation in a number of different cell types. Some of the differences and conflicting evidence could therefore be said to be cell-type specific or dependent on the particular experimental procedures used.

1.7 Chemotaxis assays

There are a wide variety of assays to aid the study of chemotaxis and cell migration. The choice of assay depends on the questions being asked and the how the results are to be collected. Described here are a few of the common chemotaxis assays as well as their advantages and disadvantages. A diagram of the set up of three of the assays can be seen in Figure 1.8.

1.7.1 Transwell assay

Transwell assays (or Boyden chambers) involve seeding cells into an insert with a porous membrane separating this insert from the lower compartment (Boyden, 1962; Toetsch et al., 2009). The lower compartment contains a chemoattractant to stimulate migration of the cells through the pores in the membrane. After the assay cells can be stained and those which have migrated can be quantified. Disadvantages of the assay include that

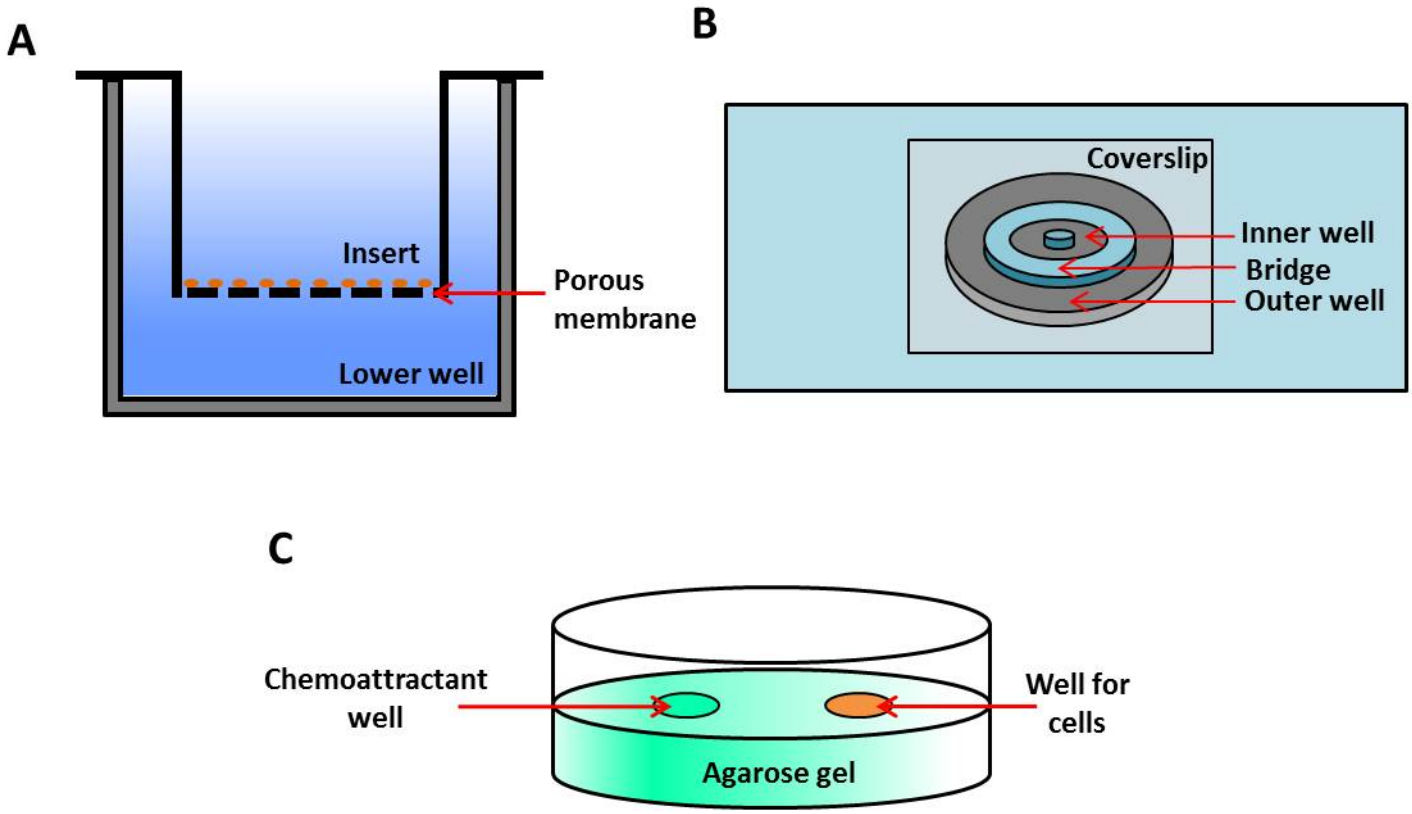

Figure 1.8: A simple diagram of some common chemotaxis assays. A) shows the set-up of a Transwell assay, B) a Dunn chamber and C) an under-agarose assay.

it cannot be imaged as migration is occurring, therefore is only an endpoint assay, and the chemoattractant gradient cannot be sustained for more than a few hours (Pouliot et al., 2013).

1.7.2 Dunn chamber

Dunn chambers were developed as a better version of the early Zigmond chamber (Zicha et al., 1991; Zigmond, 1977). They involve a slide with two precise circular chambers etched into it, separated by a bridge; cells go in one chamber and chemoattractant in the other (Pujic et al., 2009). Once a coverslip is placed on top the creation of a shallow chemoattractant gradient between the chambers occurs. Cells migrating over the bridge can be visualised by microscopy. As with the Transwell assay, the Dunn chamber is not able to maintain its gradient indefinitely (Toetsch et al., 2009). The small dimensions of the assay and requirement for the manual application of adhesive mean it is also not particularly user friendly.

1.7.3 Under-agarose assay

This assay involves punching wells into an agarose gel to which cells and chemoattractant can be added (Heit and Kubes, 2003). A gradient diffuses from the chemoattractant well and cells migrate in this direction. After several hours of migration the agarose can be removed allowing for visualisation of the migrated cells by microscopy. Adaptations also allow live cell imaging during the assay (Heit and Kubes, 2003). This assay has the flexibility of being able to study multiple chemoattractants at once (Khademhosseini, 2008).

1.7.4 Microfluidic chambers

Assays based on microfluidics allow precise control of fluids and therefore stable gradient production (Whitesides, 2006). Usually, cells are first injected into the chamber before the gradient is generated and then migration examined (Pujic et al., 2009). Advantages

of this system are the precise and rapid control of the gradient, allowing changes during experimentation. One disadvantage of these systems is the high sheer stress generated on the cells, therefore making the system unusable for some cell types (Pujic et al., 2009).

1.7.5 3D migration assays

3D assays are used to bridge the gap between migration and invasion studies, and can be used to analyse how cells react to chemoattractant in more physiological environments. There are a wide variety of 3D migration assays available. In some respects the Transwell assay can be considered a 3D migration assay as it can be modified to introduce a 3D matrix of ECM components that the cells have to crawl through while migrating along the gradient (Brekhman and Neufeld, 2009). At the other end of the spectrum of 3D migration assays there exist assays such as organotypic assays where ECM components and fibroblasts are used to create a more physiologically relevant environment, media below the matrix can contain a chemoattractant and fluorescence microscopy can allow imaging of cells migrating through the matrix (Dawson et al., 2011; Nobis et al., 2013).

1.8 TIRF microscopy

When imaging the plasma membrane microscopic techniques such as epi-flourescence and confocal microscopy are not ideal, as fluorescence originating from intracellular regions can obscure visualisation of the plasma membrane. By exciting only the adherent plasma membrane of cells TIRF microscopy (also known as evanescent wave or evanescent field microscopy) is able to overcome this.

In epi-fluorescence the incident beam hits the colver-slip-sample interface straight on, meaning that all fluorophores within the sample are excited to the same extent (Mattheyses et al., 2010). Confocal microscopy benefits from the use of a highly focussed laser combined with a small pinhole just prior to the detector which enables optical sectioning

of a sample (Amos and White, 2003; Pitkeathly et al., 2012). However, these sections are approximately 10 times the size of those achieved by TIRF and due to the incident light propagating through the whole sample images are still contaminated with out of focus fluorescence.

In TIRF the incident beam hits this interface at an angle greater than the 'critical angle', as defined by Snell's law (Mattheyses et al., 2010; Pitkeathly et al., 2012). By altering the incident angle in this way TIRF ensures that the excitation light is reflected back into the cover-slip (rather than passing straight through). As this occurs, some incident energy creates a standing wave called the evanescent field, which forms the TIRF excitation field (Figure 1.9; Axelrod 1981; Mattheyses et al. 2010). The evanescent field decays exponentially with distance from the interface, creating an imaging depth of approximately 60-100 nm. Since no light penetrates deeper into the cell only fluorophores at or near to the plasma membrane are illuminated. Consequently, images from TIRF have high signal-to-noise ratio, adding to the advantages of using TIRF as the microscopic method of choice when imaging the plasma membrane (Axelrod, 1981).

The ability of TIRF to excite fluorophores within 100 nm of the plasma membrane make it highly valuable for imaging the dynamics of molecules at or near to the cell surface. Although confocal microscopy can reduce the background fluorescence relative to epi-fluorescence microscopy, TIRF benefits from a smaller and more specific region of illumination, thereby providing clearer information about fluorophores associated with the plasma membrane.

1.8.1 Possible issues with TIRF microscopy

Due to the nature of TIRF the cell type being imaged must be adherent. One consideration to keep in mind is that the refractive index of the cells being imaged must be less than that of the numerical aperture of the objective lens (not a problem for most cell lines; Mattheyses et al. 2010).

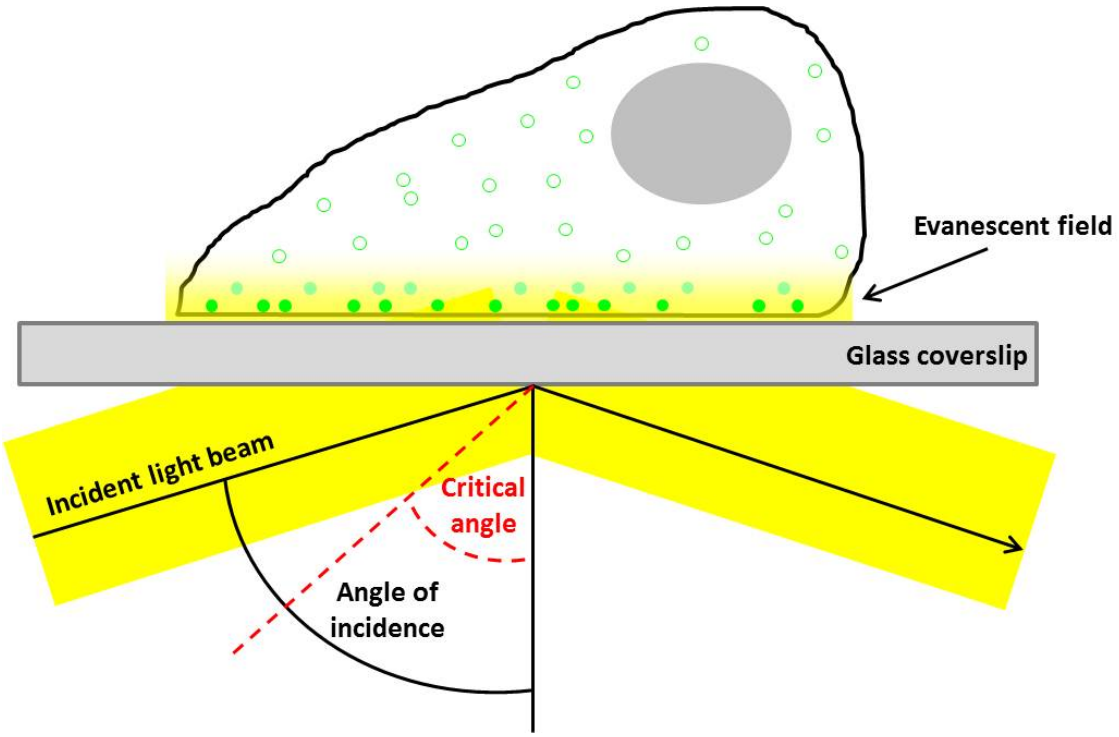

Figure 1.9: A diagram to demonstrate TIRF microscope. If the illumination light hits the coverslip-sample interface at an angle greater than the 'critical angle' TIRF will occur and an evanescent field will be created which decays exponentially with distance from the coverslip.

Ensuring that the incident angle is higher than the critical angle is also a major problem encountered by TIRF users. If light propagates into the sample the image appears similar to an epi-fluorescence image rather than TIRF, wherein background fluorescence will contaminate the image (Mattheyses et al., 2010). As a general rule if the image can be focused in more than one 'z' plane then the incident angle is too low and must be increased. A related problem is that the TIRF lasers can become misaligned, causing a field of view which is half in and half out of TIRF, or the complete inability to obtain TIRF.

As with all forms of microscopy photobleaching can be a problem. Due to the small 'z' area being excited photobleaching will occur only to those proteins which remain within the excitation field (plasma membrane and plasma membrane-associated proteins). Soluble proteins may be found to photobleach less as they move in and out of the TIRF excitation field (Mattheyses et al., 2010). This uneven photobleaching found in TIRF must be considered, so as to not draw incorrect conclusions from imaging (eg. in cases where photobleaching can be mistaken for endocytosis).

Chapter 2

Materials and Methods

2.1 Cell Culture

MDA-MB-231 cells (HPA) were incubated at 37°C in 5% (v/v) CO_2. Cells were grown in Dulbecco modified Eagle medium (DMEM; Lonza) supplemented with 10% fetal calf serum (FCS; Biosera) and 1% Pen/Strep (Lonza). PDAC cells (Kurt Anderson, The Beatson Institute, Glasgow) were maintained in the same conditions as MDA-MB-231, with the addition of G418 antibiotic to the media for the stably transfected cell lines (see below).

2.2 Transfection

For cDNA transfection 5 x 10^5 cells were plated in 35 mm dishes 24 hours prior to transfection to give approximately 80% confluence. For each dish transfection mixes of 4 μg cDNA with 250 μl of serum free media (SFM; Lonza) and 10 μl of lipofectamine 2000 (LF2000; Invitrogen) with 250 μl of SFM were made up. After waiting 5 minutes the LF2000-containing mix was added to the mix containing cDNA followed by a 20 minute incubation period. The mixture was then added dropwise to cells and the cells were incubated for 3 hours before the media was replaced. Assays with these cells were performed 24 or 48 hours post transfection (depending on the cDNA construct and

assay).

For siRNA transfections 2 x 10^5 cells were plated in 35 mm dishes 24 hours prior to transfection. For each dish transfection mixes of 3 μl of siRNA with 200 μl SFM and 3 μl DharmaFECT1 transfection reagent (Invitrogen) with 200 μl SFM were made up. After waiting 5 minutes the DharmaFECT1-containing mix was added to the mix containing siRNA followed by a 20 minute incubation period. The mixture was then added dropwise to cells and the cells. Assays with these cells were performed 72 hours post transfection.

2.3 Plasmid constructs

Table 2.1 provides details of researchers from whom cDNA plasmid constructs were obtained.

Table 2.1

Construct	Source
β3-integrin-GFP	Prof. Jonathan Jones, Northwestern University Medical School, Chicago, IL, USA.
Caveolin1-GFP	Prof. Ari Helenus, Swiss Federal Institute of Technology, Zurich, Switzerland.
Caveolin1-mRFP	Prof. Ari Helenus, Swiss Federal Institute of Technology, Zurich, Switzerland.
Clathrin-dsRed	Prof. Thomas Kirchhausen, Harvard Medical School, Boston, MA, USA.
EGFR-GFP	Dr. Alexander Sorkin, University of Pittsburgh, PA, USA.
GFP-clathrin	Dr. Alexandre Benmerah. Institure Cochin, Paris, France.
NPY-mRFP	Dr. Jyoti Jaiswal, George Washington University, Washington, DC, USA.
Rab11a-mCherry	Prof. Marino Zerial, Max Planck Institute of Molecular Cell Biology and Genetics, Dresden, Spain.
mRFP-paxillin	Dr. Maddy Parsons, King's College London, London, UK.
PKD(K618N)-GFP	Prof, Vivek Malhotra, The Centre for Genomic Regulation, Barcelona, Spain.

2.4 siRNA sequences

The non-silencing control (NSC) siRNA was a ON-TARGETplus Non-targeting pool designed for use in mouse, rat or human cell lines. The α-adaptin siRNA was custom made with target sequence 5'-AAGAGCAUGUGCACGCUGGCCA-3' as used in previous studies (Motley et al., 2003; Huang et al., 2004; Rappoport and Simon, 2009). The caveolin1 siRNA was a SMARTpool ON TARGETplus Human Cav1 siRNA from Dharmacon containing a pool of 4 siRNAs targeted to human cavolin1 (Auciello et al., 2013).

2.5 Bacterial transformation

If transforming from a previous cDNA preparation 1 μg of DNA was used, if dissolving DNA from filter paper, as little water as possible was added to dissolve the DNA off the paper and 3 μl of this was used. The DNA was added to 50 μl of MAX Efficiency DH5α Competent Cells (Invitrogen) before being incubated for 30 minutes on ice. The competent cells were then heat shocked to 42°C for 45 seconds in a water bath before being put back on ice for 2 minutes. 500 μl of Luria Broth (LB; Sigma; Supplementary methods 1) was added to the competent cells and they were then incubated with shaking for 1 hour at 37°C. Following incubating 150 μl was pipetted and spread onto an LB agar plate (Supplementary methods 2) containing antibiotic (kanamycin or ampicillin, depending on the resistance present in the particular plasmid being prepped). Plates were inverted and incubated overnight at 37°C. The following day two single colonies were picked using a pipette tip and placed in a 15 ml Falcon tube containing 2 ml LB plus 2 μl kanamycin or ampicillin. These were incubated with shaking at 37°C for 8 hours. Following this incubation 100 μl was taken from the Falcon tube and added to 100 ml of LB plus 100 μl of kanamycin and ampicillin. These were left shaking overnight at 37°C. The LB-bacteria liquid was split into two 50 ml Falcon tubes and centrifuged at 5000 rpm at 4°C for 15 minutes. The supernatant was subsequently discarded and

the Qiagen Plasmid Maxi Kit (Qiagen) protocol followed for DNA purification. Purified DNA was dissolved in 1 ml ultrapure water and the concentration calculated using a spectrophotometer.

2.6 Creating stably transfected cell lines

To first establish a concentration of G418 that kills PDAC cells after by one week post plating cells were plated into a 24 well plate. After 24 hours, when the cells had achieved confluency, media containing differing concentrations of G418 (Sigma) was added to duplicate wells. The concentrations ranged from 0-1.4 mg/ml. Media was changed and cells were observed every 2-3 days in order to find the lowest concentration that kills all the cells after one week of G418 exposure. In this case the optimal concentration was found to be 0.8 mg/ml. For making the stable cells lines cells were transfected with the desired plasmid containing G418 resistance and the following day the media was changed to that containing 0.8 mg/ml G418. Cells were cultured in the G418-containing media for the whole course of experiments utilising them.

2.7 Western blotting

Western blot analysis was used to quantify the knockdown of siRNA constructs. Briefly, cells were lysed in 1% Triton X-100 (Sigma) in phosphate-buffered saline (PBS; Lonza) with protease inhibitors (Roche) and 3X sample buffer (Supplementary methods 3) was added to a 2:1 ratio. Proteins were separated by SDS PAGE on a 12.5% acrylamide resolving gel with a 4% acrylamide stacking gel (Supplementary methods 4), and then transferred from the gel onto Immobilon-FL membrane (see Supplementary methods 5-8 for more information on solutions used). The membrane was blotted with primary antibody overnight at 4°C and then with secondary antibody for 2 hours at room temperature. Primary antibodies used were polyclonal rabbit anti-α-adaptin (Invitrogen), polyclonal rabbit anti-caveolin1 (BD Biosciences) and monoclonal mouse anti-tubulin

(Sigma). Secondary antibodies used were anti-rabbit IRDye 800 and anti-mouse IRDye 680 (Li-Cor) for use in Odyssey. Quantification of knockdowns was done relative to control tubulin using Odyssey software.

2.8 Agarose spot assay

Agarose spot assays were utilised to investigate chemotactic migration of the MDA-MB-231 cells and PDAC cells (Wiggins and Rappoport, 2010). A 0.5% solution agarose was made using low melting point agarose (Invitrogen) in PBS. The solution was heated to boiling point, mixed thoroughly and allowed to cool to 45°C. Microcentrifuge tubes were made up containing 10 μl PBS (for control) or 7 μl PBS + 3 μl EGF stock (1 mg/ml in PBS; Bachem), to which 90 μl of the agarose solution was added. These were used to plate 10 μl spots in 35 mm glass-bottomed dishes (MatTek Corporation). Dishes were cooled to 4°C in a cold room for 5 minutes. After cooling 4 x 10^5 cells were plated in each dish (same number of cells used for both MDA-MB-231 assays and PCDAC cell assays). Dishes were incubated for 4 hours to allow cells to adhere before changing to cell imaging media (see Section 2.13) with low (0.1%) serum content. Overnight time-lapse imaging began directly after media change. TIRF imaging of migrating cells began 1 hour after media change to allow cells time to begin migrating.

For assays with EGF-containing media, the low serum media given after 4 hours contained EGF at a concentration of 100 ng/ml.

For the Dynasore treatment assays the low serum media given after 4 hours contained Dynasore (Sigma; 80 mM in dimethy sulphoxide (DMSO)) diluted to a final concentration of 80 μM. The control group was given media containing DMSO (Sigma) to the equivalent volume as the Dynasore group.

2.9 Transwell assays

Chemotaxis assays were carried out using 6 well Transwell plates (Corning Life Sciences) containing 24 mm diameter semi-permeable membrane inserts with 8 μm pores. 2.6 ml of media was added to each well. In wells receiving EGF treatment 1 μg/ml EGF was also added. 5 x 10^5 cells were plated into each insert and the volume made up to 1.5 ml with media. The Dynasore group was treated with 80 μM in the media for both the lower well and the insert. After 5 hours of incubation inserts were removed from the plates, washed twice with PBS, and then fixed for 5 minutes in 4% Paraformaldehyde (PFA; Electron Microscopy Sciences). After fixing, membranes were mounted into slides using Vecta shield with DAPI (Vector Laboratories) to stain cell nuclei. Imaging was done using a Nikon TE300 Inverted Epi-fluorescence microscope with a 40 x oil objective lens (CFI Plan Apo 1.3 NA, Nikon).

2.10 Wound healing assay

For assessment of focal adhesion disassembly during wound healing cells were transfected with siRNA 72 hours prior to wounding and cDNA 48 hours prior to wounding. 24 hours before wounding cells were replated into 35 mm glass-bottomed dishes to achieve a confluent monolayer. Cells were wounded using a 200 μl pipette tip. For assessment of migration following siRNA treatment cells were transfected with siRNA 72 hours prior to wounding and then replated 24 hours before wounding onto glass-bottomed dishes. Again, cells were wounded using a 200 μl pipette tip.

2.11 Endocytosis assays

Endocytosis assays were conducted to confirm the effects of Dynasore treatment, α-adaptin knockdown and caveolin1 knockdown on endocytosis. 24 hours before the assay cells were plated onto cover slips in a 6 well plate. For assays with Dynasore each well was rinsed with 2 ml SFM before incubation with 2 ml SFM containing the Dynasore at 80

μM or the equivalent volume of DMSO for 30 minutes. A 10 minute incubation with just SFM was used for assays utilising siRNA transfected cells. After this initial incubation cells were then further incubated for 5 minutes with either Transferrin (Alexa Fluor® 568 conjugate; Tf-AF568; Invitrogen) at 10 μg/ml or cholera toxin (Alexa Fluor® 555 conjugate; CTx-AF555; Invitrogen) at 1 μg/ml in 2 ml SFM. After incubation Tf568 wells were washed with acid PBS twice followed by a PBS wash; CTx555 wells were washed twice with SFM followed by a PBS wash. Cover slips were fixed in 4% PFA for 5 minutes, before two final PBS washes. Cover slips were fixed to slides using ProLong Gold (Invitrogen) before being imaged and analysed.

2.12 Exocytosis assays

Exocytosis assays were used to determine the effect of Dynasore on trafficking from the Golgi apparatus to the plasma membrane. Cells were transfected with either an neuropeptide Y (NPY)-mRFP alone or NPY-mRFP and PKD dominant negative (PKD(K618N)-GFP) together. Transfected cells were plated onto cover slips in a 6 well plate 24 hours before the assay. Wells were washed with 2 ml SFM and then treated with 2 ml SFM containing either the Dynasore to a concentration of 80 μM or the equivalent volume of DMSO for 30 minutes. After incubation wells were washed twice with 2 ml PBS and then fixed in 2 ml 4% PFA for 5 minutes. Cover slips were then fixed to slides using ProLong Gold before being imaged and subsequently analysed.

2.13 Imaging and image analysis

All live cell imaging made use of cell imaging media (10 mM Hepes (Sigma), 9.7 g Hank's Balanced Salt Solution (Life Technologies) in 1 l dH2O, pH 7.4) with the required amount of serum dependent upon the experiment (0.1% FCS for agaose spot assay, 5% for wound healing; Jaiswal et al. 2002).

For analysis by region cells were split into front, middle and back using an axis perpen-

dicular to the spot edge (see Chapter 3 for more information on this analysis).

2.13.1 Endocytosis and exocytosis assays and Transwell assays

Imaging was achieved using a Nikon TE300 Inverted Epi-fluorescence microscope with a 40 x oil objective lens (CFI Plan Apo 1.3 NA, Nikon). Using a Red/Green/Blue multiband emission filter with excitation changed the desired colour (depending on the fluorophore being used) using a Ludl filter wheel. Random fields of view from the slides were imaged. For endocytosis and exocytosis assays analysis was done using ImageJ software which allowed the drawing of a region of interest around the cell. Increasing the contrast in brightfield images allowed accurate detection of the cell edge and switching to the fluorescent image allowed a reading of the mean fluorescence intensity within that cell to be displayed by Image J software (see Figure 2.1). Average background fluorescence was measured by selecting regions where no fluorescence could be seen and these values were taken away from the cell fluorescence values. For Transwell assays simply the number of cells which had migrated through the membrane were counted in each field of view.

2.13.2 Agarose spot assay: Overnight time-lapses

Overnight brightfield time-lapse imaging was done on a Nikon eclipse Ti inverted microscope using a 10x air objective lens (CFI Plan Fluor 0.3 NA, Nikon). The microscope was situated inside an Okolab incubator set to 37°C. The microscope system was controlled by NIS elements AR. Regions around each spot were randomly selected for imaging; generally two regions per spot. Images were taken every 10 minutes for 14 hours. For counting number of cells migrated or distance migrated perpendicular to spot edge the counting/measuring tools in NIS elements (version 3.1) were used. NIS elements manual tracking software was used for all cell tracking analysis (see Figure 2.2). Cells were chosen randomly for analysis but if at any point there was uncertainty over where a cell had migrated too e.g. because it had migrated in very close proximity to other cells,

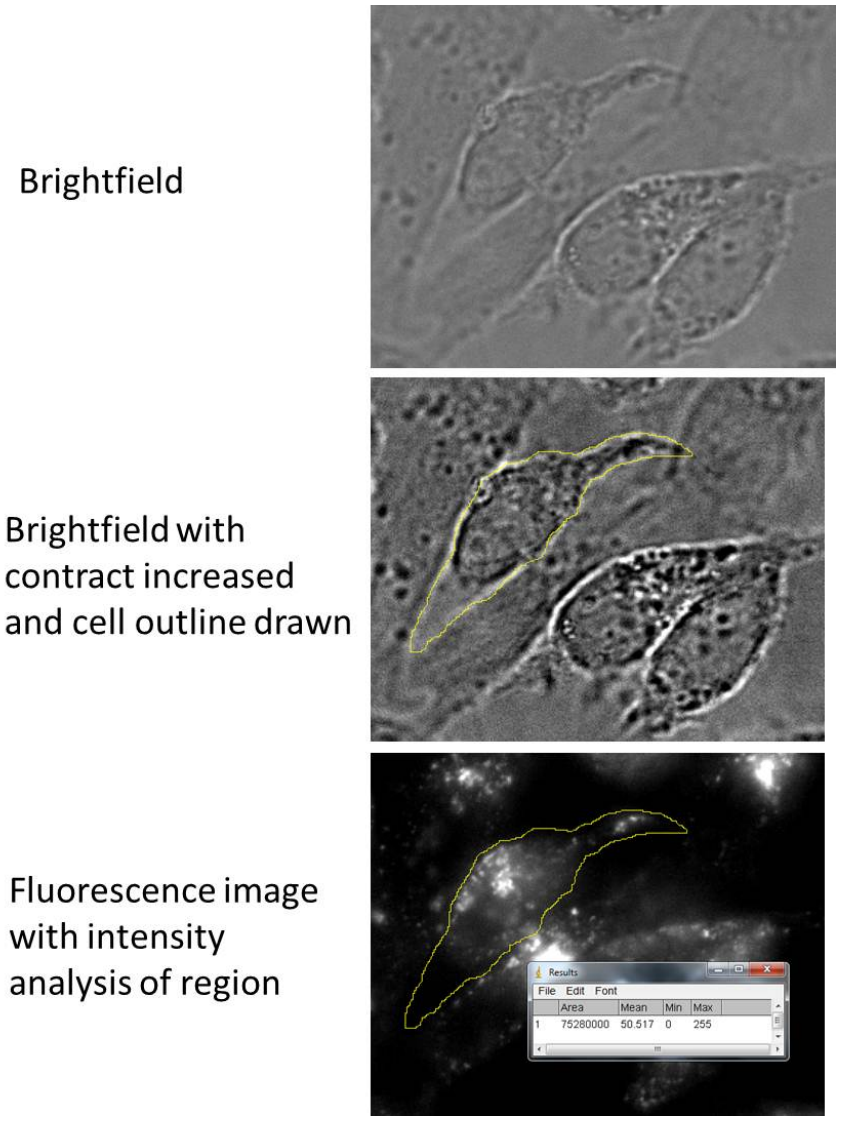

Figure 2.1: Representative images of analysis of endocytosis and exocytosis assays. Contrast of brightfield images could be increased to ensure accurate drawing around the edge of the cell. Image J software allowed quantification of mean fluorescence intensity within each region.

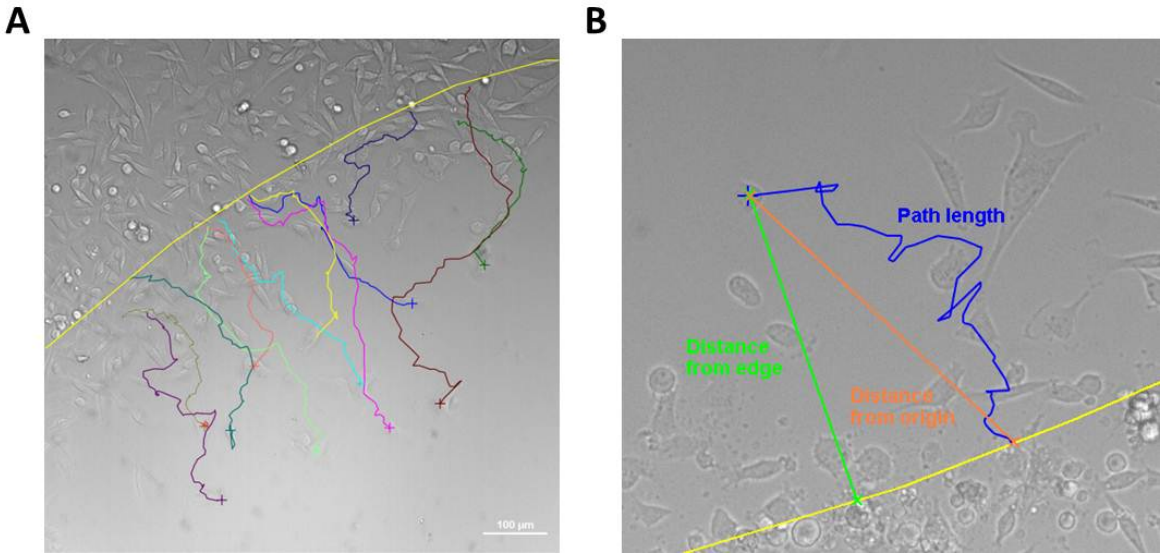

Figure 2.2: Images to show cell tracking analysis. A) Representative image cells after 14 hours timelapse. Using NIS Elements software cells can be manually tracked by clicking on the cell in question in each frame of the timelapse. B) This image shows the track produced from one cell and also details the distance measurements which would be used for both 'distance from edge' and 'distance from origin' measurements.

that analysis was ended and not counted and another cell was chosen to replace it. 100 cells were tracked per condition.

2.13.3 Agarose spot assay: TIRF imaging

Live cell TIRF imaging was performed using Nikon A1-R Ti TIRF system within in the Nikon eclipse Ti inverted microscope with a 60x oil objective lens (CFI TIRF Apo 1.49 NA, Nikon). The microscope was situated inside an Okolab incubator set to 37°C. The microscope system was controlled by NIS elements AR. All GFP constructs were excited with the 488 nm lines of an Argon-Ion laser 457-514 nm. All RFP, dsRed or mCherry constructs were excited with a green diode 561 nm laser. Image analysis was done using NIS elements (version 3.1 or higher).

2.13.4 Colocalisation analysis

Colocalisation of β3-integrin and clathrin

Live cell TIRF imaging took place, imaging every 2 minutes for a total of 40 minutes. All β3-integrin-GFP-labelled focal adhesions were circled in the green channel before assessing the proportion that colocalised with clathin-dsRed in the red channel. A technique whereby the effect of shifting one channel relative to another one pixel at a time and determining the effect of this on the Pearson's correlation coefficient was also used in this case to look at colocalisation by another method (Rappoport and Simon, 2003; Jones et al., 2014). In addition kymographs were made to assess the colocalisation between β3-integrin-GFP and clathrin-dsRed and also paxillin-mRFP and clathrin-GFP. Here a line was drawn across a 10 μm region of interest and a kymograph across this region for 40 minutes was generated using NIS elements software.

Colocalisation of EGFR and clathrin or caveolin1

Static TIRF images were taken of live cells migrating into EGF spots. For colocalisation analysis of clathrin-dsRed or caveolin1-mRFP with EGFR-GFP 50 EGFR-positive

structures in the green channel were circled, the number of these corresponding to a clathrin/caveolin1-positive structure in the red channel was then recorded (see Figure 2.3 for representation of this colocalisation analysis). To assess random colocalisation, the same 50 circled regions were moved slightly so that they corresponded to regions where EGFR-GFP was not present; the number of these control regions which corresponded to a clathrin/caveolin1-positive structure was recorded as the control value.

Colocalisation of EGFR and NPY or Rab11

Static TIRF images were taken of live cells migrating into EGF spots. NPY-mRFP or Rab11a-mCherry-positive structures were circled in the red channel. Those corresponding to EGFR-GFP-positive structures in the green channel were recorded. To assess random colocalisation, the same circled regions were moved slightly so that they corresponded to regions where NPY-mRFP or Rab11a-GFP was not present; the number of these control regions which corresponded to an EGFR-GFP-positive structure was recorded as the control value.

2.13.5 Internalisation intensity profile

To create the intensity profile of a clathrin- and EGFR-positive structure disappearing from the TIRF field a region of interest was drawn around the structure in both the red and green channels. The instensity of this region of interest was measured over the time course of the disappearance. Background intensity of each frame was taken away and this value was divided by the area of the region to give intensity per unit area for both the clathrin and EGFR clusters.

2.13.6 Cluster size analysis

For analysis of the apparent size of EGFR-GFP or clathrin-dsRed clusters the area calculation tool in NIS elements was used. Cluster were excluded from analysis if there

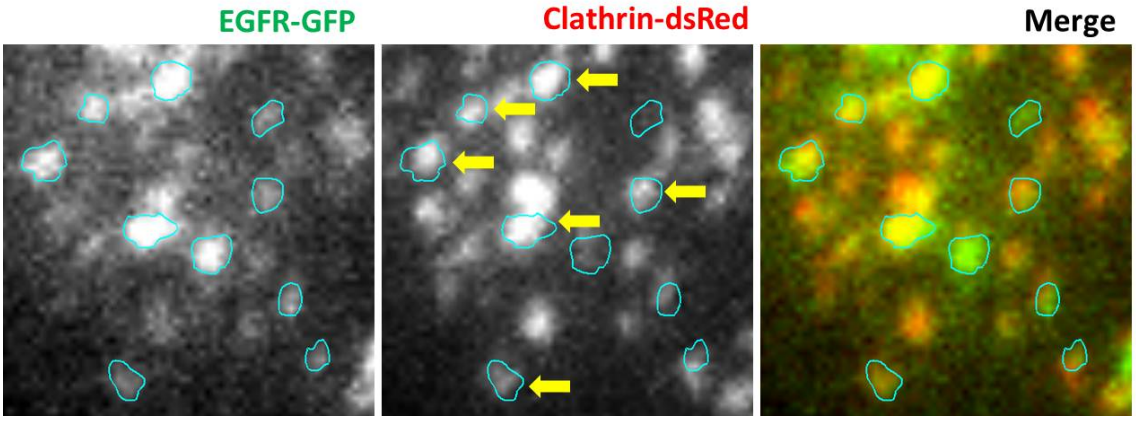

Figure 2.3: Representative image colocalisation analysis. Using EGFR-GFP and clathrin-dsRed colocalisation analysis as an example: clusters of EGFR were drawn around in the GFP image (increasing image brightness as necessary to accurately view each cluster), switching to the dsRed image allowed analysis of whether the EGFR clusters colocalised with a clathrin cluster. In the above image the arrows show representative cluster which would be viewed as colocalised.

were too close to another cluster to accurately see the edge and also in regions of excessive fluorescence possibly not stemming from cluster at the plasma membrane (eg. fluorescence from the Golgi region). To draw around clusters, channel brightness was increased to ensure entire cluster region was analysed (see Figure 2.4 for a representative image of this analysis).

2.13.7 Clathrin internalisation analysis

For MDA-MB-231 cells live cell TIRF imaging was done with $\leq$ 400 ms exposure time (corresponding to 2.5 frames per second) for one minute time-lapses. For analysis of internalisation events we looked for instances where clathrin-dsRed disappeared from the evanescent field to indicate an internalisation event, as previously described (Rappoport and Simon, 2003). The disappearance of clathrin from the evanescent field was taken to be due to endocytosis only if it was not due to photobleaching, if it occurred rapidly (within 10 frames of imaging) and if it did not reappear in the evanescent field within 10 frames of its disappearance. Analysis was done in relation to the front, middle and back of migrating cells.

For PDAC cells live cell TIRF imaging was done with $\leq$ 200 ms exposure time (corresponding to 5 frames per second) for one minute time-lapses. In the case of MDA-MB-231 cells the clathrin was generally static for the whole time-lapse or else it internalised. In PDAC cells it appeared that the majority of clathrin was highly dynamic and moving in a manner that suggested it was travelling along microtubules. Previously it has been suggested that clathrin can move along microtubules prior to internalisation (Rappoport et al., 2003b; Ezratty et al., 2009), so we analysed both the number of clathrin clusters disappearing from the TIRF field as well as the number of these dynamic clathrin clusters. Analysis was done in relation to the front, middle and back of migrating cells.

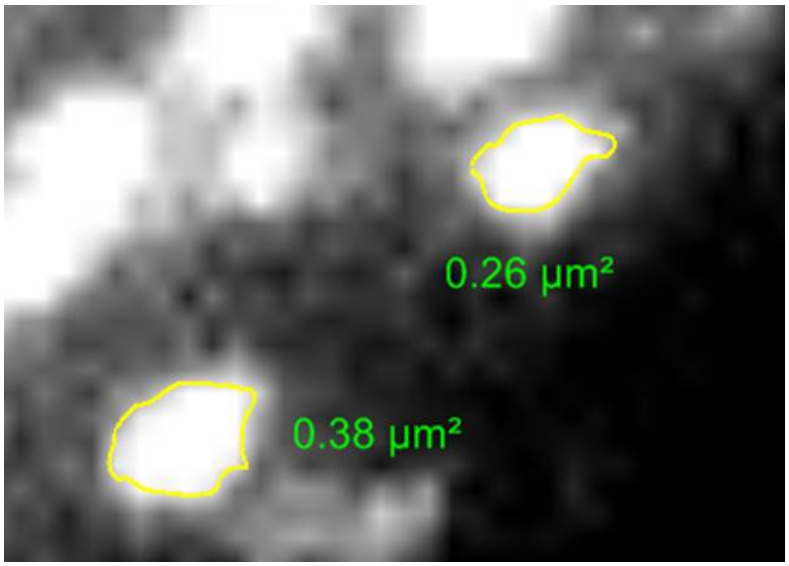

Figure 2.4: Representative image of cluster size analysis. In NIS Elements softare brightness of images was increased to ensure the most accurate region could be drawn around the cluster. NIS Element analysis software was able to analyse the area of regions selected.

2.13.8 Focal adhesion disassembly analysis

During a wound healing assay live cell TIRF imaging of paxillin-mRFP in cells at the edge of the wound took place. Regions of interest were drawn around focal adhesions and intensity over time was monitored. The time from when the focal adhesion was at its brightest until its intensity decreased to background was recorded as disassembly time.

2.13.9 Wound closure analysis

For overall assessment of migration following wounding areas of the wound were imaged by brightfield imaging using a Nikon eclipse Ti inverted microscope using a 10x air objective lens (CFI Plan Fluor 0.3 NA, Nikon). Imaging took place from the point of wounding for 14 hours, acquiring images every 15 minutes. Analysis using NIS elements software involved drawing a line along the edge of the wound at the start and the end of the time-lapse, then measuring the distance between these two lines as a number of points to give the average distance of wound closure over the course of the time-lapse, which could then be converted to average closure per hour.

2.13.10 Fusion analysis

For the verification of fusion events methods described by Schmoranzer and colleagues were used (Schmoranzer et al., 2003). TIRF microscopy was used to image time-lapses with EGFR-GFP as the cargo for vesicle fusion. Firstly, putative fusion events were identified by examining the time-lapse for instances of high fluorescent intensity appearing at the plasma membrane, before a decrease in fluorescence as the vesicle contents diffuse in the plasma membrane. To verify fusion events two analytical methods were used, the first being a line scan method using NIS elements line scan tool. A line scan was drawn across the fusion area to measure the intensity of fluorescence in each pixel along the time during the fusion process. A graph was produced plotting pixel number against fluorescent intensity with each time point represented by a different line. A true

fusion event would have a sharp peak followed by the peak decreasing and widening as the vesicle contents fuse and then diffuse laterally in the plasma membrane. The second analysis method used was the draw a circular region of interest around the fusing vesicle for each frame of the fusion and measure the fluorescence intensity of the region in each frame. As area increases the intensity should first increase as the vesicle is coming into closer proximity with the membrane and fusing with the membrane. At later stages the area of the fluorescence intensity should increase but the total intensity should remain fairly constant as the contents are diffusing within the plane of the plasma membrane.

2.13.11 FLIM-FRET imaging

Fluorescence lifetime imaging (FLIM) imaging took place at the Beatson Institute for Cancer Research, Glasgow. FLIM measurements were achieved using a Lambert Instruments fluorescent attachment on a Nikon Eclipse TE2000-U inverted microscope using a 60x objective and a filter block with a 436/20 excitation filter, a T455LP dichroic mirror, and a 480/40 emission filter. For FLIM-FRET a modulated 445 nm LED light source was used for FLIM-FRET frequency domain measurements. Fluorescein (10 μM in 0.1 M Tris-CL, pH $\geq$ 10) was used as a reference with known fluorescent lifetime of 4 ns. Donor lifetime was analysed using LI-FLIM software (version 1.2.10, Lambert Instruments). Regions of interest could be selected for lifetime measurements of a whole cell or regions within a cell.

Chapter 3

Investigating the role of vesicle trafficking in chemotactic invasion

3.1 Introduction

As mentioned previously, the process of directed cell migration towards a source of attractant is known as chemotaxis and is vital to the intravasation and extravasation stages of metastasis (Condeelis and Segall, 2003). Chemotaxis is triggered by the binding of chemoattractant molecules to cell surface receptors (e.g. EGF binding to its receptor) (Bagorda et al., 2006). Activation of such receptors results in a complex signalling cascade that leads to polarisation of the cell in the direction of migration, increased contractility and subsequent directed motility (Bagorda and Parent, 2008).

In order to fully control important aspects of migration cells must have the ability to regulate surface localisation of both chemoattractant receptors and adhesion molecules. The process of vesicle trafficking affords the cell such control and therefore must be taken into account for a detailed understanding of cell migration (Fletcher and Rappoport, 2010). As previously mentioned vesicle trafficking can be split into three main pathways (endocytosis, endosomal recycling and exocytosis) each of which is split further into sub-pathways (eg. short-loop recycling and long-loop recycling as two sub-pathways

in the wider trafficking process of endosomal recycling). Here we concentrate specifically on endocytosis and aim to elucidate the endocytic transport routes necessary to MDA-MB-231 cells migrating towards EGF.

Many assays exist to study cell directed cell migration, from Dunn chambers and Transwell assays, to more recently developed assays such as the Insall chamber (Zicha et al., 1991; Boyden, 1962; Muinonen-Martin et al., 2010). In the present study we use a relatively new assay which is simple and cheap to perform and allows for use in multiple microscopy set-ups. Figure 3.1 depicts a diagram of the agarose spot assay from the view of the user. For more information about the agarose spot assay please refer to Wiggins and Rappoport 2010 or Section 2.8. In this chapter we aim to further characterise the assay and then use it to investigate the importance of endocytosis in EGF-directed chemotactic invasion of MDA-MB-231 cells.

3.2 Results

3.2.1 Characterisation of the agarose spot assay

To study the response of cells to the chemoattractant EGF we employed a chemotactic invasion assay in which cells migrate into an agarose spot containing EGF (hereafter referred to as EGF spots; Wiggins and Rappoport 2010). Further characterisation of the assay was necessary to rule out that chemokinesis could be the cause of migration. Control experiments were undertaken using agarose spots containing PBS (hereafter referred to as PBS spots) to represent an unstimulated condition. The same condition with the addition of EGF to the media was used to stimulate chemokinesis (hereafter referred to as chemokinetic control), in order to compare the migration seen in this condition with that seen into EGF spots.

Data obtained from 14 hour brightfield time-lapses of these control conditions includes the number of cells which migrated into the spot area, as well as the distance migrated,

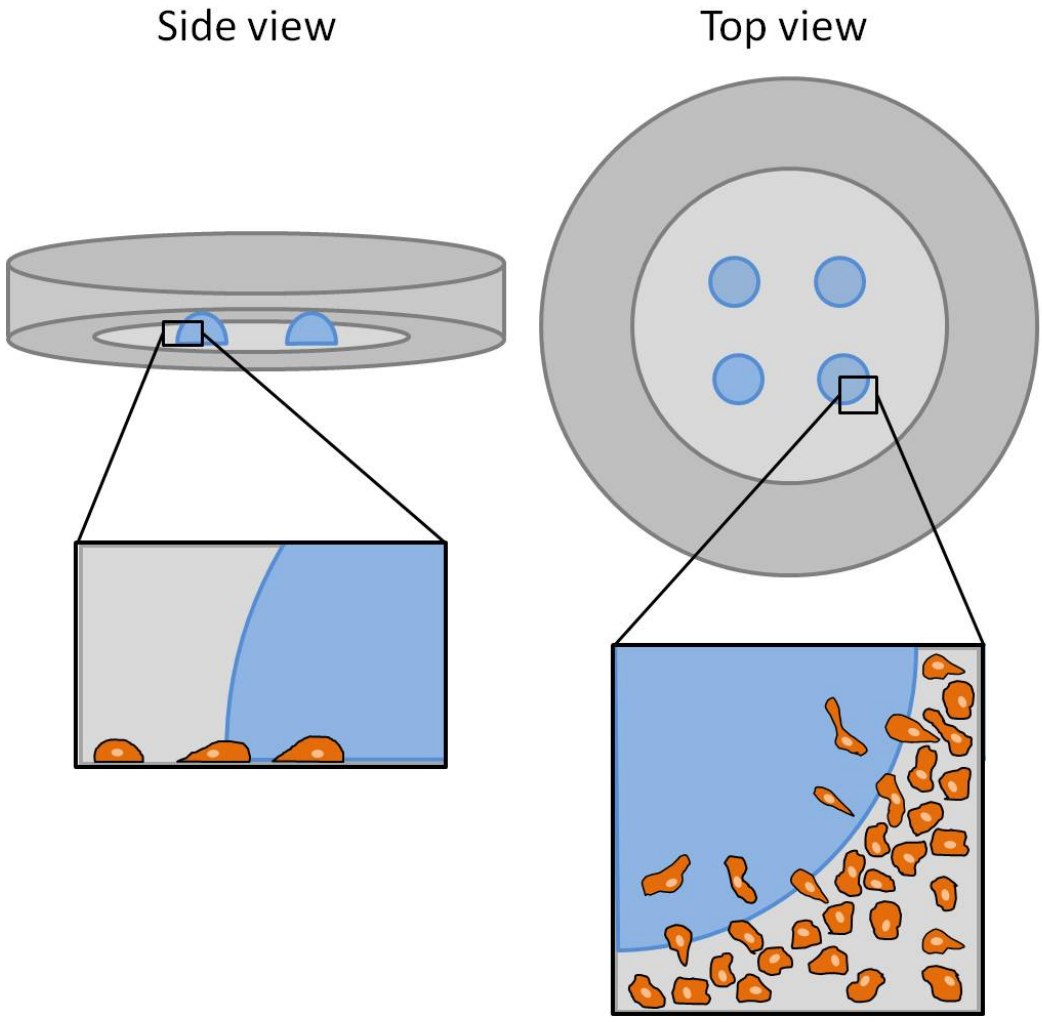

Figure 3.1: Diagram of the agarose spot assay; side-on view and a view from above. The assay is done in 35mm glass-bottom dishes. Depicted in blue are the agarose spots, four of which can fit comfortably in one dish. The close-up views show cells around the agarose spots and those migrating under the spots.

the average velocity of migrating cells and the directionality of the migrating cells. As expected the number of cells which had migrated into the agarose spots was significantly higher for those containing EGF than PBS (Figure 3.2). In the case of the chemotactic control the number of cells which had migrated was intermediate to these results indicating that the EGF in the media is able to stimulate migration but not to the same extent as the EGF spots themselves (Figure 3.2).

In order to determine whether cells not in the direct vicinity of the agarose spots were affected by chemoattractant cells were tracked using NIS elements tracking software to ascertain the velocity and total path length over the course of the time-lapse. Cells away from the spots in dishes with PBS or EGF spots were not significantly different from one another in terms of distance migrated and average velocity, but the cells of the chemotactic control migrated significantly further and faster than the other two conditions (Figure 3.3A). This therefore suggests to us that cells undergo chemokinesis when in EGF media but that the EGF from the agarose spots does not affect cells in regions away from the spots in this chemokinetic way.

Similar tracking analysis was applied to cells migrating into the agarose spots. Results indicate that cells migrate much further and faster into EGF spots than PBS spots, even when EGF is present in the media of the PBS spot dishes as in the chemotactic control (Figure 3.3B). When comparing velocity of cells tracked from inside and outside the agarose spots it is evident that there is no real different between cells of the PBS spots and cells of the chemotactic control, however a significant increase is seen in the average velocity of those cells with EGF spots (Figure 3.3C). This indicates that the EGF in the agarose spots is causing directed migration within the spot, and that any migration seen as a result of EGF in the media is as a result of chemokinesis rather than chemoattractant-directed migration. The distance migrated by cells in the chemotactic control is much lower inside the agarose spot than out of it, suggesting that the agarose spot itself poses a physical barrier to normal migration. This result adds to the point that EGF spots stimulate migration into them as these cells travel significantly further

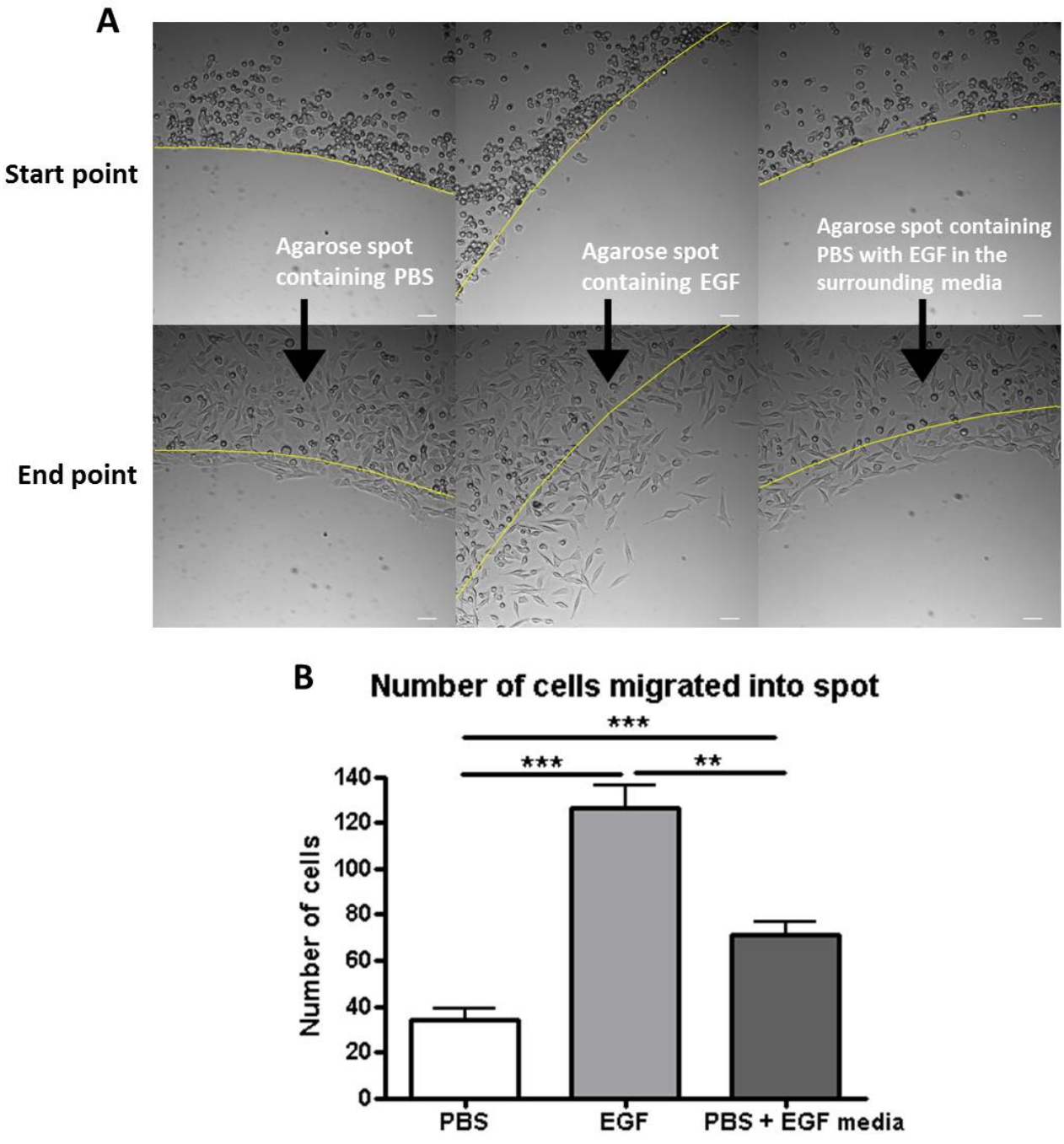

Figure 3.2: Migration of MDA-MB-231 cells into PBS and EGF spots and PBS spots with EGF-containing media. A) Representative images taken from the start point and end point of 14 hour time-lapses in control experiments. The top panel shows migration into a PBS spot, the middle shows migration into an EGF spot and the bottom panel shows migration into a PBS spot with EGF present in the surrounding media. The line denotes the edge of the agarose spot. All scale bars are 50 μm. B) Graph to show the total number of cells migrated in the three conditions. n = 3 experiments with a total of 24 spots analysed per condition. Error bars represent standard error of the mean, significance determined by one way ANOVA followed by Tukey's post-test, ** denotes p-value < 0.01, *** denotes p-value < 0.001.

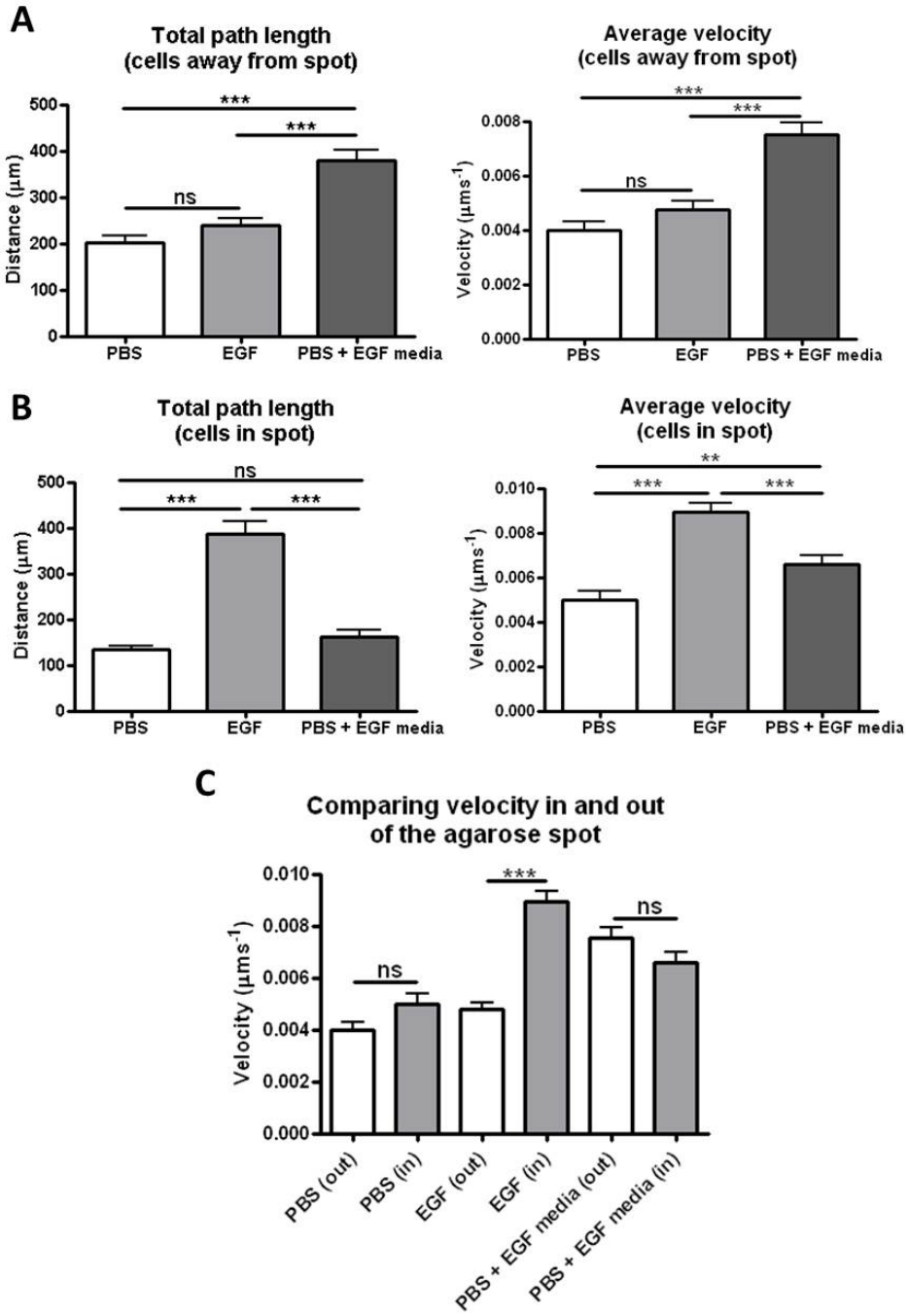

Figure 3.3: Graphs to show the total path length and the average velocity of migrating MDA-MB-231 cells both away from (A) and in the agarose spot (B). In (A) it can be seen that cells away from the spot in dishes containing PBS and EGF spots do not migrate significantly differently from one another, but that those in the chemotactic control migrate significantly further and faster. When looking at cells migrating into agarose spots in (B) it can be seen that both the distance migrated and velocity of cells is significantly increased only for those migrating into EGF spots, compared to the other two conditions. (C) compares the velocity data from the graphs on the right of (A) and (B) in order to directly compare the affect the spot has on the average velocity of migration. n = 3 experiments with a total of 35 cells analysed per condition. Error bars represent standard error of the mean, significance determined by one way ANOVA followed by Tukey's post-test, 'ns' denotes p-value ≥ 0.05 (not significant), ** denotes p-value < 0.01, *** denotes p-value < 0.001.

in the spots even with this barrier to overcome.

Control time-lapses were also used to establish the overall direction of migration taken by cells within agarose spots. For later analyses following TIRF imaging we wanted to split cells into regions of front, middle and back. For this analysis it would not be possible to tell the direction that the cell was travelling in as this imaging involved taking short rapid time-lapses or static images, and were therefore not over a long enough time course to view the direction of migration at the time of imaging. From observation it was also noted that the migrating MDA-MB-231 cells do not always have a well-defined lamellipodia region, therefore we also have to discount this as a way of identifying the front of the cells.

One theory was to assume the cells were travelling perpendicular to the spot edge and use this axis to assign the front, middle and back of migrating cells. We decided to investigate this assumption further in order to decide whether this was a satisfactory method of splitting the cell into regions. We used two methods to calculate the trajectory of migrating cells with regards to the perpendicular. In each case we noted the position of the cell when it entered the agarose spot and the position at the end of the time-lapse. We then drew a line perpendicular to the edge of the agarose spot at the time the cell was at the spot edge (green line in Figure 3.4) and another straight line from the cell's start position to its end position (blue line in Figure 3.4). We then measured the angle between these two lines. In our first method our aim was to see whether cells have a propensity to travel to the left or right of the perpendicular axis or straight on into the spot. For this reason we recorded angles to the right as positive numbers and angles to the left as negative; in the diagram in Figure 3.4A we would therefore record the angle of the red cell as $+10^\circ$ and the angle of the blue cell as -30°. Repeating this analysis over 91 cells gave us an average angle of $+5.04^\circ$ with a standard error of the mean (SEM) of 2.20° showing that overall the cells have a very slight deviation to the right of the perpendicular and that the spread of the data is low. The second method aimed to test the directionality of cells regardless of whether it was to the right or the

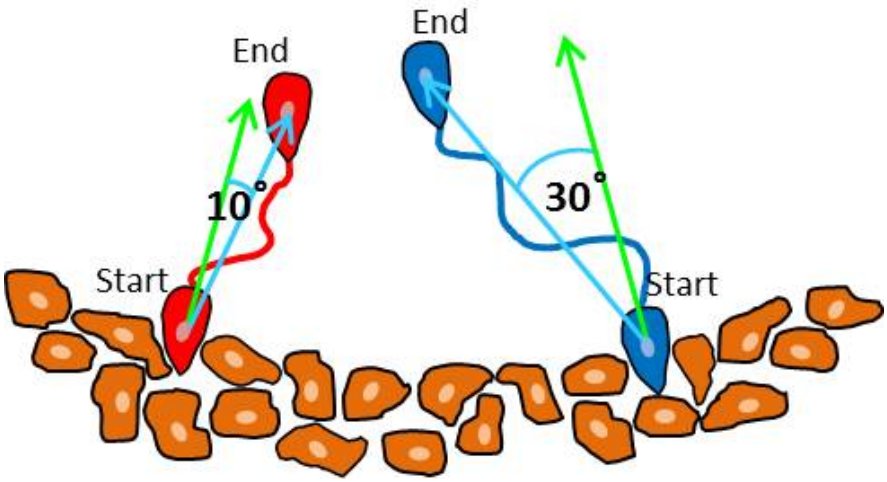

Figure 3.4: A diagram of a field a view of an agarose spot with trajectories for two migrating cells. The diagram shows how the angles were measured to determine how far cells travelled from a perpendicular axis at their start point. The perpendicular is shown by a green line and the actual overall direction of the cell shown by a blue line. n = 3 experiments with a total of 91 cells analysed.

left of the perpendicular, so the values from diagram in Figure 3.4 would simply be 10° and 30°. Repeating this analysis over 91 cells gave us an average angle of 16.97° with an SEM of 1.38°. In this way the cells are migrating slightly off course from the perpendicular but not to a large degree and the spread of the data is low. This data supports observations by Wiggins et al. who noted that the movement of cells into agarose spots was 'progressive and directed' (Wiggins and Rappoport, 2010). For later analysis involving establishing the front, middle and back of migrating cells splitting the cell into these regions was achieved using a line perpendicular to the edge of the agarose spot and dividing this into three equal lengths. Where stated, analyses were then normalised to the area of each region to account for their different sizes.

3.2.2 Inhibition of dynamin-dependent mechanisms of endocytosis decreases chemotactic invasion

Dynamin2 is a large GTPase shown to be vital for both clathrin-mediated and caveolar routes of endocytosis (Hill et al., 2001; Nabi and Le, 2003). Dynasore is a small molecule inhibitor of dynamin and was used to inhibit dynamin-dependent endocytosis in the chemotactic invasion assay (Macia et al., 2006). We tracked cells exposed to Dynasore in 14 hour time-lapses to elucidate the necessity for these routes of endocytosis on EGF-directed cell migration. In order to establish the success of our inhibition strategy we analysed how efficiently Dynasore inhibited the internalisation of transferrin and Cholera toxin Subunit B (as markers of clathrin-mediated endocytosis and caveolar endocytosis, respectively; see Figure 3.5).

Tracking data from 14 hour time-lapses of cells treated with Dynasore showed a significant decrease in the number of cells able to migrate into the EGF spots as well as the total path length migrated, the distance from the origin and the average velocity (see Figure 3.6). Interestingly, Dynasore also affected the elliptical factor of cells (as found by measuring the longest axis of the cell and measuring the width at the middle point

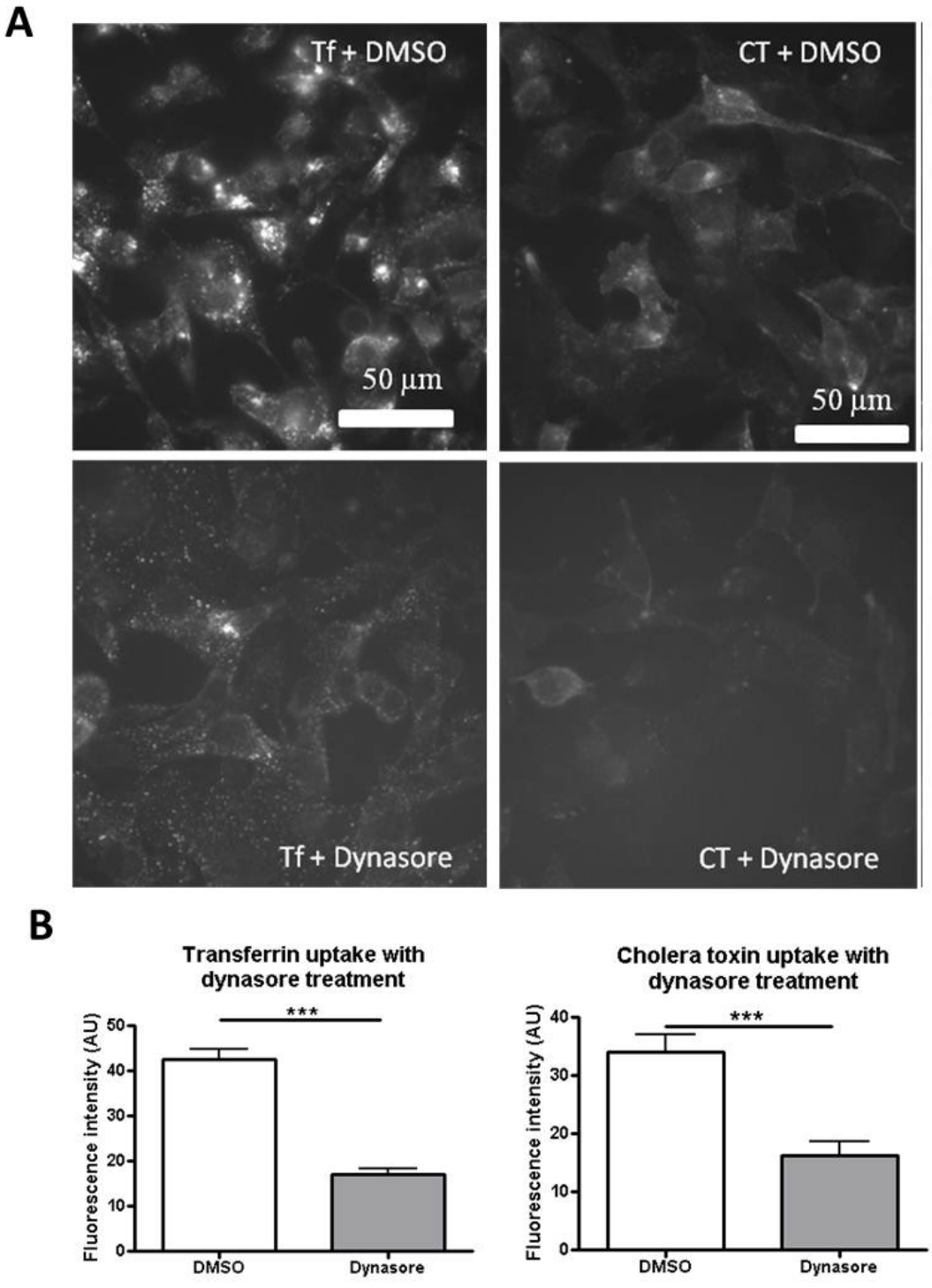

Figure 3.5: Endocytosis controls for Dynasore treatment. A) Representative images of Tf568 (left panels) and CTx555 (right panels) endocytosis ligands in MDA-MB-231 cells treated with DMSO (as control) or 80 μm Dynasore (to inhibit endocytosis). Ligand uptake was allowed to occur for 5 minutes before excess ligand was washed off and cells were fixed. Scale bars are 50 μm. B) Graph of transferrin uptake showing 60% inhibition in cells treated with Dynasore and graph of Cholera toxin uptake showing 52% inhibition in cells treated with Dynasore. n = 3 experiments with a total of 60 cells analysed per condition. Error bars represent standard error of the mean, significance determined by two-tailed unpaired student's t-test. *** denotes p-value < 0.001.

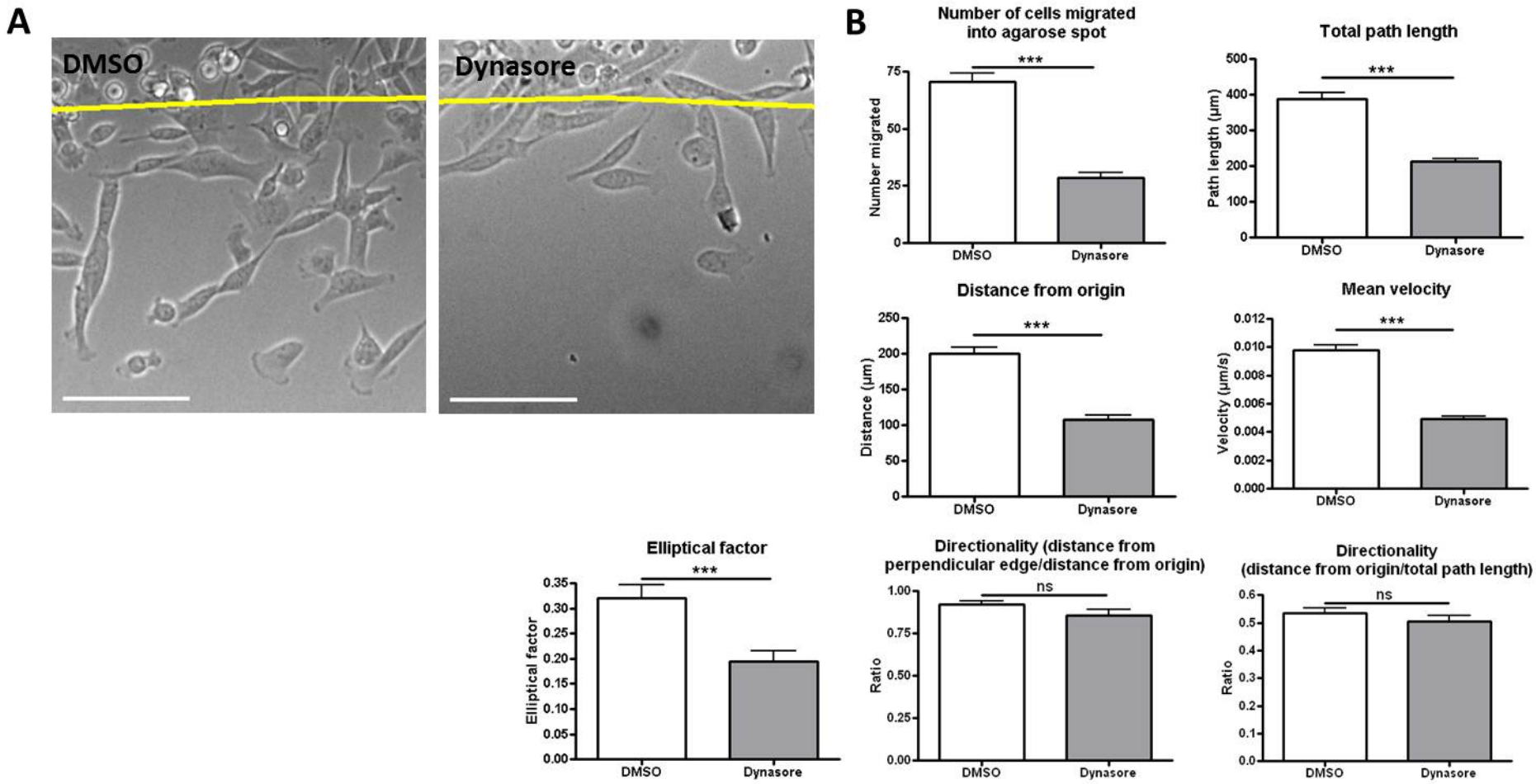

Figure 3.6: Dynasore inhibits MDA-MB-231 cell migration into EGF spots. A) Representative images of MDA-MB-231 cells treated with DMSO or Dynasore after 14 hours migration into an agarose spot containing EGF. Line denotes edge of the agarose spot. Scale bars are 100 μm. B) Results of tracking cells over the course of the time-lapses. Parameters analysed were total number of cells migrated, total path length, distance from origin, average velocity, elliptical factor and two measures of directionality. n = 3 experiments with a total of $\geq$ 100 cells analysed per condition. Error bars represent standard error of the mean, significance determined by two-tailed unpaired student's t-test, 'ns' denotes p-value ≥ 0.05, *** denotes p-value < 0.001.

of the length, then dividing the width by the length to give a number between 0 and 1, where 1 would be a perfectly round cell), causing them to become significantly more elongated (Figure 3.6). However, Dynasore had no effect on the directionality of the migrating cells as calculated either by the distance of the cell from its origin divided by its total path length or by the straight line distance of the cell perpendicular to the edge of the agarose spot divided by the distance from its origin (Figure 3.6).

In combination with the agarose spot assay we also used Transwells as another means of testing the effect of Dynasore on EGF-directed migration. Transwells are an end-point chemotaxis assay that allows the production of a gradient of chemoattractant between an upper and lower well separated by a membrane. Cells travel towards higher chemoattractant concentrations by crawling through pores in the membrane to the lower surface of the membrane and can then be visualised by staining and using fluorescent microscopy. The results of this assay corroborated those of our agarose spot assay, namely that migration was inhibited by 94% in the presence of the drug when compared with the control condition (see Figure 3.7).

Although the above data suggest that inhibition of dynamin-dependent endocytosis prevents chemotactic invasion, such a conclusion cannot be drawn from this data alone. Dynamin has roles in other cellular processes including exocytosis from the Golgi (Jones et al., 1998), Dynasore treatment may therefore affect other pathways in addition to endocytosis. Exocytosis assays were used to assess the impact of Dynasore on exocytic trafficking from the Golgi-apparatus. We utilised the secretory cargo neuropeptide Y tagged to red fluorescent protein (NPY-mRFP) as a marker for PKD-mediated exocytic traffic (Fletcher, 2012). Fluorescence intensity was measured in cells treated with DMSO as a reference for NPY-mRFP intensity under normal trafficking conditions and this was compared with Dynasore treated cells. We also made use of a dominant-negative form of PKD (PKD(K618N)), which is a kinase dead mutant shown to inhibit vesicle production at the trans-Golgi-network and fission of vesicles with the plasma membrane (Liljedahl et al., 2001). This dominant-negative PKD was used as a comparison; if Dynasore was

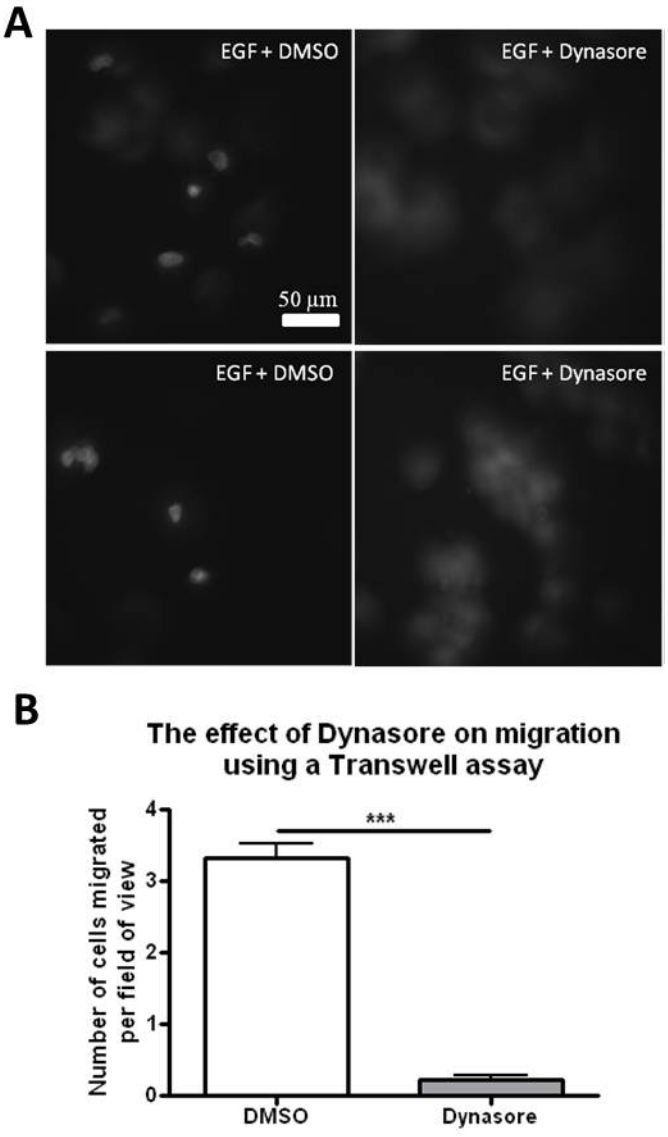

Figure 3.7: Dynasore inhibits MDA-MB-231 cell chemotaxis towards EGF in Transwells. A) Representative images of cells on the Transwell membrane focussed on the underside of the membrane. Scale bars are 50 μm. B) Quantification of cells migrated per field of view following DMSO and Dynasore treatment. n = 3 experiments with a total of $\geq$ 45 cells analysed per condition. Error bars represent standard error of the mean, significance determined by two-tailed unpaired student's t-test, *** denotes p-value $<$ 0.001.

to inhibit NPY-mRFP exocytosis we wanted to know whether this is to the same or a lesser extent of the PKD dominant-negative.

Treatment of NPY-mRFP transfected cells with Dynasore increased NPY retention by 68% over control DMSO cells, to a level comparable to cells expressing a PKD dominant negative (84% retention compared to control DMSO cells, Figure 3.8) Thus, in our system Dynasore also has a significant inhibitory effect on post-Golgi exocytic trafficking.

3.2.3 Clathrin-mediated endocytosis, but not caveolar endocytosis, is required for EGF-directed cell migration

To more specifically inhibit endocytosis siRNAs were employed against proteins found to be vital for clathrin-mediated and caveolar endocytosis. siRNA against α-adaptin (a subunit of AP2) was used to inhibit clathrin-mediated endocytosis and was found to give consistant knockdown with an average of 32% protein remaining (Figure 3.9A, B). To specifically inhibit caveolar endocytosis siRNA against caveolin1 was used, this construct consistently knocked-down caveolin1 with an average of 8% protein remaining (Figure 3.9A, B). The ability of the siRNAs to inhibit transferrin uptake and Cholera toxin Subunit B uptake, respectively, was also established (Figure 3.9C, D). Transferrin uptake was inhibited by 45% under α-adaptin knockdown conditions, and Cholera toxin uptake was inhibited by 50% under caveolin1 knockdown conditions.

Analysis of cells migrating into EGF spots showed the siRNA against α-adaptin significantly inhibited the number of cells able to migrate (Figure 3.10). The cells still able to migrate showed a number of differences including a decrease in directionality and the cells were slightly more rounded than control, however these differences were only small compared to the earlier results with Dyansore treatment. Inhibition of caveolar endocytosis by knockdown of caveolin1 had no effect on the number of cells able to migrate and no significant differences in most of the tracking parameters analysed (Figure 3.10). The

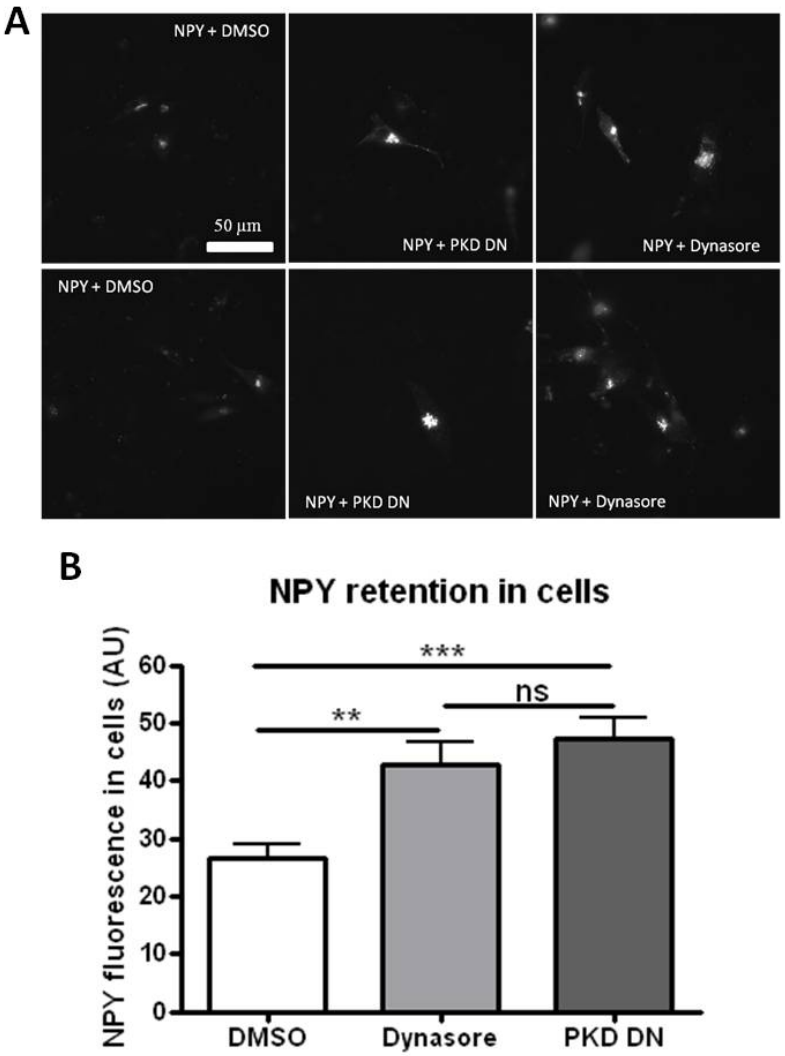

Figure 3.8: Inhibition of NPY-mRFP exocytic trafficking by Dynasore. NPY-mRFP was transfected into MDA-MB-231 cells and used as a marker of exocytic trafficking. DMSO treatment was used to assess normal trafficking, while cells also transfected with dominant negative PKD (known to inhibit vesicle production at the Golgi) were used to assess NPY-mRFP build up when its trafficking is inhibited. These controls could be used to compare the effect of Dynasore treatment on Golgi-derived trafficking. A) shows representative images of NPY-mRFP under conditions of DMSO (negative control), PKD-dominant negative (positive control) and Dynsore. B) Treatment with Dynasore increased intracellular accumulation of NPY-mRFP to a level comparable to that of the PKD dominant negative. n = 3 experiments with a total of 40 cells analysed per condition. Error bars represent standard error of the mean, significance determined by one way ANOVA followed by Tukey's post-test, 'ns' denotes p-value $\geq$0.05, ** denotes p-value < 0.01, *** denotes p-value < 0.001.

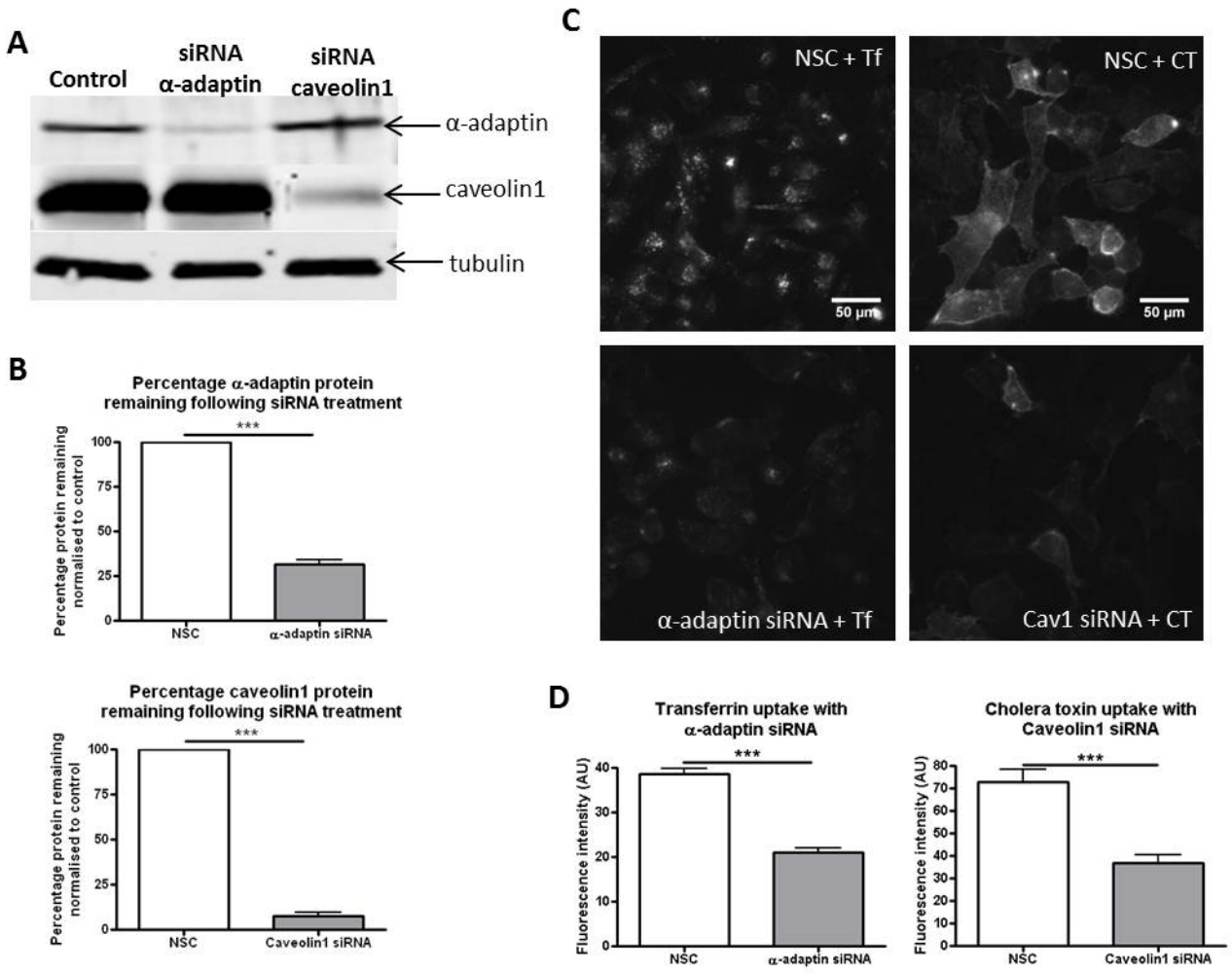

Figure 3.9: Controls for α-adaptin and caveolin1 siRNA. A) Western blot of remaining protein following treatment with non-silencing siRNA (NSC), α-adaptin siRNA and caveolin1 siRNA. B) Graphs show the quantification analysis of protein knockdown. In each case the NSC is normalised to 100% and percentage protein remaining is calculated. Average amount of α-adaptin remaining was 32% in α-adaptin siRNA treated cells; average amount of caveolin1 remaining in caveolin1 siRNA treated cells was 8%. n $\geq$ 3 western blots per quantification analysis. Error bars represent standard error of the mean, significance determined by two-tailed unpaired student's t-test, *** denotes p-value < 0.001. C) Representative images of Tf568 uptake in NSC α-adaptin siRNA treated cells (left panel) and CTx555 uptake in caveolin1 siRNA treated cells (right panel). D) Quantification of transferrin and Cholera toxin uptake; transferrin uptake was inhibited by 45% in α-adaptin siRNA treated cells and Cholera toxin was inhibited by 50% in caveolin1 siRNA treated cells. n = 3 experiments with a total of 60 cells analysed per condition. Error bars represent standard error of the mean, significance determined by two-tailed unpaired student's t-test, *** denotes p-value < 0.001.

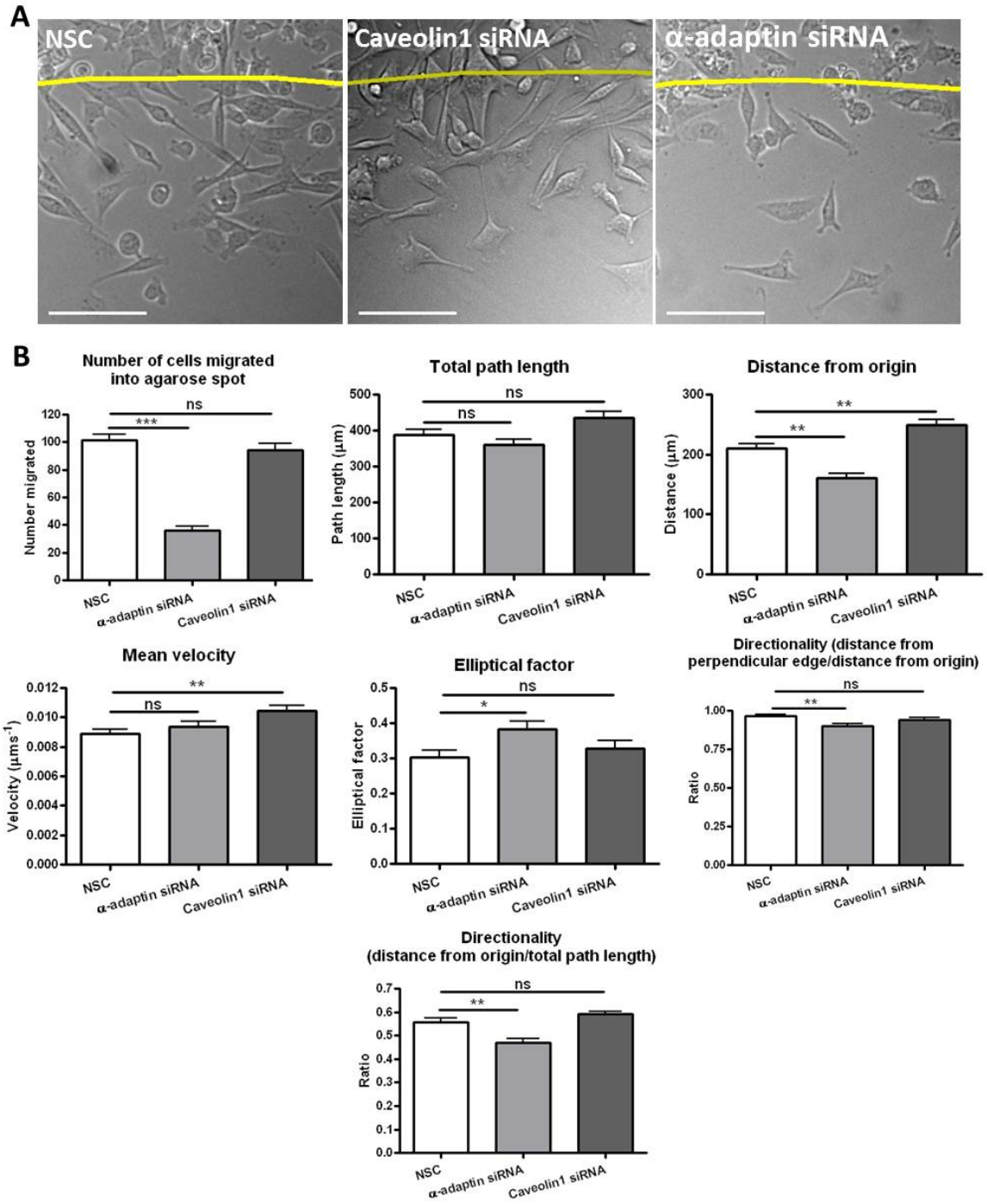

Figure 3.10: α-adaptin siRNA inhibits MDA-MB-231 cell migration into EGF spots, Cav1 siRNA does not inhibit MDA-MB-231 cell migration into EGF spots. A) Representative images of cells treated with control siRNA, α-adaptin siRNA and caveolin1 siRNA after 14 hours migration into EGF spots. Line denotes edge of the agarose spot. Scale bars 100 μm. B) Results of tracking cells over the course of the time-lapses. Parameters analysed were total number of cells migrated, total path length, distance from origin, average velocity, elliptical factor and two measures of directionality. n = 4 experiments with 100 cells analysed per condition. Error bars represent standard error of the mean, significance determined by one way ANOVA followed by Dunnett's post-test, 'ns' denotes p-value ≥ 0.05, * denotes p-value < 0.05, ** denotes p-value < 0.01, *** denotes p-value < 0.001.

caveolin1 knockdown cells did have a higher average velocity and distance from origin, compared to control, but again these differences were only minor.

3.3 Discussion

The agarose spot assay was first developed by Wiggins and Rappoport as an inexpensive, relatively simple assay for chemotactic invasion (Wiggins and Rappoport, 2010). They showed that the assay could give highly reproducible results and that migration into EGF spots was significantly higher than migration into control PBS spots. The results of their preliminary studies, however, couldn't rule out the possibility that EGF was increasing chemokinesis of the cells in general and that it wasn't specific to the cells crawling under the spot. Control assays of PBS spots with EGF present in the surrounding media were undertaken to stimulate chemokinesis and compare this condition with those of PBS or EGF spots alone (Figures 3.2 & 3.3). The migration into these chemotactic control was significantly slower and less far than migration into EGF spots, but faster than those into regular PBS spots, indicating that the migration we observe into EGF spots is in fact, not chemokinesis.

Analysis of the migration of cells not directly in the vicinity of the agarose spots also took place (Figure 3.3A, C). It was found that cells in dishes with PBS or EGF spots behave very similarly in terms of path length and velocity, suggesting that the EGF affects only cells close to the spot and does not seep out to cause chemokinesis of cells further from the spot edge. The cells in the chemotactic control migrate much further and faster than either of the other two groups when tracked in areas away from the spot, providing further evidence that this mode of migration is chemokenesis.

On analysis of the directionality of cells migrating under the EGF spots it was found that the average trajectory was 5.4° to the right of a perpendicular axis from the spot edge, meaning overall the cells are migrating in a directional manner. If direction is dis-

counted from this analysis the angle becomes 16.97° which is still only a minor deviation from the perpendicular. Overall this result suggests that within the spots cells migrate in a directional manner; and this can be used to establish front, middle and back regions of the cell for later analysis.

The agarose spot assay was used to analyse migration of a large population of MDA-MB-231 cells under various inhibitory conditions. We showed that Dynasore inhibits the number of cells able to migrate as well as a number of other parameters analysed (Figure 3.6). However, we also showed that Dynasore affected exocytosis in these cells, thereby meaning we have to be cautious when interpreting results as a consequence of this drug (Figure 3.8). With Dynasore affecting exocytosis it is possible that the results we saw were due to a decrease in receptors and adhesion molecules made available to the cell surface through this inhibition, rather than due to a decrease in their internalisation. From our results there is no way to distinguish between these possibilities. However, it seems likely that both plasma membrane-based endocytic events as well as Golgi-derived fission events would be necessary for migration and thus it can be stated that dynamin is required for EGF-directed migration in our system.

We used siRNA to more specifically inhibit two endocytic pathways: α-adaptin siRNA to inhibit clathrin-mediated endocytosis and caveolin1 siRNA to inhibit caveolar endocytosis. In the case of α-adaptin siRNA we saw a large decrease in the number of cells able to migrate but of those still able to migrate differences in the other parameters measured were either small or non-existent. This was different to the case of Dynasore where large differences were seen in the total path length, velocity and other parameters. The α-adaptin protein knockdown in these cells was 68% meaning 32% of the protein remained. We do not know whether this means that all cells had 32% of the protein remaining or that 68% of cells were knocked down to 100% leaving 32% of cells with no knockdown, or somewhere in between. Since the cells that still migrate aren't very dissimilar to control cells in most parameters we postulate that these represent a population of cells unaffected or only partially affected by the siRNA. It therefore seems

that α-adaptin (and therefore clathrin-mediated endocytosis) is necessary for migration of MDA-MB-231 cells.

In contrast to this caveolin1 knock-down had little effect on any of the migratory parameters measured and so it seems likely that in our system clathrin-mediated endocytosis but not caveolar endocytosis is necessary for MDA-MB-231 cell migration. However, an argument must be made for a possible compensatory role for caveolin2 in migration when caveolin1 is knocked-down. Caveolin2 is often thought of as unnecessary for caveolar endocytosis and in fact caveolin2-null mice have been shown to form normal caveolae (**?**). However, this does not fully discount a role for caveolin2 in caveolar formation in all systems. Experiments in MDA-MB-231 cells have shown a role for caveolin2 in tumour progression, specifically enhancing tumour proliferation and survival, though this tumour promoting role was not linked to an ability to undergo caveolar endocytosis (Shatseva et al., 2011). Other studies back-up the previously discussed lack of a role for caveolin2 in caveolae formation. Sotgia et al. found that caveolin2 expression could not rescue caveolae formation in caveolin1-null cells, but that caveolin1 or caveolin3 expression could (Sotgia et al., 2002). Conclusions drawn from other studies propose that caveolin1 is necessary for transport of caveolin2 to the plasma membrane and that in its absence, caveolin2 is simply degraded (Sowa, 2011). Taking the above into account, a role for caveolin2 in caveolar endocytosis cannot be ruled out, therefore there is a chance of a compensatory role for this protein when caveolin1 is knocked-down. In light of the evidence, however, it seems likely then that by knocking down caveolin1 we were preventing all caveolar endocytosis in our system and therefore our results show that in MDA-MB-231 cells caveolar endocytosis is not required for EGF-directed migration.

3.4 Key chapter findings

- Our chemotactic invasion assay is specific for chemotaxis and not chemokinesis and cells move directionally under the agarose spots.

- Dynamin is necessary for EGF-directed migration of MDA-MB-231 cells in our chemotactic invasion assay.
- Clathrin-mediated endocytosis is necessary for EGF-directed migration of MDA-MB-231 cells in our chemotactic invasion assay, but caveolar endocytosis is not.

Chapter 4

Clathrin mediated endocytosis is not required for focal adhesion disassembly in migrating MDA-MB-231 cells

4.1 Introduction

Research into the role of endocytosis during chemotactic invasion is currently limited. Both chemoattractant receptors and focal adhesion components represent potential endocytic cargoes which are also likely to have roles in cell migration. Focal adhesions serve as points of contact between the ECM and the actin cytoskeleton (Ridley et al., 2003). Fully formed focal adhesions are complexes multiple proteins including those which link the adhesion to actin, signalling proteins and integrins which link the actin cytoskeleton to the ECM (Huttenlocher and Horwitz, 2011). Integrins are integral to focal adhesions as they are membrane bound heterodimers that bind ECM ligands as well as providing sites for binding of structural and signalling proteins that make up the focal adhesion itself. Through interaction with myosin II via actin focal adhesions serve as sites for traction force, thereby allowing the cell to move (Lauffenburger and Horwitz, 1995; Sheetz et al., 1998; Beningo et al., 2001). Factors affecting focal adhesion dynamics, including their turnover, can affect many aspects of migration.

Endocytosis of integrins has been proposed as a mechanism of focal adhesion disassembly under certain conditions (Fabbri et al., 2005; Panicker et al., 2006; Nishimura and Kaibuchi, 2007; Caswell and Norman, 2008). Most β-integrin subunits have NXXY motifs in their cytoplasmic regions which points to an involvement of clathrin-mediated endocytosis in their internalisation, however until recently little other evidence could be gleamed that this motif does in fact aid internalisation of these integrins and even mutating the motif was shown to have no effect on the rate of internalisation of β-integrins (Ylänne et al., 1995). More recently studies have found that a subpopulation of β1-integrins which associate with the tetraspanin CD151 internalise via an AP2-dependent route (Liu et al., 2007; Nishimura and Kaibuchi, 2007). However, there is much evidence for clathrin-independent internalisation routes for the internalisation of integrins, with studies linking particular integrins to caveolae (Caswell and Norman, 2008). Caswell and Norman conclude that the types of internalisation pathways followed by integrins is determined by multiple factors including the region of the cell the integrin is in, the migratory status of the cell and the method of detection of integrin internalisation (Caswell and Norman, 2008).

During migration there is a need for focal adhesions to be present at the front of migrating cells for the migratory traction force to control cell movement. Early work has shown recycling of integrins from the rear of migrating cells as a way to provide integrins to newly forming adhesions at the leading edge (Bretscher, 1989; Lawson and Maxfield, 1995; Pierini et al., 2000). Laukaitis and colleagues propose a model for endocytosis of integrins to serve two functions; the first being internalisation of unliganded integrins at the lamellipodial region and the second being internalisation at the cell rear followed by trafficking to a PNRC (Laukaitis et al., 2001). The group also suggest that focal adhesion disassembly is preceded by cleavage of the integrin-substrate complex from the rest of the adhesion, a process which marks the initiation of disassembly.

Two papers from 2009 discuss a necessity for clathrin in integrin endocytosis, and thereby focal adhesion disassembly, during cell migration (Chao and Kunz, 2009; Ezratty et al.,

2009). The first study used human fibrosarcoma HT1080 cells to show colocalisation between β1-integrin and components of the clathrin internalisation machinery and also found that knockdown of dynamin2 on its own or DAB2 and AP2 together led to a build-up of β1-integrins on the cell surface (Chao and Kunz, 2009). They postulate that two NPXY motifs in the integrin bind to AP2 and DAB2 to enable its endocytosis by the clathrin-mediated pathway. They also indicate that the lack of evidence of this motif leading to internalisation of integrins thus far might be due to the necessity of integrin activation to occur before this motif can bind endocytic machinery (Chao and Kunz, 2009). In the second study, using NIH3T3 fibroblasts, Gunderson's group showed that knocking down CHC led to an inhibition of focal adhesion disassembly of up to 80% (Ezratty et al., 2009). They also used TIRF microscopy to show recruitment of clathrin to β1-integrin-GFP as focal adhesions were disassembling, and in many cases clathrin was seen to leave the TIRF field at the same time as β1-integrin punctae. Ezratty et al. also point to a requirement for the alternative adaptor Dab2 (Ezratty et al., 2009).

In contrast to the two above mentioned studies in 2011 Gu et al. found integrin trafficking to occur via circular dorsal ruffles (CDR) and marcopinocytosis as the adhesion was being disassembled (Gu et al., 2011). The group showed β3-integrin to colocalise with markers of CDR when fibroblasts were stimulated with platelet derived growth factor (PDGF; Gu et al. 2011). The study was also expanded to other cell types and growth factors (including EGF-stimulated MDA-MB-231 cells) and integrins were also found to redistribute to CDRs in these situations. Gu et al. found this CDR-based internalisation of integrins to be dependent on brefeldin A-ADP-ribosylated substrate (BARS; a molecule necessary for micropinocytosis) but independent of both clathrin and caveolin1. The authors state that perhaps clathrin or caveolin1-dependent endocytosis of integrins may represent a basal internalisation method for integrin internalisation but that under growth factor stimulation macropinocytosis may be necessary to ensure correct integrin internalisation and recycling (Gu et al., 2011). In a similar vein Fletcher et al. examined focal adhesions during wound healing of MDCK epithelial cells (Fletcher et al., 2012).

They saw no colocalisation between clathrin-dsRed and β3-integrin-GFP nor between clathrin-GFP and paxillin-mRFP in migrating cells and also found no increase in the number or size of focal adhesions present in migrating cells when clathrin-mediated endocytosis was inhibited using Eps15 EH29 mutant or caveolar endocytosis was inhibited using Cav1Y14F mutant (Fletcher et al., 2012).

Here we aim to elucidate whether clathrin-mediated endocytosis is important for focal adhesion turnover in MDA-MB-231 cells during EGF-directed migration.

4.2 Results

4.2.1 Colocalisation of endocytosis markers and focal adhesions

As shown previously in Figure 3.6 treating migrating cells with Dynasore to inhibit dynamin causes a dramatic decrease in the number of cells able to migrate. Interestingly those still able to migrate exhibit an elongated phenotype compared to control cells. This elongated phenotype led us to postulate that a fault was occurring in the disassembly of focal adhesions and therefore that perhaps clathrin-mediated endocytosis was involved in their disassembly under normal conditions. Such necessity for clathrin in focal adhesion disassembly has been observed in other cell types (as outlined previously) but has not been universally observed.

To test this hypothesis of a role for clathrin in focal adhesion disassembly in migrating MDA-MB-231 cells we used TIRF microscopy, a technique which allows illumination of only fluorophores present within $\sim$100 nm of the adherent plasma membrane (see Figure 1.9). In this way we examined the colocalisation between clathrin-dsRed and β3-integrin-GFP in cells migrating towards EGF in the agarose spot assay (Figure 4.1A). β3-integrin-GFP expressing focal adhesions were circled and the proportion which also contained clathrin was noted. Only 7.33% of focal adhesions could be seen to colocalise with clathrin. We also investigated the effect on Pearson's correlation coefficient of

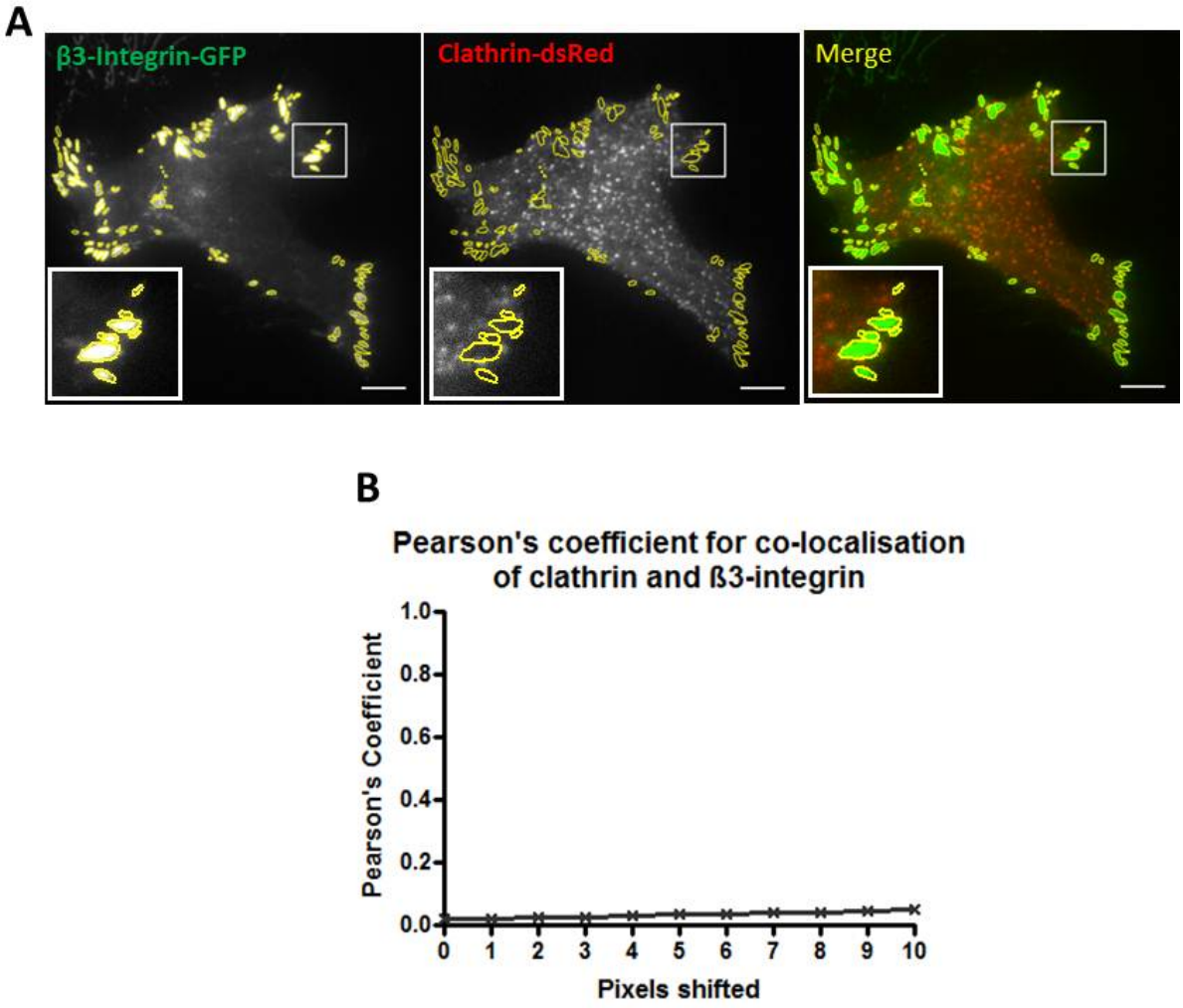

Figure 4.1: Clathrin does not colocalise with focal adhesions in MDA-MB-231 cells using β3-integrin-GFP as the focal adhesion marker. A) Representative images with focal adhesions circled in the β3-integrin-GFP image to assess colocalisation with clathrin-dsRed. Scale bars are 10 μm. n = 3 experiments with a total of 30 cells analysed. B) Pearson's coefficient of β3-integrin-GFP with clathrin-dsRed. Pearson's coefficient looks at the amount of colocalisation between the two markers as one imaged is shifted relative to the other one pixel at a time. Collaborative work with Emma Jenner is acknowledged for the analysis of data used in this figure.

shifting one channel relative to another one pixel at a time, which confirmed a lack of colocalisation between the two (Figure 4.1; Rappoport et al. 2003a,b). We investigated whether clathrin was being recruited to sites of focal adhesion disassembly after the process had already begun. We produced a kymograph by assessing a 10 μm region across two focal adhesions over time and saw no clathrin recruitment to the sites where focal adhesions had previously been established (Figure 4.2).

The use of β3-integrin-GFP as our marker of focal adhesions was chosen for a number of reasons. Firstly this integrin is known to be endogenously expressed in MDA-MB-231 cells, therefore adding physiological relevance to our studies. Secondly, the construct itself has been shown to express normally with correct dimerisation with its integrin partner αIIb and have normal surface expression levels (Plançon et al., 2001). Finally, being membrane bound in focal adhesions means that integrins represent potential cargo for endocytic machinery. However, we realise that this particular integrin may not be present in all focal adhesions and thus we sought to repeat the above experiment using a focal adhesion marker that binds intracellularly to other focal adhesion components and thus is present in all focal adhesions. For this we chose paxillin-mRFP. In an identical experiment to those with β3-integrin-GFP we sought to examine the colocalisation between paxillin-mRFP and clathrin-GFP in cells migrating in an EGF spot. Again, we saw no colocalisation between these two markers and a kymograph showing focal adhesions over time showed no recruitment of clathrin during or immediately after focal adhesion disassembly (Figure 4.3).

An additional study was undertaken to further examine whether β3-integrin-GFP was a valid marker for focal adhesions in our experimental system. We investigated colocalisation between β3-integrin-GFP and paxillin-mRFP to see the proportion of focal adhesions β3-integrin-GFP was recruited to in migrating MDA-MB-231 cells. We found all regions of paxillin-mRFP to contain β3-integrin-GFP and vice versa (Figure 4.4). This leads us to conclude that, at least in our experimental system, β3-integrin-GFP can be used to study focal adhesions and represent the whole focal adhesion population.

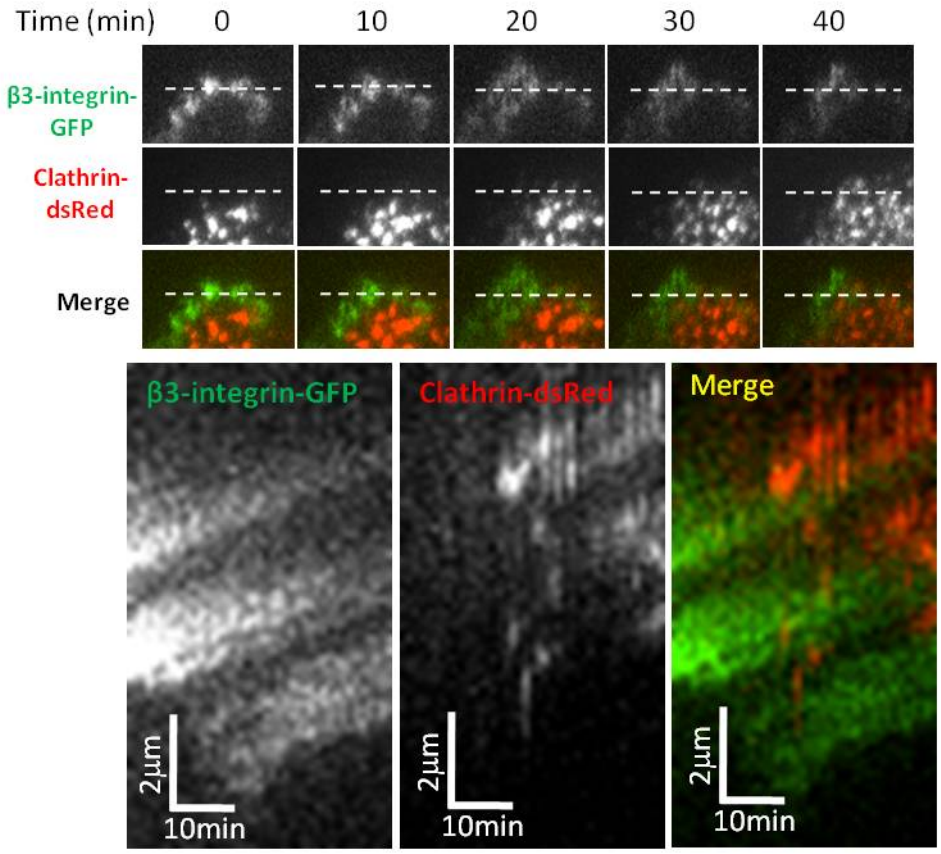

Figure 4.2: Kymograph to show lack of colocalisation between clathrin-dsRed and β3-integrin-GFP labelled focal adhesions in MDA-MB-231 cells. A 10 μm line was drawn across two disassembling focal adhesions and a kymograph produced to show the degree of clathrin and β3-integrin present within this region over time. The khymograph demonstrated no co-localisation of clathrin with β3-integrin during focal adhesion disassembly.

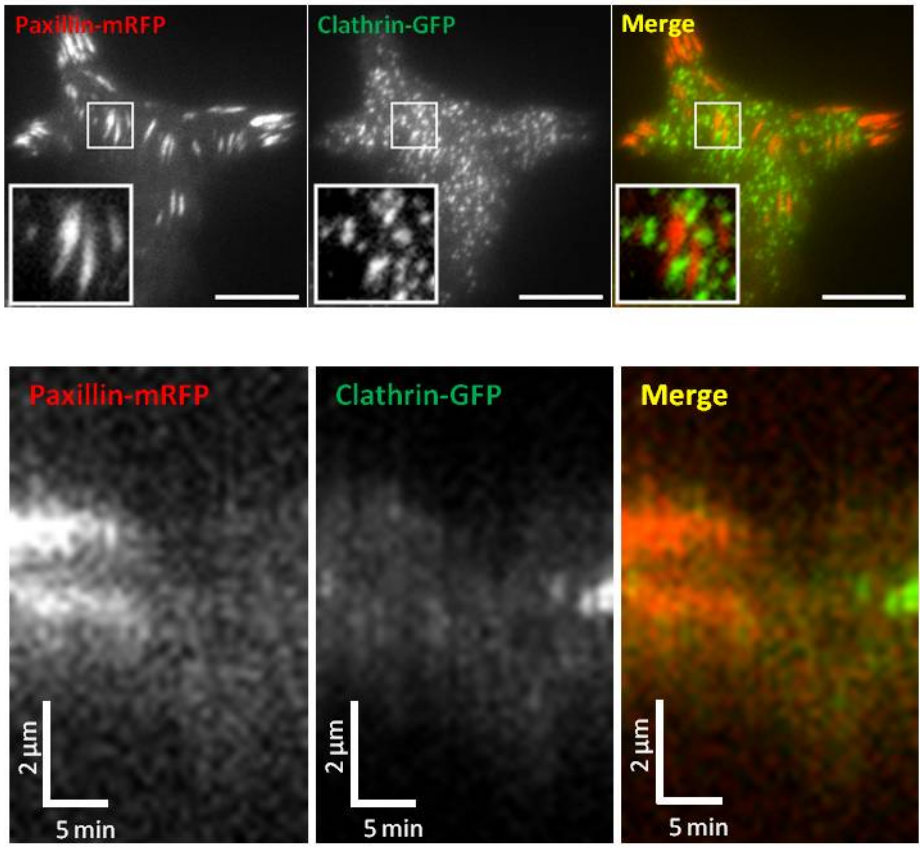

Figure 4.3: Clathrin does not colocalise with focal adhesions in MDA-MB-231 cells using paxillin as the focal adhesion marker. A) Representative images of paxillin-mRFP and clathrin-GFP in migrating cells. Scale bars are 10 μm. n = 1 experiment, 20 cells imaged. B) Kymograph to show lack of co-localisation between paxillin-mRFP labelled focal adhesions and clathrin-GFP over time. A 10 μm line was drawn across two disassembling focal adhesions and a kymograph across this region demonstrated no colocalisation of clathrin during focal adhesion disassembly.

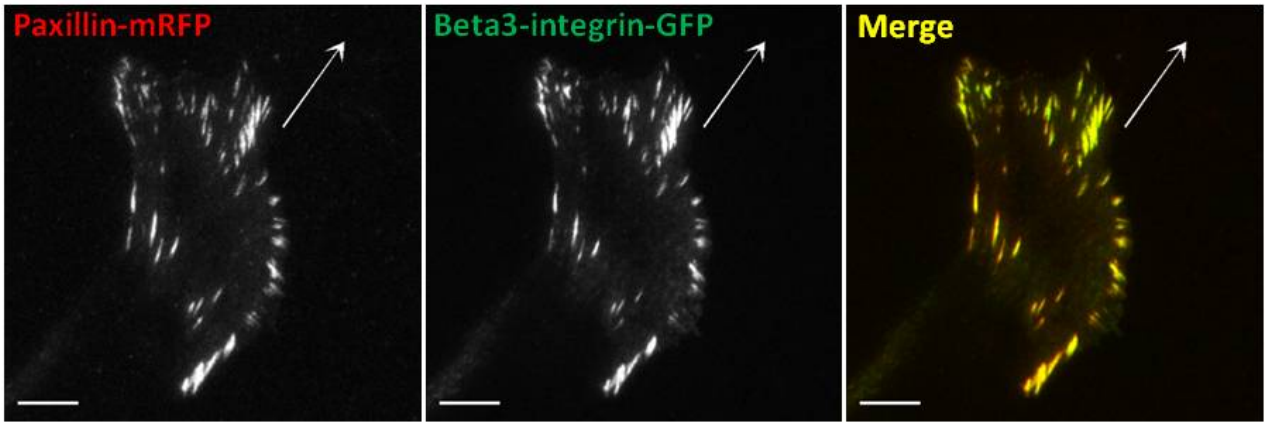

Figure 4.4: Colocalisation of focal adhesion markers in migrating MDA-MB-231 cells. Representative image showing a high degree of colocalisation between paxillin-mRFP and β3-integrin-GFP. Arrows denote the direction of migration. Scale bars are 10 μm. n = 1 experiment, 20 cells imaged.

Caveolar endocytosis was found not to be necessary for migration towards EGF in our system, however some groups have shown it to be involved in integrin internalisation, and therefore possibly also focal adhesion disassembly, in some cases (Caswell and Norman, 2008). Thus we examined the potential for colocalisation between β3-integrin-GFP and caveolin1-mRFP. We saw no colocalisation between the two and, as such (Figure 4.5), think it is unlikely that caveolar endocytosis could be involved in focal adhesion disassembly during EGF-directed migration.

As a non-colocalisation based strategy to test for the involvement of endocytosis in focal adhesion turnover following Dynasore treatment we imaged paxillin-mRFP in cells migrating in EGF spots. We examined the total number of focal contacts in migrating cells, assuming that if their disassembly was being prevented there would be an increase in focal contact number, and found no overall increase (Figure 4.6A, B). We also specifically examined the number of focal contacts present in the front, middle and back regions of the cells in case there was a build-up in one particular region but found that this was not apparent when looking at the total number present in each cell. We counted the number in each region and normalised to the size of the regions (Figure 4.6C). No differences were seen in the number of focal adhesions present in any region with Dynasore treatment leading us to conclude that endocytosis is not important for focal adhesion disassembly in MDA-MB-231 cells in our EGF-directed migration system.

4.2.2 Focal adhesion disassembly time following inhibition of clathrin-mediated endocytosis

As an alternative to using static images to assess focal adhesion colocalisation or number we wanted to investigate whether an altered rate of focal adhesion disassembly occurred when cells were treated with siRNA against α-adaptin to inhibit clathrin-mediated endocytosis. Our spot assay migration system posed a problem for this experiment, in

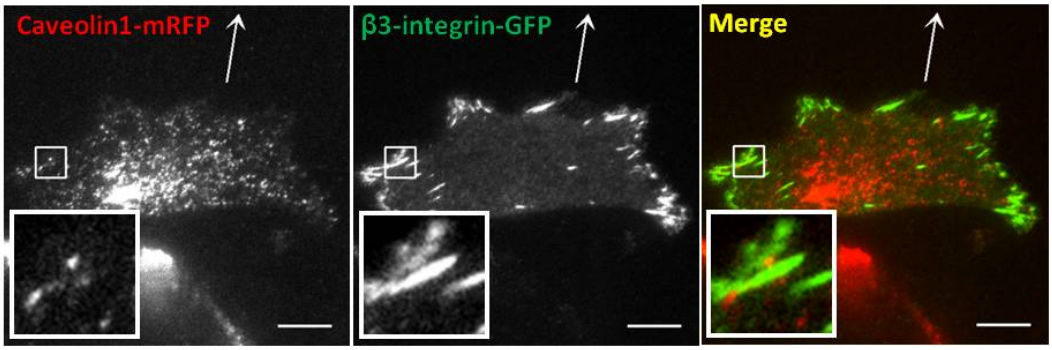

Figure 4.5: Representative image showing a lack of colocalisation between caveolin1-mRFP and β3-integrin-GFP in MDA-MB-231 cells. Arrows denote the direction of migration. Scale bars are 10 μm. n = 1 experiment, 20 cells imaged.

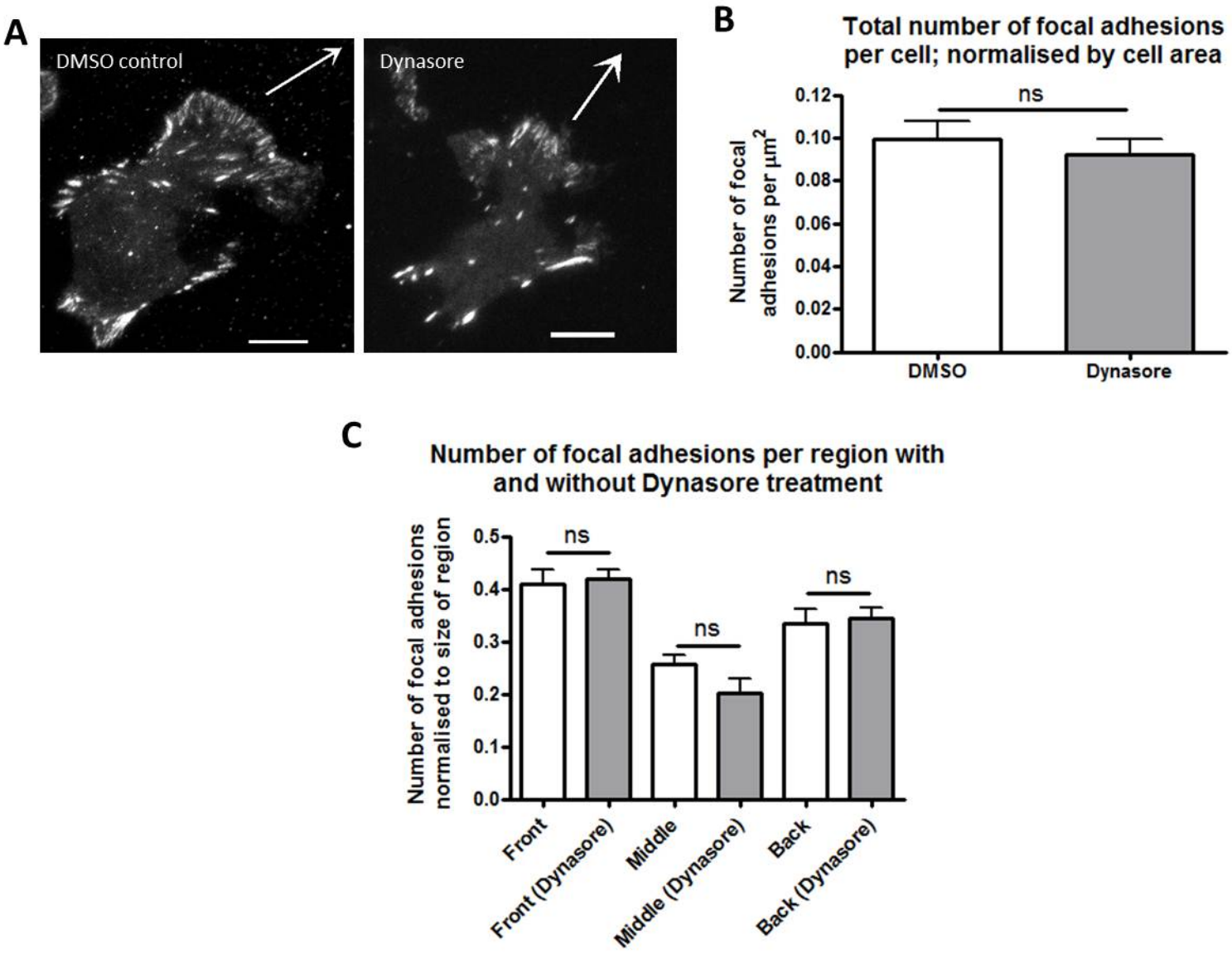

Figure 4.6: Dynasore does not cause redistribution of focal contacts during chemotactic invasion of MDA-MB-231 cells. A) Representative images of paxillin-mRFP in cell migrating towards EGF. Arrows denote the direction of migration. Scale bars are 10 μm. B) Overall there is no significant increase in the number of focal contacts following 80 μm Dynasore treatment. Data is normalised to the area of each cell to ensure comparison between them. Error bars represent standard error of the mean, significance determined by two-tailed unpaired student's t-test, 'ns' denotes p-value ≥ 0.05. C) Quantification of number of focal contacts in the front, middle and back regions of migrating cells. Data is normalised to the area of each region to ensure comparison between regions of different sizes. n = 3 experiments with a total of 25 cells analysed per treatment. Error bars represent standard error of the mean, significance determined by one way ANOVA followed by Tukey's post-test.

that not many α-adaptin siRNA treated cells migrate into EGF spots and those that do migrate in a similar manner to control cells and therefore may represent a population of cells unaffected by the siRNA. We decided instead to use a wound healing assay for this experiment and imaged cells at the edge of the wound since these should be stimulated to migrate due to loss of contact inhibition by the occurrence of the wound. Focal adhesions labelled with paxillin-mRFP were circled and fluorescence intensity was measured over time. The time from when the focal adhesions were the brightest to when this decreased to match background fluorescence was recorded as a measure of focal adhesion disassembly time, a strategy previously used (Fletcher et al., 2012). In this experimental system we found no difference in focal adhesion disassembly time between control and siRNA treated cells (Figure 4.7), providing further evidence for a lack of necessity for clathrin in focal adhesion dynamics in migrating MDA-MB-231 cells. However, adding complexity to this result we also examined the effect α-adaptin siRNA had on wound closure in MDA-MB-231 cells. Interestingly we saw no significant inhibition of wound closure compared to control cells when measuring distance closed over time (Figure 4.8).

4.3 Discussion

Other groups have previously reported a role for clathrin in focal adhesion dynamics of migrating cells (Chao and Kunz, 2009; Ezratty et al., 2009), however this observation is not seen in all cases (Gu et al., 2011; Fletcher et al., 2012). We had previously seen a phenotype of less migratory but more elongated cells upon treatment with the dynamin inhibitor Dynasore (Figure 3.6). Perhaps the observed phenotype was as a result of inability of the cells to undergo focal adhesion disassembly meaning that the rear or the cells remained attached rather than retracting as in a normal migrating cell. This led us to postulate whether there might be a role for clathrin-mediated endocytosis in the turnover of focal adhesions in our system. In this current study we therefore investigated whether a role for clathrin in focal adhesion disassembly could be found in cells

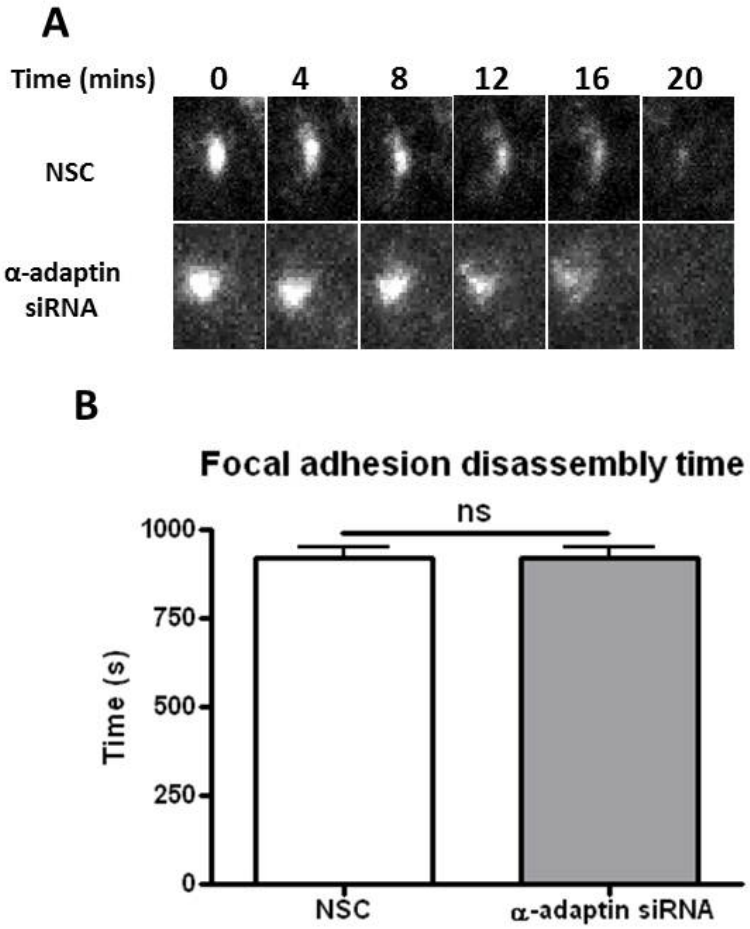

Figure 4.7: α-adaptin siRNA does not inhibit focal adhesion disassembly in wound healing MDA-MB-231 cells. A) Representative image of paxillin-mRFP disappearing over time in cells treated with NSC or α-adaptin siRNA. B) Graph showing mean focal adhesion disassembly time for cells treated with NSC and α-adaptin siRNA. n = 3 experiments with a total of 100 focal adhesions analysed per treatment. Error bars represent standard error of the mean, significance determined by two-tailed unpaired student's t-test, 'ns' denotes p-value ≥ 0.05. Collaborative work with Emma Jenner is acknowledged image analysis contributing to this figure.

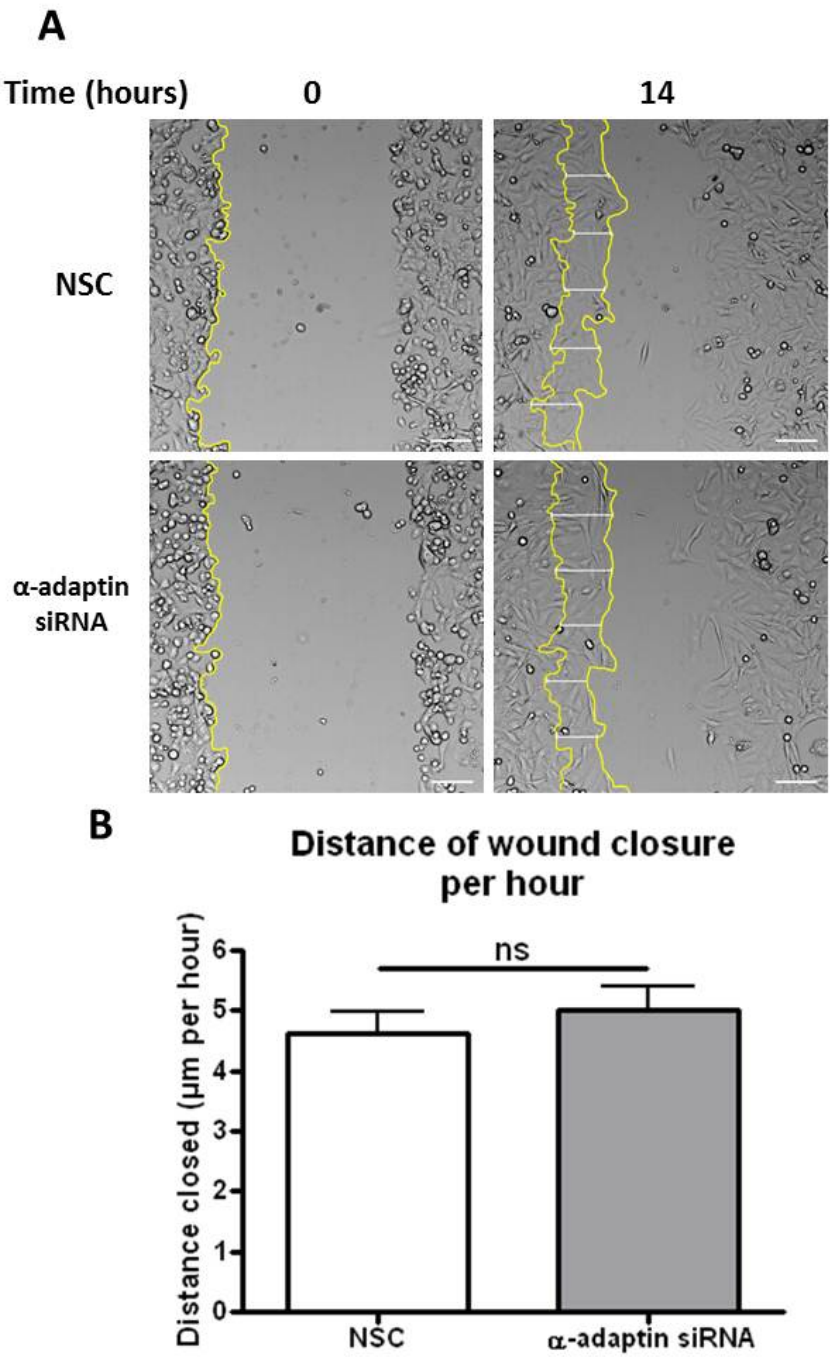

Figure 4.8: Wound healing assay with α-adaptin knock-down in MDA-MB-231 cells. A) Representative images of wounds at time 0 and after 14 hours. In the images on the left yellow lines denote the edge of the wound at time 0. In the images on the right the time 0 lines are shown again and the new lines denote the egde of the wound at time 14 hours. Distances between cells at time 0 and 14 hours were measured at various points in each image to give an average distance migrated in NSC and α-adaptin siRNA treated cells (white lines). B) Quantification of distance moved by siRNA treated cells. n = 3 experiments with a total of 22 fields of view analysed per treatment. Error bars represent standard error of the mean, significance determined by two-tailed unpaired student's t-test, 'ns' denotes p-value ≥ 0.05. Collaborative work with Emma Jenner is acknowledged image analysis contributing to this figure.

migrating towards EGF.

For a number of the studies in this chapter we chose to use β3-integrin-GFP as our focal adhesion marker. Since there is a link between β1-integrin and EGFR signalling, using a fluorescent-tagged β1-integrin might have been an apparent choice at this stage (Caswell et al., 2008b; Morello et al., 2011). However, this construct is known for being hard to express to detectable levels unless used in cells devoid of the endogenous protein (Parsons et al., 2008). In addition to this, our lab already had experience using the β3-integrin-GFP marker in the MDA-MB-231 cell line. We therefore chose to use this construct (β3-integrin-GFP) rather than travel the more complicated route of ensuring protein knockdown before expression of a construct, which would have been the case if we chose to use β1-integrin-GFP. As with any decision relating to use of single constructs to investigate a point, there may be details we are missing out on. Given more time the use of β1-integrin-GFP in addition to β3-integrin-GFP may have proven useful and delivered more insights into the role of endocytosis in focal adhesion turnover.

We investigated the possibility of clathrin being involved in focal adhesion turnover in a number of ways. We examined colocalisation between fluorescent labelled clathrin and either β3-integrin-GFP (as a focal adhesion protein and a potential endocytic membrane cargo) and paxillin-mRFP (to account for the fact that β3-integrin-GFP might not be present in all focal adhesions). We found only a very low amount of colocalisation and the small amount seen most likely represents random migration due to the sheer number of clathrin spots present these migrating cells (Figures 4.1 & 4.3). Perhaps, however, the focal adhesion components begin their disassembly prior to the arrival of clathrin and, as such, have a fluorescence intensity below the limit of our imaging system by the time of clathrin recruitment. To test this we examined clathrin recruitment to sites of focal adhesion disassembly in the period of time following their disassembly (Figures 4.2 & 4.3). In the cases of both focal adhesion markers we found no clathrin recruitment, so this theory appears not to be the case.

In addition to these colocalisation studies we looked at focal adhesion disassembly time in cells treated with siRNA to inhibit clathrin-mediated endocytosis. In this case we used wound healing as the migratory model due to the lack of migration we see in the agarose spot assay when we employ α-adaptin siRNA. We saw no difference in the time for focal adhesion disassembly in either control or siRNA treated cells, showing again that clathrin appears not to be necessary for this process in migrating MDA-MB-231 cells.

The previously mentioned studies that saw a role for clathrin in focal adhesion disassembly were performed in fibroblasts (Chao and Kunz, 2009; Ezratty et al., 2009). Our results stem both from migration towards a chemoattractant in the agarose spot assay and from wound healing, adding weight to the lack of necessity for clathrin in focal adhesion dynamics in migrating MDA-MB-231 cells. However, most likely the discrepancies between our results and those of other groups are due to cell type specific differences in the requirement for clathrin in this process. Interestingly, we actually found that α-adaptin siRNA did not inhibit migration during wound healing with MDA-MB-231 cells, in contrast to our results observed during chemotactic invasion. This further emphasises that different migratory models require different pathways; thus, clathrin-mediated endocytosis appears to not be necessary for either wound healing or for focal adhesion disassembly in this cell type, but may be a requirement in other cell types or experimental systems.

If clathrin is not necessary for focal adhesion disassembly or integrin internalisation in our system then it begs the question, what is? Since caveolar endocytosis wasn't necessary for cell migration towards EGF in our system we thought it unlikely to be involved in focal adhesion turnover, however, in the interest of completeness we tested this by looking at colocalisation between β3-integrin-GFP and caveolin1-mRFP. As expected we saw no colocalisation between the two and so see this as a highly unlikely route of integrin internalisation in MDA-MB-231 cells (Figure 4.5). As previously discussed work by Gu and colleagues found that in PDGF-stimulated fibroblasts CDRs were re-

sponsible for focal adhesion disassembly, and that similar results could be observed in EGF-stimulated MDA-MB-231 cells (Gu et al., 2011). The aforementioned studies by Ezratty et al. and Chao et al. used wound healing and Transwell migration models, respectively, without the addition of growth factors (other than those that those that occur in FCS), perhaps clathrin is necessary for focal adhesion turnover in these cases but not in growth factor stimulated conditions (Ezratty et al., 2009; Chao and Kunz, 2009). Given more time it would be interesting to investigate whether CDRs have a role in the internalisation of integrins in our EGF-directed migration assay.

4.4 Key chapter findings

- Focal adhesion markers do not colocalise with clathrin in cells migrating in an EGF-directed manner.
- Inhibiting endocytosis does not affect focal adhesion number or distribution.
- Clathrin-mediated endocytosis is not necessary for wound closure in MDA-MB-231 cells.

Chapter 5

Clathrin-mediated endocytosis is polarised towards the front of migrating cells and is responsible for EGFR internalisation in cells migrating towards EGF

5.1 Introduction

Polarisation is very important to the migrating cell. In order to control directionality of migration cells must have methods to respond to chemoattractant gradients and polarise actin-based protrusions to the regions where concentrations of chemoattractant are the highest. Following the binding of attractant molecules to cell surface receptors, signalling cascades lead to the activation of Cdc42 and Rac at this region of highest chemoattractant gradient (Srinivasan et al., 2003). This local activation serves to restrict the area of actin polymerisation, and therefore lamellipodia and filopodia formation, to this area and hence denotes the leading edge (Srinivasan et al., 2003). Complex feedback loops involving both Cdc42 and Rac are in place to ensure sustained activity of both in this

area (Li et al., 2003). Through one particular feedback loop Rac plays a role in establishing more focal contacts at the front of the cell, thereby further enhancing the cells migratory ability (del Pozo et al., 2000; Schwartz and Shattil, 2000). Rho activity is inhibited at the front of the cell by Rac. Similarly due to low Rac activity at the rear of the cell Rho is able to build up in this area and so define it as the back (Sander et al., 1999). Rho prevents the polymerisation of actin at the rear of cells and thus prevents unwanted lamellipodia formation.

With regards to vesicle trafficking the polarisation of pathways is important to ensure the correct localisation of cell surface proteins such as integrins. Integrins are components of focal adhesions which form at the front of cells and are sites of traction to enable migration to occur (Sheetz et al., 1998). The requirement for their disassembly and trafficking to sites of new focal adhesions at the front of cells is therefore apparent. In certain situations, endocytosis of integrins from disassembling focal adhesions in the cell rear has been observed (Bretscher and Aguado-Velasco, 1998; Laukaitis et al., 2001; Lawson and Maxfield, 1995). As well as disassembly of focal adhesions in the rear of migrating cells, a subset appears to be disassembled just behind the lamellipodium (Caswell et al., 2009). A study has shown that the alternative clathrin adaptor, Numb, localises to this region and colocalises with specific integrins (Nishimura and Kaibuchi, 2007). When Numb is inhibited in these cells integrin endocytosis is perturbed, as is the ability of cells to migrate on particular integrin substrates, pointing to a role for Numb polarisation in integrin endocytosis during directed cell migration (Nishimura and Kaibuchi, 2007).

Polarisation of particular vesicle trafficking pathways during migration has also been shown in some cases. Rappoport et al. used live cell TIRF imaging to shown that clathrin-mediated endocytosis is polarised towards the middle-front regions of migrating epithelial cells and others have shown that endocytic recycling is polarised back to the leading edge (Hopkins et al., 1994; Lawson and Maxfield, 1995; Rappoport and Simon, 2003; Strachan and Condic, 2004; Caswell and Norman, 2006). Conversely, caveolar

endocytosis has been observed to occur at the rear of migrating cells, the significance of which is largely unknown (Isshiki et al., 2002; Parat et al., 2003; Fletcher and Rappoport, 2010). Importantly, these studies only encompass a small selection of cell types and migratory models; such polarisation may well depend on the cell type and experimental system as well as other factors.

The EGFR receptor is the receptor for the chemoattractant and signalling molecule EGF. There is evidence that EGFR is able to continue signalling when located on early endosomes in a fashion that seems distinct from its plasma membrane signalling (Di Guglielmo et al., 1994; von Zastrow and Sorkin, 2007; Vieira et al., 1996). As such, there is much interest in studying the internalisation and trafficking of this receptor. The route of internalisation of EGFR is subject to much debate and evidence exists for both clathrin-dependent and clathrin-independent pathways (Sorkina et al., 2002; Motley et al., 2003; Hinrichsen et al., 2003; Huang et al., 2004; Sigismund et al., 2005; Johannessen et al., 2006; Orlichenko et al., 2006; Rappoport and Simon, 2009). Two studies previously reported a clathrin-independent route by showing that AP2 was dispensable for EGFR endocytosis (Motley et al., 2003; Hinrichsen et al., 2003). Two later studies, however, found a necessity for clathrin and AP2, respectively (Huang et al., 2004; Rappoport and Simon, 2009). Importantly, the studies concluding that AP2 was not necessary for EGFR internalisation were mostly conducted at 4°C which may therefore account for the differences between those and the later studies (Boucrot et al., 2010). Further to this, groups have reported a possible role of caveolae in EGFR internalisation, although debate exists over whether this is indeed internalisation or whether caveolae might represent a method of EGFR sequestration prior to EGF stimulation (Sigismund et al., 2005; Orlichenko et al., 2006).

We aim here to elucidate the route of EGFR internalisation in a system of directed migration towards EGF. We also aim to investigate whether this internalisation is polarised in the context of migration.

5.2 Results

5.2.1 EGFR colocalises with clathrin but not caveolin1 in migrating MDA-MB-231 cells

Since inhibiting clathrin-mediated endocytosis caused a decrease in the migration of cells towards EGF we predicted that clathrin-mediated endocytosis could play a role in the internalisation of EGFR during migration. We examined the potential for colocalisation between EGFR and clathrin in migrating cells. Notably when we image EGFR in cells away from EGF spots it appears diffuse in the plasma membrane but when imaged in cells migrating in EGF spots it appears as punctae on the plasma membrane (as seen in Figures 5.1A, B). Results from Chapter 3 established a lack of a role for caveolin1 in MDA-MB-231 cell migration, therefore we used colocalisation between EGFR and caveolin1 as a control in this experiment.

We used TIRF microscopy to image only the adherent plasma membrane of cells migrating towards EGF in agarose spots. Cells were transfected with both EGFR-GFP and clathrin-dsRed and cells migrating into the spot were imaged. During analysis cells were split into front, middle and back regions using the axis perpendicular to the spot edge. At least 50 EGFR clusters were circled per cell, split evenly between the three regions, and the number of these which were also positive for clathrin was noted. As a control for random colocalisation the circles drawn around EGFR clusters were moved to regions not containing EGFR and the number of these which were positive for clathrin was noted. The same analysis was repeated with EGFR-GFP and caveolin1-mRFP. As can be seen in Figure 5.1B & C there is a much higher degree of colocalisation between EGFR-GFP and clathrin-dsRed, compared to EGFR-GFP and caveolin1-mRFP. When control values were accounted for the colocalisation between EGFR-GFP and caveolin1-mRFP is about 5%, with colocalisation between EGFR-GFP and clathrin-dsRed being close to 50%, almost 10-fold higher.

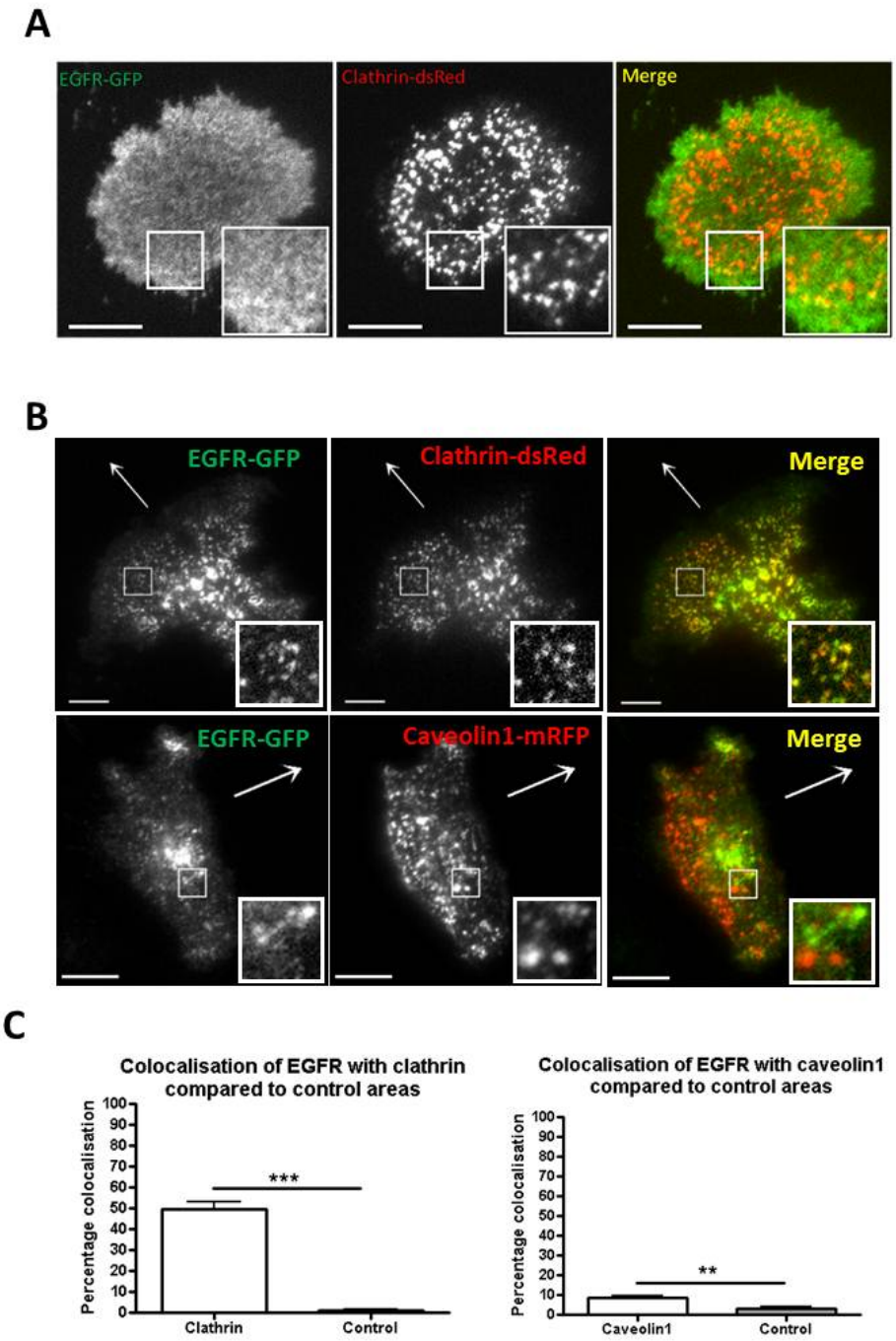

Figure 5.1: Colocalisation between clathrin-dsRed and EGFR-GFP in migrating cells. A) Imaging of clathrin-dsRed and EGFR-GFP in cells with no EGF stimulation. Scale bars are 10 μm. n = 1 experiment with 20 cells imaged to ensure consistency. B) Representative images of EGFR-GFP with clathrin-dsRed or caveolin1-mRFP in cells migrating towards EGF. Arrows denote the direction of migration. Scale bars are 10 μm. C) Quantification of colocalisation of EGFR-GFP with clathrin-dsRed and caveolin1-mRFP. n = 3 experiments with a total of 14 cells analysed for each condition. Error bars represent standard error of the mean, significance determined by two-tailed unpaired student's t-test, ** denotes p-value < 0.01, *** denotes p-value < 0.001.

We next performed live cell rapid TIRF imaging of EGFR-GFP and clathrin-dsRed in migrating cells. We found that we could observe instances of both internalising together, verifying that some of these colocalisation events result in internalisation. Figure 5.2A and B shows a timecourse of one such internalisation event. Interestingly, we were also able to observe instances of EGFR without clathrin colocalisation moving in the plane of the plasma membrane (Figure 5.2C); likely post-endocytic structures or post-Golgi vesicles. Since we observed such structures quite regularly this could mean that some EGFR clusters counted in the previous experiment (Figure 5.1) were of this category and therefore our quantification of colocalisation between clathrin and EGFR on the plasma membrane may be even higher than originally thought.

We tested whether Dynasore treatment would have any effect on the colocalisation between EGFR and clathrin. Perhaps if EGFR entry was inhibited we would see an increase in colocalisation as more clathrin structures contain EGFR trying to internalise, or if EGFR were to be internalised via an alternative pathway following inhibition perhaps we would see a decrease in colocalisation. We repeated the above analysis with the addition of Dynasore or DMSO for the control cells. As can be seen in Figure 5.3, Dynasore has no effect on the colocalisation between EGFR and clathrin. As an alternative we also decided to analyse whether inhibiting endocytosis with Dynasore had any effect on either the size of clathrin clusters or the number present on the plasma membrane of migrating cells. We performed this analysis on cells as a whole and also broken down by area to see if there were any region specific effects. For the cluster size analysis cells were split into front, middle and back regions and 10 clusters per region in each cell were measured to establish their area. As can be seen in Figure 5.4A, the average apparent cluster size over the cell as a whole increased by 18% following Dynasore treatment, and this increase was more pronounced at the front and back of migrating cells, but less so in the middle (Figure 5.4B). It should be noted that these cluster area measurements were approaching the resolution limit of a light microscope, therefore numbers might not be as accurate as intended. However the error bars for this analysis were small meaning

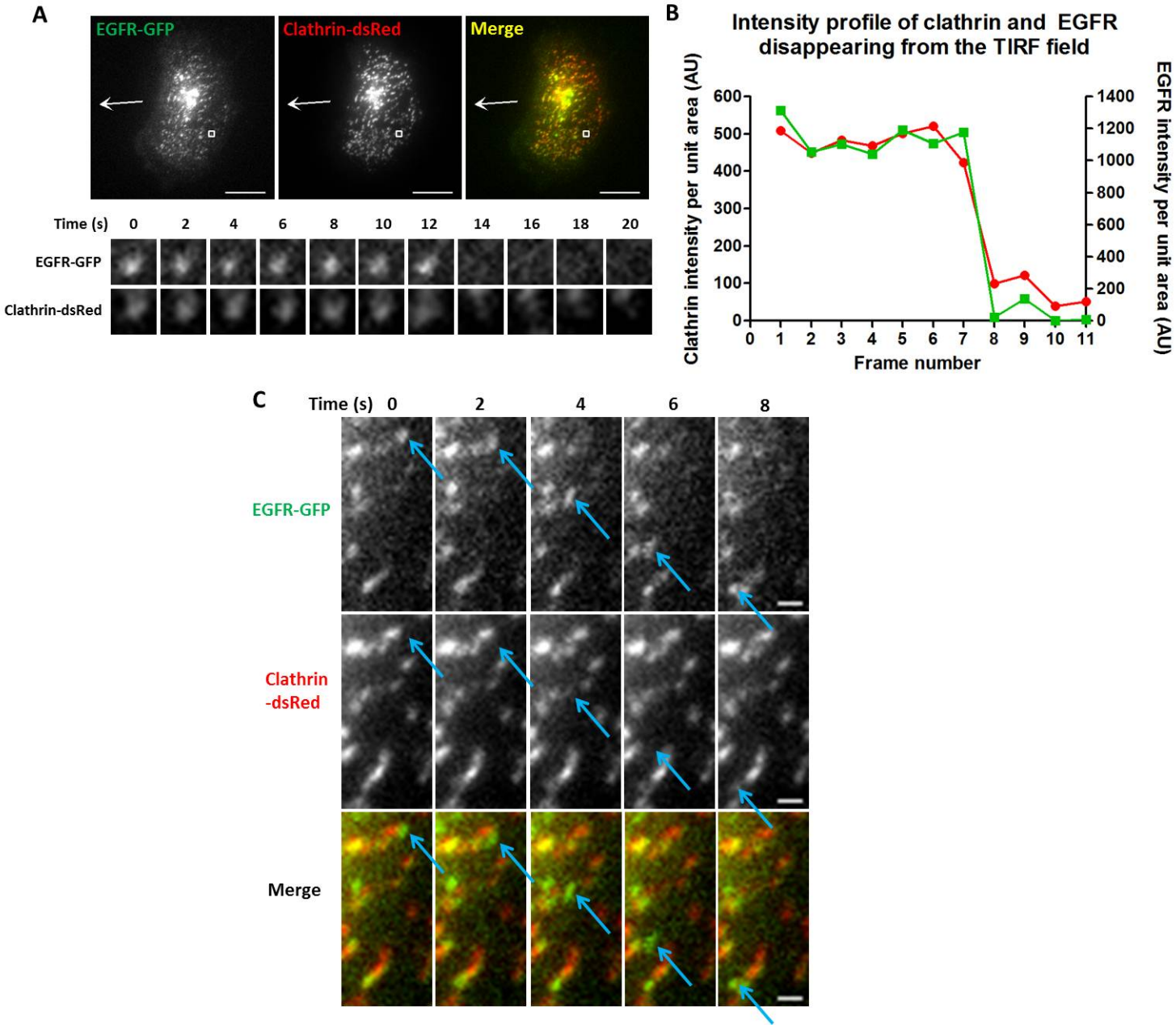

Figure 5.2: Live cell TIRF imaging of clathrin-dsRed and EGFR-GFP. A) Representative image to show instance of both markers leaving the TIRF field at the same time. Time between frames is 2 seconds. Arrows denote the direction of migration. Scale bars are 10 μm. B) Graph shows a quantification of the intensity over time for the clathrin/EGFR spot identified in (A), the clathrin-dsRed intensity is shown by the red line (circular points), the EGFR-GFP intensity is shown by the green line (square points). C) An instance showing directed motility of an EGFR cluster devoid of clathrin. Scale bars are 1 μm.

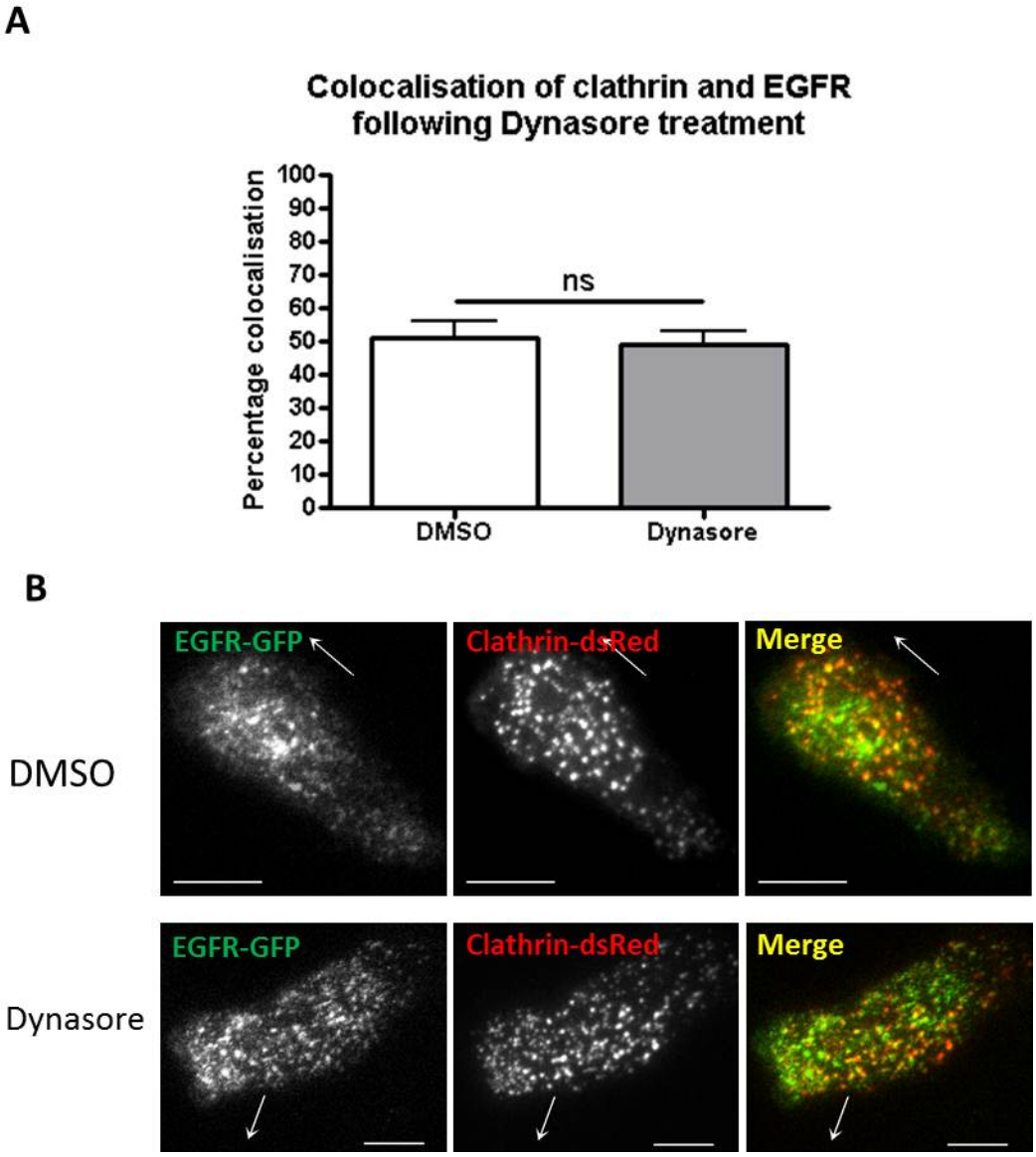

Figure 5.3: Colocalisation between clathrin-dsRed and EGFR-GFP in migrating cells following Dynasore treatment. A) Quantification of the total number of EGFR clusters that colocalise with clathrin in cells migrating towards EGF treated with either DMSO or Dynasore. B) Representative images of EGFR-GFP and clathrin-dsRed in cells with and without Dynasore treatment. n = 3 experiments with a total of 13 cells analysed per treatment. Error bars represent standard error of the mean, significance determined by two-tailed unpaired student's t-test, 'ns' denotes p-value ≥ 0.05.

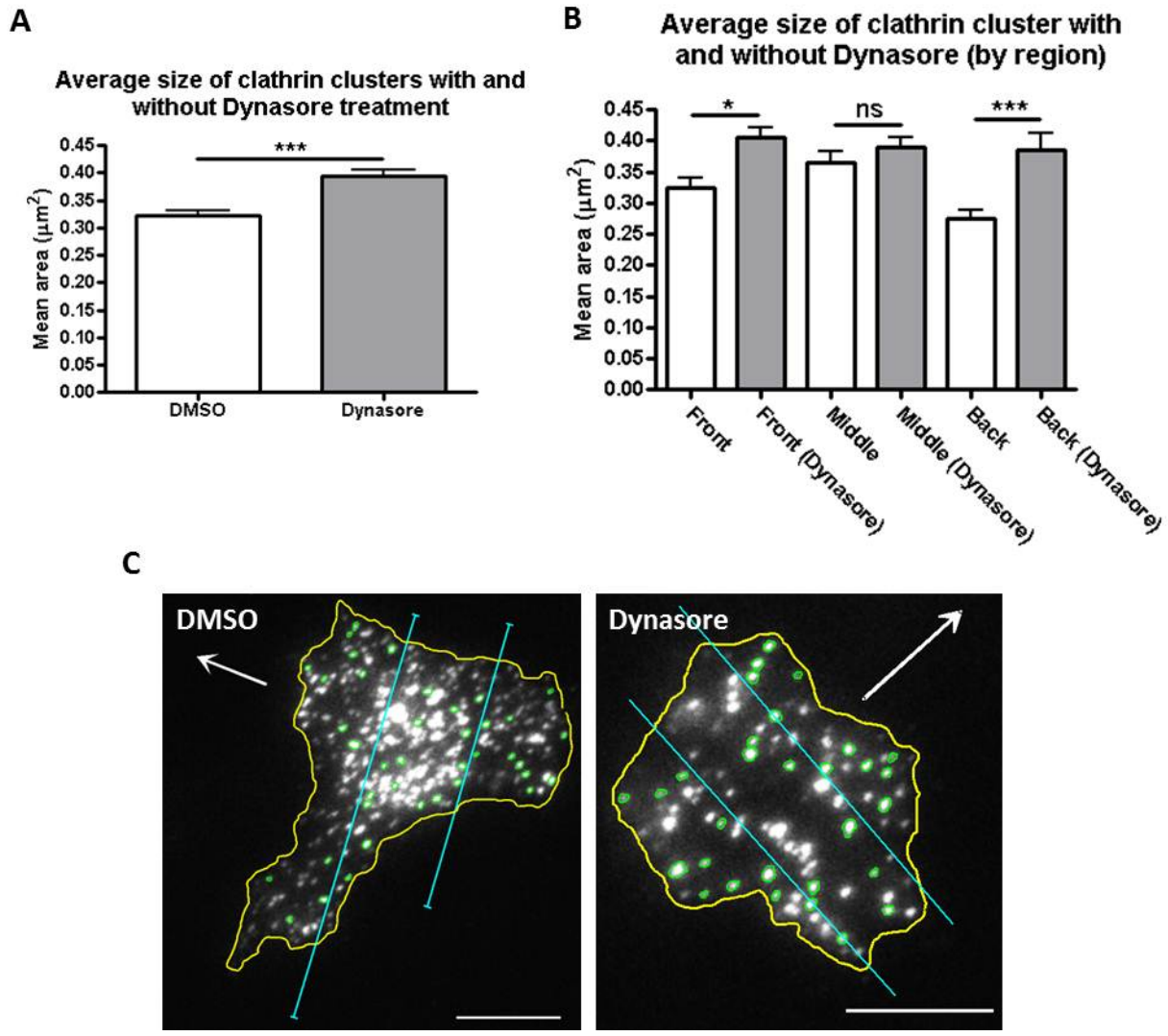

Figure 5.4: Investigating whether any changes occur to the size of clathrin-dsRed clusters in migrating cells following Dynasore treatment. A) Mean area of clathrin clusters over the whole cell. Error bars represent standard error of the mean, significance determined by two-tailed unpaired student's t-test, *** denotes p-value < 0.001. B) Mean area of clathrin clusters broken down by region. C) Representative images of clathrin cluster size analysis. Green circles show clusters analysed for their area. Arrows denote the direction of migration. Scale bars are 10 μm. n = 3 experiments with ≥ 9 cells analysed per treatment and a minimum of 10 clusters being analysed per cell (total 90 clusters analysed per treatment). Error bars represent standard error of the mean, significance determined by one way ANOVA followed by Tukey's post-test, 'ns' denotes p-value ≥ 0.05, * denotes p-value < 0.05, *** denotes p-value < 0.001.

that whether the actual values were accurate or not there is still likely to be a significant difference between the two treatments. No differences were observed in the number of clathrin clusters present in these cells, whether analysing the cell as a whole or by region (Figure 5.5).

We performed the same analysis on EGFR-GFP clusters in these migrating cells treated with Dynasore. We found no differences in the average area of EGFR clusters per cell, nor were there any differences in the areas in any particular region following Dynasore treatment (Figure 5.6). The total number of EGFR clusters per cell was also no different following Dynasore treatment (Figure 5.7A) but when analysed by region the number of EGFR clusters was skewed following Dynasore treatment with there being a slight build up at the front (Figure 5.7B and C).

5.2.2 Clathrin-mediated endocytosis events occur more frequently at the front of migrating cells

In order to establish whether endocytosis events were polarised in our model of migration we imaged clathrin-dsRed in migrating cells. TIRF microscopy was employed again to rapidly image clathrin at the plasma membrane of migrating cells for one minute time-lapses. The disappearance of clathrin from the evanescent field was taken to be due to endocytosis only if it was not due to photobleaching, if it occurred rapidly and if it did not reappear in the evanescent field for the duration of the time-lapse (Rappoport and Simon, 2003).

Using the previously established method for denoting the front, middle and back of migrating cells, the number of endocytosis events within each of these regions during the one minute time-lapses was analysed (Figure 5.8). After normalising the data to ensure equal weighting we felt a cut-off was necessary to ensure that cells with very low numbers of events would not skew the analysis. For this reason we only counted cells with three or more internalisation events. It was found that endocytosis occurred

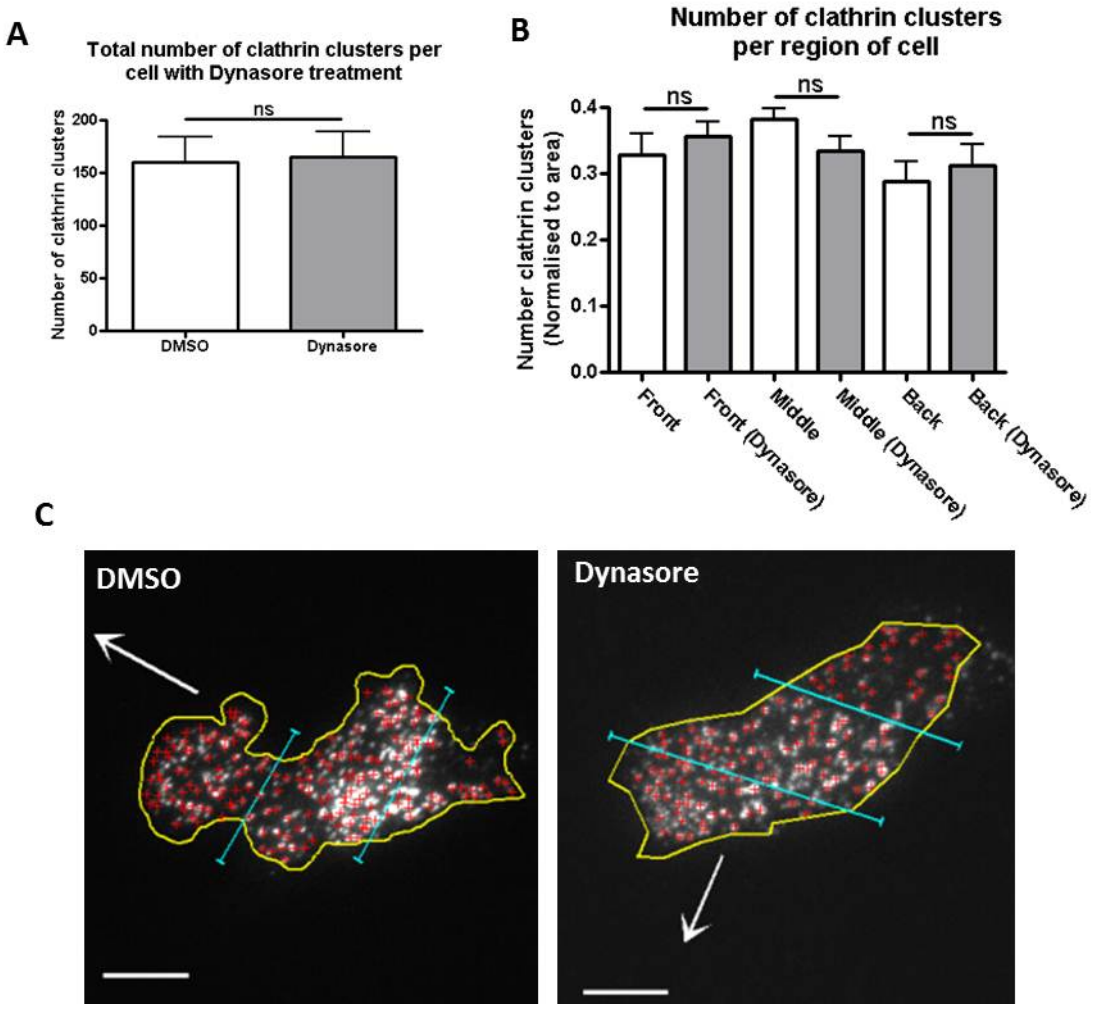

Figure 5.5: Investigating to number of clathrin-dsRed clusters at the plasma membrane of migrating cells with Dynasore treatment. A) Overall there is no significant increase in the number of clusters following Dynasore treatment. Error bars represent standard error of the mean, significance determined by two-tailed unpaired student's t-test, 'ns' denotes p-value ≥ 0.05. B) Quantification of clathrin clusters by cell region with and without Dynasore treatment, number normalised relative to the area of the region. C)Representative images of clathrin cluster counts in migrating cells. Arrows denote the direction of migration. Scale bars are 10 μm. n = 3 experiments with a total of 12 cells analysed per treatment. Error bars represent standard error of the mean, significance determined by one way ANOVA followed by Tukey's post-test, 'ns' denotes p-value $\geq$ 0.05.

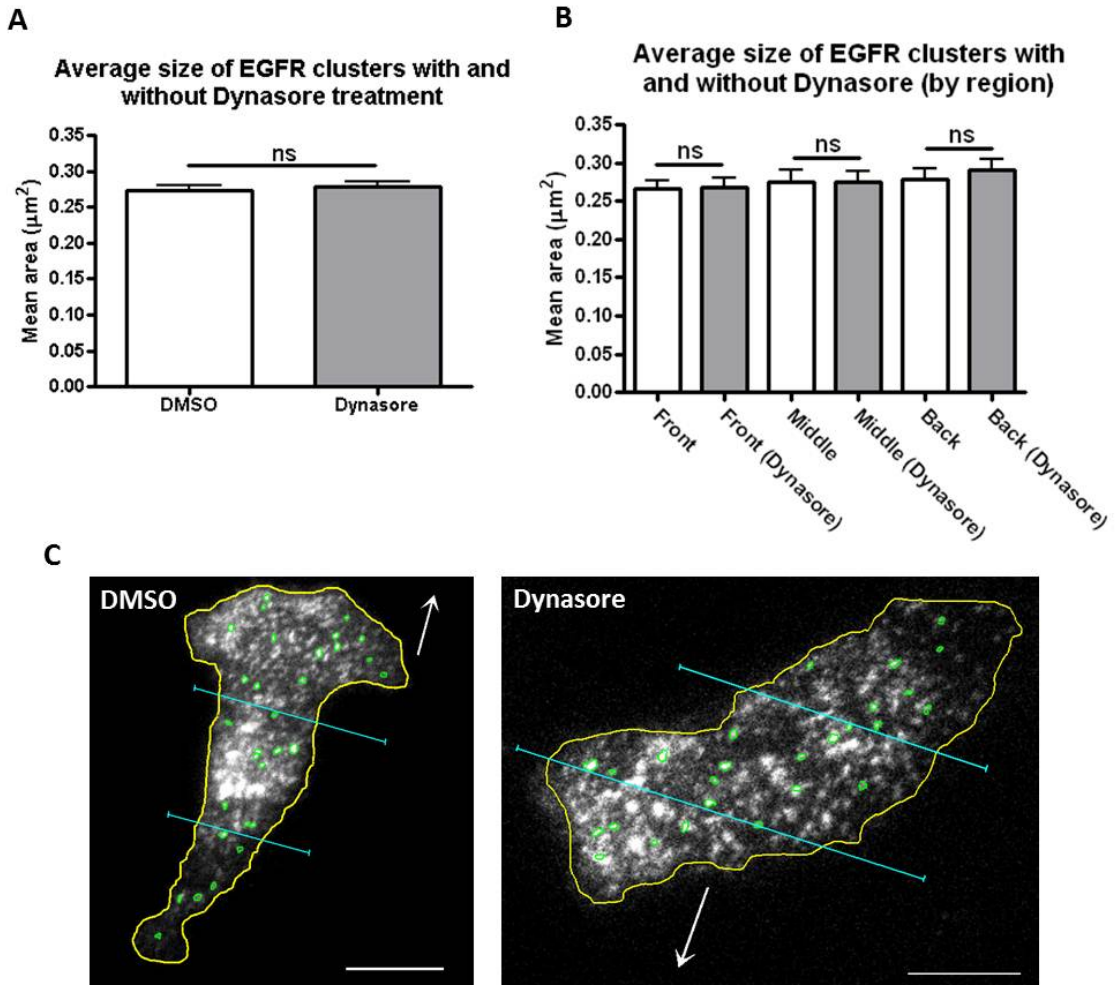

Figure 5.6: Investigating whether any changes occur to the size of EGFR clusters in migrating cells following Dynasore treatment. A) Mean area of EGFR clusters over the whole cell. Error bars represent standard error of the mean, significance determined by two-tailed unpaired student's t-test, 'ns' denotes p-value ≥ 0.05. B) Mean area of EGFR clusters broken down by region. No significant differences were observed in any case. C) Representative images of EGFR cluster size analysis. Green circles show clusters analysed for their area. Arrows denote the direction of migration. Scale bars are 10 μm. n = 3 experiments with ≥ 9 cells analysed per treatment and a minimum of 10 clusters being analysed per cell (total 90 clusters analysed per treatment). Error bars represent standard error of the mean, significance determined by one way ANOVA followed by Tukey's post-test, 'ns' denotes p-value ≥ 0.05.

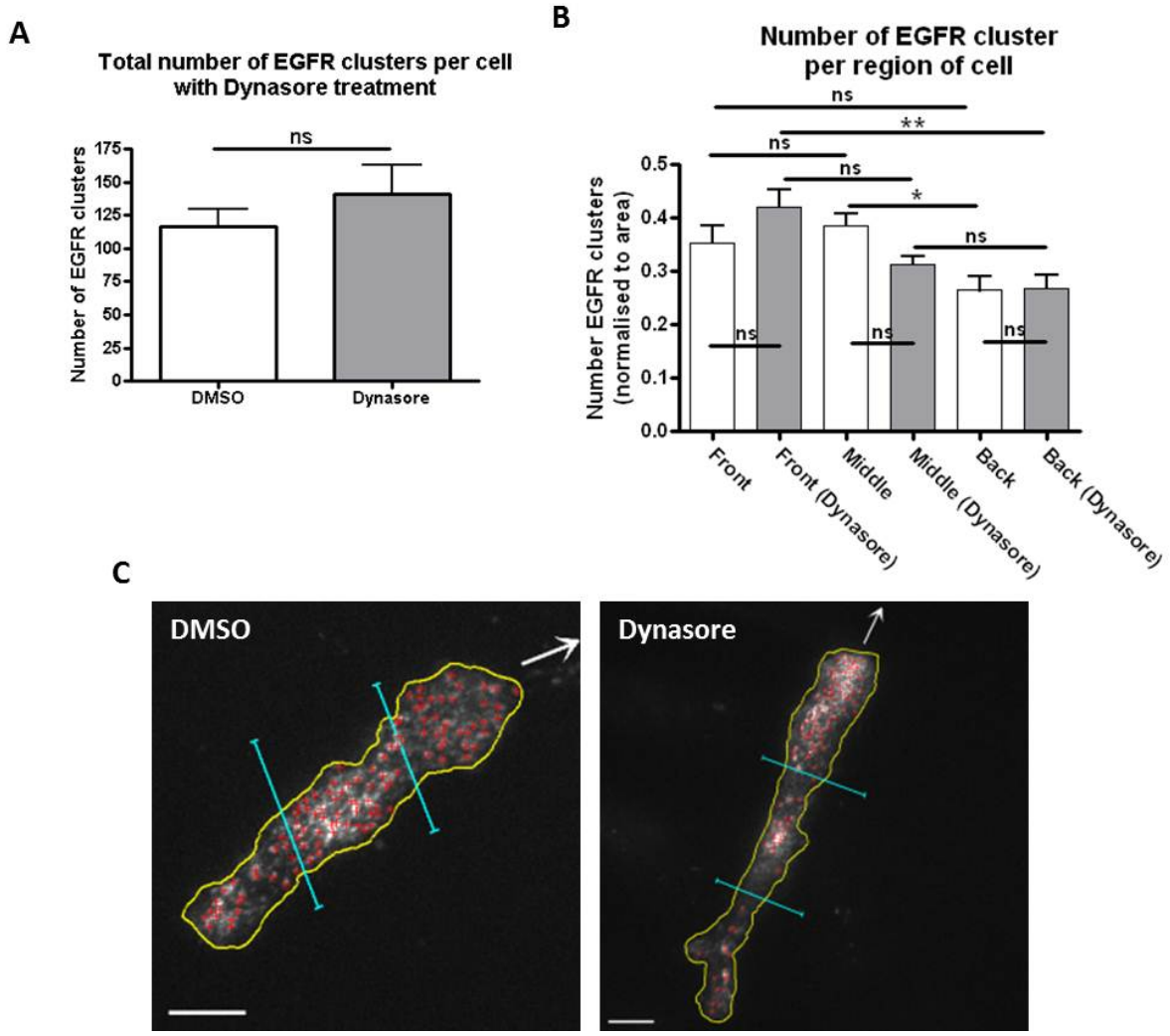

Figure 5.7: Investigating to number of EGFR clusters at the plasma membrane of migrating cells with Dynasore treatment. A) Overall there is no significant increase in the number of clusters following Dynasore treatment. Error bars represent standard error of the mean, significance determined by two-tailed unpaired student's t-test, 'ns' denotes p-value ≥ 0.05. B) Representative images of EGFR cluster counts in migrating cells. Arrows denote the direction of migration. Scale bars are 10 μm. C) Quantification of EGFR clusters by cell region with and without Dynasore treatment, numbers normalised relative to the area of the region. n = 3 experiments with 12 cells analysed per treatment. Error bars represent standard error of the mean, significance determined by one way ANOVA followed by Tukey's post-test, 'ns' denotes p-value ≥ 0.05, * denotes p-value < 0.05, *** denotes p-value < 0.001.

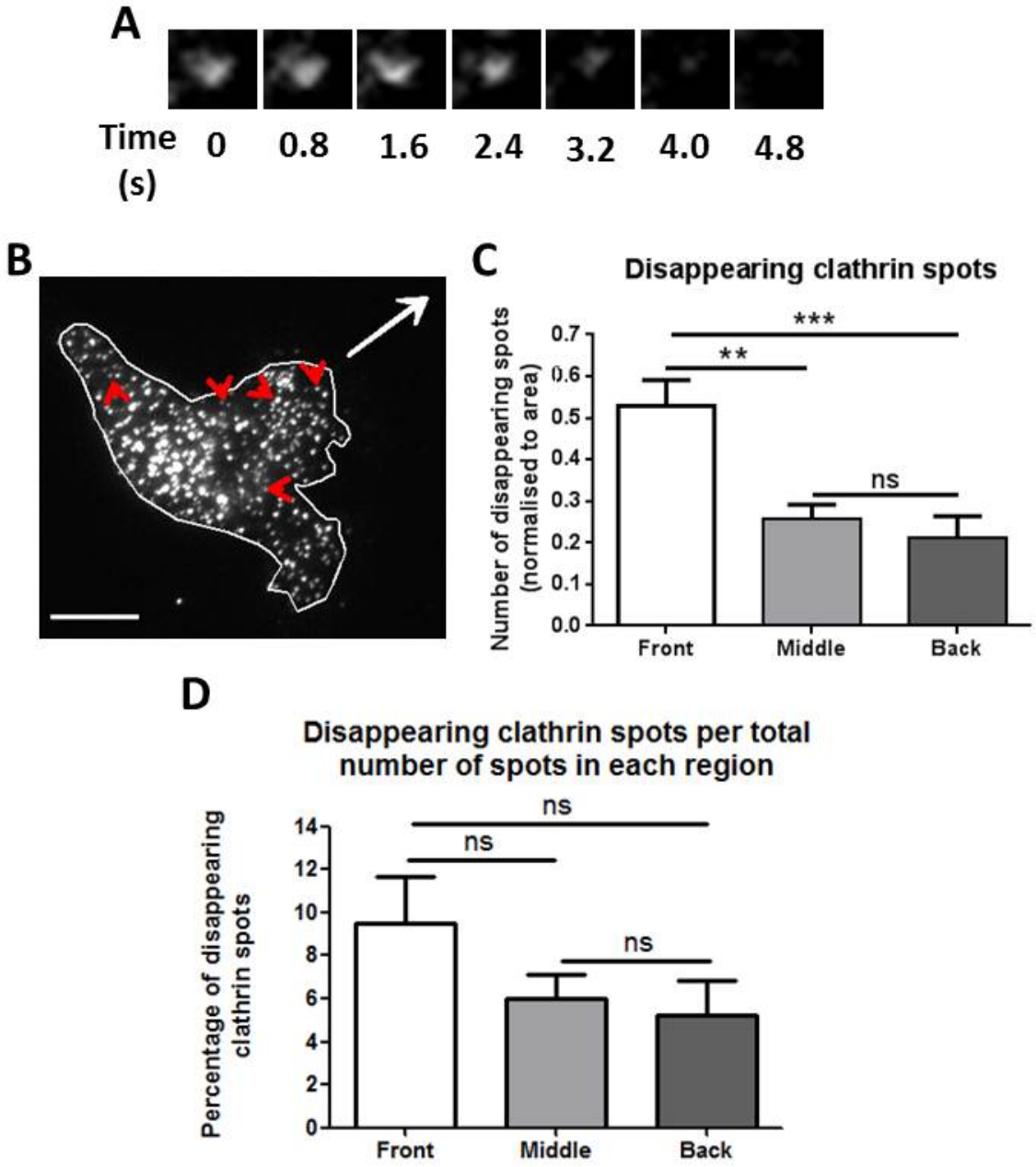

Figure 5.8: Clathrin spot disappearance is polarised to the front of migrating cells. A) Representative images of a clathrin spot disappearing from the TIRF imaging field. B) Representative image of a clathrin-dsRed expressing migrating cell with arrows to indicate instances of clathrin disappearance. Arrow denotes the direction of migration. Scale bars are 10 μm. C) Quantification of clathrin disappearance by cell region. D) Quantification of clathrin disappearance compared to total number of spots in each region. For C) and D) cells were used for quantification if they contained 3 or more internalisation events. n = 4 experiments with a total of 18 cells analysed. Error bars represent standard error of the mean, significance determined by one way ANOVA followed by Tukey's post-test, 'ns' denotes p-value ≥ 0.05, ** denotes p-value < 0.01, *** denotes p-value < 0.001.

significantly more frequently at the front of migrating cells than the middle or the back. Furthermore, we tested whether the likelihood of occurrence of endocytic events was increased at the front of the cells and found this not to be the case (Figure 5.8D). Thus we can conclude that more clathrin-mediated endocytosis is occurring in this region and so the pathway appears to be polarised towards the front in cells migrating towards EGF.

5.3 Discussion

As a means to try and establish the route of EGFR internalisation in cells migrating towards EGF we assessed colocalisation of EGFR-GFP with clathrin-dsRed in the agarose spot assay. Using TIRF microscopy we were able to image only events at or close to the plasma membrane thereby increasing the probability that clathrin-positive structures present were potential sites of endocytosis. As a control we also assessed the colocalisation between the EGFR-GFP construct and caveolin1-mRFP. After controlling for random colocalisation the colocalisation between EGFR-GFP and clathrin-dsRed was almost 10-fold that between EGFR-GFP and caveolin1-mRFP (Figure 5.1). We also established that by TIRF imaging we could view instances of EGFR-GFP and clathrin-dsRed internalisation together, although this imaging was not rigorous enough to assess all internalisation events (Figure 5.2). These results indicate a clathrin-mediated endocytosis route for the EGFR in cells migrating in an EGF-dependent manner.

In the literature there is much support for a clathrin-dependent route of EGFR endocytosis (Sorkina et al., 2002; Huang et al., 2004; Johannessen et al., 2006; Rappoport and Simon, 2009) but also contrary evidence supporting a clathrin-independent route in certain situations (Hinrichsen et al., 2003; Motley et al., 2003; Sigismund et al., 2005; Orlichenko et al., 2006; Sigismund et al., 2008). In support of our findings, previous work by Huang et al. and Rappoport et al. demonstrated that in non-migrating cells the EGFR enters primarily through clathrin-coated pits and not through caveolae (Huang

et al., 2004; Rappoport and Simon, 2009). To assess whether we could see endocytosis events happening in real time we undertook TIRF time-lapse experiments of clathrin-dsRed and EGFR-GFP in migrating cells. We were able to see many instances of both markers disappearing from the same point together, suggesting that clathrin-mediated endocytosis is the main route of internalisation of the EGFR in our migratory model.

We investigated whether using Dynasore to inhibit endocytosis in cells migrating in the spot assay would have any effect on the colocalisation of clathrin-dsRed and EGFR-GFP. In this case we saw no observed differences between the control (DMSO) and Dynasore treated groups (Figure 5.3). Dynasore inhibits dynamin and therefore the stage of endocytosis where the vesicle is detached from the membrane, it is therefore likely that EGFR recruitment to the forming pit was still able to occur prior to endocytosis being halted at the stage of vesicle fission. However, when we tested the effect of Dynasore on the area of clathrin structures on the plasma membrane we saw an 18% increase in size in the Dynasore treated group (Figure 5.4). This could indicate that clathrin is continuing to be recruited to sites of vesicle formation under circumstances when they are not able to pinch off the membrane. The increase in clathrin cluster size was more exaggerated at the front and rear of migrating cells, although we are unsure of the significance of this observation. It might also be expected that the number of clathrin clusters present at the plasma membrane might increase following Dynasore treatment, although in our system we found this not to be the case (Figure 5.5).

In addition to analysing the effect Dynasore had on clathrin structures on the plasma membrane of migrating cells, we looked to see if there were any similar effects on EGFR clusters. Unlike clathrin, the size of EGFR clusters remained the same, which could mean that after a certain point no further cargo is recruited to the forming pits, although more clathrin might be (Figure 5.6). Perhaps this lack of further cargo recruitment is due to the pit being in a closed state with dynamin at the neck ready to pinch off the membrane, and so no further cargo incorporation can occur.

An emerging idea is that polarised vesicle trafficking is involved in the regulation of directed cell migration. A link between polarised trafficking of cell adhesion components has been shown in a number of cell types (Nishimura and Kaibuchi, 2007; Caswell et al., 2009; Ulrich and Heisenberg, 2009; Thapa et al., 2012). The occurrence of polarised trafficking of chemoattractant receptors is less well studied than that of focal adhesions, but it is becoming more apparent that it may play a role in the regulation of directed cell migration. A recent study by Assaker et al. found that particular endocytic proteins were necessary to control the trafficking, and hence spatial polarisation, of receptor tyrosine kinases during Drosophila border cell migration (Assaker et al., 2010). Another study by Belleudi et al. found endocytosis and polarised recycling of the keratinocyte growth factor receptor regulated receptor polarisation at the plasma membrane, and that this was necessary for keratinocyte migration (Belleudi et al., 2011). In order to investigate the possibility of polarised receptor trafficking during chemotactic invasion in MDA-MB-231 cells, we tested whether Dynasore treatment produced a redistribution of EGFR localisation. The results of these studies demonstrated an accumulation of EGFR towards the front of migrating cells (Figure 5.7). This implies that EGFR internalisation is polarised to the front of migrating cells, as inhibition of endocytosis caused a build-up in this region.

We were then led to test whether clathrin-mediated endocytosis is polarised in MDA-MB-231 cells during EGF direct chemotactic invasion. As expected, we saw an increase in the number of internalisation events at the front of cells migrating towards EGF rather than at the middle or back (Figure 5.8). In addition to the necessity for clathrin-mediated endocytosis for migration in this model, these results imply that polarised endocytosis of the EGFR is important for migration in this breast cancer cell line.

5.4 Key chapter findings

- EGFR colocalises with in MDA-MB-231 cells migrating in an EGF-dependent manner, but does not colocalise with caveolin1.
- When endocytosis is inhibited more EGFR is present at the front of migrating cells than at the back, as opposed to a uniform distribution under control conditions.
- Clathrin internalisation events are polarised towards the front of EGF-directed migrating cells.

Chapter 6

Endosomal recycling and exocytosis

6.1 Introduction

As discussed earlier, the process of endocytosis is important to cell migration as it may affect signalling from chemoattractant receptors, availability of such receptors and also the localisation of adhesion molecules. Similarly trafficking of receptors and adhesion molecules to the cell surface must also be important for cell migration. Trafficking to the cell surface can occur either through the biosynthetic secretory route or by pathways which recycle internalised proteins back to a location on the cell surface.

Trafficking of newly synthesised cargo is a process which has been shown to be necessary for cell migration in fibroblasts (Bershadsky and Futerman, 1994; Prigozhina and Waterman-Storer, 2004). As previously mentioned, using strategies to disrupt post-Golgi secretion of cargo prevented Swiss 3T3 fibroblasts from polarising in the direction of migration and inhibited the migration of these cells. The orientation of the Golgi towards the leading edge of migrating cells also appears to be important for cell migration (Gotlieb et al., 1981; Yadav et al., 2009). In wound healing experiments Yadav et al. showed polarised protein secretion from the Golgi, which was abrogated when Golgi position was disrupted and this led to a failure of these cells to close the wound (Yadav et al., 2009). These results indicate that the polarised positioning of the Golgi

is important for polarised protein secretion and consequently for correct cell migration.

Recycling pathways exist to traffic internalised cargo back to the plasma membrane. The Rab4-dependent short-loop recycling pathway traffics cargo directly from the early endosome back to the plasma membrane (Grant and Donaldson, 2009; Maxfield and McGraw, 2004). This pathway has been shown to be the major route of transferrin receptor recycling as well as for some integrins and has been shown to be important for polarised integrin recycling in fibroblasts as inhibition prevents directional migration in this system (Woods et al., 2004; Jones et al., 2006; White et al., 2007). The other major recycling pathway is Rab11-dependent and involves trafficking of cargo via the juxtanuclear PNRC in a long-loop recycling route (Maxfield and McGraw, 2004). This route is also thought to be necessary for recycling of some integrins which are seen in a juxtanuclear compartment after internalisation (Jones et al., 2006; Caswell and Norman, 2006). Like the short-loop pathway this Rab-11 dependent route has been implicated in cell migration; dominant-negative Rab11 expression perturbs migration in various cell types and migration systems (Mammoto et al., 1999; Prigozhina and Waterman-Storer, 2006).

Since these exocytic pathways have been shown to be necessary for migration in some cell types we decided to try and deduce which pathway or pathways are important for EGFR exocytic trafficking and whether this trafficking was polarised in migrating cells.

6.2 Results

To assess EGFR fusions we used TIRF microscopy to image cells expressing EGFR-GFP migrating in EGF spots. We imaged every 100 ms for a total of one minute. True fusions events were validated in two ways. The first method used a line scan where a line was draw across the fusion region and the fluorescence intensity of each pixel of the line was measured over the course of the fusion event. As fusion occurs the intensity should be high and localised in the centre of the line scan and as the fluorescent marker

diffuses laterally in the plasma membrane the intensity should give a lower but wider peak. A line scan of one fusion event is shown in Figure 6.1. The second method to validate a fusion event is to measure the area and fluorescence intensity of the fluorescent marker over the course of a fusion. The fluorescence intensity should firstly increase as the vesicle approaches and subsequently fuses with the plasma membrane, the intensity should then remain approximately constant as the area increases as the vesicle contents diffuse laterally in the plane of the plasma membrane. An area/intensity analysis of a fusion event is shown in Figure 6.2.

Once confident that we could identify and validate fusion events we analysed the TIRF time-lapses of EGFR-GFP transfected cells migrating in EGF spots to assess the localisation of fusion events. We split the cells into front, middle and back regions, as previously described, and normalised the data. As with the clathrin internalisation data (Figure 5.8) we only counted cells with three or more events to ensure that cells with very low numbers of events would not skew the analysis. The data shows a trend whereby the most fusion events occur at the front (48%), followed by the middle (34%) and then back (18%), however the data is only significant between the front and back regions (Figure 6.3). This suggests that exocytosis of EGFR is polarised towards the front of MDA-MB-231 cells migrating in an EGF spot.

Following the investigation of the localisation of fusions events we next sought to test which pathways played a significant role in EGFR trafficking to the plasma membrane. We decided to investigate the secretory pathway and the long-loop recycling pathways. Ideally we would have also included the short-loop pathway in this investigation however time constraints prevented us from doing so. We again utilised NPY-mRFP as a marker for biosynthetic cargo and undertook TIRF imaging of live cells expressing this construct migrating in EGF spots. To assess colocalisation we circled all NPY-mRFP clusters in the migrating cells (this was between 13 and 50 clusters, dependent on the cell) then switched to the green EGFR-GFP image and counted the number that were positive for EGFR clusters. To assess the likelihood of colocalisation happening by random

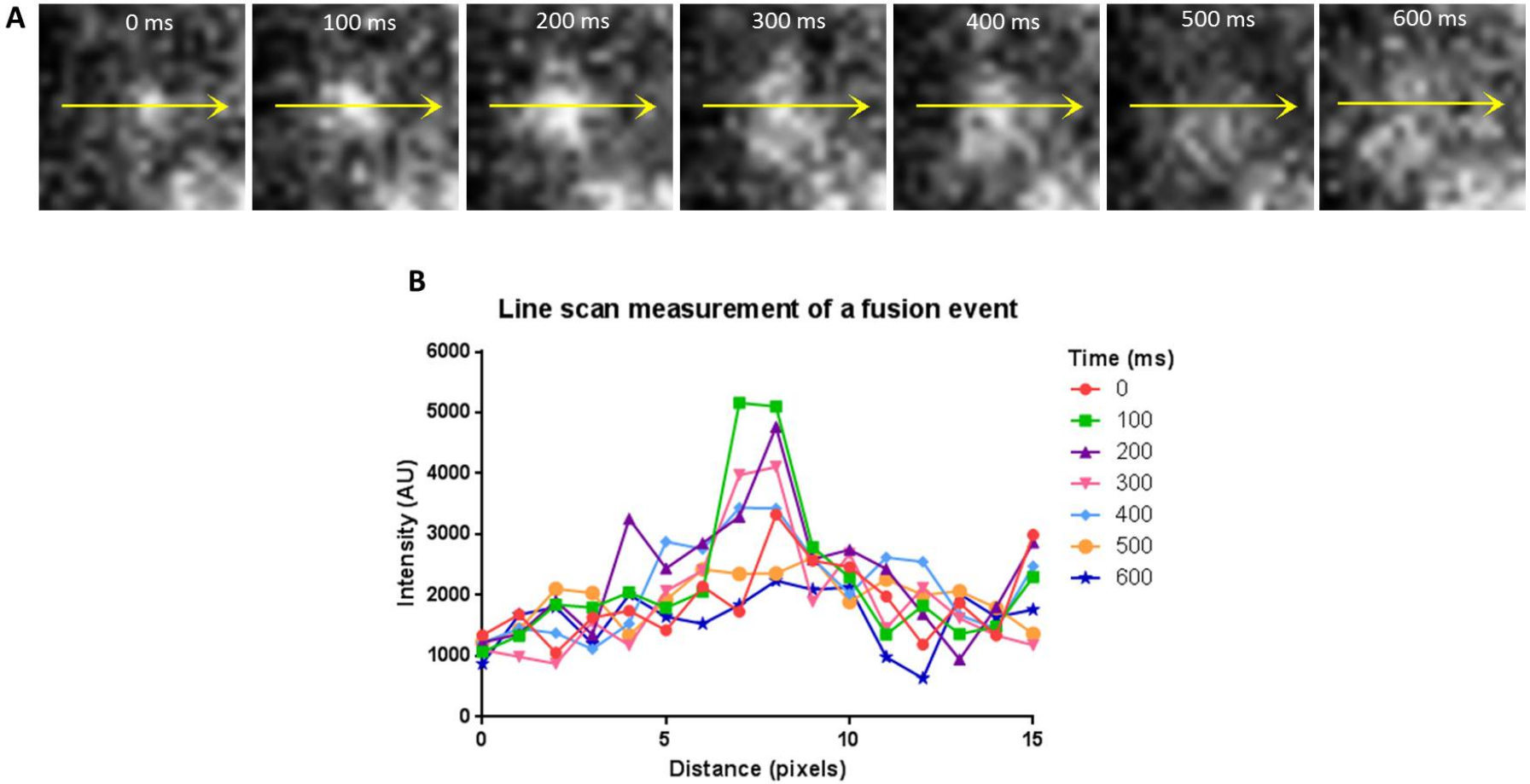

Figure 6.1: Validation of a fusion event by line scan. A) Shows TIRF images of a vesicle fusing with the plasma membrane and subsequent diffusion of the EGFR-GFP marker in the plane of the membrane. The line denotes the region of the line scan used for validation analysis. B) Shows the fluorescence intensity of each pixel of the line scan over the course of fusion.

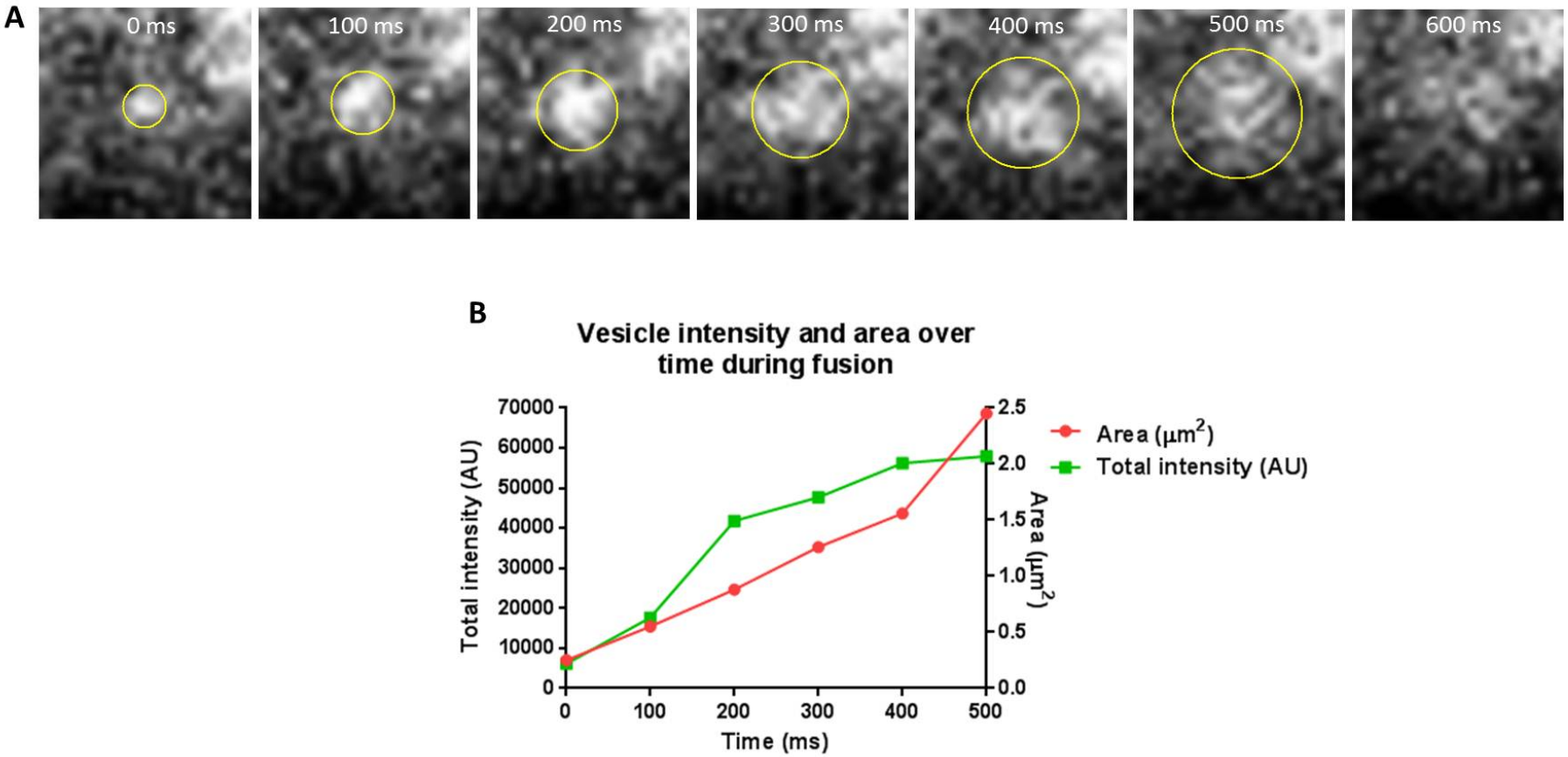

Figure 6.2: Validation of a fusion event by area/intensity analysis. A) Shows TIRF images of a vesicle fusing with the plasma membrane and subsequent diffusion of the EGFR-GFP marker in the plane of the membrane. The circle shows the area analysed for each frame. B) Shows the area and fluorescence intensity within each area for each time point.

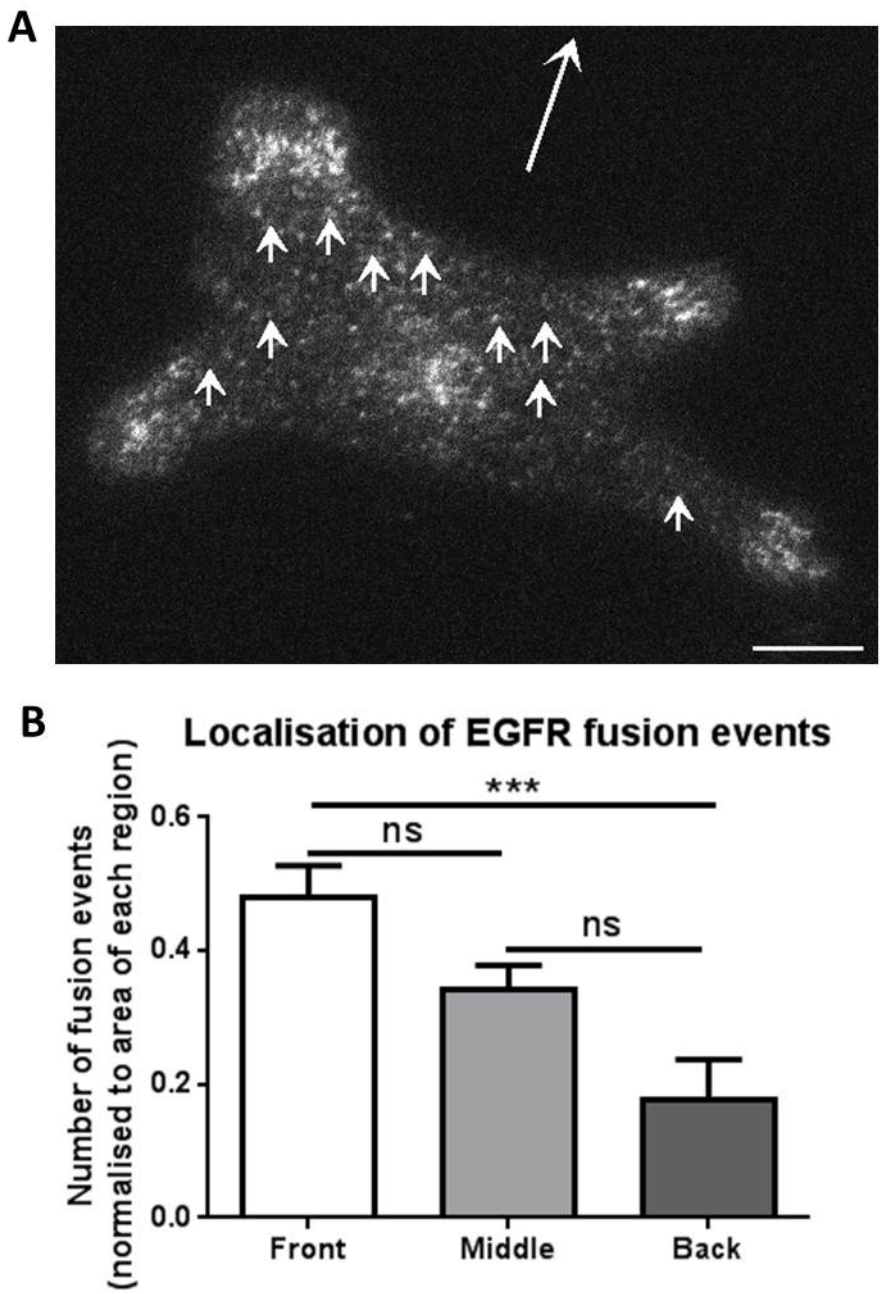

Figure 6.3: Localisation of EGFR-GFP exocytic fusion events. A) Shows a representative TIRF image of a cell expressing EGFR-GFP and migrating in an EGF spot. Regions where fusion events occurred within the one minute time-lapse are indicated by the arrows. Arrow denotes the direction of migration. Scale bars 10 μm. B) Quantification of the localisation of EGFR-GFP fusion events in migrating cells normalised to the area of each region. Cells were used for quantification if they contained 3 or more fusion events. n = 4 experiments with a total of 22 cells analysed. Error bars represent standard error of the mean, significance determined by one way ANOVA followed by Tukey's post-test, 'ns' denotes p-value ≥ 0.05, *** denotes p-value < 0.001. Collaborative work with Robert Lees is acknowledged for performing experiments and imaging which contributed to this figure.

chance we took the circled regions in the red channel image and moved them to regions not containing NPY-mRFP clusters, we then counted how many of these regions were positive for EGFR in the green channel. For this analysis we found the number of NPY clusters colocalised with EGFR to be 21% and the amount of random colocalisation to be 13% (Figure 6.4). The biosynthetic pathway therefore likely counts for a small portion of the EGFR being trafficked to the plasma membrane when cells are migrating in an EGF-dependent manner.

In order to assess the role of the long-loop recycling pathways in EGFR trafficking we repeated the above colocalisation analysis using Rab11a-mCherry in place of NPY-mRFP, as the marker for long-loop recycling. When analysing colocalisation we circled all distinguishable Rab11a-mCherry punctae in the red channel (between 24 and 258 punctae) and counted how many colocalised with EGFR-GFP clusters in the green channel. We assessed for random colocalisation by the same methods as with NPY-mRFP. The percentage of Rab11a punctae that colocalised with EGFR was 44% with 6% random colocalisation, meaning that 38% of this was true colocalisation of the two markers (Figure 6.5). This shows that the Rab11-dependent long-loop recycling pathway likely accounts for a significant proportion of EGFR present on the plasma membrane during migration.

6.3 Discussion

As stated previously polarised trafficking has long been thought to play a role in directed migration, especially in the context of integrins (Nishimura and Kaibuchi, 2007; Caswell et al., 2009; Ulrich and Heisenberg, 2009; Thapa et al., 2012). Many studies have therefore sought to investigate the trafficking pathways taken by integrins into and around the migrating cell. Studies into the trafficking of chemoattractant receptors have mostly taken place in the context of non-migratory cells, although some studies are emerging that investigate receptor trafficking in the context of migration (Caswell et al.,

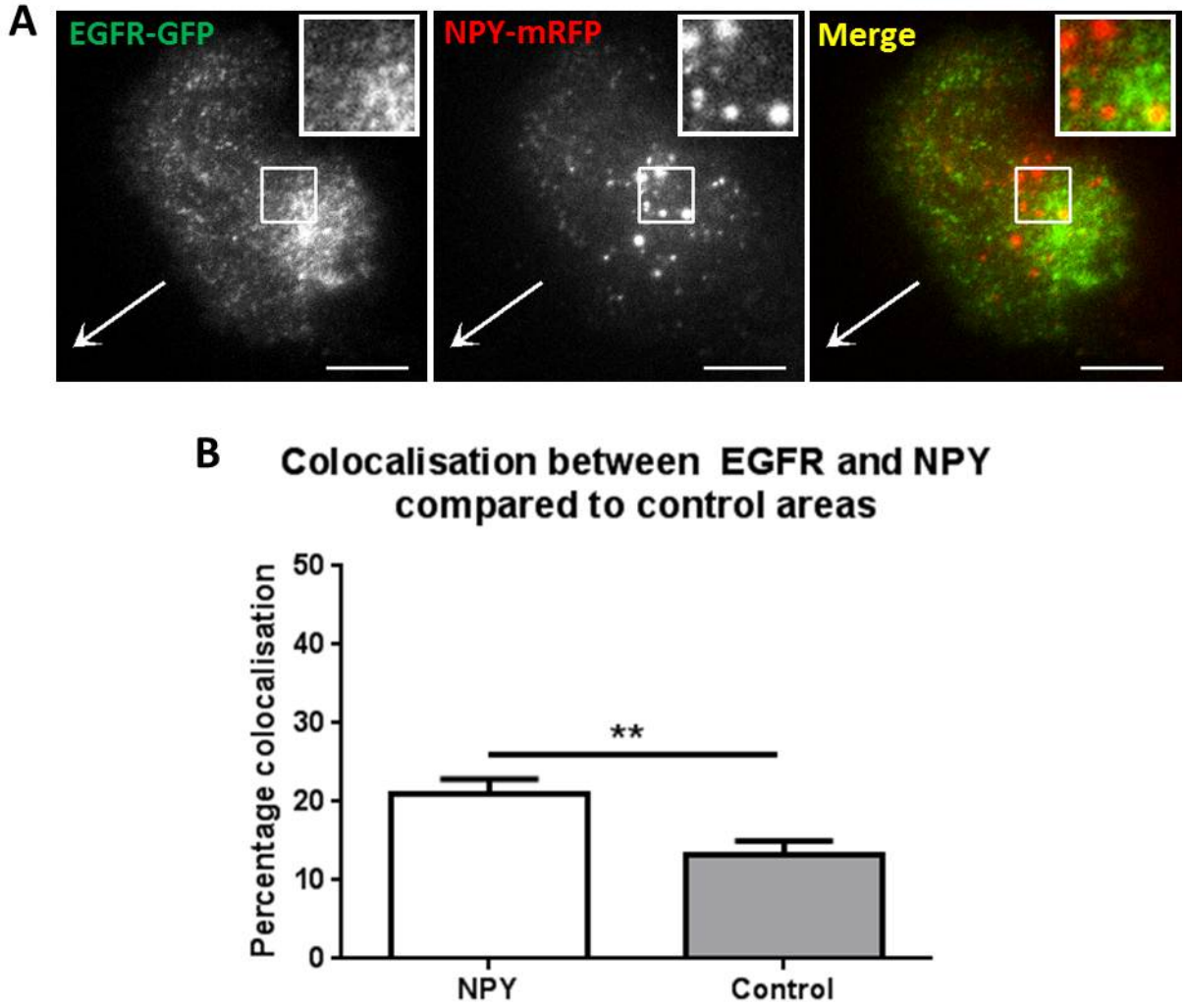

Figure 6.4: Colocalisation between NPY-mRFP and EGFR-GFP. A) Representative TIRF images of a cell with NPY-mRFP and EGFR-GFP. Arrows denote the direction of migration. Scale bars are 10 μm. B) Percentage colocalisation of NPY-mRFP clusters with EGFR-GFP and of random instances of EGFR-GFP colocalisation with regions devoid of NPY-mRFP. n = 3 experiments with a total of 20 cells analysed. Error bars represent standard error of the mean, significance determined by two-tailed unpaired student's t-test, ** denotes p-value < 0.01. Collaborative work with Robert Lees is acknowledged for performing experiments and imaging which contributed to this figure.

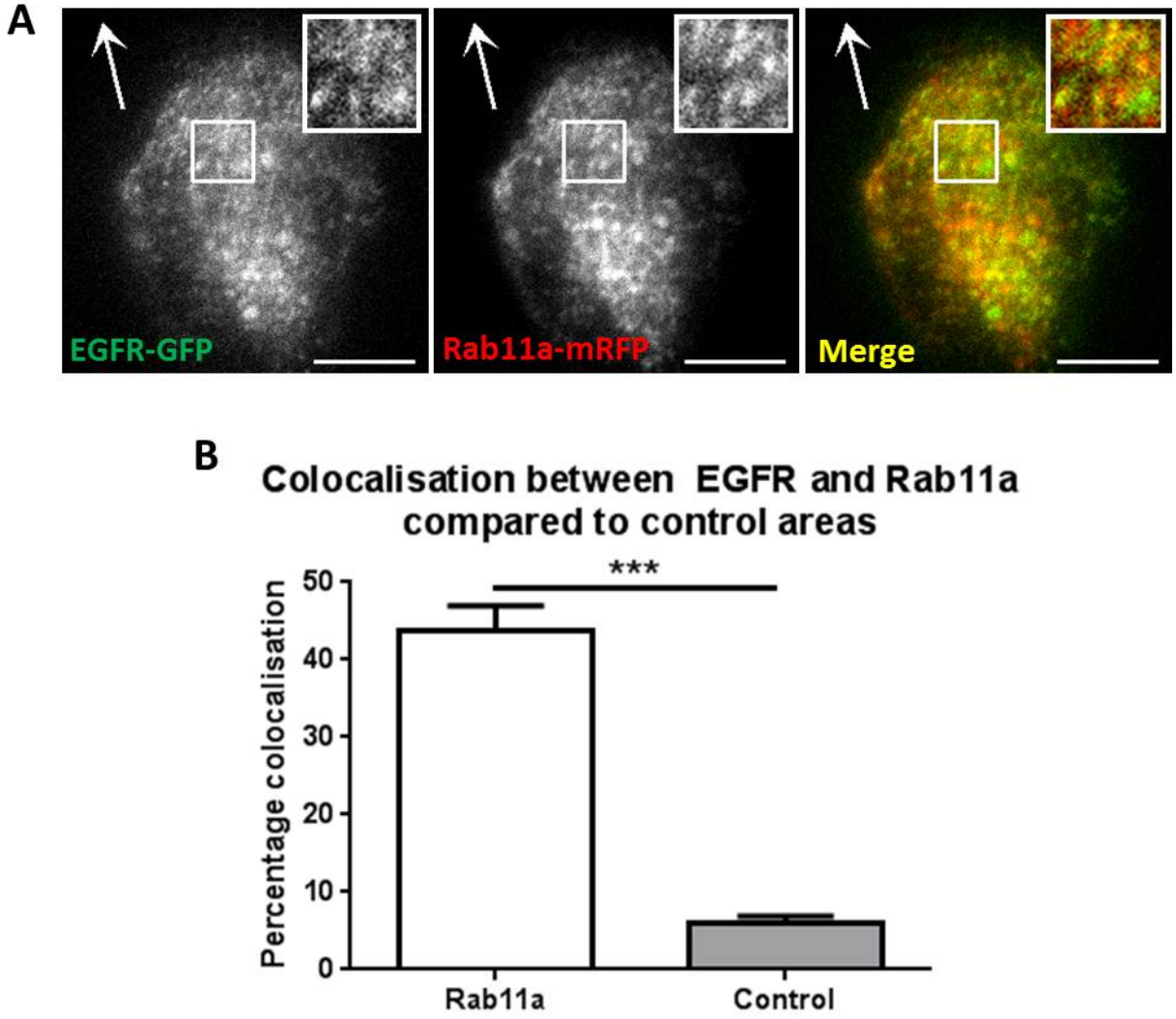

Figure 6.5: Colocalisation between Rab11a-mCherry and EGFR-GFP. A) Representative TIRF images of a cell with Rab11a-mCherry and EGFR-GFP. Arrows denote the direction of migration. Scale bars are 10 μm. B) Percentage colocalisation of Rab11a-mCherry clusters with EGFR-GFP and of random instances of EGFR-GFP colocalisation with regions devoid of Rab11a-mCherry. n = 3 experiments with a total of 20 cells analysed. Error bars represent standard error of the mean, significance determined by two-tailed unpaired student's t-test, *** denotes p-value < 0.001. Collaborative work with Robert Lees is acknowledged for performing experiments and imaging which contributed to this figure.

2008a; Assaker et al., 2010). In Figure 5.8 we showed that endocytosis is polarised in our chemotactic invasion assay and in Figure 5.7 show that EGFR clusters are uniform throughout the cell in control conditions. This could point to EGFR exocytosis also being polarised towards the front to maintain this uniform distribution, we therefore sought to test this. We used previously established methods for validating exocytic fusions events and used these methods to analyse EGFR fusion events in cells migrating in EGF spots in the chemotactic invasion assay (Schmoranzer et al. 2000; Figures 6.1 & 6.2). We used these methods to show EGFR exocytosis is in fact polarised towards the front of migrating cells. This could explain how the cell is able to maintain a uniform distribution of receptor even though more internalisation is happening at the front of the cell. This polarised endocytosis will enable the cell to continue sensing directional cues from its front region during migration.

The Golgi complex is important for maintaining cell polarity during cell migration and trafficking form the Golgi has been shown to be important for maintenance of the lamellipodium (Yadav et al., 2009; Prigozhina and Waterman-Storer, 2004). In addition, recycling pathways, such as the Rab11-dependent long-loop pathway have been proposed to be important for migration (Jones et al., 2006; Caswell and Norman, 2006; Mammoto et al., 1999; Prigozhina and Waterman-Storer, 2006). We investigated the contributions of these two pathways to the trafficking of the EGFR in our migratory system. We showed a small but significant degree of colocalisation between NPY (our marker of the secretory pathway) and EGFR, suggesting that at least some EGFR on the cell surface is newly synthesised protein (Figure 6.4). A higher degree of colocalisation was seen between Rab11a and EGFR, suggesting that the long-loop recycling pathway plays a larger role than the secretory pathway in delivering EGFR to the plasma membrane under these conditions (Figure 6.5).

Ubiquitination of EGFR by proteins which bind to phosphorylation sites on the receptor occurs following ligand binding at the plasma membrane (Levkowitz et al., 1998). This ubiquitination is shown to have roles in the internalisation of the receptor but also in

targeting it for degradation. It might be that one cue which decides the fate of the receptor is whether it remains ligand bound following internalisation. In the case of TGFα ligand dissociation occurs once the ligand-receptor complex reaches the early endosome, this process is followed by deubiquitination of the receptor preventing it from being targeted to the lysosome for degradation (French et al., 1995; Roepstorff et al., 2009). EGF does not dissociate from the receptor as easily and so the receptor remains targeted for degradation (French et al., 1995). This research seems to conflict with our results; if the receptor was being degraded we would most likely see a higher proportion of newly synthesised receptor travelling from the Golgi to the plasma membrane to replace the degraded portion, however we see long-loop recycling playing a much large role than the synthetic pathway. However, the work by the groups of French and Roepstorff was done in HeLa cells or HeLa-derived cells and therefore the same might not be occurring in the MDA-MB-231 cells used in this study. Recently, di Fiore's group have shown that different concentrations of ligand can affect the amount of ubiquitination the receptor receives, which in turn affects whether the receptor is degraded or recycled (Sigismund et al., 2013). Taking this research into account it might be that in our system only a minimal amount of ubiquitination occurs leading to most of the receptor being recycled. It is also of note that in cases where overexpression of EGFR/ErbB2 dimers occurs increased recycling has been observed (Peschard and Park, 2003). MDA-MB-231 cells have been reported to overexpress EGFR but have normal levels of ErbB2, however perhaps this would be enough to account for increased recycling.

The time-lapses used for Figure 6.3 were made using rapid TIRF imaging (every 100 ms) which was achievable due to the construct being bright enough for this speed of imaging. It was necessary to image this fast for fusion events since they are themselves a fast event (the fusion event in Figure 6.1 being 600 ms). It would have been preferable to image the NPY and Rab11a experiments in the same way in order to see whether we could view fusion events of each pathway marker along with EGFR. As it stands the switch time between imaging red and green in our imaging system takes approximately

two seconds, meaning that the vast majority of fusion events would be missed if we were to image like this. As the next best option we chose to use static TIRF imaging and assess colocalisation. This allowed us to know that the vesicles were at least in close proximity to the plasma membrane (approximately 100 nm), meaning that they could have been in the process of fusing, but without the rapid time-lapse imaging as in Figure 6.3 we can't be sure of this. It would be preferable to repeat such experiments using a microscope set-up cable of simultaneous imaging of two fluorophores. Another experiment we would have liked to include here would be colocalisation of Rab4 and EGFR, as this would assess the contribution of the short-loop pathway in replenishing EGFR at the plasma membrane during migration.

Further to using a better imaging system to view fusions of EGFR vesicles also containing recycling or biosynthetic pathway markers it could be an interesting addition to see what effect inhibiting these pathways has on migration. We could use dominant-negative versions of the Rab4 and Rab11a plasmids to inhibit recycling pathways and dominant-negative PKD to disrupt biosecretory traffic. Finally, investigating the effect of inhibiting long-loop recycling on EGF-directed migration might be fitting to this study since we propose from the above studies that it plays a significant role in replenishing EGFR on the plasma membrane.

6.4 Key chapter findings

- We are able to observe and verify exocytic fusion events in cells in our chemotactic invasion assay.
- More EGFR fusions events occur at the front than the back of migrating MDA-MB-231 cells.
- Colocalisation of EGFR with a marker of the biosecretory pathway is minimal; significant colocalisation occurs between EGFR and a marker of the long-loop recycling pathway.

Chapter 7

Signalling during chemotactic invasion

7.1 Introduction

Growth factor signalling is a complex, and poorly understood, process. As mentioned previously, ligand binding causes receptor dimerisation and subsequent transphosphorylation (Schlessinger, 2002; Riese et al., 2007; Foley et al., 2010). These phosphorylation sites can act as binding sites for protein kinases, whose activation leads to signalling cascades (Normanno et al., 2006). The response of a signalling cascade might be to alter transcriptional output of the cell, or it might be to initiate a process within the cell.

Growth factor receptor signalling can activate a multitude of pathways leading to a variety of cellular responses. EGFR signalling has been shown to be involved in processes such as cell differentiation, proliferation, survival and migration through regulating the PI3K-AKT and Ras-ERK pathways, among others (Jones and Rappoport, 2014; Mendoza et al., 2011). The pathways can regulate cell migration by modulating protein function via phosphorylation as well as altering gene transcription (Jones and Rappoport, 2014). EGFR-related signalling pathways can also have structural effects on the cell which can influence cell migration, including activation of Rho and Rac which can influence the actin/myosin dynamics in cell migration, and the activation of Src which can activate FAK and thereby stimulate focal adhesion turnover and cell migra-

tion (Spiering and Hodgson, 2011; Ray et al., 2012). Having more knowledge about these and other pathways can lead to more specific targets for future anticancer therapies; however the complexity of these pathways shouldn't be underestimated. A recent study looking at chemoattractant directed migration and invasion in just one cell type, MDA-MB-231, found that the three chemoattractants studied elicited different signalling pathways within the cell to provide the same general outcome (Harrison et al., 2013). The authors also found that some pathways were dispensable when particular chemoattractants were used; while LPA-stimulated migration and invasion required the MAPK pathway, EGF-directed migration did not (Harrison et al., 2013). Such studies are necessary to systematically provide information about signalling during migration.

There are many examples of polarised signalling during chemoattractant directed migration. Such polarisation is necessary to ensure the correct signalling pathways are stimulated at the proper localisation within the cell for migration with a defined direction and magnitude. In *Dictyostelium discoideum* binding of a chemoattractant to GPCRs at the front of the cell stimulates a polarised dissociation of Gα subunit and therefore activation of signalling pathways which cause reorganisation of actin only in this region (van Hemert et al., 2010). The process of axon guidance in neurons has been shown to involve polarised signalling due to chemoattractant; polarised PIP_3 accumulation and subsequent Akt activation was shown to occur in this system, and this asymmetric activation of Akt was also shown to be necessary for the process *in vivo* (Henle et al., 2011). A similar observation has been made in fibroblasts where polarised PDGF activation led to a steeper gradient of PIP_3 at the front of cells leading to activation of Akt in this region (Haugh et al., 2000). The polarised signalling in these examples is necessary to ensure processes required for migration, such as actin reorganisation, happen only in specified regions of the cell.

In recent years there has been much work on the localisation of EGFR signalling and what affects this has on outcome within the cell; thereby linking the process of receptor trafficking with signalling outcome. The longstanding view with regards to receptor

internalisation was that this process led to signal attenuation and degradation of the receptor. For EGFR in particular, evidence by many groups now points to a role for endosomes in the continued signalling of the receptor (Miaczynska et al., 2004; von Zastrow and Sorkin, 2007; Murphy et al., 2009; French et al., 1995; Vieira et al., 1996; Di Guglielmo et al., 1994; Wu et al., 2012). In some cases this signalling is distinct from that at the plasma membrane and can result in different signalling outcomes (von Zastrow and Sorkin, 2007; Wu et al., 2012). Roles for signalling from endosomes might include temporal regulation, increasing the length of time a receptor signals, or spatial regulation, controlling the subset of signalling molecules with which a receptor interacts (French et al., 1995; Miaczynska et al., 2004).

The studies mentioned above show the important link between trafficking and signalling, however, such a link has scarcely been studied in the context of migration. This is likely to be because biochemical signalling assays only allow analysis of signalling from a whole group of cells. Newly established techniques are emerging for the study of signalling in single cells in a variety of contexts, from migration in a 2D environment to within a tumour environment in a living organism. Here we take advance of a FLIM-FRET technique which allows measurement of the activity of certain signalling proteins and use this in conjunction with our agarose spot chemotactic invasion assay. This FLIM-FRET technique has already recently been used in the context of migrating PDAC cells by Nobis and colleagues who used it to investigate Src signalling in cells migrating *in vivo* tumour environments (Nobis et al., 2013).

7.2 Results

Mouse pancreatic ductal adenocarcinoma (PDAC) cells established for use with FLIM-FRET Biosensors were obtained. The primary aim was to use this cell line in our EGF-directed chemotactic invasion assay to assess signalling downstream of EGFR, polarisation in signalling and whether inhibition of receptor trafficking altered signalling.

To verify that PDAC cells were an appropriate model we conducted preliminary studies using the agarose spot assay. Figure 7.1 shows that a significantly higher number of PDAC cells migrated into EGF spots compared to control PBS spots, and that cells travelled much further into EGF spots than control. Since we wanted to later test whether signalling downstream of EGFR was affected by inhibition of internalisation we tested whether treating the PDAC cells with Dynasore gave us the same results as with MDA-MB-231 cells. Figure 7.2 shows that when treated with Dynasore 69% less cells migrated than into control spots and those that still migrated travelled significantly less far than control DMSO treated cells.

As well as verifying that PDAC cells migrate in EGF spots and that this is inhibited when endocytosis is prevented we thought it would be beneficial to verify whether clathrin-mediated endocytosis is polarised in this cell type as it was in MDA-MB-231 cells (Figure 5.8). As previously, we imaged one minute time-lapses of clathrin-dsRed in cells migrating in EGF spots. This analysis proved to be different to that of the MDA-MB-231 cells as the clathin in this case was highly dynamic thereby making judgement of disappearance from the TIRF field difficult. Previous work by Rappoport and colleagues has shown clathrin to be either static, laterally mobile or disappearing vertically into the cell (Rappoport et al., 2003b; Rappoport and Simon, 2003). It has also been suggested that movement of clathrin along microtubules can occur prior to endocytosis (Ezratty et al., 2009; Rappoport et al., 2003b). Therefore in the case of PDAC cells we chose to count the number of dynamic clathrin spots (those moving laterally in the plane of the membrane as well as those disappearing from the TIRF field). To prevent re-counting of a clathrin spot that had already been analysed (for example, in the case of clathrin spots shown to move along microtubules which have been shown to sometimes curve axially away from the TIRF field and back again (Yang et al., 2011)) we followed the fate of only those clathrin spots present at the start of the time-lapse. As with the previous analysis we split the cells into front, middle and back regions for analysis. We looked at the total number of dynamic clathrin spots compared to the total number of

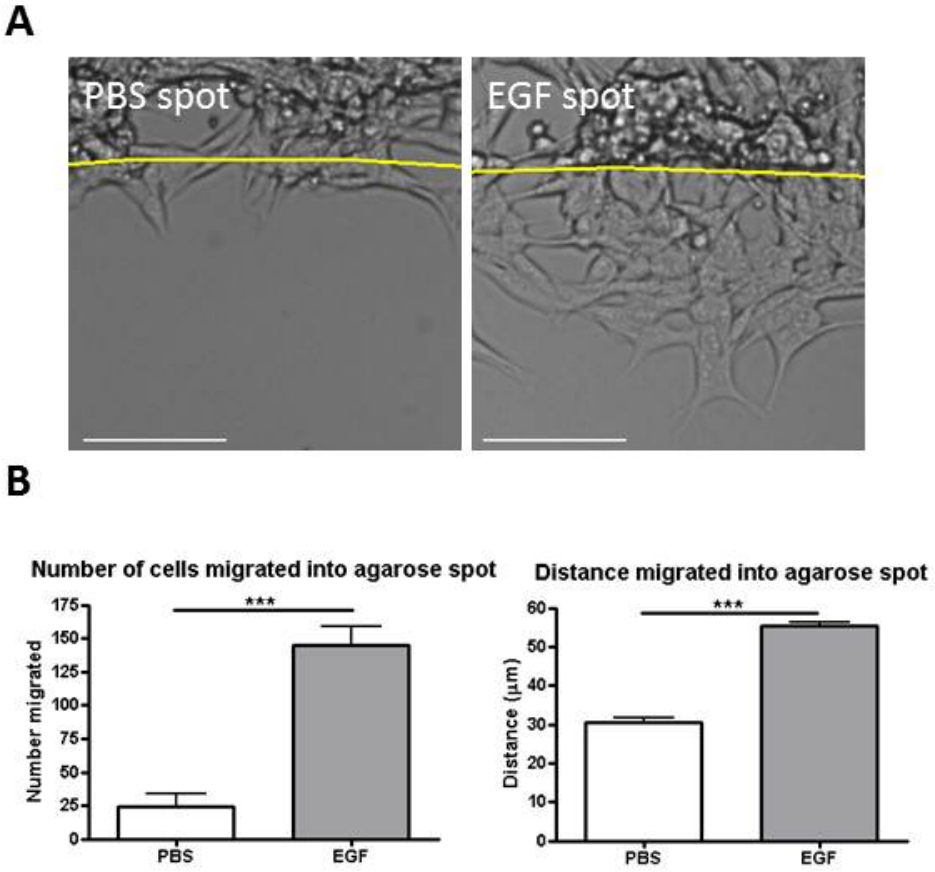

Figure 7.1: PDAC cell migration in the agarose spot assay. A) Representative images of PDAC cells after 14 hours of migration under PBS spots and EGF spots. Line denotes the edge of the agarose spot. Scale bars are 100 μm. B) Quantification of the total number of cells which migrated and the distance migrated into PBS and EGF spots. n = 3 experiments witha $\geq$ 12 fields of view analysed per treatment. Error bars represent standard error of the mean, significance determined by two-tailed unpaired student's t-test, *** denotes p-value < 0.001.

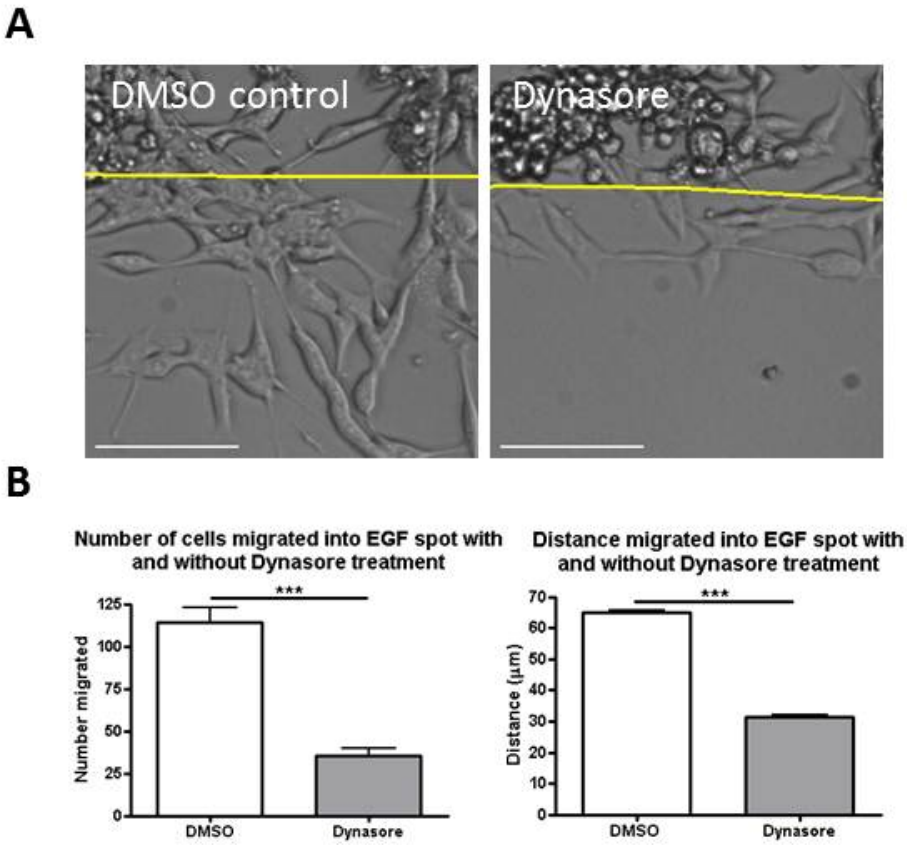

Figure 7.2: Dynasore inhibits PDAC chemotactic invasion into EGF spots. A) Representative images of PDAC cells after 14 hours of migration under EGF spots with DMSO or Dynasore treatment. Line denotes the edge of the agarose spot. Scale bars are 100 μm. B) Quantification of number of cells migrated and distance migrated with DMSO and Dynasore treatment. n = 4 experiments with $\geq$ 12 fields of view analysed per treatment. Error bars represent standard error of the mean, significance determined by two-tailed unpaired student's t-test, *** denotes p-value < 0.001.

clathrin spots in each region and also the number of dynamic spots normalised to the total area of each region. In both cases we found significantly more dynamic clathrin spots at the front of migrating cells than the middle or the back (Figure 7.3A, B). We also took this opportunity to image both clathrin-dsRed and EGFR-GFP together in migrating cells and were able to observe instances of colocalisation and disappearance from the TIRF field together as in Figure 7.3C.

FLIM-FRET imaging allows measurement of the fluorescence lifetime of a Biosensor. We chose to use previously validated Biosensors: a membrane-bound Akt Biosensor, a cytosolic Akt Biosensor and a Src Biosensor. Each of the Biosensors had two domains, one of which would be a FRET donor and one the acceptor. During imaging the fluorescence lifetime of the FRET donor would be measured. The Biosensors were engineered so that in the inactive confirmation the two domains were close enough for FRET to occur, in this case energy from the donor would be transferred to the acceptor and the donor fluorescence lifetime would be low. In the active confirmation the two domains were not close enough for FRET to occur meaning the fluorescence lifetime of the donor would be comparatively increased (see Figure 7.4 for a diagram).

In the case of the Src Biosensor ECFP and an SH2 domain are joined by a flexible linker to a Src substrate peptide and YPet (FRET-optimised yellow fluorescent protein). Unphosphorylated Biosensor is in a folded conformation bringing the ECFP and YPet close together resulting in FRET. Following phosphorylation induced by Src, the Src substrate peptide binds to the SH2 domain causing separation of the fluorophores and thereby decreasing FRET and increasing fluorescence lifetime of the donor. For the Akt Biosensors the mCFP and mYFP fluorophores are separated by a FHA2 phosphothreonine-binding domain and a PKB phosphorylation sequence. Again, when unphosphorylated the fluorophores are in close proximity resulting in FRET; upon phosphorylation of the PKB consensus sequence this domain binds the FHA2 domain moving the fluorophores further apart and minimising FRET and increasing fluorescence lifetime of the donor. The membrane-bound Akt Biosensor is identical to its cytosolic counterpart except for the

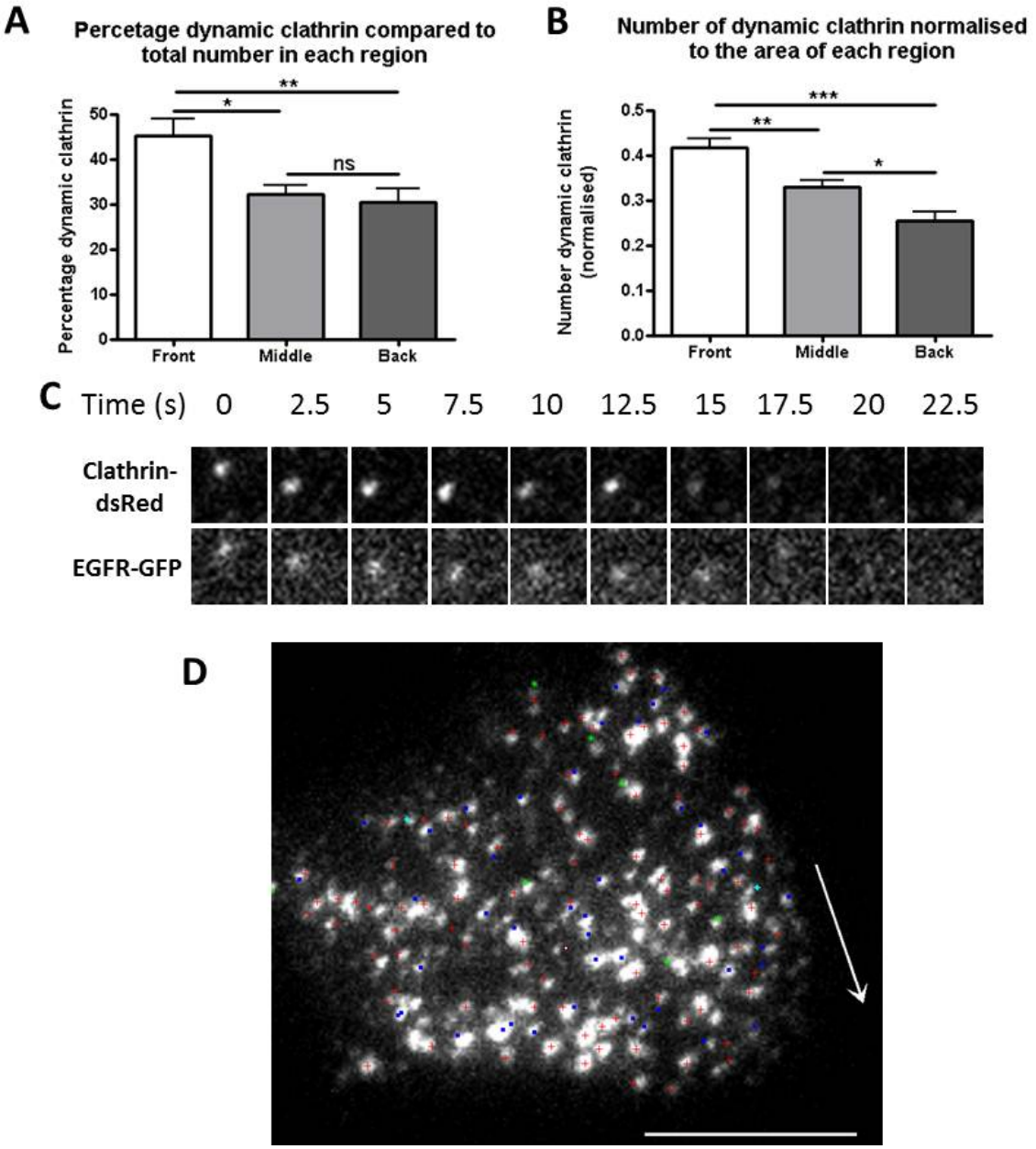

Figure 7.3: Dynamic clathrin in migrating PDAC cells. A) Graph to show that there is a higher proportion of dynamic clathrin compared to total clathrin at the front of migrating PDAC cells compared to the middle or the back. B) Graph to show that there is more dynamic clathrin at the front of migrating PDAC cells when normalised to the area of each region. C) Representative images of a clathrin spot disappearing from the TIRF imaging field. D) Representative image of a clathrin-dsRed expressing migrating cell. Different symbols were used during analysis to catagorise every clathrin cluster that was present at the start of the timelapse. Arrow denotes the direction of migration. Scale bars are 10 μm.n = 4 experiments with a total of 12 cells analysed per treatment. Error bars represent standard error of the mean, significance determined by one way ANOVA followed by Tukey's post-test, * denotes p-value <0.05, * denotes p-value <0.05, ** denotes p-value <0.01, *** denotes p-value <0.001. C) An instance to show clathrin-dsRed and EGFR-GFP internalising from the TIRF field together.

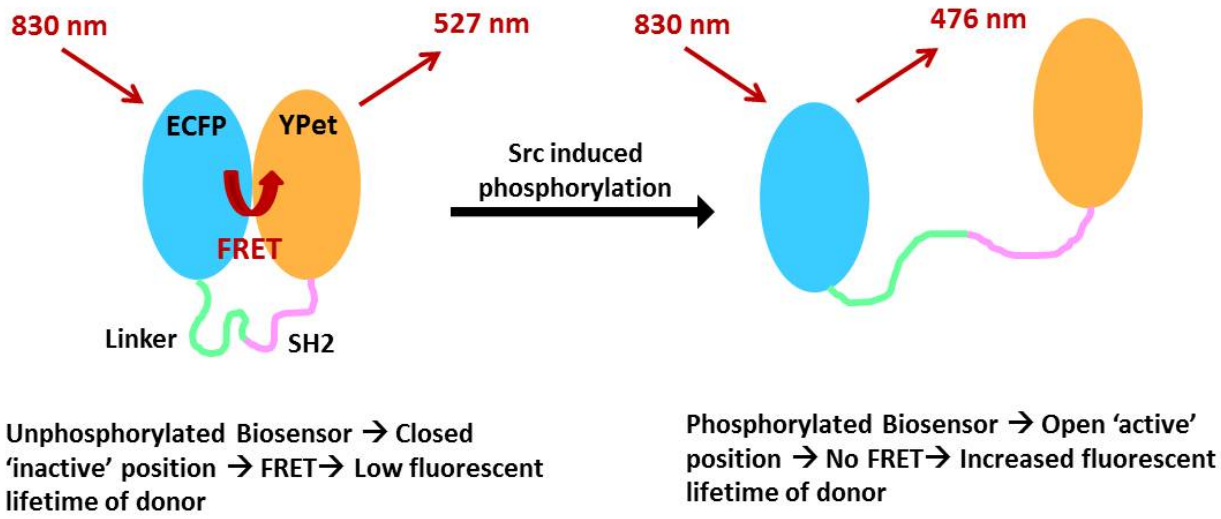

Figure 7.4: Diagram to show how the fluorescent lifetime of a Biosensor changes when the probe is in the inactive of active conformations. When unphosphorylated the Biosensor is in a closed position bringing the FRET donor and acceptor in close proximity, thereby allowing FRET to occur. This decreases the fluorescent lifetime of the donor fluorophore. When phosphorylated by Src the Biosensor adopts an open conformation, preventing FRET and increasing the fluorescent lifetime of the donor fluorophore.

addition of a myristoylation and palmitoylation tag to target it to the membrane.

We made stable cell lines of PDAC cells expressing each of the Biosensors using G418 selection (see Section 2.6). As an initial experiment to test the activity of the Biosensors in these stable cells lines we imaged fluorescence lifetimes of cells without stimulation, we then added 100 ng/ml EGF and incubated for 15 minutes before imaging fluorescence lifetimes again. Using LI-FLIM analysis software we could establish average fluorescence lifetime for the cells stably transfected with each Biosensor, with and without EGF stimulation. The purpose of this experiment was to define a cut-off below which we could say the Biosensor was inactive and above which it would be active (as in Nobis et al. 2013 Figure 1C & D). Unfortunately, as shown in Figure 7.5, no difference was seen in average fluorescence lifetime of cells with or without EGF stimulation for any of the Biosensors used.

Nonetheless, we next used the agarose spot assay to assess signalling in cells migrating in EGF spots with and without treatment with Dynasore to assess signalling with inhibition of endocytosis. We firstly analysed these results on a whole cell basis. Figure 7.6 shows that in the case of each Biosensor fluorescence lifetime, and therefore signalling, was increased in cells migrating into EGF spots compared to those away from the spots. This conflicted with results from the previous experiment (Figure 7.5), however it shows that in our EGF-directed spot assay signalling by Src and Akt is increased compared to control. When repeated this experiment with the addition of Dynasore to the media to inhibit endocytosis and therefore perturb migration, we unexpectedly saw a significant increase in the signalling of each Biosensor (Figure 7.6).

To see if there was any polarisation of signalling during migration in the EGF spots we split the cells into front, middle and back regions and looked at average fluorescence lifetimes for these regions. We repeated this analysis in the Dynasore treated cells to see if inhibiting endocytosis had any effect on polarisation of signalling. As can be seen in Figure 7.7 neither the cytoplasmic Akt nor the Src Biosensors showed any

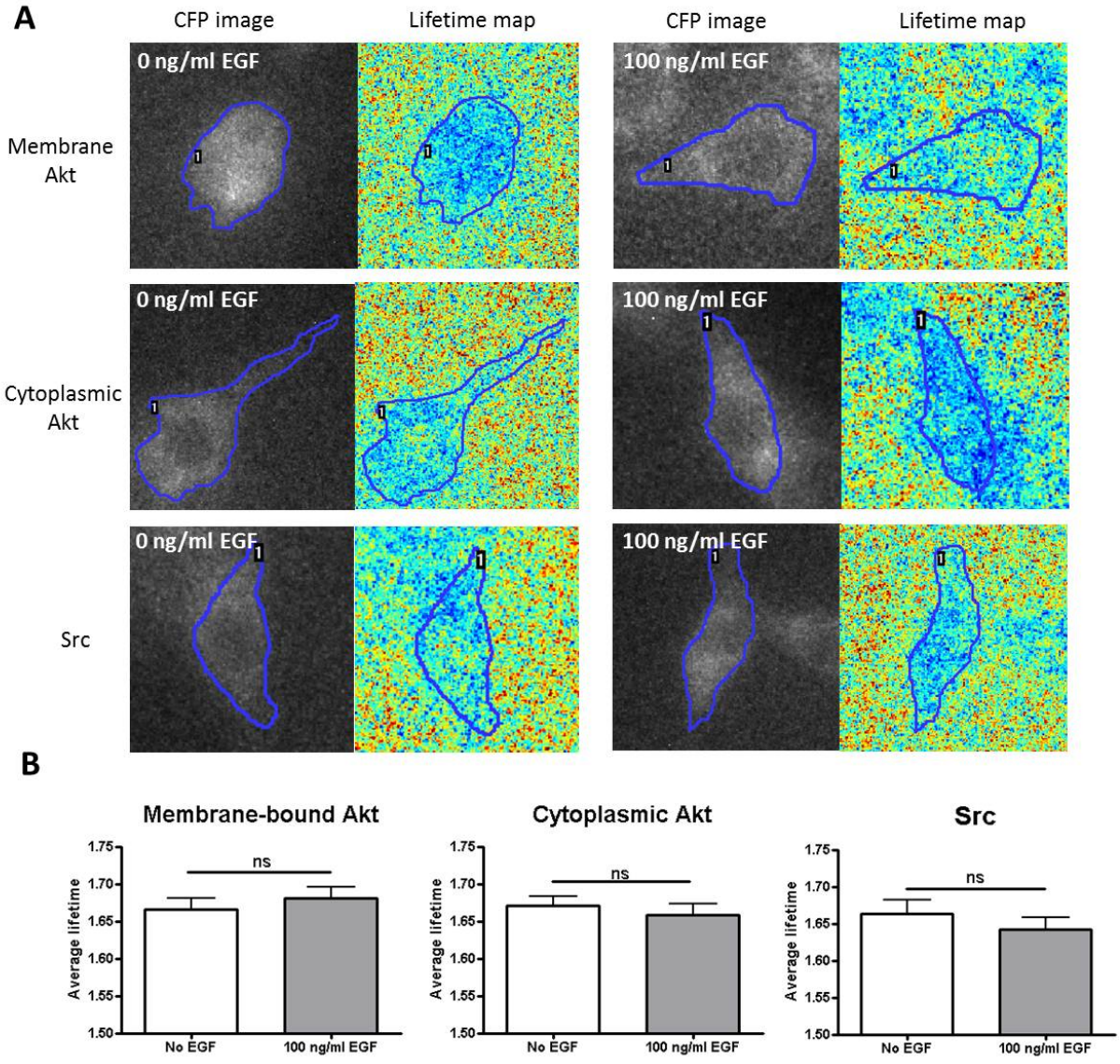

Figure 7.5: Average fluorescence lifetimes of cells stably transfected with each Biosensor construct. Fluorescence lifetimes were measured with and without 15 minutes stimulation with 100 ng/ml EGF. A) Representative CFP and lifetime map images of cells with and without EGF treatment. B) Quantification of fluorescence lifetimes of cells with and without EGF treatment. n = 3 experiments with a total of 60 cells analysed per condition. Error bars represent standard error of the mean, significance determined by two-tailed unpaired student's t-test, 'ns' denotes p-value ≥ 0.05.

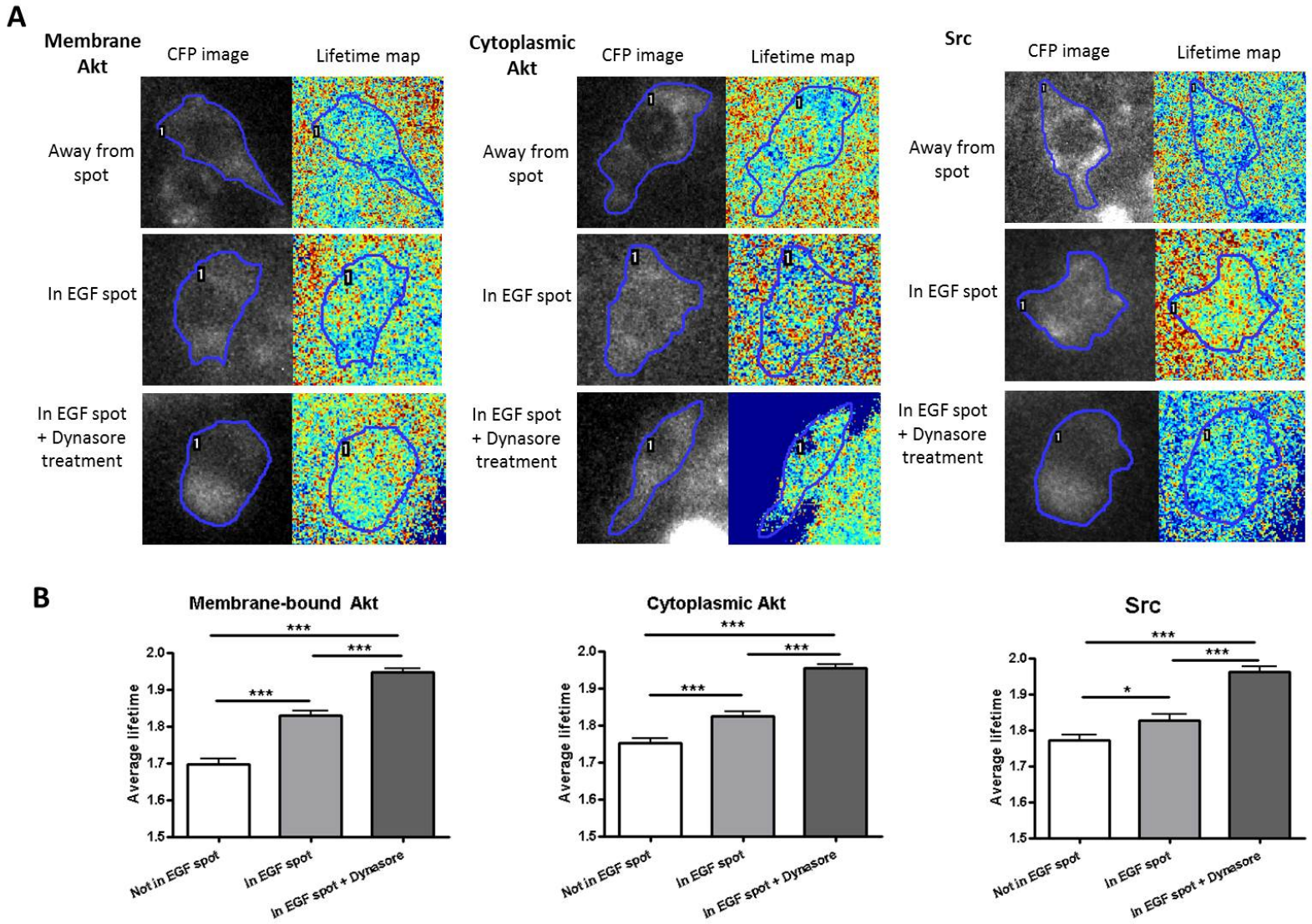

Figure 7.6: Average fluorescence lifetimes of cells stably transfected with each Biosensor construct. Lifetimes were measured from cells not in EGF spots, those in EGF spots and those in EGF spots with the addition of Dynasore to the media. A) Representative CFP and fluorescence lifetime images of cells expressing each Biosensor, under all three conditions. B) Quantification of fluorescence lifetimes. n = 4 experiments with $\geq$ 65 cells analysed per condition. Error bars represent standard error of the mean, significance determined by one way ANOVA followed by Tukey's post-test, * denotes p-value < 0.05, *** denotes p-value < 0.001.

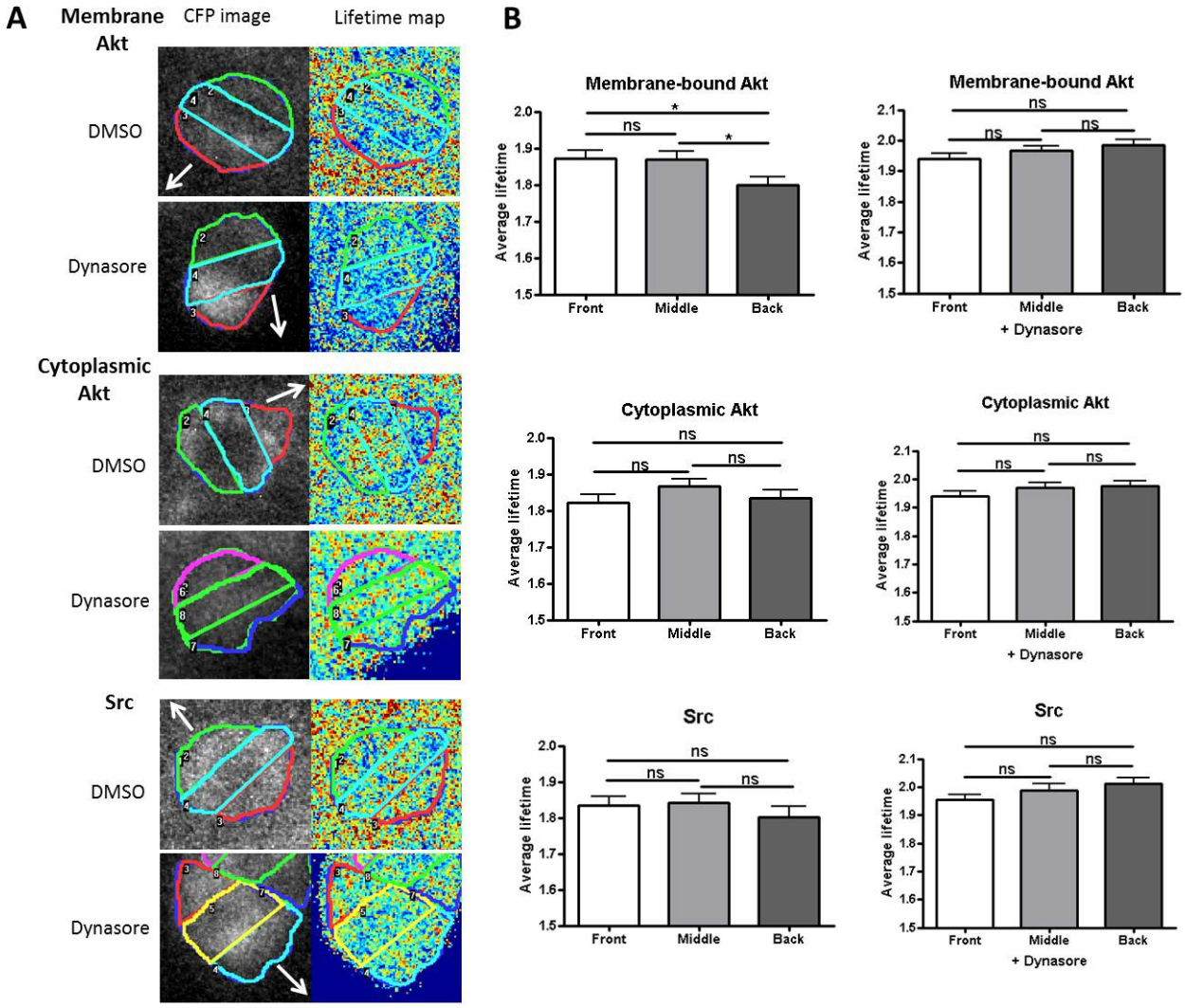

Figure 7.7: Average fluorescence lifetimes of front, middle and back regions of cells stably transfected with each Biosensor construct with the addition of Dynasore to the media. A) Representative CFP and fluorescence lifetime images of cells with and without Dynasore treatment for each Biosensor. Front, middle and back regions can be seen. Arrows denote direction of migration. B) Quantification of fluorescence lifetimes for front, middle and back regions of cells with and without Dynasore treatment. n = 4 experiments with ≥ 65 cells analysed per condition. Error bars represent standard error of the mean, significance determined by one way ANOVA followed by Tukey's post-test, 'ns' denotes p-value ≥ 0.05, * denotes p-value < 0.05.

polarised signalling with or without treatment with Dynasore. Membrane-bound Akt has significant polarisation of activity towards the front and middle of migrating cells, which was abrogated with Dynasore treatment.

7.3 Discussion

In this study we were attempting to look at signalling in live cells during the process of migration. This work was done at the Beatson Institute for Cancer Research using their FLIM-FRET Biosensors and imaging system. At the time of planning we decided to use the PDAC cell line that was already set up for use in a mouse model for pancreatic cancer using this system. One reason for this choice was that it would facilitate potential future *in vivo* work as PDAC cells can be studied in immuno-competant mice, whereas MDA-MB-231 cells cannot. The initial work verified that the PDAC cell line behaved as expected form our previous results in MDA-MB-231 cells. In Figure 7.1 we show that more cells migrate into EGF spots than into control PBS spots and we show that, as with MDA-MB-231 cells, this migration can be inhibited by treatment with Dynasore (Figure 7.2). These data show that, not only do the PDAC cells migrate when stimulated with EGF and require dynamin for this migration, but that the agarose spot assay can give highly reproducible results in another cell line. We also showed that more dynamic clathrin is present on the plasma membrane at the front of the migrating cells, rather than the middle or the back (Figure 7.3). This dynamic clathrin includes clathrin clusters which disappear from the TIRF field, therefore likely to be internalisation events, and clathrin moving rapidly and directionally in the plane of the membrane, presumably along microtubules. In some cases this movement along microtubules has been suggested to occur just prior to endocytosis and we therefore took these clathrin clusters to represent an endocytosis intermediate (Yang et al., 2011). In this case we were able to repeat our results from MDA-MB-231 cells to show that in PDAC cells more endocytic events occur at the front of cells migration in EGF-directed conditions.

The range of signalling of each Biosensor construct was tested to estimate a threshold for the inactive and active forms of each Biosensor. Unexpectedly there were no changes in fluorescence lifetime of any of the Biosensors with and without EGF treatment, as shown in Figure 7.5. A similar experiment was done by Nobis and colleagues using the same cell line with the Src construct stably transfected (Nobis et al., 2013). Rather than stimulate signalling with a growth factor or similar, they chose to inhibit signalling by using the Src inhibitor Dasatinib and were able to image lifetimes ranging from 1.9 ns to 2.8 ns. Perhaps the reason we saw no difference was due to the concentration of EGF chosen or the timepoint used. We used 100 ng/ml, which is considered a high concentration, but in this case we wanted to elicit a large signalling response to see the range of the Biosensors, this is also the same concentration as others have used in EGFR trafficking studies (Rappoport and Simon, 2009; Jones et al., 2014). Ideally the experiment would be repeated with a range of EGF concentrations and timepoints post-EGF addition, however, time prevented this.

Contrary to the aforementioned result, when we imaged cells migrating in EGF spots and compared their lifetimes to cells away from the spot regions we saw a significant increase in fluorescence lifetimes for each of the constructs (Figure 7.6). Without further study it is difficult to speculate why this result is different to the previous, however it serves to show that during EGF stimulation in our migration assay activity of all Biosensors is increased over control.

Dyansore treatment inhibits migration of PDAC cells (Figure 7.2); from this we might expect that Dynasore treatment would yield a decreasing in migration-dependent signalling. As shown in Figure 7.7 this was not found to be the case and in fact activity of all three Biosensors was increased during Dynasore treatment. The role trafficking plays in signalling events is very complicated and is only really at the beginning of being investigated. EGFR has been shown to signal from endosomes and this signalling is distinct from signalling at the plasma membrane (Miaczynska et al., 2004; von Zastrow and Sorkin, 2007; Murphy et al., 2009; French et al., 1995; Vieira et al., 1996; Di Guglielmo

et al., 1994; Wu et al., 2012). Perhaps our results point to a spatially restricted endosomal signalling pathway that is necessary for migration and when we inhibit endocytosis we see increased Biosensor activity stemming from the plasma membrane due to lack of receptor internalisation and degradation, but that this signalling is unable to stimulate migration. The imaging system does not have enough resolution to further analyse signalling from endosomes in uninhibited cells as a possibility but this would be useful for further investigation. There are likely other explanations for our results but much more work would be needed to fully elucidate the reason for the increase in signalling seen when internalisation is prevented in these migrating cells.

Finally, the polarisation of membrane-bound Akt signalling was interesting as it follows our result of polarised endocytosis in migrating cells. Perhaps internalisation of EGFR is necessary for Akt signalling and more EGF is binding in this front-middle region leading to increased internalisation and therefore signalling in this region. This could explain why the polarisation is abrogated when Dynasore treatment is applied, but doesn't explain why it only occurs for the membrane-bound Akt and not the cytoplasmic version. Again, more work would be needed before an explanation might become apparent.

7.4 Key chapter findings

- Earlier results can be verified in a PDAC cell line, proving the use of the chemotactic invasion assay in another cell type.
- Signalling of Src and Akt Biosensor probes is increased within migrating cells in EGF spots, compared to in cells not migrating in these spots.
- Signalling of Src and Akt Biosensor probes is increased further when endocytosis is inhibited.

Chapter 8

Discussion

8.1 Final discussion

The aim of my work has been to show a link between directed cell migration and endocytic trafficking. Firstly we wanted to establish that the agarose spot assay was suitable for chemoattractant-directed migration studies. Wiggins and Rappoport already showed that the assay gave highly reproducible results and that migration was significantly increased into chemoattractant (EGF)-containing agarose spots relative to those containing PBS as a control (Wiggins and Rappoport, 2010). The results of their preliminary studies, however, couldn't rule out the possibility that EGF was increasing chemokinesis of the cells and wasn't specific to the cells crawling under the spot. By investigating the migration of cells under the spot when EGF was present in the media rather than in the spot and also by analysing migration of cells away from the agarose spots, we were able to establish that the assay is specific to chemotactic invasion and not chemokinesis (Figures 3.2 and 3.3). Analysis of the cell trajectories also showed that cells are migrating in a directed manner into EGF spots (Figure 3.4).

Rappoport and Wiggins also touched upon the use of the assay in multiple imaging systems; including imaging using a 10 x objective lens on a Nikon TE300 inverted microscope and looking at the cells crawling under the spot in more detail using Scannning

Electron Microscopy (SEM). This current study involved imaging using a 10 x objective, static and live cell TIRF microscopy, FLIM-FRET Biosensor imaging and also studies using confocal microscopy, finding the system robust under all methods. This multiple imaging ability of the assay allows us to gain a wide variety of information from which to build up a model of cell migration in the highly motile MDA-MB-231 cell line. We have also used the assay for preliminary studies in another cell line, PDAC, and found results to be highly comparable to those of MDA-MB-231 cells (Figures 7.1, 7.2 and 7.3), thereby confirming reproducible use of the assay in another cell line. In conclusion, we can say in the agarose spot assay cells migrate in a directed manner towards the EGF-containing spots and that this assay can be used to analyse EGF-directed migration under many different conditions with a variety of methods.

Using the agarose spot assay we were able to analyse various parameters of the migration of MDA-MB-231 cells towards EGF, under a number of inhibitory conditions. We used both a small molecule inhibitor and an RNAi approach to show that both dynamin and the process of clathrin-mediated endocytosis are necessary for migration of these cells towards EGF, but that caveolar endocytosis is dispensable in this system (Figures 3.6 and 3.10).

In the cell tracking analysis Dynasore was also found to cause a more elongated phenotype of the MDA-MB-231 cells when compared to control (Figure 3.6). This elongation led us to consider whether focal adhesion dynamics may be affected by inhibiting endocytosis. We analysed the colocalisation of clathrin with two focal adhesion markers, paxillin-mRFP and β3-integrin-GFP, but found no colocalisation in either case (Figures 4.1, 4.2 and 4.3). This was in agreement with work by Fletcher et al. in MDCK cells where no colocalisation was seen between clathrin and various focal adhesion markers (Fletcher et al., 2012). The contrast in these results compared to some studies performed in fibroblasts indicates that effects seen on focal adhesions may be cell type specific and although there may be a requirement for clathrin in focal adhesion disassembly in fibroblasts that does not seem to be the case for all cell lines (Chao and Kunz, 2009;

Ezratty et al., 2009). Interestingly, we actually found that α-adaptin siRNA did not inhibit migration during wound healing with MDA-MB-231 cells, in contrast to our results observed during chemotactic invasion. This further emphasises that different migratory models require different pathways; thus, clathrin-mediated endocytosis appears to be unnecessary for both wound healing and focal adhesion disassembly in this cell type.

Since clathrin-mediated endocytosis was found to be necessary for chemotactic invasion in our model we wanted to establish whether this was the route of internalisation taken by EGFR in these cells. We found a high degree of colocalisation between clathrin-dsRed and EGFR-GFP in migrating cells (Figure 5.1). As a control we also imaged EGFR-GFP in conjunction with caveolin1-mRFP and found a relative lack of colocalisation. Taken together this provides strong evidence for clathrin-mediated endocytosis of EGFR during EGF-directed chemotactic invasion. Such a result fits with the literature but conflicts with evidence for clathrin-independent routes of EGFR internalisation (Sorkina et al., 2002; Motley et al., 2003; Hinrichsen et al., 2003; Huang et al., 2004; Sigismund et al., 2005; Johannessen et al., 2006; Orlichenko et al., 2006; Rappoport and Simon, 2009). Ultimately, these results are likely to be dependent on the experimental system and cell type being studied.

We also assessed whether EGFR localisation was polarised in migrating cells, however this was not found to be the case. Though, interestingly, when treated with Dynasore the localisation of the EGFR became skewed with more receptor clusters present at the front of migrating cells (Figure 5.7). This led to the suggestion that although EGFR localisation was not polarised under normal conditions, its endocytosis may be polarised, as seen by a build-up of receptors at the front of the cell when dynamin-dependent endocytosis is inhibited. In recent years some studies have found a role for polarised vesicle trafficking in directed cell migration (Bailly et al., 2000; Caswell and Norman, 2006; Caswell et al., 2009; Fletcher and Rappoport, 2010). We found a polarisation of clathrin-dsRed internalisation events at the front of migrating cells. In a separate experiment we were able to image instances of colocalised clathrin-dsRed and EGFR-GFP

internalising at the same time, but imaging limitations meant we weren't able to expand this anaylsis further. Taken together these results suggest that polarised endocytosis of EGFR is important for migration in this breast cancer cell line and adds to emerging evidence of the importance of polarised vesicle trafficking in directed cell migration.

Since endocytosis was polarised in our migratory model but EGFR remained uniform on the cell surface during migration, we decided to further investigate EGFR trafficking during EGF-directed chemotactic invasion. We found fusion of EGFR-containing vesicles to be polarised towards the front of migrating cells, perhaps to replenish the receptor in this region and allow continued sensing of chemoattractant molecules at the front of the cell (Figure 6.3). We examined colocalisation of EGFR with NPY-mRFP as a marker for biosecretory traffic and Rab11a-GFP as a marker for the long-loop recycling pathway. A low degree of colocalisation was found with NPY but almost 40% colocalisation with Rab11a was found, perhaps pointing to the proportionate role each of these pathways plays with regards to replenishing EGFR on the plasma membrane (Figures 6.4 and 6.5). However, this work is lacking live TIRF time-lapse imaging to see how many of these colocalised structures result in fusions and also would benefit from analysis of Rab4 and EGFR to account for the short-loop recycling pathway.

In the final chapter of work we tested a link between our trafficking results and signalling downstream of EGFR. We used a PDAC cell line, established for use with the FLIM-FRET Biosensors we intended to work with. Our results showed an increase in both Akt and Src signalling in cells migrating into EGF spots, and this signalling increased further when Dynasore was used to inhibit dynamin-dependent endocytosis pathways (Figure 7.6). Since Dynasore inhibits migration we might expect signalling to be decreased in these circumstances, however the complexity of signalling pathways means what we expect might not necessarily be the case. Perhaps by preventing internalisation we prevented a necessary aspect of signalling which allows migration to occur; signalling from endosomes has been shown to play a role in EGFR signalling and might be the case in this instance. Further work is needed before any conclusions can be made from

these results.

EGFR and EGFR family members are overexpressed in many cancers, most notably in breast carcinoma (Eccles, 2011; Roskoski Jr, 2004). EGF has been found to physiologically promote metastasis of these cancer cells by stimulating EGF-directed migration (Hynes, 2002; Lu and Kang, 2009). This current study utilised an EGF-directed migration assay to answer questions about the vesicle trafficking pathways and signalling pathways involved in the migration of particular cell lines and the trafficking routes taken by the major cargo proteins involved. We propose that dynamin and clathrin are both necessary for the migration of MDA-MB-231 cells, but that caveolin1 is not. We find no role for clathrin in focal adhesion disassembly in our migratory model but do find it to be the route of internalisation of EGFR. We find that clathrin-mediated endocytosis and also exocytosis of EGFR to be polarised towards the front of cells migrating towards EGF. Using PDAC cells we find signalling of Src and Akt Biosensors to be increased following dynamin inhibition; a result which we are unable to explain at this stage but may leave the door open for future studies. Comparing some of our results with other studies provides significant evidence of differences between cell types, as well as migratory models. Ultimately, until a more systematic approach is taken to the study of directed cell migration we will be without a thorough picture of what is really occurring during chemotaxis and metastasis.

8.2 Future work

This thesis is one in only a few studies which has investigated the polarisation of receptor trafficking during chemoattractant-directed cell migration. At various points within the study there were many other directions the work could have taken, some of which are discussed below.

Clathrin-mediated endocytosis and caveolar endocytosis represent the two most highly studied endocytic routes used by cells, however several other less well characterised and

possibly overlapping pathways exist. These include the CLIC/GEEC pathway, Flotillin-dependent endocytosis and the Arf-6 dependent pathway (Doherty and McMahon, 2009). It would be interesting to investigate the contribution each of these pathways has to EGF-dependent migration in our migratory model. However, most of these additional pathways don't have specific markers and/or inhibitors so specifically investigating each in studies such as these has not yet been practical. Such work would be useful to establish whether alternative internalisation pathways are necessary for chemotactic invasion towards EGF.

Our study found that α-adaptin, and therefore presumably clathrin-mediated endocytosis was necessary for EGF-dependent migration of MDA-MB-231 cells. Since α-adaptin is necessary for clathrin-mediated endocytosis it does not pose a particularly attractive target for anti-cancer therapies, as healthy cells also need this process to enable their survival. However, if we could find a protein specific for the internalisation of EGFR this might prove a better target for anti-cancer therapies for tumours overexpressing the receptor; since inhibiting its endocytosis prevented cell migration it might be an option to prevent metastasis. A large siRNA screen could find targets which inhibit EGF-directed migration and with comparisons to other endocytic screens in the literature could find targets not yet studied in this context. Further experiments could include creating fluorescent protein fusions of these target proteins to assess colocalisation with internalising receptor, or mutations in the target proteins to assess their role in the EGFR endocytic process.

Further to our work on the route of internalisation of EGFR it would be beneficial to elucidate the trafficking of the receptor once inside the cell. The fate of the internalised receptor may impact on the signalling stemming from its activation and more knowledge of this process might open it up to manipulation in future. We began this investigation in Chapter 6, with experiments designed to see which exocytic routes played a role in replenishing EGFR at the plasma membrane. In addition to what we achieved in Chapter 6 it would be beneficial to show live cell TIRF time-lapses of vesicles containing

EGFR and a pathway marker fuse with the plasma membrane, and also to use additional pathway markers than we were able to in Chapter 3, such as a marker for the Rab4-short loop recycling pathway. Further knowledge about the route of the receptor immediately after internalisation would also be useful to future researchers. Knowing what portion of the receptor is recycled compared to the portion degraded and the cues that control these pathways could be useful to try and increase the proportion targeted for degradation in the case of some cancers overexpressing the receptor.

Since its publication in 2010 the agarose spot assay for chemotactic invasion has been used by a number of other groups in their research (Wiggins and Rappoport, 2010; Chung et al., 2011; Vinader et al., 2011; Al Saleh et al., 2011; Haemmerle et al., 2013; Cheng et al., 2014). The groups have used a range of different cells lines, from the same MDA-MB-231 cell line that we used to lymphatic endothelial cells, pancreatic cancer cells lines and mesothelioma cell lines. It iss promising that other groups have started using such a new assay in their varied fields of research. Another way to ensure its use in the future could be to investigate its use with a number of different cell types of different metastatic and migratory potentials and also with a range of chemoattractants/chemokines. This type of analysis, in conjunction with its low cost, will hopefully ensure it is routinely used for chemoattractant-based motility studies in future research.

Our research in Chapter 7 on signalling during migration and how this might relate to trafficking could open doors for a variety of further work. Our results brought up the role EGFR signalling at endosomes is playing in migration. To investigate this further higher resolution microscopy would be needed to discern endosomal structures in the migrating cells and assess the signalling emanating from these regions. Using TIRF microscopy in combination with the FLIM-FRET system would also help us localise the signalling events taking place in the migrating cells. Combined use of Biosensors with siRNAs to silence trafficking proteins of interest could resolve how trafficking influences signalling during the process of migration. As advances are made this research could be widened to include other signalling Biosensors to further build up understanding of the

migratory process.

In order to take the current results further it would be useful to apply a more physiological approach; this could range from 3D *in vitro* migration assays up to *in vivo* whole animal imaging. An invasion assay called the matrigel plug assay, pioneered by Hannigan in 2004 and used by a number of other groups, is particularly appealing (Mongroo et al., 2004; Muller et al., 2009). It involves cells migrating through Transwell membranes and into Matrigel or other ECM-based derivatives, it then allows for confocal microscopy to assess 3D migration into the Matrigel. This assay is appealing as it can investigate many of the parameters of the agarose spot assay but in a 3D setting, thereby improving the physiological relevance of results. Another interesting 3D migration assay is an organotypic invasion assay which uses collagen imbedded with fibroblasts to mimic the *in vivo* tumour environment (Timpson et al., 2011; Nobis et al., 2013). Using fluorescent labelled tumour cells and fibroblasts in conjunction with second harmonic imaging to view the collagen allows detailed imaging of invasion occurring in the 3D environment. Nobis et al. used this organotypic assay in conjunction with the same Src FLIM-FRET signalling Biosensor that we used in Chapter 7, thereby providing another possible avenue of research following the signalling route (Nobis et al., 2013).

Following successful 3D invasion assays the next stage would likely be *in vivo* work, to assess whether the proteins found necessary for chemotactic invasion in earlier work are also necessary *in vivo*. Again, a range of systems could be used for this stage of research. Injecting tumour cells expressing mutated genes of interest into mice before undertaking whole animal imaging in a system such as the Caliper IVIS would allow us to gain information about their roles in metastasis. We could investigate the number and size of metastases as well as their locations in the body. To more specifically investigate the migratory process we could use multiphoton imaging of mice. In this case we would again inject tumours carrying mutations in our genes of interest and allow them to grow. We could then image cells in the tumour/stroma interface migrating into the ECM and towards blood vessels. We would hope this would give us increased information on the

roles of our genes of interest in cancer metastasis.

Bibliography

F. Aguet, C. N. Antonescu, M. Mettlen, S. L. Schmid, and G. Danuser. Advances in analysis of low signal-to-noise images link dynamin and ap2 to the functions of an endocytic checkpoint. *Developmental cell*, 26(3):279–291, 2013.

S. Al Saleh, F. Al Mulla, and Y. A. Luqmani. Estrogen receptor silencing induces epithelial to mesenchymal transition in human breast cancer cells. *PloS one*, 6(6): e20610, 2011.

W. E. Allen, G. E. Jones, J. W. Pollard, and A. J. Ridley. Rho, rac and cdc42 regulate actin organization and cell adhesion in macrophages. *Journal of Cell Science*, 110(6): 707–720, 1997.

W. Amos and J. White. How the confocal laser scanning microscope entered biological research. *Biology of the Cell*, 95(6):335–342, 2003.

C. N. Antonescu, F. Aguet, G. Danuser, and S. L. Schmid. Phosphatidylinositol-(4, 5)-bisphosphate regulates clathrin-coated pit initiation, stabilization, and size. *Molecular biology of the cell*, 22(14):2588–2600, 2011.

A. Arkhipov, Y. Shan, R. Das, N. F. Endres, M. P. Eastwood, D. E. Wemmer, J. Kuriyan, and D. E. Shaw. Architecture and membrane interactions of the egf receptor. *Cell*, 152(3):557–569, 2013.

G. Assaker, D. Ramel, S. K. Wculek, M. González-Gaitán, and G. Emery. Spatial restriction of receptor tyrosine kinase activity through a polarized endocytic cycle controls border cell migration. *Proceedings of the National Academy of Sciences*, 107 (52):22558–22563, 2010.

G. Auciello, D. L. Cunningham, T. Tatar, J. K. Heath, and J. Z. Rappoport. Regulation of fibroblast growth factor receptor signalling and trafficking by src and eps8. *Journal of cell science*, 126(2):613–624, 2013.

D. Axelrod. Cell-substrate contacts illuminated by total internal reflection fluorescence. *The Journal of cell biology*, 89(1):141–145, 1981.

A. Bagorda and C. Parent. Eukaryotic chemotaxis at a glance. *Journal of cell science*, 121(16):2621–2624, 2008.

A. Bagorda, V. Mihaylov, and C. Parent. Chemotaxis: moving forward and holding on to the past. *Thrombosis and Haemostasis*, 95(1):12, 2006.

M. Bailly, J. Wyckoff, B. Bouzahzah, R. Hammerman, V. Sylvestre, M. Cammer, R. Pestell, and J. E. Segall. Epidermal growth factor receptor distribution during chemotactic responses. *Molecular biology of the cell*, 11(11):3873–3883, 2000.

J. Baselga and S. M. Swain. Cleopatra: a phase iii evaluation of pertuzumab and trastuzumab for her2-positive metastatic breast cancer. *Clinical breast cancer*, 10(6): 489–491, 2010.

P. V. Bashkirov, S. A. Akimov, A. I. Evseev, S. L. Schmid, J. Zimmerberg, and V. A. Frolov. A partnership between dynamin and lipids defines dynamics and intermediates of membrane fission. *Cell*, 135(7):1276, 2008a.

P. V. Bashkirov, S. A. Akimov, A. I. Evseev, S. L. Schmid, J. Zimmerberg, and V. A. Frolov. Gtpase cycle of dynamin is coupled to membrane squeeze and release, leading to spontaneous fission. *Cell*, 135(7):1276–1286, 2008b.

M. Bastiani and R. G. Parton. Caveolae at a glance. *Journal of cell science*, 123(22): 3831–3836, 2010.

M. Bastiani, L. Liu, M. M. Hill, M. P. Jedrychowski, S. J. Nixon, H. P. Lo, D. Abankwa, R. Luetterforst, M. Fernandez-Rojo, M. R. Breen, et al. Murc/cavin-4 and cavin family members form tissue-specific caveolar complexes. *The Journal of cell biology*, 185(7):1259–1273, 2009.

F. Belleudi, C. Scrofani, M. R. Torrisi, and P. Mancini. Polarized endocytosis of the keratinocyte growth factor receptor in migrating cells: role of src-signaling and cortactin. *PloS one*, 6(12):e29159, 2011.

K. A. Beningo, M. Dembo, I. Kaverina, J. V. Small, and Y.-l. Wang. Nascent focal adhesions are responsible for the generation of strong propulsive forces in migrating fibroblasts. *The Journal of cell biology*, 153(4):881–888, 2001.

A. Benmerah, B. Bègue, A. Dautry-Varsat, and N. Cerf-Bensussan. The ear of-adaptin interacts with the cooh-terminal domain of the eps15 protein. *Journal of Biological Chemistry*, 271(20):12111–12116, 1996.

A. D. Bershadsky and A. H. Futerman. Disruption of the golgi apparatus by brefeldin a blocks cell polarization and inhibits directed cell migration. *Proceedings of the National Academy of Sciences*, 91(12):5686–5689, 1994.

G. S. Blank and F. M. Brodsky. Site-specific disruption of clathrin assembly produces novel structures. *The EMBO journal*, 5(9):2087, 1986.

G. S. Blank and F. M. Brodsky. Clathrin assembly involves a light chain-binding region. *The Journal of cell biology*, 105(5):2011–2019, 1987.

T. Böcking, F. Aguet, S. C. Harrison, and T. Kirchhausen. Single-molecule analysis of a molecular disassemblase reveals the mechanism of hsc70-driven clathrin uncoating. *Nature structural & molecular biology*, 18(3):295–301, 2011.

G. Bonuccelli, M. C. Casimiro, F. Sotgia, C. Wang, M. Liu, S. Katiyar, J. Zhou, E. Dew, F. Capozza, K. M. Daumer, et al. Caveolin-1 (p132l), a common breast cancer mutation, confers mammary cell invasiveness and defines a novel stem cell/metastasis-associated gene signature. *The American journal of pathology*, 174(5):1650–1662, 2009.

E. Boucrot, S. Saffarian, R. Massol, T. Kirchhausen, and M. Ehrlich. Role of lipids and actin in the formation of clathrin-coated pits. *Experimental cell research*, 312(20): 4036–4048, 2006.

E. Boucrot, S. Saffarian, R. Zhang, and T. Kirchhausen. Roles of ap-2 in clathrin-mediated endocytosis. *PloS one*, 5(5):e10597, 2010.

E. Boucrot, A. Pick, G. Camdere, N. Liska, E. Evergren, H. T. McMahon, and M. M. Kozlov. Membrane fission is promoted by insertion of amphipathic helices and is restricted by crescent bar domains. *Cell*, 149(1):124–136, 2012.

S. Boyden. The chemotactic effect of mixtures of antibody and antigen on polymorphonuclear leucocytes. *The Journal of experimental medicine*, 115(3):453–466, 1962.

S. Braun, G. Schlimok, I. Heumos, G. Schaller, L. Riethdorf, G. Riethmüller, and K. Pantel. Erbb2 overexpression on occult metastatic cells in bone marrow predicts poor clinical outcome of stage i–iii breast cancer patients. *Cancer research*, 61(5):1890–1895, 2001.

V. Brekhman and G. Neufeld. A novel asymmetric 3d in-vitro assay for the study of tumor cell invasion. *BMC cancer*, 9(1):415, 2009.

M. Bretscher. Moving membrane up to the front of migrating cells. *Cell*, 85(4):465–467, 1996.

M. S. Bretscher. Endocytosis and recycling of the fibronectin receptor in cho cells. *The EMBO journal*, 8(5):1341, 1989.

M. S. Bretscher and C. Aguado-Velasco. Membrane traffic during cell locomotion. *Current opinion in cell biology*, 10(4):537–541, 1998.

R. E. Bridgewater, J. C. Norman, and P. T. Caswell. Integrin trafficking at a glance. *Journal of cell science*, 125(16):3695–3701, 2012.

F. M. Brodsky. Diversity of clathrin function: new tricks for an old protein. *Annual review of cell and developmental biology*, 28(1):309, 2012.

J. A. Broussard, D. J. Webb, and I. Kaverina. Asymmetric focal adhesion disassembly in motile cells. *Current opinion in cell biology*, 20(1):85–90, 2008.

M. L. Burness, T. A. Grushko, and O. I. Olopade. Epidermal growth factor receptor in triple-negative and basal-like breast cancer: promising clinical target or only a marker? *The Cancer Journal*, 16(1):23–32, 2010.

K. Burridge and K. Wennerberg. Rho and rac take center stage. *Cell*, 116(2):167–179, 2004.

D. A. Calderwood, Y. Fujioka, J. M. de Pereda, B. García-Alvarez, T. Nakamoto, B. Margolis, C. J. McGlade, R. C. Liddington, and M. H. Ginsberg. Integrin β cytoplasmic domain interactions with phosphotyrosine-binding domains: a structural prototype for diversity in integrin signaling. *Proceedings of the National Academy of Sciences*, 100(5):2272–2277, 2003.

H. Cao, W. E. Courchesne, and C. C. Mastick. A phosphotyrosine-dependent protein interaction screen reveals a role for phosphorylation of caveolin-1 on tyrosine 14 recruitment of c-terminal src kinase. *Journal of Biological Chemistry*, 277(11):8771–8774, 2002.

P. Caswell and J. Norman. Endocytic transport of integrins during cell migration and invasion. *Trends in cell biology*, 18(6):257–263, 2008.

P. T. Caswell and J. C. Norman. Integrin trafficking and the control of cell migration. *Traffic*, 7(1):14–21, 2006.

P. T. Caswell, M. Chan, A. J. Lindsay, M. W. McCaffrey, D. Boettiger, and J. C. Norman. Rab-coupling protein coordinates recycling of $\alpha 5\beta 1$ integrin and egfr1 to promote cell migration in 3d microenvironments. *The Journal of cell biology*, 183(1): 143–155, 2008a.

P. T. Caswell, M. Chan, A. J. Lindsay, M. W. McCaffrey, D. Boettiger, and J. C. Norman. Rab-coupling protein coordinates recycling of $\alpha 5\beta 1$ integrin and egfr1 to promote cell migration in 3d microenvironments. *The Journal of cell biology*, 183(1): 143–155, 2008b.

P. T. Caswell, S. Vadrevu, and J. C. Norman. Integrins: masters and slaves of endocytic transport. *Nature Reviews Molecular Cell Biology*, 10(12):843–853, 2009.

W.-T. Chao and J. Kunz. Focal adhesion disassembly requires clathrin-dependent endocytosis of integrins. *FEBS letters*, 583(8):1337–1343, 2009.

J. S. Chappie, J. A. Mears, S. Fang, M. Leonard, S. L. Schmid, R. A. Milligan, J. E. Hinshaw, and F. Dyda. A pseudoatomic model of the dynamin polymer identifies a hydrolysis-dependent powerstroke. *Cell*, 147(1):209–222, 2011.

C.-Y. Chen, M. L. Reese, P. K. Hwang, N. Ota, D. Agard, and F. M. Brodsky. Clathrin light and heavy chain interface: α-helix binding superhelix loops via critical tryptophans. *The EMBO journal*, 21(22):6072–6082, 2002.

J.-M. Cheng, M. Ding, A. Aribi, P. Shah, and K. Rao. Loss of rab25 expression in breast cancer. *International journal of cancer*, 118(12):2957–2964, 2006.

J.-M. Cheng, L. Volk, D. K. M. Janaki, S. Vyakaranam, S. Ran, and K. A. Rao. Tumor suppressor function of rab25 in triple-negative breast cancer. *International Journal of Cancer*, 126(12):2799–2812, 2010.

K. W. Cheng, J. P. Lahad, W.-l. Kuo, A. Lapuk, K. Yamada, N. Auersperg, J. Liu, K. Smith-McCune, K. H. Lu, D. Fishman, et al. The rab25 small gtpase determines aggressiveness of ovarian and breast cancers. *Nature medicine*, 10(11):1251–1256, 2004.

N. C. Cheng, N. van Zandwijk, and G. Reid. Cilengitide inhibits attachment and invasion of malignant pleural mesothelioma cells through antagonism of integrins $\alpha v\beta 3$ and $\alpha v\beta 5$. *PloS one*, 9(3):e90374, 2014.

C. K. Choi, M. Vicente-Manzanares, J. Zareno, L. A. Whitmore, A. Mogilner, and A. R. Horwitz. Actin and α-actinin orchestrate the assembly and maturation of nascent adhesions in a myosin ii motor-independent manner. *Nature cell biology*, 10(9):1039–1050, 2008.

C. Chung, C. C. Mader, J. C. Schmitz, J. Atladottir, P. Fitchev, M. L. Cornwell, A. J. Koleske, S. E. Crawford, and F. Gorelick. The vacuolar-atpase modulates matrix metalloproteinase isoforms in human pancreatic cancer. *Laboratory Investigation*, 91 (5):732–743, 2011.

E. Cocucci, F. Aguet, S. Boulant, and T. Kirchhausen. The first five seconds in the life of a clathrin-coated pit. *Cell*, 150(3):495–507, 2012.

S. Cohen. Egf and its receptor: historical perspective. *Journal of Mammary Gland Biology and Neoplasia*, 2(2):93–96, 1997.

S. Cohen. Origins of growth factors: Ngf and egf. *Annals of the New York Academy of Sciences*, 1038(1):98–102, 2004.

B. M. Collins, A. J. McCoy, H. M. Kent, P. R. Evans, and D. J. Owen. Molecular architecture and functional model of the endocytic ap2 complex. *Cell*, 109(4):523–535, 2002.

M. Colombo, F. Corsi, D. Foschi, E. Mazzantini, S. Mazzucchelli, C. Morasso, E. Occhipinti, L. Polito, D. Prosperi, S. Ronchi, et al. Her2 targeting as a two-sided strategy for breast cancer diagnosis and treatment: Outlook and recent implications in nanomedical approaches. *Pharmacological research*, 62(2):150–165, 2010.

J. Condeelis and J. E. Segall. Intravital imaging of cell movement in tumours. *Nature Reviews Cancer*, 3(12):921–930, 2003.

J. Condeelis, R. H. Singer, and J. E. Segall. The great escape: when cancer cells hijack the genes for chemotaxis and motility. *Annu. Rev. Cell Dev. Biol.*, 21:695–718, 2005.

L. M. Coussens and Z. Werb. Matrix metal loproteinases and the development of cancer. *Chemistry & biology*, 3(11):895–904, 1996.

R. Crowther, J. Pinch, and B. Pearse. On the structure of coated vesicles. *Journal of molecular biology*, 103(4):785–798, 1976.

A. Czuchra, X. Wu, H. Meyer, J. Van Hengel, T. Schroeder, R. Geffers, K. Rottner, and C. Brakebusch. Cdc42 is not essential for filopodium formation, directed migration, cell polarization, and mitosis in fibroblastoid cells. *Molecular biology of the cell*, 16 (10):4473–4484, 2005.

E.-M. Damm, L. Pelkmans, J. Kartenbeck, A. Mezzacasa, T. Kurzchalia, and A. Helenius. Clathrin-and caveolin-1–independent endocytosis entry of simian virus 40 into cells devoid of caveolae. *The Journal of cell biology*, 168(3):477–488, 2005.

E. H. Danen, J. van Rheenen, W. Franken, S. Huveneers, P. Sonneveld, K. Jalink, and A. Sonnenberg. Integrins control motile strategy through a rho–cofilin pathway. *The Journal of cell biology*, 169(3):515–526, 2005.

P. N. Dannhauser and E. J. Ungewickell. Reconstitution of clathrin-coated bud and vesicle formation with minimal components. *Nature cell biology*, 14(6):634–639, 2012.

E. Daro, P. Van Der Sluijs, T. Galli, and I. Mellman. Rab4 and cellubrevin define different early endosome populations on the pathway of transferrin receptor recycling. *Proceedings of the National Academy of Sciences*, 93(18):9559–9564, 1996.

O. Daumke, A. Roux, and V. Haucke. Bar domain scaffolds in dynamin-mediated membrane fission. *Cell*, 156(5):882–892, 2014.

J. C. Dawson, P. Timpson, G. Kalna, and L. M. Machesky. Mtss1 regulates epidermal growth factor signaling in head and neck squamous carcinoma cells. *Oncogene*, 31 (14):1781–1793, 2011.

P. G. De Deyne, A. O'Neill, W. G. Resneck, G. M. Dmytrenko, D. W. Pumplin, and R. J. Bloch. The vitronectin receptor associates with clathrin-coated membrane domains via the cytoplasmic domain of its beta5 subunit. *Journal of cell science*, 111(18): 2729–2740, 1998.

M. A. del Pozo, L. S. Price, N. B. Alderson, X.-D. Ren, and M. A. Schwartz. Adhesion to the extracellular matrix regulates the coupling of the small gtpase rac to its effector pak. *The EMBO journal*, 19(9):2008–2014, 2000.

M. A. del Pozo, N. Balasubramanian, N. B. Alderson, W. B. Kiosses, A. Grande-García, R. G. Anderson, and M. A. Schwartz. Phospho-caveolin-1 mediates integrin-regulated membrane domain internalization. *Nature cell biology*, 7(9):901–908, 2005a.

M. A. del Pozo, N. Balasubramanian, N. B. Alderson, W. B. Kiosses, A. Grande-García, R. G. Anderson, and M. A. Schwartz. Phospho-caveolin-1 mediates integrin-regulated membrane domain internalization. *Nature cell biology*, 7(9):901–908, 2005b.

P. Devreotes and C. Janetopoulos. Eukaryotic chemotaxis: distinctions between directional sensing and polarization. *Journal of biological chemistry*, 278(23):20445–20448, 2003.

G. Di Guglielmo, P. Baass, W. Ou, B. Posner, and J. Bergeron. Compartmentalization of shc, grb2 and msos, and hyperphosphorylation of raf-1 by egf but not insulin in liver parenchyma. *The EMBO journal*, 13(18):4269, 1994.

G. M. Di Guglielmo, C. Le Roy, A. F. Goodfellow, and J. L. Wrana. Distinct endocytic pathways regulate tgf-β receptor signalling and turnover. *Nature cell biology*, 5(5): 410–421, 2003.

D. J. Dietzen, W. R. Hastings, and D. M. Lublin. Caveolin is palmitoylated on multiple cysteine residues palmitoylation is not necessary for localization of caveolin to caveolae. *Journal of Biological Chemistry*, 270(12):6838–6842, 1995.

G. Doherty and H. McMahon. Mechanisms of endocytosis. *Annual review of biochemistry*, 78:857–902, 2009.

M. Drab, P. Verkade, M. Elger, M. Kasper, M. Lohn, B. Lauterbach, J. Menne, C. Lindschau, F. Mende, F. C. Luft, et al. Loss of caveolae, vascular dysfunction, and pulmonary defects in caveolin-1 gene-disrupted mice. *Science*, 293(5539):2449–2452, 2001.

K. W. Dunn, T. E. McGraw, and F. R. Maxfield. Iterative fractionation of recycling receptors from lysosomally destined ligands in an early sorting endosome. *The Journal of cell biology*, 109(6):3303–3314, 1989.

S. A. Eccles. The epidermal growth factor receptor/erb-b/her family in normal and malignant breast biology. *International Journal of Developmental Biology*, 55(7):685, 2011.

S. Eden, R. Rohatgi, A. V. Podtelejnikov, M. Mann, and M. W. Kirschner. Mechanism of regulation of wave1-induced actin nucleation by rac1 and nck. *Nature*, 418(6899): 790–793, 2002.

S. Etienne-Manneville and A. Hall. Rho gtpases in cell biology. *Nature*, 420(6916): 629–635, 2002.

H. Ewers, W. Römer, A. E. Smith, K. Bacia, S. Dmitrieff, W. Chai, R. Mancini, J. Kartenbeck, V. Chambon, L. Berland, et al. Gm1 structure determines sv40-induced membrane invagination and infection. *Nature cell biology*, 12(1):11–18, 2010.

E. J. Ezratty, C. Bertaux, E. E. Marcantonio, and G. G. Gundersen. Clathrin mediates integrin endocytosis for focal adhesion disassembly in migrating cells. *The Journal of cell biology*, 187(5):733–747, 2009.

M. Fabbri, S. Di Meglio, M. C. Gagliani, E. Consonni, R. Molteni, J. R. Bender, C. Tacchetti, and R. Pardi. Dynamic partitioning into lipid rafts controls the endo-exocytic cycle of the αl/β2 integrin, lfa-1, during leukocyte chemotaxis. *Molecular biology of the cell*, 16(12):5793–5803, 2005.

K. Faelber, Y. Posor, S. Gao, M. Held, Y. Roske, D. Schulze, V. Haucke, F. Noé, and O. Daumke. Crystal structure of nucleotide-free dynamin. *Nature*, 477(7366):556–560, 2011.

G.-H. Fan, L. A. Lapierre, J. R. Goldenring, J. Sai, and A. Richmond. Rab11-family interacting protein 2 and myosin vb are required for cxcr2 recycling and receptor-mediated chemotaxis. *Molecular biology of the cell*, 15(5):2456–2469, 2004.

S. M. Ferguson and P. De Camilli. Dynamin, a membrane-remodelling gtpase. *Nature Reviews Molecular Cell Biology*, 13(2):75–88, 2012.

S. Fletcher and J. Rappoport. Moving forward: polarised trafficking in cell migration. *Trends in cell biology*, 20(2):71–78, 2010.

S. J. Fletcher. *Investigating the role of vesicle trafficking in epithelial cell migration.* PhD thesis, The University of Birmingham, 2012.

S. J. Fletcher, N. S. Poulter, E. J. Haining, and J. Z. Rappoport. Clathrin-mediated endocytosis regulates occludin, and not focal adhesion, distribution during epithelial wound healing. *Biology of the Cell*, 104(4):238–256, 2012.

J. Foley, N. K. Nickerson, S. Nam, K. T. Allen, J. L. Gilmore, K. P. Nephew, and D. J. Riese II. Egfr signaling in breast cancer: bad to the bone. *Seminars in cell & developmental biology*, 21(9):951–960, 2010.

M. G. Ford, I. G. Mills, B. J. Peter, Y. Vallis, G. J. Praefcke, P. R. Evans, and H. T. McMahon. Curvature of clathrin-coated pits driven by epsin. *Nature*, 419(6905): 361–366, 2002.

A. Fotin, Y. Cheng, N. Grigorieff, T. Walz, S. C. Harrison, and T. Kirchhausen. Structure of an auxilin-bound clathrin coat and its implications for the mechanism of uncoating. *Nature*, 432(7017):649–653, 2004.

A. R. French, D. K. Tadaki, S. K. Niyogi, and D. A. Lauffenburger. Intracellular trafficking of epidermal growth factor family ligands is directly influenced by the ph sensitivity of the receptor/ligand interaction. *Journal of Biological Chemistry*, 270(9):4334–4340, 1995.

S. Funamoto, R. Meili, S. Lee, L. Parry, and R. A. Firtel. Spatial and temporal regulation of 3-phosphoinositides by pi 3-kinase and pten mediates chemotaxis. *Cell*, 109(5):611–623, 2002.

I. Gaidarov, Q. Chen, J. R. Falck, K. K. Reddy, and J. H. Keen. A functional phosphatidylinositol 3, 4, 5-trisphosphate/phosphoinositide binding domain in the clathrin adaptor ap-2 α subunit. implications for the endocytic pathway. *Journal of Biological Chemistry*, 271(34):20922–20929, 1996.

F. Galbiati, J. A. Engelman, D. Volonte, X. L. Zhang, C. Minetti, M. Li, H. Hou, B. Kneitz, W. Edelmann, and M. P. Lisanti. Caveolin-3 null mice show a loss of caveolae, changes in the microdomain distribution of the dystrophin-glycoprotein complex, and t-tubule abnormalities. *Journal of Biological Chemistry*, 276(24):21425–21433, 2001.

J. L. Gilmore, J. A. Scott, Z. Bouizar, A. Robling, S. E. Pitfield, D. J. Riese II, and J. Foley. Amphiregulin-egfr signaling regulates pthrp gene expression in breast cancer cells. *Breast cancer research and treatment*, 110(3):493–505, 2008.

A. Glading, D. A. Lauffenburger, and A. Wells. Cutting to the chase: calpain proteases in cell motility. *Trends in cell biology*, 12(1):46–54, 2002.

J. Goldenring, K. R. Shen, H. D. Vaughan, and I. M. Modlin. Identification of a small gtp-binding protein, rab25, expressed in the gastrointestinal mucosa, kidney, and lung. *Journal of Biological Chemistry*, 268(25):18419–18422, 1993.

A. I. Gotlieb, L. M. May, L. Subrahmanyan, and V. I. Kalnins. Distribution of microtubule organizing centers in migrating sheets of endothelial cells. *The Journal of cell biology*, 91(2):589–594, 1981.

A. Grande-García, A. Echarri, J. de Rooij, N. B. Alderson, C. M. Waterman-Storer, J. M. Valdivielso, and M. A. del Pozo. Caveolin-1 regulates cell polarization and directional migration through src kinase and rho gtpases. *The Journal of cell biology*, 177(4):683–694, 2007.

B. D. Grant and J. G. Donaldson. Pathways and mechanisms of endocytic recycling. *Nature Reviews Molecular Cell Biology*, 10(9):597–608, 2009.

Z. Gu, E. H. Noss, V. W. Hsu, and M. B. Brenner. Integrins traffic rapidly via circular dorsal ruffles and macropinocytosis during stimulated cell migration. *The Journal of cell biology*, 193(1):61–70, 2011.

T. A. Guise, J. J. Yin, S. Taylor, Y. Kumagai, M. Dallas, B. Boyce, T. Yoneda, and G. Mundy. Evidence for a causal role of parathyroid hormone-related protein in the pathogenesis of human breast cancer-mediated osteolysis. *Journal of Clinical Investigation*, 98(7):1544, 1996.

M. Haemmerle, T. Keller, G. Egger, H. Schachner, C. W. Steiner, D. Stokic, C. Neumayer, M. K. Brown, D. Kerjaschki, and B. Hantusch. Enhanced lymph vessel density, remodelling and inflammation is reflected by gene expression signatures in dermal lymphatic endothelial cells in type 2 diabetes. *Diabetes*, page DB_120844, 2013.

D. Hanahan and R. A. Weinberg. Hallmarks of cancer: the next generation. *Cell*, 144 (5):646–674, 2011.

R. C. Harris, E. Chung, and R. J. Coffey. Egf receptor ligands. *The EGF receptor family biologic mechanisms and role in cancer. Elsevier, California*, pages 3–14, 2004.

S. M. Harrison, T. Knifley, M. Chen, and K. L. O'Connor. Lpa, hgf, and egf utilize distinct combinations of signaling pathways to promote migration and invasion of mda-mb-231 breast carcinoma cells. *BMC cancer*, 13(1):501, 2013.

J. M. Haugh, F. Codazzi, M. Teruel, and T. Meyer. Spatial sensing in fibroblasts mediated by 3' phosphoinositides. *The Journal of cell biology*, 151(6):1269–1280, 2000.

A. Hayer, M. Stoeber, D. Ritz, S. Engel, H. H. Meyer, and A. Helenius. Caveolin-1 is ubiquitinated and targeted to intralumenal vesicles in endolysosomes for degradation. *The Journal of cell biology*, 191(3):615–629, 2010.

B. Heit and P. Kubes. Measuring chemotaxis and chemokinesis: the under-agarose cell migration assay. *Science Signaling*, 2003(170):pl5, 2003.

S. J. Henle, G. Wang, E. Liang, M. Wu, M.-m. Poo, and J. R. Henley. Asymmetric pi (3, 4, 5) p3 and akt signaling mediates chemotaxis of axonal growth cones. *The Journal of Neuroscience*, 31(19):7016–7027, 2011.

W. M. Henne, E. Boucrot, M. Meinecke, E. Evergren, Y. Vallis, R. Mittal, and H. T. McMahon. Fcho proteins are nucleators of clathrin-mediated endocytosis. *Science*, 328(5983):1281–1284, 2010.

E. Hill, J. Van Der Kaay, C. Downes, and E. Smythe. The role of dynamin and its binding partners in coated pit invagination and scission. *The Journal of cell biology*, 152(2):309–324, 2001.

M. M. Hill, N. Scherbakov, N. Schiefermeier, J. Baran, J. F. Hancock, L. A. Huber, R. G. Parton, and M.-O. Parat. Reassessing the role of phosphocaveolin-1 in cell adhesion and migration. *Traffic*, 8(12):1695–1705, 2007.

M. M. Hill, M. Bastiani, R. Luetterforst, M. Kirkham, A. Kirkham, S. J. Nixon, P. Walser, D. Abankwa, V. M. Oorschot, S. Martin, et al. Ptrf-cavin, a conserved cytoplasmic protein required for caveola formation and function. *Cell*, 132(1):113–124, 2008.

L. Hinrichsen, J. Harborth, L. Andrees, K. Weber, and E. J. Ungewickell. Effect of clathrin heavy chain-and α-adaptin-specific small inhibitory rnas on endocytic accessory proteins and receptor trafficking in hela cells. *Journal of Biological Chemistry*, 278(46):45160–45170, 2003.

S. Hiratsuka, A. Watanabe, H. Aburatani, and Y. Maru. Tumour-mediated upregulation of chemoattractants and recruitment of myeloid cells predetermines lung metastasis. *Nature cell biology*, 8(12):1369–1375, 2006.

A. M. Hommelgaard, K. Roepstorff, F. Vilhardt, M. L. Torgersen, K. Sandvig, and B. van Deurs. Caveolae: stable membrane domains with a potential for internalization. *Traffic*, 6(9):720–724, 2005.

C. R. Hopkins, A. Gibson, M. Shipman, D. K. Strickland, and I. S. Trowbridge. In migrating fibroblasts, recycling receptors are concentrated in narrow tubules in the pericentriolar area, and then routed to the plasma membrane of the leading lamella. *The Journal of Cell Biology*, 125(6):1265–1274, 1994.

F. Huang, A. Khvorova, W. Marshall, and A. Sorkin. Analysis of clathrin-mediated endocytosis of epidermal growth factor receptor by rna interference. *Journal of Biological Chemistry*, 279(16):16657–16661, 2004.

J. D. Humphries, A. Byron, and M. J. Humphries. Integrin ligands at a glance. *Journal of cell science*, 119(19):3901–3903, 2006.

A. Huttenlocher and A. R. Horwitz. Integrins in cell migration. *Cold Spring Harbor perspectives in biology*, 3(9):a005074, 2011.

R. O. Hynes. Integrins: bidirectional, allosteric signaling machines. *Cell*, 110(6):673–687, 2002.

M. Iijima and P. Devreotes. Tumor suppressor pten mediates sensing of chemoattractant gradients. *Cell*, 109(5):599–610, 2002.

M. Isshiki, J. Ando, K. Yamamoto, T. Fujita, Y. Ying, and R. G. Anderson. Sites of ca2+ wave initiation move with caveolae to the trailing edge of migrating cells. *Journal of cell science*, 115(3):475–484, 2002.

T. Itoh, K. S. Erdmann, A. Roux, B. Habermann, H. Werner, and P. De Camilli. Dynamin and the actin cytoskeleton cooperatively regulate plasma membrane invagination by bar and f-bar proteins. *Developmental cell*, 9(6):791–804, 2005.

J. Ivaska, R. D. Whelan, R. Watson, and P. J. Parker. Pkcε controls the traffic of β1 integrins in motile cells. *The EMBO journal*, 21(14):3608–3619, 2002.

J. K. Jaiswal, N. W. Andrews, and S. M. Simon. Membrane proximal lysosomes are the major vesicles responsible for calcium-dependent exocytosis in nonsecretory cells. *The Journal of cell biology*, 159(4):625–635, 2002.

L. E. Johannessen, N. M. Pedersen, K. W. Pedersen, I. H. Madshus, and E. Stang. Activation of the epidermal growth factor (egf) receptor induces formation of egf receptor-and grb2-containing clathrin-coated pits. *Molecular and cellular biology*, 26 (2):389–401, 2006.

M. C. Jones, P. T. Caswell, and J. C. Norman. Endocytic recycling pathways: emerging regulators of cell migration. *Current opinion in cell biology*, 18(5):549–557, 2006.

S. Jones and J. Z. Rappoport. Interdependent epidermal growth factor receptor signalling and trafficking. *The international journal of biochemistry & cell biology*, 51:23–28, 2014.

S. Jones, D. L. Cunningham, J. Z. Rappoport, and J. K. Heath. The non-receptor tyrosine kinase ack1 regulates the fate of activated egfr by inducing trafficking to the p62/nbr1 pre-autophagosome. *Journal of cell science*, 127(5):994–1006, 2014.

S. M. Jones, K. E. Howell, J. R. Henley, H. Cao, and M. A. McNiven. Role of dynamin in the formation of transport vesicles from the trans-golgi network. *Science*, 279(5350): 573–577, 1998.

H. Katoh, K. Hiramoto, and M. Negishi. Activation of rac1 by rhog regulates cell migration. *Journal of cell science*, 119(1):56–65, 2006.

P. A. Keyel, S. K. Mishra, R. Roth, J. E. Heuser, S. C. Watkins, and L. M. Traub. A single common portal for clathrin-mediated endocytosis of distinct cargo governed by cargo-selective adaptors. *Molecular biology of the cell*, 17(10):4300–4317, 2006.

A. Khademhosseini. *Micro and nanoengineering of the cell microenvironment: technologies and applications*. Artech House, 2008.

A. S. Kim, L. T. Kakalis, N. Abdul-Manan, G. A. Liu, and M. K. Rosen. Autoinhibition and activation mechanisms of the wiskott–aldrich syndrome protein. *Nature*, 404 (6774):151–158, 2000.

W. B. Kiosses, S. J. Shattil, N. Pampori, and M. A. Schwartz. Rac recruits high-affinity integrin αvβ3 to lamellipodia in endothelial cell migration. *Nature cell biology*, 3(3): 316–320, 2001.

T. Kirchhausen. Adaptors for clathrin-mediated traffic. *Annual review of cell and developmental biology*, 15(1):705–732, 1999.

T. Kirchhausen. Clathrin. *Annual review of biochemistry*, 69(1):699–727, 2000.

T. Kirchhausen. Bending membranes. *Nature cell biology*, 14(9):906–908, 2012.

T. Kirchhausen and S. C. Harrison. Protein organization in clathrin trimers. *Cell*, 23 (3):755–761, 1981.

C. Knuehl, C.-Y. Chen, V. Manalo, P. K. Hwang, N. Ota, and F. M. Brodsky. Novel binding sites on clathrin and adaptors regulate distinct aspects of coat assembly. *Traffic*, 7(12):1688–1700, 2006.

E. Korsching, S. S. Jeffrey, W. Meinerz, T. Decker, W. Boecker, and H. Buerger. Basal carcinoma of the breast revisited: an old entity with new interpretations. *Journal of clinical pathology*, 61(5):553–560, 2008.

C. Lamaze, A. Dujeancourt, T. Baba, C. G. Lo, A. Benmerah, and A. Dautry-Varsat. Interleukin 2 receptors and detergent-resistant membrane domains define a clathrin-independent endocytic pathway. *Molecular cell*, 7(3):661–671, 2001.

D. Lauffenburger and A. Horwitz. Cell migration: a physically integrated molecular process. *Cell*, 84(3):359–369, 1995.

C. M. Laukaitis, D. J. Webb, K. Donais, and A. F. Horwitz. Differential dynamics of $\alpha 5$ integrin, paxillin, and α-actinin during formation and disassembly of adhesions in migrating cells. *The Journal of cell biology*, 153(7):1427–1440, 2001.

M. A. Lawson and F. R. Maxfield. Ca2+-and calcineurin-dependent recycling of an integrin to the front of migrating neutrophils. *Nature*, 377(6544):75–79, 1995.

K. R. Legate, S. A. Wickström, and R. Fässler. Genetic and cell biological analysis of integrin outside-in signaling. *Genes & development*, 23(4):397–418, 2009.

M. A. Lemmon, Z. Bu, J. E. Ladbury, M. Zhou, D. Pinchasi, I. Lax, D. M. Engelman, and J. Schlessinger. Two egf molecules contribute additively to stabilization of the egfr dimer. *The EMBO Journal*, 16(2):281–294, 1997.

S. K. Lemmon and L. M. Traub. Getting in touch with the clathrin terminal domain. *Traffic*, 13(4):511–519, 2012.

G. Levkowitz, H. Waterman, E. Zamir, Z. Kam, S. Oved, W. Y. Langdon, L. Beguinot, B. Geiger, and Y. Yarden. c-cbl/sli-1 regulates endocytic sorting and ubiquitination of the epidermal growth factor receptor. *Genes & development*, 12(23):3663–3674, 1998.

J. Li, B. A. Ballif, A. M. Powelka, J. Dai, S. P. Gygi, and V. W. Hsu. Phosphorylation of acap1 by akt regulates the stimulation-dependent recycling of integrin $\beta 1$ to control cell migration. *Developmental cell*, 9(5):663–673, 2005.

X. Li, A. G. Garrity, and H. Xu. Regulation of membrane trafficking by signalling on endosomal and lysosomal membranes. *The Journal of physiology*, 591(18):4389–4401, 2013.

Z. Li, M. Hannigan, Z. Mo, B. Liu, W. Lu, Y. Wu, A. V. Smrcka, G. Wu, L. Li, M. Liu, et al. Directional sensing requires g$\beta\gamma$-mediated pak1 and pixα-dependent activation of cdc42. *Cell*, 114(2):215–227, 2003.

M. Liljedahl, Y. Maeda, A. Colanzi, I. Ayala, J. Van Lint, and V. Malhotra. Protein kinase d regulates the fission of cell surface destined transport carriers from the trans-golgi network. *Cell*, 104(3):409–420, 2001.

C. J. Lim, K. H. Kain, E. Tkachenko, L. E. Goldfinger, E. Gutierrez, M. D. Allen, A. Groisman, J. Zhang, and M. H. Ginsberg. Integrin-mediated protein kinase a activation at the leading edge of migrating cells. *Molecular biology of the cell*, 19(11): 4930–4941, 2008.

L. Liu and P. F. Pilch. A critical role of cavin (polymerase i and transcript release factor) in caveolae formation and organization. *Journal of biological chemistry*, 283 (7):4314–4322, 2008.

L. Liu, B. He, W. M. Liu, D. Zhou, J. V. Cox, and X. A. Zhang. Tetraspanin cd151 promotes cell migration by regulating integrin trafficking. *Journal of Biological Chemistry*, 282(43):31631–31642, 2007.

Y. Liu, M. Surka, T. Schroeter, V. Lukiyanchuk, and S. Schmid. Isoform and splice-variant specific functions of dynamin-2 revealed by analysis of conditional knock-out cells. *Molecular biology of the cell*, 19(12):5347–5359, 2008.

X. Lu and Y. Kang. Epidermal growth factor signalling and bone metastasis. *British journal of cancer*, 102(3):457–461, 2009.

L. M. Machesky and A. Hall. Role of actin polymerization and adhesion to extracellular matrix in rac-and rho-induced cytoskeletal reorganization. *The Journal of cell biology*, 138(4):913–926, 1997.

L. M. Machesky, S. J. Atkinson, C. Ampe, J. Vandekerckhove, and T. D. Pollard. Purification of a cortical complex containing two unconventional actins from acanthamoeba by affinity chromatography on profilin-agarose. *The Journal of cell biology*, 127(1): 107–115, 1994.

E. Macia, M. Ehrlich, R. Massol, E. Boucrot, C. Brunner, and T. Kirchhausen. Dynasore, a cell-permeable inhibitor of dynamin. *Developmental cell*, 10(6):839–850, 2006.

A. Mallavarapu and T. Mitchison. Regulated actin cytoskeleton assembly at filopodium tips controls their extension and retraction. *The Journal of cell biology*, 146(5):1097–1106, 1999.

A. Mammoto, T. Ohtsuka, I. Hotta, T. Sasaki, and Y. Takai. Rab11bp/rabphilin-11, a downstream target of rab11 small g protein implicated in vesicle recycling. *Journal of Biological Chemistry*, 274(36):25517–25524, 1999.

C. Margadant, H. N. Monsuur, J. C. Norman, and A. Sonnenberg. Mechanisms of integrin activation and trafficking. *Current opinion in cell biology*, 23(5):607–614, 2011.

B. Marks, M. H. Stowell, Y. Vallis, I. G. Mills, A. Gibson, C. R. Hopkins, and H. T. McMahon. Gtpase activity of dynamin and resulting conformation change are essential for endocytosis. *Nature*, 410(6825):231–235, 2001.

J. M. Mato, A. Losada, V. Nanjundiah, and T. M. Konijn. Signal input for a chemotactic response in the cellular slime mold dictyostelium discoideum. *Proceedings of the National Academy of Sciences*, 72(12):4991–4993, 1975.

A. L. Mattheyses, S. M. Simon, and J. Z. Rappoport. Imaging with total internal reflection fluorescence microscopy for the cell biologist. *Journal of cell science*, 123 (21):3621–3628, 2010.

S. Maubant, D. Saint-Dizier, M. Boutillon, F. Perron-Sierra, P. J. Casara, J. A. Hickman, G. C. Tucker, and E. Van Obberghen-Schilling. Blockade of $\alpha v\beta 3$ and $\alpha v\beta 5$ integrins by rgd mimetics induces anoikis and not integrin-mediated death in human endothelial cells. *Blood*, 108(9):3035–3044, 2006.

M. E. Maurer and J. A. Cooper. The adaptor protein dab2 sorts ldl receptors into coated pits independently of ap-2 and arh. *Journal of cell science*, 119(20):4235–4246, 2006.

F. R. Maxfield and T. E. McGraw. Endocytic recycling. *Nature reviews Molecular cell biology*, 5(2):121–132, 2004.

F. R. Maxfield and D. J. Yamashiro. Acidification of organelles and the intracellular sorting of proteins during endocytosis. *Intracellular Trafficking of Proteins*, pages 157–182, 1991.

M. W. McCaffrey, A. Bielli, G. Cantalupo, S. Mora, V. Roberti, M. Santillo, F. Drummond, and C. Bucci. Rab4 affects both recycling and degradative endosomal trafficking. *FEBS letters*, 495(1):21–30, 2001.

H. T. McMahon and E. Boucrot. Molecular mechanism and physiological functions of clathrin-mediated endocytosis. *Nature reviews Molecular cell biology*, 12(8):517–533, 2011.

M. Meinecke, E. Boucrot, G. Camdere, W.-C. Hon, R. Mittal, and H. T. McMahon. Cooperative recruitment of dynamin and bin/amphiphysin/rvs (bar) domain-containing proteins leads to gtp-dependent membrane scission. *Journal of Biological Chemistry*, 288(9):6651–6661, 2013.

M. C. Mendoza, E. E. Er, and J. Blenis. The ras-erk and pi3k-mtor pathways: cross-talk and compensation. *Trends in biochemical sciences*, 36(6):320–328, 2011.

M. Miaczynska, L. Pelkmans, and M. Zerial. Not just a sink: endosomes in control of signal transduction. *Current opinion in cell biology*, 16(4):400–406, 2004.

A. E. Miele, P. J. Watson, P. R. Evans, L. M. Traub, and D. J. Owen. Two distinct interaction motifs in amphiphysin bind two independent sites on the clathrin terminal domain β-propeller. *Nature structural & molecular biology*, 11(3):242–248, 2004.

H. Miki, S. Suetsugu, and T. Takenawa. Wave, a novel wasp-family protein involved in actin reorganization induced by rac. *The EMBO journal*, 17(23):6932–6941, 1998.

C. Mim and V. M. Unger. Membrane curvature and its generation by bar proteins. *Trends in biochemical sciences*, 37(12):526–533, 2012.

J. A. Mindell. Lysosomal acidification mechanisms*. *Annual review of physiology*, 74: 69–86, 2012.

K. Mohrmann and P. van der Sluijs. Regulation of membrane transport through the endocytic pathway by rabgtpases. *Molecular membrane biology*, 16(1):81–87, 1999.

P. S. Mongroo, C. N. Johnstone, I. Naruszewicz, C. Leung-Hagesteijn, R. K. Sung, L. Carnio, A. K. Rustgi, and G. E. Hannigan. β-parvin inhibits integrin-linked kinase signaling and is downregulated in breast cancer. *Oncogene*, 23(55):8959–8970, 2004.

S. Monier, R. G. Parton, F. Vogel, J. Behlke, A. Henske, and T. Kurzchalia. Vip21-caveolin, a membrane protein constituent of the caveolar coat, oligomerizes in vivo and in vitro. *Molecular biology of the cell*, 6(7):911, 1995.

V. Morello, S. Cabodi, S. Sigismund, M. Camacho-Leal, D. Repetto, M. Volante, M. Papotti, E. Turco, and P. Defilippi. β1 integrin controls egfr signaling and tumorigenic properties of lung cancer cells. *Oncogene*, 30(39):4087–4096, 2011.

A. Motley, N. A. Bright, M. N. Seaman, and M. S. Robinson. Clathrin-mediated endocytosis in ap-2–depleted cells. *The Journal of cell biology*, 162(5):909–918, 2003.

A. J. Muinonen-Martin, D. M. Veltman, G. Kalna, and R. H. Insall. An improved chamber for direct visualisation of chemotaxis. *PloS one*, 5(12):e15309, 2010.

P. A. Muller, P. T. Caswell, B. Doyle, M. P. Iwanicki, E. H. Tan, S. Karim, N. Lukashchuk, D. A. Gillespie, R. L. Ludwig, P. Gosselin, et al. Mutant p53 drives invasion by promoting integrin recycling. *Cell*, 139(7):1327–1341, 2009.

A. Murali and K. Rajalingam. Small rho gtpases in the control of cell shape and mobility. *Cellular and Molecular Life Sciences*, pages 1–19, 2013.

J. E. Murphy, B. E. Padilla, B. Hasdemir, G. S. Cottrell, and N. W. Bunnett. Endosomes: a legitimate platform for the signaling train. *Proceedings of the National Academy of Sciences*, 106(42):17615–17622, 2009.

I. Nabi and P. Le. Caveolae/raft-dependent endocytosis. *The Journal of cell biology*, 161(4):673–677, 2003.

I. S. Näthke, J. Heuser, A. Lupas, J. Stock, C. W. Turck, and F. M. Brodsky. Folding and trimerization of clathrin subunits at the triskelion hub. *Cell*, 68(5):899–910, 1992.

S. Neumann and S. L. Schmid. Dual role of bar domain-containing proteins in regulating vesicle release catalyzed by the gtpase, dynamin-2. *Journal of Biological Chemistry*, 288(35):25119–25128, 2013.

R. E. Nisato, J.-C. Tille, A. Jonczyk, S. L. Goodman, and M. S. Pepper. αvβ3 and αvβ5 integrin antagonists inhibit angiogenesis in vitro. *Angiogenesis*, 6(2):105–119, 2003.

T. Nishimura and K. Kaibuchi. Numb controls integrin endocytosis for directional cell migration with apkc and par-3. *Developmental cell*, 13(1):15–28, 2007.

M. Nobis, E. J. McGhee, J. P. Morton, J. P. Schwarz, S. A. Karim, J. Quinn, M. Edward, A. D. Campbell, L. C. McGarry, T. J. Evans, et al. Intravital flim-fret imaging reveals dasatinib-induced spatial control of src in pancreatic cancer. *Cancer research*, 73(15): 4674–4686, 2013.

N. Normanno, A. De Luca, C. Bianco, L. Strizzi, M. Mancino, M. R. Maiello, A. Carotenuto, G. De Feo, F. Caponigro, and D. S. Salomon. Epidermal growth factor receptor (egfr) signaling in cancer. *Gene*, 366(1):2–16, 2006.

R. Nossal. Energetics of clathrin basket assembly. *Traffic*, 2(2):138–147, 2001.

P. Oh, D. P. McIntosh, and J. E. Schnitzer. Dynamin at the neck of caveolae mediates their budding to form transport vesicles by gtp-driven fission from the plasma membrane of endothelium. *The Journal of cell biology*, 141(1):101–114, 1998.

H. Ohno, J. Stewart, M.-C. Fournier, H. Bosshart, I. Rhee, S. Miyatake, T. Saito, A. Gallusser, T. Kirchhausen, and J. S. Bonifacino. Interaction of tyrosine-based sorting signals with clathrin-associated proteins. *Science*, 269(5232):1872–1875, 1995.

O. Olusanya, P. D. Andrews, J. R. Swedlow, and E. Smythe. Phosphorylation of threonine 156 of the μ2 subunit of the ap2 complex is essential for endocytosis in vitro and in vivo. *Current Biology*, 11(11):896–900, 2001.

L. Orlichenko, B. Huang, E. Krueger, and M. McNiven. Epithelial growth factor-induced phosphorylation of caveolin 1 at tyrosine 14 stimulates caveolae formation in epithelial cells. *Journal of Biological Chemistry*, 281(8):4570, 2006.

U. Örtegren, M. Karlsson, N. Blazic, M. Blomqvist, F. H. Nystrom, J. Gustavsson, P. Fredman, and P. Strålfors. Lipids and glycosphingolipids in caveolae and surrounding plasma membrane of primary rat adipocytes. *European Journal of Biochemistry*, 271(10):2028–2036, 2004.

D. J. Owen and P. R. Evans. A structural explanation for the recognition of tyrosine-based endocytotic signals. *Science*, 282(5392):1327–1332, 1998.

A. F. Palazzo, H. L. Joseph, Y. J. Chen, D. L. Dujardin, A. S. Alberts, K. K. Pfister, R. B. Vallee, and G. G. Gundersen. Cdc42, dynein, and dynactin regulate mtoc reorientation independent of rho-regulated microtubule stabilization. *Current Biology*, 11(19):1536–1541, 2001.

A. K. Panicker, M. Buhusi, A. Erickson, and P. F. Maness. Endocytosis of β1 integrins is an early event in migration promoted by the cell adhesion molecule l1. *Experimental cell research*, 312(3):299–307, 2006.

M.-O. Parat, B. Anand-Apte, and P. L. Fox. Differential caveolin-1 polarization in endothelial cells during migration in two and three dimensions. *Molecular biology of the cell*, 14(8):3156–3168, 2003.

J. T. Parsons, A. R. Horwitz, and M. A. Schwartz. Cell adhesion: integrating cytoskeletal dynamics and cellular tension. *Nature reviews Molecular cell biology*, 11(9):633–643, 2010.

M. Parsons, A. J. Messent, J. D. Humphries, N. O. Deakin, and M. J. Humphries. Quantification of integrin receptor agonism by fluorescence lifetime imaging. *Journal of cell science*, 121(3):265–271, 2008.

R. G. Parton and A. A. Richards. Lipid rafts and caveolae as portals for endocytosis: new insights and common mechanisms. *Traffic*, 4(11):724–738, 2003.

R. G. Parton and K. Simons. The multiple faces of caveolae. *Nature reviews Molecular cell biology*, 8(3):185–194, 2007.

S. Pathak, G. Sarno, Q. M. Nunes, and G. J. Poston. Synchronous resection for colorectal liver metastasis: the future. *European Journal of Surgical Oncology*, 36(11):1004–1006, 2010.

B. Pearse. Clathrin: a unique protein associated with intracellular transfer of membrane by coated vesicles. *Proceedings of the National Academy of Sciences*, 73(4):1255–1259, 1976.

L. Pelkmans and M. Zerial. Kinase-regulated quantal assemblies and kiss-and-run recycling of caveolae. *Nature*, 436(7047):128–133, 2005.

L. Pelkmans, D. Püntener, and A. Helenius. Local actin polymerization and dynamin recruitment in sv40-induced internalization of caveolae. *Science*, 296(5567):535–539, 2002.

L. Pelkmans, T. Bürli, M. Zerial, and A. Helenius. Caveolin-stabilized membrane domains as multifunctional transport and sorting devices in endocytic membrane traffic. *Cell*, 118(6):767–780, 2004.

P. Peschard and M. Park. Escape from cbl-mediated downregulation: a recurrent theme for oncogenic deregulation of receptor tyrosine kinases. *Cancer cell*, 3(6):519–523, 2003.

B. J. Peter, H. M. Kent, I. G. Mills, Y. Vallis, P. J. G. Butler, P. R. Evans, and H. T. McMahon. Bar domains as sensors of membrane curvature: the amphiphysin bar structure. *Science*, 303(5657):495–499, 2004.

L. M. Pierini, M. A. Lawson, R. J. Eddy, B. Hendey, and F. R. Maxfield. Oriented endocytic recycling of $\alpha 5 \beta 1$ in motile neutrophils. *Blood*, 95(8):2471–2480, 2000.

W. T. Pitkeathly, N. S. Poulter, E. Claridge, and J. Z. Rappoport. Auto-align–multimodality fluorescence microscopy image co-registration. *Traffic*, 13(2):204–217, 2012.

S. Plançon, M. C. Morel-Kopp, E. Schaffner-Reckinger, P. Chen, and N. Kieffer. Green fluorescent protein (gfp) tagged to the cytoplasmic tail of alphaiib or beta3 allows the expression of a fully functional integrin alphaiib(beta3): effect of beta3gfp on alphaiib(beta3) ligand binding. *Biochemical Journal*, 357(2):529–536, 2001.

A. Pol, S. Martin, M. A. Fernández, M. Ingelmo-Torres, C. Ferguson, C. Enrich, and R. G. Parton. Cholesterol and fatty acids regulate dynamic caveolin trafficking through the golgi complex and between the cell surface and lipid bodies. *Molecular biology of the cell*, 16(4):2091–2105, 2005.

T. D. Pollard and G. G. Borisy. Cellular motility driven by assembly and disassembly of actin filaments. *Cell*, 112(4):453–465, 2003.

D. Poteryaev, S. Datta, K. Ackema, M. Zerial, and A. Spang. Identification of the switch in early-to-late endosome transition. *Cell*, 141(3):497–508, 2010.

N. Pouliot, H. B. Pearson, and A. Burrows. Investigating metastasis using in vitro platforms. *Madame Curie Bioscience Database [Internet]*, 2013.

A. M. Powelka, J. Sun, J. Li, M. Gao, L. M. Shaw, A. Sonnenberg, and V. W. Hsu. Stimulation-dependent recycling of integrin β1 regulated by arf6 and rab11. *Traffic*, 5(1):20–36, 2004.

N. L. Prigozhina and C. M. Waterman-Storer. Protein kinase d-mediated anterograde membrane trafficking is required for fibroblast motility. *Current Biology*, 14(2):88–98, 2004.

N. L. Prigozhina and C. M. Waterman-Storer. Decreased polarity and increased random motility in ptk1 epithelial cells correlate with inhibition of endosomal recycling. *Journal of Cell Science*, 119(17):3571–3582, 2006.

Z. Pujic, D. Mortimer, J. Feldner, and G. J. Goodhill. Assays for eukaryotic cell chemotaxis. *Combinatorial chemistry & high throughput screening*, 12(6):580–588, 2009.

V. Puri, R. Watanabe, R. D. Singh, M. Dominguez, J. C. Brown, C. L. Wheatley, D. L. Marks, and R. E. Pagano. Clathrin-dependent and-independent internalization of plasma membrane sphingolipids initiates two golgi targeting pathways. *The Journal of cell biology*, 154(3):535–548, 2001.

R. Ramachandran, T. J. Pucadyil, Y.-W. Liu, S. Acharya, M. Leonard, V. Lukiyanchuk, and S. L. Schmid. Membrane insertion of the pleckstrin homology domain variable loop 1 is critical for dynamin-catalyzed vesicle scission. *Molecular biology of the cell*, 20(22):4630–4639, 2009.

I. Rapoport, M. Miyazaki, W. Boll, B. Duckworth, L. C. Cantley, S. Shoelson, and T. Kirchhausen. Regulatory interactions in the recognition of endocytic sorting signals by ap-2 complexes. *The EMBO journal*, 16(9):2240–2250, 1997.

J. Z. Rappoport and S. M. Simon. Real-time analysis of clathrin-mediated endocytosis during cell migration. *Journal of cell science*, 116(5):847–855, 2003.

J. Z. Rappoport and S. M. Simon. Endocytic trafficking of activated egfr is ap-2 dependent and occurs through preformed clathrin spots. *Journal of cell science*, 122(9): 1301–1305, 2009.

J. Z. Rappoport, B. W. Taha, S. Lemeer, A. Benmerah, and S. M. Simon. The ap-2 complex is excluded from the dynamic population of plasma membrane-associated clathrin. *Journal of Biological Chemistry*, 278(48):47357–47360, 2003a.

J. Z. Rappoport, B. W. Taha, and S. M. Simon. Movement of plasma-membrane-associated clathrin spots along the microtubule cytoskeleton. *Traffic*, 4(7):460–467, 2003b.

R. M. Ray, C. Li, S. Bhattacharya, A. P. Naren, and L. R. Johnson. Spermine, a molecular switch regulating egfr, integrin β3, src, and fak scaffolding. *Cellular signalling*, 24(4):931–942, 2012.

B. Razani, J. A. Engelman, X. B. Wang, W. Schubert, X. L. Zhang, C. B. Marks, F. Macaluso, R. G. Russell, M. Li, R. G. Pestell, et al. Caveolin-1 null mice are viable but show evidence of hyperproliferative and vascular abnormalities. *Journal of Biological Chemistry*, 276(41):38121–38138, 2001.

B. Razani, X. B. Wang, J. A. Engelman, M. Battista, G. Lagaud, X. L. Zhang, B. Kneitz, H. Hou, G. J. Christ, W. Edelmann, et al. Caveolin-2-deficient mice show evidence of severe pulmonary dysfunction without disruption of caveolae. *Molecular and cellular biology*, 22(7):2329–2344, 2002.

C. M. Regen and A. F. Horwitz. Dynamics of beta 1 integrin-mediated adhesive contacts in motile fibroblasts. *The Journal of cell biology*, 119(5):1347–1359, 1992.

A. R. Reynolds, I. R. Hart, A. R. Watson, J. C. Welti, R. G. Silva, S. D. Robinson, G. Da Violante, M. Gourlaouen, M. Salih, M. C. Jones, et al. Stimulation of tumor growth and angiogenesis by low concentrations of rgd-mimetic integrin inhibitors. *Nature medicine*, 15(4):392–400, 2009.

A. Ridley, M. Schwartz, K. Burridge, R. Firtel, M. Ginsberg, G. Borisy, J. Parsons, and A. Horwitz. Cell migration: integrating signals from front to back. *Science*, 302 (5651):1704–1709, 2003.

K. Riento and A. J. Ridley. Rocks: multifunctional kinases in cell behaviour. *Nature Reviews Molecular Cell Biology*, 4(6):446–456, 2003.

D. J. Riese, R. M. Gallo, and J. Settleman. Mutational activation of erbb family receptor tyrosine kinases: insights into mechanisms of signal transduction and tumorigenesis. *Bioessays*, 29(6):558–565, 2007.

M. S. Roberts, A. J. Woods, T. C. Dale, P. van der Sluijs, and J. C. Norman. Protein kinase b/akt acts via glycogen synthase kinase 3 to regulate recycling of αvβ3 and α5β1 integrins. *Molecular and cellular biology*, 24(4):1505–1515, 2004.

D. G. Rodionov and O. Bakke. Medium chains of adaptor complexes ap-1 and ap-2 recognize leucine-based sorting signals from the invariant chain. *Journal of Biological Chemistry*, 273(11):6005–6008, 1998.

O. C. Rodriguez, A. W. Schaefer, C. A. Mandato, P. Forscher, W. M. Bement, and C. M. Waterman-Storer. Conserved microtubule–actin interactions in cell movement and morphogenesis. *Nature cell biology*, 5(7):599–609, 2003.

K. Roepstorff, M. V. Grandal, L. Henriksen, S. L. J. Knudsen, M. Lerdrup, L. Grøvdal, B. M. Willumsen, and B. Van Deurs. Differential effects of egfr ligands on endocytic sorting of the receptor. *Traffic*, 10(8):1115–1127, 2009.

R. Roskoski Jr. The erbb/her receptor protein-tyrosine kinases and cancer. *Biochemical and biophysical research communications*, 319(1):1–11, 2004.

T. F. Roth and K. R. Porter. Yolk protein uptake in the oocyte of the mosquito aedes aegypti. l. *The Journal of cell biology*, 20(2):313–332, 1964.

K. G. Rothberg, J. E. Heuser, W. C. Donzell, Y.-S. Ying, J. R. Glenney, and R. G. Anderson. Caveolin, a protein component of caveolae membrane coats. *Cell*, 68(4): 673–682, 1992.

E. E. Sander, P. Jean, S. van Delft, R. A. van der Kammen, and J. G. Collard. Rac downregulates rho activity reciprocal balance between both gtpases determines cellular morphology and migratory behavior. *The Journal of cell biology*, 147(5):1009–1022, 1999.

J. Schlessinger. Ligand-induced, receptor-mediated dimerization and activation of egf receptor. *Cell*, 110(6):669–672, 2002.

J. Schmoranzer, M. Goulian, D. Axelrod, and S. M. Simon. Imaging constitutive exocytosis with total internal reflection fluorescence microscopy. *The Journal of cell biology*, 149(1):23–32, 2000.

J. Schmoranzer, G. Kreitzer, and S. M. Simon. Migrating fibroblasts perform polarized, microtubule-dependent exocytosis towards the leading edge. *Journal of cell science*, 116(22):4513–4519, 2003.

E. Schonteich, G. M. Wilson, J. Burden, C. R. Hopkins, K. Anderson, J. R. Goldenring, and R. Prekeris. The rip11/rab11-fip5 and kinesin ii complex regulates endocytic protein recycling. *Journal of cell science*, 121(22):3824–3833, 2008.

W. X. Schulze, L. Deng, and M. Mann. Phosphotyrosine interactome of the erbb-receptor kinase family. *Molecular systems biology*, 1(1), 2005.

M. A. Schwartz and S. J. Shattil. Signaling networks linking integrins and rho family gtpases. *Trends in biochemical sciences*, 25(8):388–391, 2000.

D. K. Sharma, J. C. Brown, A. Choudhury, T. E. Peterson, E. Holicky, D. L. Marks, R. Simari, R. G. Parton, and R. E. Pagano. Selective stimulation of caveolar endocytosis by glycosphingolipids and cholesterol. *Molecular biology of the cell*, 15(7): 3114–3122, 2004.

D. K. Sharma, J. C. Brown, Z. Cheng, E. L. Holicky, D. L. Marks, and R. E. Pagano. The glycosphingolipid, lactosylceramide, regulates β1-integrin clustering and endocytosis. *Cancer research*, 65(18):8233–8241, 2005.

M. Sharma, N. Naslavsky, and S. Caplan. A role for ehd4 in the regulation of early endosomal transport. *Traffic*, 9(6):995–1018, 2008.

T. Shatseva, D. Y. Lee, Z. Deng, and B. B. Yang. Microrna mir-199a-3p regulates cell proliferation and survival by targeting caveolin-2. *Journal of cell science*, 124(16): 2826–2836, 2011.

M. Shatz, G. Lustig, R. Reich, and M. Liscovitch. Caveolin-1 mutants p132l and y14f are dominant negative regulators of invasion, migration and aggregation in h1299 lung cancer cells. *Experimental cell research*, 316(10):1748–1762, 2010.

M. Sheetz, D. Felsenfeld, C. Galbraith, and D. Choquet. Cell migration as a five-step cycle. *Biochemist Society Spymposia*, 65:233–243, 1999.

M. P. Sheetz, D. P. Felsenfeld, and C. G. Galbraith. Cell migration: regulation of force on extracellular-matrix-integrin complexes. *Trends in cell biology*, 8(2):51–54, 1998.

S. Sigismund, T. Woelk, C. Puri, E. Maspero, C. Tacchetti, P. Transidico, P. P. Di Fiore, and S. Polo. Clathrin-independent endocytosis of ubiquitinated cargos. *Proceedings of the National Academy of Sciences of the United States of America*, 102(8):2760–2765, 2005.

S. Sigismund, E. Argenzio, D. Tosoni, E. Cavallaro, S. Polo, and P. P. Di Fiore. Clathrin-mediated internalization is essential for sustained egfr signaling but dispensable for degradation. *Developmental cell*, 15(2):209–219, 2008.

S. Sigismund, V. Algisi, G. Nappo, A. Conte, R. Pascolutti, A. Cuomo, T. Bonaldi, E. Argenzio, L. G. Verhoef, E. Maspero, et al. Threshold-controlled ubiquitination of the egfr directs receptor fate. *The EMBO journal*, 32(15):2140–2157, 2013.

R. D. Singh, D. L. Marks, E. L. Holicky, C. L. Wheatley, T. Kaptzan, S. B. Sato, T. Kobayashi, K. Ling, and R. E. Pagano. Gangliosides and β1-integrin are required for caveolae and membrane domains. *Traffic*, 11(3):348–360, 2010.

T. Sorkina, F. Huang, L. Beguinot, and A. Sorkin. Effect of tyrosine kinase inhibitors on clathrin-coated pit recruitment and internalization of epidermal growth factor receptor. *Journal of Biological Chemistry*, 277(30):27433–27441, 2002.

F. Sotgia, B. Razani, G. Bonuccelli, W. Schubert, M. Battista, H. Lee, F. Capozza, A. L. Schubert, C. Minetti, J. T. Buckley, et al. Intracellular retention of glycosylphosphatidyl inositol-linked proteins in caveolin-deficient cells. *Molecular and cellular biology*, 22(11):3905–3926, 2002.

L. Sousa, I. Lax, H. Shen, S. Ferguson, P. De Camilli, and J. Schlessinger. Suppression of egfr endocytosis by dynamin depletion reveals that egfr signaling occurs primarily at the plasma membrane. *Proceedings of the National Academy of Sciences*, 2012.

G. Sowa. Novel insights into the role of caveolin-2 in cell-and tissue-specific signaling and function. *Biochemistry research international*, 2011, 2011.

D. Spiering and L. Hodgson. Dynamics of the rho-family small gtpases in actin regulation and motility. *Cell adhesion & migration*, 5(2):170, 2011.

M. Sporn. The war on cancer: A review. *Annals of the New York Academy of Sciences*, 833(1):137–146, 1997.

S. Srinivasan, F. Wang, S. Glavas, A. Ott, F. Hofmann, K. Aktories, D. Kalman, and H. R. Bourne. Rac and cdc42 play distinct roles in regulating pi (3, 4, 5) p3 and polarity during neutrophil chemotaxis. *The Journal of cell biology*, 160(3):375–385, 2003.

J. C. Stachowiak, E. M. Schmid, C. J. Ryan, H. S. Ann, D. Y. Sasaki, M. B. Sherman, P. L. Geissler, D. A. Fletcher, and C. C. Hayden. Membrane bending by protein–protein crowding. *Nature cell biology*, 14(9):944–949, 2012.

L. R. Strachan and M. L. Condic. Cranial neural crest recycle surface integrins in a substratum-dependent manner to promote rapid motility. *The Journal of cell biology*, 167(3):545–554, 2004.

N. Taub, D. Teis, H. Ebner, M. Hess, and L. Huber. Late endosomal traffic of the epidermal growth factor receptor ensures spatial and temporal fidelity of mitogen-activated protein kinase signaling. *Molecular biology of the cell*, 18(12):4698–4710, 2007.

M. J. Taylor, D. Perrais, and C. J. Merrifield. A high precision survey of the molecular dynamics of mammalian clathrin-mediated endocytosis. *PLoS biology*, 9(3):e1000604, 2011.

E. Ter Haar, S. C. Harrison, and T. Kirchhausen. Peptide-in-groove interactions link target proteins to the β-propeller of clathrin. *Proceedings of the National Academy of Sciences*, 97(3):1096–1100, 2000.

N. Thapa, Y. Sun, M. Schramp, S. Choi, K. Ling, and R. A. Anderson. Phosphoinositide signaling regulates the exocyst complex and polarized integrin trafficking in directionally migrating cells. *Developmental cell*, 22(1):116–130, 2012.

J. A. Thorley, J. A. McKeating, and J. Z. Rappoport. Mechanisms of viral entry: sneaking in the front door. *Protoplasma*, 244(1-4):15–24, 2010.

P. Timpson, E. J. Mcghee, Z. Erami, M. Nobis, J. A. Quinn, M. Edward, and K. I. Anderson. Organotypic collagen i assay: a malleable platform to assess cell behaviour in a 3-dimensional context. *Journal of visualized experiments: JoVE*, (56), 2011.

S. Toetsch, P. Olwell, A. Prina-Mello, and Y. Volkov. The evolution of chemotaxis assays from static models to physiologically relevant platforms. *Integrative Biology*, 1 (2):170–181, 2009.

M. L. Torgersen, G. Skretting, B. van Deurs, and K. Sandvig. Internalization of cholera toxin by different endocytic mechanisms. *Journal of cell science*, 114(20):3737–3747, 2001.

L. M. Traub. Sorting it out ap-2 and alternate clathrin adaptors in endocytic cargo selection. *The Journal of cell biology*, 163(2):203–208, 2003.

O. Ullrich, S. Reinsch, S. Urbé, M. Zerial, and R. G. Parton. Rab11 regulates recycling through the pericentriolar recycling endosome. *The Journal of cell biology*, 135(4): 913–924, 1996.

F. Ulrich and C.-P. Heisenberg. Trafficking and cell migration. *Traffic*, 10(7):811–818, 2009.

P. Umasankar, S. Sanker, J. R. Thieman, S. Chakraborty, B. Wendland, M. Tsang, and L. M. Traub. Distinct and separable activities of the endocytic clathrin-coat components fcho1/2 and ap-2 in developmental patterning. *Nature cell biology*, 14(5): 488–501, 2012.

E. Ungewickell, H. Ungewickell, S. E. Holstein, R. Lindner, K. Prasad, W. Barouch, B. Martini, L. E. Greene, and E. Eisenberg. Role of auxilin in uncoating clathrin-coated vesicles. *Nature*, 378(6557):632–635, 1995.

P. Upla, V. Marjomäki, P. Kankaanpää, J. Ivaska, T. Hyypiä, F. G. Van Der Goot, and J. Heino. Clustering induces a lateral redistribution of $\alpha 2\beta 1$ integrin from membrane rafts to caveolae and subsequent protein kinase c-dependent internalization. *Molecular biology of the cell*, 15(2):625–636, 2004.

P. van der Sluijs, M. Hull, P. Webster, P. Mâle, B. Goud, and I. Mellman. The small gtp-binding protein rab4 controls an early sorting event on the endocytic pathway. *Cell*, 70(5):729–740, 1992.

F. van Hemert, M. D. Lazova, B. E. Snaar-Jagaska, and T. Schmidt. Mobility of g proteins is heterogeneous and polarized during chemotaxis. *Journal of cell science*, 123(17):2922–2930, 2010.

M. Vicente-Manzanares, C. K. Choi, and A. R. Horwitz. Integrins in cell migration–the actin connection. *Journal of cell science*, 122(2):199–206, 2009.

A. V. Vieira, C. Lamaze, and S. L. Schmid. Control of egf receptor signaling by clathrin-mediated endocytosis. *Science*, 274(5295):2086–2089, 1996.

V. Vinader, Y. Al-Saraireh, H. L. Wiggins, J. Z. Rappoport, S. D. Shnyder, L. H. Patterson, and K. Afarinkia. An agarose spot chemotaxis assay for chemokine receptor antagonists. *Journal of Pharmacological and Toxicological Methods*, 64(3):213–216, 2011.

M. von Zastrow and A. Sorkin. Signaling on the endocytic pathway. *Current opinion in cell biology*, 19(4):436–445, 2007.

C. M. Waterman-Storer, R. A. Worthylake, B. P. Liu, K. Burridge, and E. Salmon. Microtubule growth activates rac1 to promote lamellipodial protrusion in fibroblasts. *Nature Cell Biology*, 1(1):45–50, 1999.

M. Way and R. G. Parton. M-caveolin, a muscle-specific caveolin-related protein. *FEBS letters*, 378(1):108–112, 1996.

D. J. Webb, K. Donais, L. A. Whitmore, S. M. Thomas, C. E. Turner, J. T. Parsons, and A. F. Horwitz. Fak–src signalling through paxillin, erk and mlck regulates adhesion disassembly. *Nature cell biology*, 6(2):154–161, 2004.

B. Weigelt, J. L. Peterse, and L. J. Van't Veer. Breast cancer metastasis: markers and models. *Nature reviews cancer*, 5(8):591–602, 2005.

H. C. Welch, W. J. Coadwell, L. R. Stephens, and P. T. Hawkins. Phosphoinositide 3-kinase-dependent activation of rac. *FEBS letters*, 546(1):93–97, 2003.

M. D. Welch and R. D. Mullins. Cellular control of actin nucleation. *Annual review of cell and developmental biology*, 18(1):247–288, 2002.

D. P. White, P. T. Caswell, and J. C. Norman. $\alpha v\beta 3$ and $\alpha 5\beta 1$ integrin recycling pathways dictate downstream rho kinase signaling to regulate persistent cell migration. *The Journal of cell biology*, 177(3):515–525, 2007.

G. M. Whitesides. The origins and the future of microfluidics. *Nature*, 442(7101):368–373, 2006.

H. Wiggins and J. Rappoport. An agarose spot assay for chemotactic invasion. *Biotechniques*, 48:121–124, 2010.

J. D. Wilbur, P. K. Hwang, and F. M. Brodsky. New faces of the familiar clathrin lattice. *Traffic*, 6(4):346–350, 2005.

A. J. Woods, D. P. White, P. T. Caswell, and J. C. Norman. Pkd1/pkcμ promotes $\alpha v\beta 3$ integrin recycling and delivery to nascent focal adhesions. *The EMBO journal*, 23(13): 2531–2543, 2004.

R. A. Worthylake and K. Burridge. Rhoa and rock promote migration by limiting membrane protrusions. *Journal of Biological Chemistry*, 278(15):13578–13584, 2003.

P. Wu, P. Wee, J. Jiang, X. Chen, and Z. Wang. Differential regulation of transcription factors by location-specific egf receptor signaling via a spatio-temporal interplay of erk activation. *PloS one*, 7(9):e41354, 2012.

J. B. Wyckoff, J. G. Jones, J. S. Condeelis, and J. E. Segall. A critical step in metastasis: in vivo analysis of intravasation at the primary tumor. *Cancer research*, 60(9):2504–2511, 2000.

S. Yadav, S. Puri, and A. D. Linstedt. A primary role for golgi positioning in directed secretion, cell polarity, and wound healing. *Molecular biology of the cell*, 20(6):1728–1736, 2009.

E. Yamada. The fine structure of the gall bladder epithelium of the mouse. *The Journal of biophysical and biochemical cytology*, 1(5):445, 1955.

L. Yang, L. Wang, and Y. Zheng. Gene targeting of cdc42 and cdc42gap affirms the critical involvement of cdc42 in filopodia induction, directed migration, and proliferation in primary mouse embryonic fibroblasts. *Molecular biology of the cell*, 17(11): 4675–4685, 2006.

Q. Yang, A. Karpikov, D. Toomre, and J. S. Duncan. 3-d reconstruction of microtubules from multi-angle total internal reflection fluorescence microscopy using bayesian framework. *Image Processing, IEEE Transactions on*, 20(8):2248–2259, 2011.

Y. Yarden, M. Sliwkowski, et al. Untangling the erbb signalling network. *Nat Rev Mol Cell Biol*, 2(2):127–137, 2001.

J. A. Ybe, F. M. Brodsky, K. Hofmann, K. Lin, S.-H. Liu, L. Chen, T. N. Earnest, R. J. Fletterick, and P. K. Hwang. Clathrin self-assembly is mediated by a tandemly repeated superhelix. *Nature*, 399(6734):371–375, 1999.

J. Ylänne, J. Huuskonen, T. E. O'Toole, M. H. Ginsberg, I. Virtanen, and C. G. Gahmberg. Mutation of the cytoplasmic domain of the integrin subunit differential effects on cell spreading, recruitment to adhesions plaques, endocytosis, and phagocytosis. *Journal of Biological Chemistry*, 270(16):9550–9557, 1995.

S.-O. Yoon, S. Shin, and A. M. Mercurio. Hypoxia stimulates carcinoma invasion by stabilizing microtubules and promoting the rab11 trafficking of the $\alpha 6\beta 4$ integrin. *Cancer research*, 65(7):2761–2769, 2005.

A. Young. Structural insights into the clathrin coat. *Seminars in cell & developmental biology*, 18(4):448–458, 2007.

W. Zhang, B. Razani, Y. Altschuler, B. Bouzahzah, K. E. Mostov, R. G. Pestell, and M. P. Lisanti. Caveolin-1 inhibits epidermal growth factor-stimulated lamellipod extension and cell migration in metastatic mammary adenocarcinoma cells (mtln3) transformation suppressor effects of adenovirus-mediated gene delivery of caveolin-1. *Journal of Biological Chemistry*, 275(27):20717–20725, 2000.

D. Zicha, G. A. Dunn, and A. F. Brown. A new direct-viewing chemotaxis chamber. *Journal of Cell Science*, 99(4):769–775, 1991.

S. H. Zigmond. Ability of polymorphonuclear leukocytes to orient in gradients of chemotactic factors. *The Journal of Cell Biology*, 75(2):606–616, 1977.

R. Zoncu, R. M. Perera, R. Sebastian, F. Nakatsu, H. Chen, T. Balla, G. Ayala, D. Toomre, and P. V. De Camilli. Loss of endocytic clathrin-coated pits upon acute depletion of phosphatidylinositol 4, 5-bisphosphate. *Proceedings of the National Academy of Sciences*, 104(10):3793–3798, 2007.

Appendix I

Supplementary methods

1. LB Broth

20 g of LB Broth (Sigma) was dissolved in 1 l distilled H_20 and autoclaved at 121°C for 20 minutes.

2. LB agar plates

35 g of LB Agar (Sigma) was dissolved in 1 l distilled H_20 and autoclaved at 121°C for 20 minutes. Kanamycin or ampicillin was then added to give a final concentration of 50 μg/ml or 100 μg/ml, respectively. 50 ml was then poured into each 12 cm plastic dish and allowed to set. Agar plates were stored at 4°C in a sealed bag.

3. Sample buffer

3X sample buffer was made using 18.8 ml of Tris-HCl (1 M; pH 6.8) 6 g SDS, 15 ml Beta mercaptoethanol (Sigma) and 30 ml glycerol (Fisher Scientific), this was made up to 100 ml with distilled H_20. A small spatula of bromophenol blue was added before thorough mixing.

4. Acrylamide gel solutions

50 ml of 4% stacking gel was made up with 30 ml distilled H_20, 12.5 ml Tris HCl (0.5 M, pH 6.8; Fisher Scientific), 6.7 ml acrylamide (Protogel), 0.5 ml 10% sodium dodecyl sulphate (SDS; Sigma), 500 μl ammonium per sulphate (APS; Sigma) and 75 μl Tetramethylethylenediamine (TEMED; Sigma).

50 ml of 12.5% resolving gel was made up with 16.1 ml distilled H_20, 12.5 ml Tris-HCl (1.5 M, pH 8.8; Fisher Scientific), 20.8 ml acrylamide (Protogel), 0.5 ml 10% SDS, 500 μl APS and 75 μl TEMED.

5. Gel running buffer

Running buffer was made up with 14.4 g Glycine (Fisher Scientific), 3 g Tris and 0.4 g SDS made up to 1 l with distilled H_20.

6. Gel transfer buffer

Transfer buffer was made up with 14.4 g Glycine, 3 g Tris with 200 ml methanol (Fisher Scientific) and made up to 1 l with distilled H_20.

7. TBST

TBST was made up using 20 ml of Tris-HCl (1 M, pH 7.5), 30 ml NaCl (Fisher Scientific; 5 M) plus 1 ml Tween20 (Sigma) made up to 1 l with distilled H_20.

8. Blocking buffer

Milk solution (Marvel) was dissolved in TBST (2.5 g in 50 ml).

Appendix II

Published work

Mutch L.J., Howden J.D., Jenner E.P., Poulter N.S., Rappoport J.Z. Polarised clathrin-mediated endocytosis of EGFR during chemotactic invasion. *Traffic*, 15(6):648-64, 2014.

Traffic

doi:10.1111/tra.12165

Polarised Clathrin-Mediated Endocytosis of EGFR During Chemotactic Invasion

Laura Jane Mutch[1], Jake Davey Howden[1], Emma Poppy Louise Jenner[1], Natalie Sarah Poulter[2] and Joshua Zachary Rappoport[1,*]

[1]School of Biosciences, The University of Birmingham, Edgbaston, Birmingham B15 2TT, UK

[2]Centre for Cardiovascular Research, Institute for Biomedical Research, The College of Medical and Dental Sciences, The University of Birmingham, Edgbaston, Birmingham B15 2TT, UK

*Corresponding author: Joshua Z. Rappoport, j.rappoport@bham.ac.uk

Abstract

Directed cell migration is critical for numerous physiological processes including development and wound healing. However chemotaxis is also exploited during cancer progression. Recent reports have suggested links between vesicle trafficking pathways and directed cell migration. Very little is known about the potential roles of endocytosis pathways during metastasis. Therefore we performed a series of studies employing a previously characterised model for chemotactic invasion of cancer cells to assess specific hypotheses potentially linking endocytosis to directed cell migration. Our results demonstrate that clathrin-mediated endocytosis is indispensable for epidermal growth factor (EGF) directed chemotactic invasion of MDA-MB-231 cells. Conversely, caveolar endocytosis is not required in this mode of migration. We further found that chemoattractant receptor (EGFR) trafficking occurs by clathrin-mediated endocytosis and is polarised towards the front of migrating cells. However, we found no role for clathrin-mediated endocytosis in focal adhesion disassembly in this migration model. Thus, this study has characterised the role of endocytosis during chemotactic invasion and has identified functions mechanistically linking clathrin-mediated endocytosis to directed cell motility.

Keywords breast cancer, chemotactic invasion, EGFR, endocytosis, MDA-MB-231

Received 11 July 2013, revised and accepted for publication 14 February 2014, uncorrected manuscript published online 20 February 2014, published online 20 March 2014

Introduction

Directed cell migration underlies many physiological processes. Under most circumstances, including embryonic development, wound repair and immune responses, cell migration is beneficial to the normal growth and survival of an organism. However, cell migration can also promote progression of cancer through angiogenesis and metastasis and, under these circumstances, has a negative impact on the survival of the organism. Cancer metastasis is strongly associated with a poor prognosis and chance of survival; as such the prevention of metastasis is a key target for therapeutic intervention (1).

During the intravasation and extravasation stages of metastasis, cells migrate towards a source of chemoattractant in a process called chemotaxis (2). This process is triggered by the binding of chemoattractant molecules to cell surface receptors. Epidermal growth factor (EGF) binding to its receptor (EGFR) has been identified as a potent chemoattractant stimulus for metastatic cancer cells (3). Activation of chemoattractant receptors results in a complex signalling cascade that leads to polarisation of the cell in the direction of migration, increased contractility and subsequent directed motility (4).

In order to control the directionality and magnitude of migration, the availability of chemoattractant receptors and cell adhesion molecules on the cell surface must be carefully regulated. Endocytosis is the first step of endocytic recycling and, as such, is important for regulation of receptor signalling, and has also been shown to be important for migration in a number of different systems (5,6). Recently, it has been demonstrated

Traffic

doi:10.1111/tra.12165

Polarised Clathrin-Mediated Endocytosis of EGFR During Chemotactic Invasion

Laura Jane Mutch[1], Jake Davey Howden[1], Emma Poppy Louise Jenner[1], Natalie Sarah Poulter[2] and Joshua Zachary Rappoport[1,*]

[1]School of Biosciences, The University of Birmingham, Edgbaston, Birmingham B15 2TT, UK

[2]Centre for Cardiovascular Research, Institute for Biomedical Research, The College of Medical and Dental Sciences, The University of Birmingham, Edgbaston, Birmingham B15 2TT, UK

*Corresponding author: Joshua Z. Rappoport, j.rappoport@bham.ac.uk

Abstract

Directed cell migration is critical for numerous physiological processes including development and wound healing. However chemotaxis is also exploited during cancer progression. Recent reports have suggested links between vesicle trafficking pathways and directed cell migration. Very little is known about the potential roles of endocytosis pathways during metastasis. Therefore we performed a series of studies employing a previously characterised model for chemotactic invasion of cancer cells to assess specific hypotheses potentially linking endocytosis to directed cell migration. Our results demonstrate that clathrin-mediated endocytosis is indispensable for epidermal growth factor (EGF) directed chemotactic invasion of MDA-MB-231 cells. Conversely, caveolar endocytosis is not required in this mode of migration. We further found that chemoattractant receptor (EGFR) trafficking occurs by clathrin-mediated endocytosis and is polarised towards the front of migrating cells. However, we found no role for clathrin-mediated endocytosis in focal adhesion disassembly in this migration model. Thus, this study has characterised the role of endocytosis during chemotactic invasion and has identified functions mechanistically linking clathrin-mediated endocytosis to directed cell motility.

Keywords breast cancer, chemotactic invasion, EGFR, endocytosis, MDA-MB-231

Received 11 July 2013, revised and accepted for publication 14 February 2014, uncorrected manuscript published online 20 February 2014, published online 20 March 2014

Introduction

Directed cell migration underlies many physiological processes. Under most circumstances, including embryonic development, wound repair and immune responses, cell migration is beneficial to the normal growth and survival of an organism. However, cell migration can also promote progression of cancer through angiogenesis and metastasis and, under these circumstances, has a negative impact on the survival of the organism. Cancer metastasis is strongly associated with a poor prognosis and chance of survival; as such the prevention of metastasis is a key target for therapeutic intervention (1).

During the intravasation and extravasation stages of metastasis, cells migrate towards a source of chemoattractant in a process called chemotaxis (2). This process is triggered by the binding of chemoattractant molecules to cell surface receptors. Epidermal growth factor (EGF) binding to its receptor (EGFR) has been identified as a potent chemoattractant stimulus for metastatic cancer cells (3). Activation of chemoattractant receptors results in a complex signalling cascade that leads to polarisation of the cell in the direction of migration, increased contractility and subsequent directed motility (4).

In order to control the directionality and magnitude of migration, the availability of chemoattractant receptors and cell adhesion molecules on the cell surface must be carefully regulated. Endocytosis is the first step of endocytic recycling and, as such, is important for regulation of receptor signalling, and has also been shown to be important for migration in a number of different systems (5,6). Recently, it has been demonstrated

that inhibiting endocytosis had a negative effect on Madin-Darby canine kidney (MDCK) epithelial cell migration in a wound healing model (7). Similarly, endocytosis has been shown to be important for platelet-derived growth factor-dependent chemotaxis of fibroblasts in a Boyden chamber (8).

Polarisation of vesicle trafficking pathways, such as endocytosis, along the migratory axis has been suggested as important for the promotion of cell migration (9–11). This area is widely debated due to uncertainty in the precise vesicle trafficking pathways involved and the specific membrane domains to which these might be polarised. It has recently been suggested that during epithelial wound healing clathrin-mediated endocytosis takes place in the middle-to-front area of the cell (12). Conversely, in this same system caveolar endocytosis is polarised towards the rear of the cell (6,7). This polarisation, however, may vary in different cell types and experimental systems.

To date there has been limited research into the role of endocytosis during chemotactic invasion. Potential endocytic cargo which may have a role in migration include focal adhesion components and chemoattractant receptors. Focal adhesions are involved in connecting cells to the extra-cellular matrix and providing the traction force allowing cells to move (13–15). Thus, factors affecting the disassembly of focal adhesions could have roles in controlling the rate and magnitude of migration, and endocytosis of integrin cell adhesion molecules from disassembling focal adhesions has been proposed to occur in certain situations (10,11,16,17).

Chemoattractant receptors are utilised to sense the surrounding gradient of chemoattractant and enable directionality of cell migration. The EGFR (also known as ErbB1 and Her1) is linked to many vital cellular processes such as cell survival, proliferation, differentiation and migration (18), and deregulation of EGFR can be oncogenic. EGFRs are frequently overexpressed in breast cancer and this overexpression appears to correlate with increased aggressiveness of the cancer (19).

There is conflicting evidence over which route(s) of internalisation EGFR employ(s) and what its fate is following endocytosis. Some groups describe a clathrin-dependent route for internalisation while others provide evidence that the route can be clathrin-independent (20–23). Here we aim to specifically elucidate the route of internalisation of the EGFR during chemotactic invasion of the highly migratory breast cancer cell line MDA-MB-231 and test specific hypotheses mechanistically linking endocytosis to chemotactic invasion. Our results demonstrate that dynamin-dependent clathrin-mediated endocytosis is essential for EGF-directed migration. Alternatively we found caveolar endocytosis to be entirely dispensable. While we find no role for clathrin-mediated endocytosis in focal adhesion disassembly during chemotactic invasion, we have demonstrated that clathrin-mediated endocytosis is polarised towards the front of migrating cells and that EGFR internalises via this route. In summary, we propose a model where clathrin-mediated endocytosis of EGFR is polarised towards the front of migrating cells and this polarised trafficking is necessary for migration in an EGF-containing environment. Additionally we suggest that clathrin-mediated endocytosis does not play a role in focal adhesion disassembly in this migratory model.

Results

The effect of dynamin inhibition on chemotactic invasion

In order to investigate potential mechanistic roles for endocytosis during chemotactic invasion we began by assessing the effect of inhibiting different endocytic pathways during EGF-directed migration in an assay system we recently developed (24). Briefly, our agarose spot assay for chemotactic invasion suspends chemoattractants (e.g. EGF) in a small drop of low melting point agarose adhered to a coverslip. Cells subsequently plated into wells containing agarose spots exhibit directed chemotactic invasion underneath the agarose spots, and can be observed through a wide variety of microscopy techniques.

The GTPase dynamin is known to be involved in both clathrin-mediated endocytosis and caveolar endocytosis, as well as having possible roles in other less characterised endocytosis pathways (5,25,26). Therefore, we utilised Dynasore, a small module inhibitor of dynamin, to determine if dynamin-dependent endocytosis is required for chemotactic invasion (27). In preliminary control experiments using fluorescent transferrin as a marker for

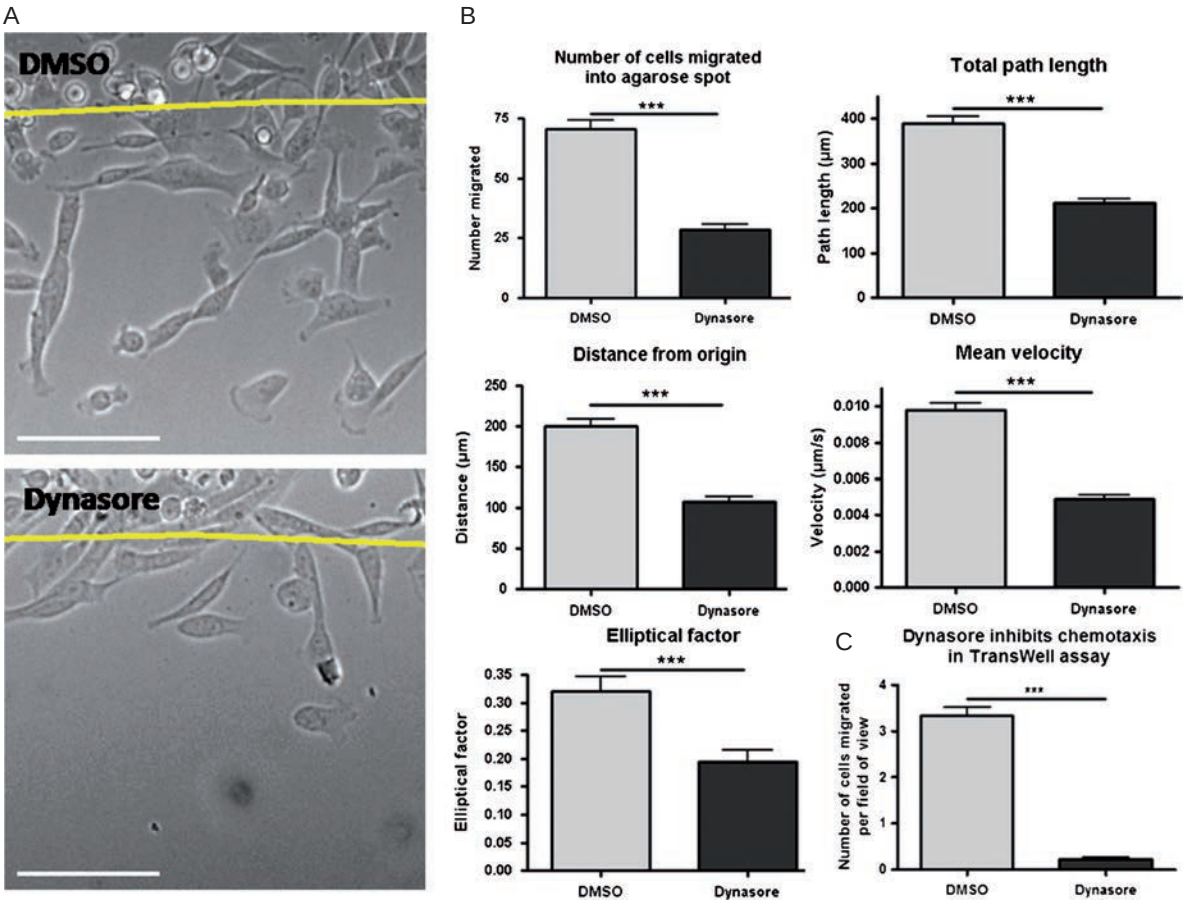

Figure 1: Dynasore inhibits MDA-MB-231 chemotactic invasion into EGF spots. A) Representative images treated with DMSO or Dynasore after 14 h migration into an agarose spot containing EGF. Line denotes edge of the agarose spot. Scale bars 100 μm. B) Results of tracking cells over the course of the timelapses. Parameters analysed include total number of cells migrated, total path length, distance from origin, average velocity and elliptical factor (found by dividing width of cell by length to give a number between 0 and 1). $n = 36$ fields of view per treatment for 'number of cell migrated' graph, $n = 100$ cells per treatment for all other analyses. C) Dynasore inhibits chemotaxis towards EGF in Transwells. Number of cells migrated per field of view following DMSO and Dynasore treatment. $n \geq 50$ fields of view per treatment.

clathrin-mediated endocytosis and fluorescent cholera toxin B (CTxB) as a marker for caveolar endocytosis we confirmed that Dynasore inhibits both these routes of internalisation (Figure S1, Supporting Information). When we treated MDA-MB-231 cells in the chemotactic invasion assay with Dynasore we saw significant differences in a number of parameters investigated, including an overall reduction in the total number of cells which migrated (60% decrease, Figure 1A and B). Investigating the 40% of cells which still migrated led us to find perturbations in the total path length travelled (45% decrease), the distance travelled from their start point (46% decrease) and their average velocity (50% decrease, Figure 1B). We next chose to validate these results with conventional Transwell-based experiments. As depicted in Figure 1C, Dynasore treatment resulted in a nearly complete inhibition of EGF-directed motility in these studies. Thus, dynamin-dependent endocytosis plays a major role in EGF-directed chemotactic invasion in MDA-MB-231 cells.

In order to further expand the applicability of our studies we analysed a second cell line. Pancreatic ductal adenocarcinoma (PDAC) cells derived from a pancreatic tumour, have been previously characterised and are chemotactic

and metastatic (28–30). As depicted in Figure 2A, as with MDA-MB-231 cells, PDACs demonstrate chemotactic invasion into agarose spots containing EGF. Both the number of migratory cells, and distance travelled were significantly greater in EGF spots compared to control spots containing PBS in place of chemoattractant. Furthermore, as with MDA-MB-231 cells, chemotactic invasion of PDACs was sensitive to Dynasore treatment (Figure 2B). Importantly these results are similar to those obtained following Dynasore treatment in PDACs cells in studies employing other cell migration models, including EGF stimulated wound healing (30), and suggest that dynamin function is required for chemotactic invasion in multiple cell platforms.

Previously we have shown that activated growth factor receptors cluster to sites of endocytosis (21,31). As depicted in Figure 3 when we visualised GFP-tagged EGFR by total internal reflection fluorescence (TIRF) microscopy performed on cells undergoing EGF-directed chemotactic invasion we observed EGFR clusters in the front, middle and back of the adherent plasma membrane (32,33). Importantly, in non-stimulated cells not exposed to EGF this construct does not form clusters in the plasma membrane of MDA-MB-231 cells (Figure S2). Thus, we next set out to determine if Dynasore treatment altered the distribution of EGFR clusters.

As depicted in Figure 3, when comparing the distribution of EGFR clusters in the adherent plasma membrane of cells migrating in EGF spots Dynasore treatment caused a decrease in the proportion of clusters in the middle of the cell, and an increase in those towards the front, although only the former was statistically significant. In further analyses we found that following Dynasore treatment, but not in untreated control cells, there were more EGFR clusters in the front of the cell relative to the middle and back of the adherent plasma membrane. Thus, Dynasore treatment causes a redistribution of EGFR clusters, potentially suggesting that endocytosis of activated EGFR is polarised during EGF-directed chemotactic invasion. Furthermore, consistent with our previous work investigating the endocytic trafficking of activated EGFR in non-motile cells, Dynasore treatment did not increase the total number of EGFR clusters in the adherent plasma membrane (Figure 3C); previously we demonstrated that inhibition

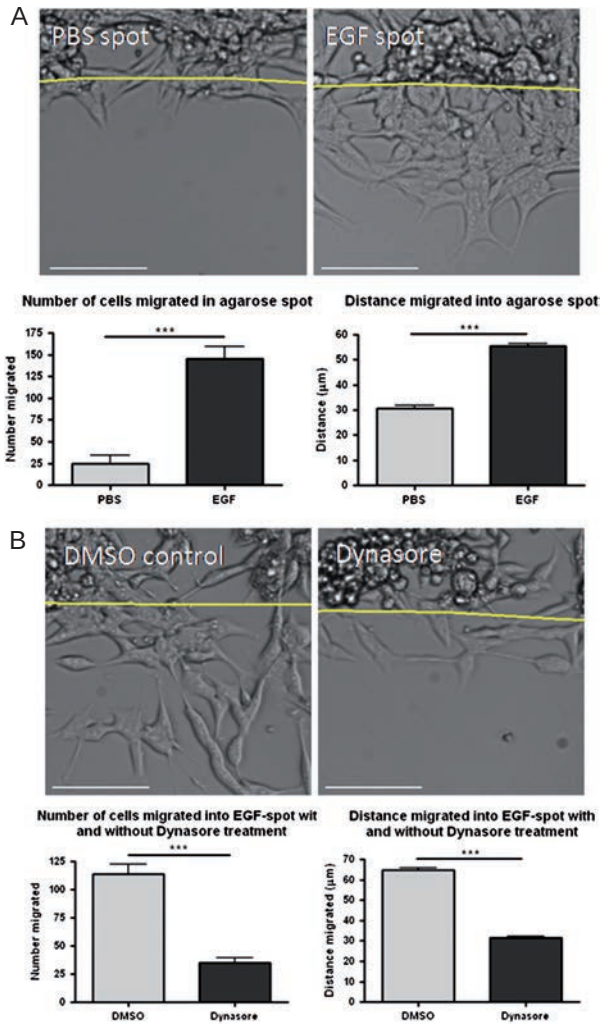

Figure 2: Dynasore inhibits PDACs chemotactic invasion into EGF spots. A) The total number of PDACs cells migrated into the spot and the distance migrated by cells was significantly higher in EGF spots compared to control PBS spots. Line denotes edge of the agarose spot. B) Dynasore treatment caused a decrease in the number of PDACs cells migrated and distance migrated into EGF spots. Scale bars are 100 µm. $n \geq 12$ fields of view per treatment.

of clathrin-mediated endocytosis with siRNA silencing of α-adaptin similarly did not increase the number of EGFR clusters in EGF stimulated cells (21).

One potential role previously suggested for endocytosis in cell migration is internalisation of integrins from disassembling focal adhesions, although this phenomenon has not been universally observed (7,34–36). Thus we

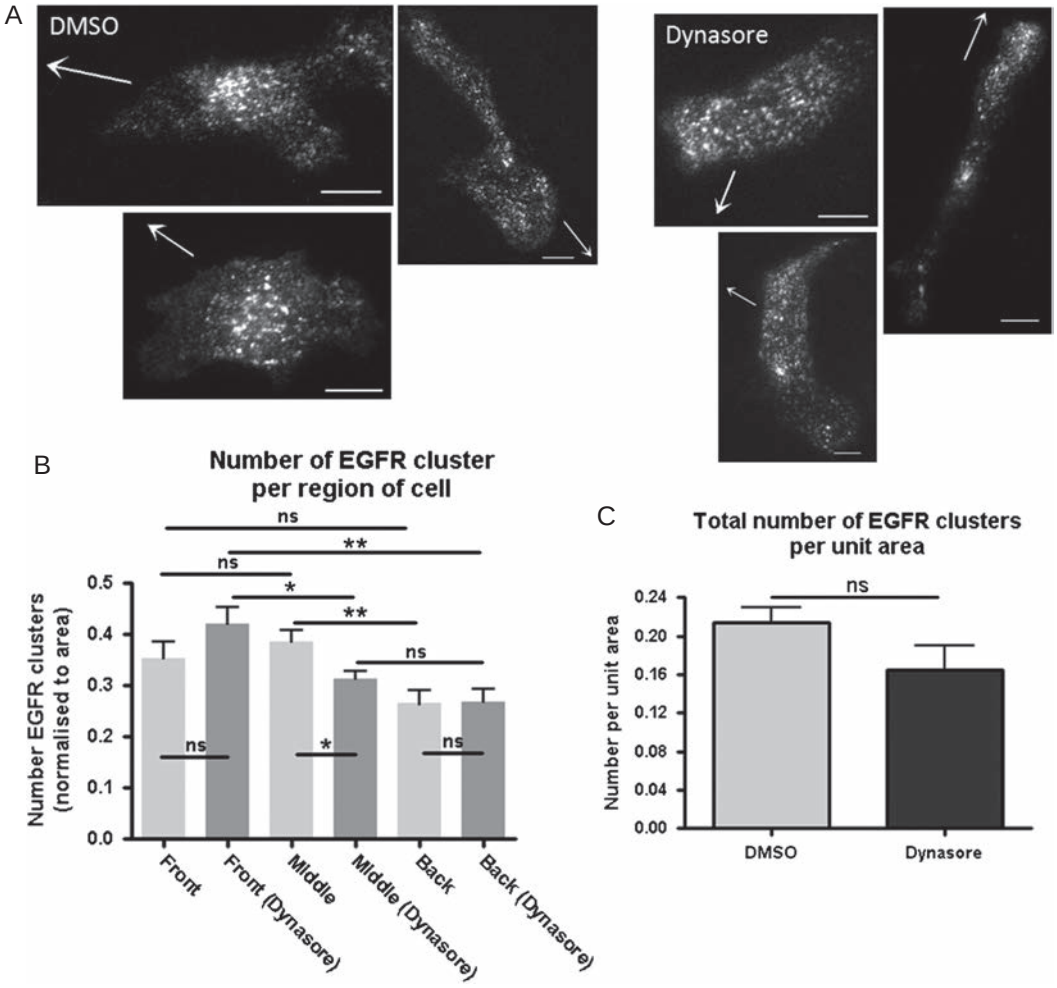

Figure 3: Dynasore causes redistribution of EGFR during chemotactic invasion. A) Representative images of cells used for EGFR cluster number counts in migrating cells treated with DMSO and Dynasore. Scale bars 10 μm. B) Quantification of EGFR clusters by cell region with and without Dynasore treatment. C) Overall there is no significant increase in the number of clusters following Dynasore treatment. $n = 12$ cells per treatment.

investigated whether Dynasore treatment causes a similar alteration in the distribution of focal adhesions in migrating MDA-MB-231 cells.

We chose to employ paxillin-mRFP for these studies, which should be present in all focal adhesions (37). As depicted in Figure 4, Dynasore treatment did not cause a redistribution of focal adhesions, within each cell region (front, middle and back), the number of focal adhesions was similar with and without Dynasore treatment. Additionally, Dynasore treatment did not increase the total number of focal adhesions per cell (Figure 4C). Thus, in contrast with EGFR, focal adhesion distribution does not seem, in this model, to depend on dynamin function.

Clathrin-mediated endocytosis of EGFR during chemotactic invasion

Dynamin functions in multiple endocytosis pathways, as well as in other cellular processes relevant to cell migration (5,25,26,38). In order to specifically determine the endocytosis pathway(s) that might be important for EGF-directed migration we performed a series of RNAi studies. We employed previously validated siRNA sequences to achieve silencing of α-adaptin, a component of the AP2 complex necessary for clathrin-medicated

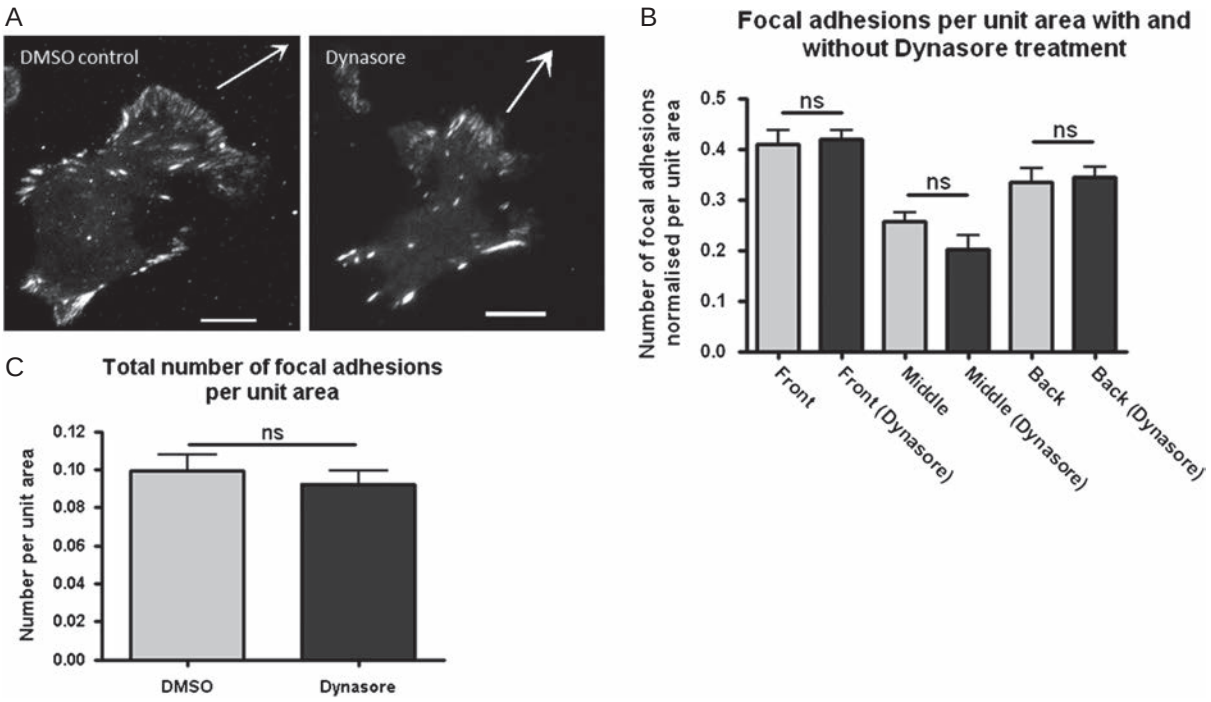

Figure 4: Dynasore does not cause redistribution of focal adhesions during chemotactic invasion. A) Representative images of paxillin-mRFP in cells migrating towards EGF. Scale bars are 10 μm. B) Quantification of number of focal adhesions in the front, middle and back regions of migrating cells. C) Overall there is no significant increase in the number of focal adhesions following Dynasore treatment. $n = 25$ cells per treatment.

endocytosis, and caveolin1, necessary for caveolar endocytosis (31). Knock-down was confirmed by western blot (Figure S3A), and inhibition of clathrin-mediated endocytosis and caveolar endocytosis were validated by inhibition of transferrin and CTxB uptake, respectively (Figure S3B). Using siRNA against α-adaptin we saw a large decrease in the total number of cells able to migrate into the agarose spot (65% decrease), conversely, knock-down of caveolin1 had no effect on cell migration (Figure 5A and B). Thus these results indicate that there is a requirement for clathrin-mediated endocytosis in the process of EGF-directed chemotactic invasion, but that caveolar endocytosis is dispensable.

Becausewe had observed a necessity for clathrin-mediated endocytosis in EGF-directed migration we predicted that this pathway might be the route of internalisation of EGFR following ligand binding in this model of migration. Thus, in the agarose spot assay migrating cells expressing GFP-tagged EGFR and clathrin-dsRed were imaged by TIRF microscopy and the degree of colocalisation between the two was quantified. As depicted in Figure 6, significant colocalisation between EGFR and clathrin was observed when compared to 'control' regions devoid of EGFR spots. As clathrin-independent endocytosis, such as caveolar endocytosis, has been suggested to play a role in EGFR internalisation in certain situations (20–23) we performed similar analyses assessing the degree of colocalisation between EGFR-GFP and caveolin1-mRFP. In stark contrast to the colocalisation observed between EGFR and clathrin, only approximately 5% of EGFR clusters colocalised with caveolin1, almost 10-fold less than the colocalisation seen with clathrin (Figure 6A and B).

Clathrin and EGFR colocalisation during endocytosis was also validated by live cell TIRF imaging and instances of both markers simultaneously disappearing from the TIRF field were observed (Figure 7A and B). However, in these live-cell studies dynamic EGFR spots devoid of clathrin were also tracked. As depicted in Figure 7C, laterally motile EGFR spots, potentially uncoated endocytic structures or post-Golgi carriers, were observed. Thus, these data

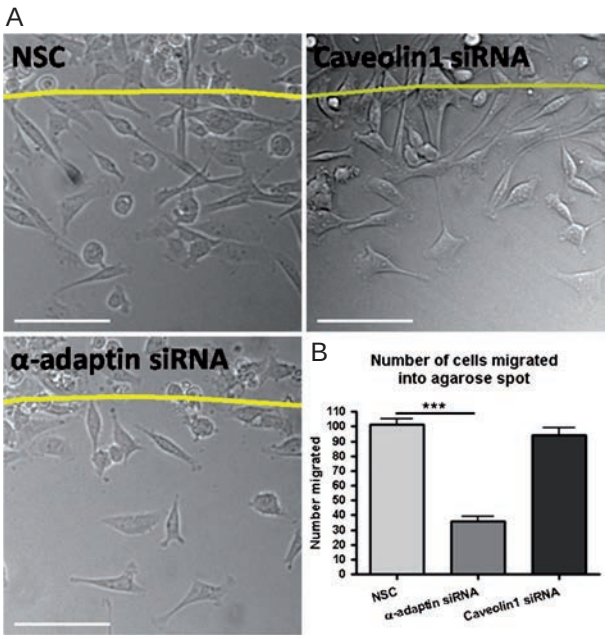

Figure 5: siRNA silencing of α-adaptin inhibits MDA-MB-231 migration into EGF spots. A) Representative images treated with control siRNA, α-adaptin siRNA and caveolin1 siRNA after 14 h migration into an agarose spot containing EGF. Scale bars are 100 μm. B) Quantification of total number of cells migrated under siRNA conditions. Line denotes edge of the agarose spot. $n = 22$ fields of view per treatment. NSC = non-silencing control siRNA.

suggest that during EGF-directed chemotactic invasion activated EGFR enters the cell via clathrin-mediated endocytosis.

Dynasore treatment caused a redistribution of EGFR spots in migrating cells (Figure 3), suggesting the possibility of polarised endocytosis in migrating cells. In order to further investigate this possibility we imaged clathrin-dsRed by live-cell TIRF microscopy in cells migrating in the agarose spot assay. We looked for instances where clathrin disappeared from the evanescent field to indicate an internalisation event. The disappearance of clathrin from the evanescent field was taken to be due to endocytosis only if it was not due to photobleaching, if it occurred rapidly (within 10 frames of imaging) and if it did not reappear in the evanescent field within 10 frames of its disappearance. It was found that over the course of these timelapses significantly more clathrin internalisation events occurred at the front of migrating cells, as opposed to the middle or the back (Figure 8A–C). Furthermore, although it seemed that clathrin-coated pits at the front of the cell are more likely to undergo endocytosis, this effect was not statistically significant (Figure 8D). Thus, taken together with the above results, during EGF-directed migration EGFR is internalised by clathrin-mediated endocytosis and that this internalisation is polarised towards the front of migrating cells.

We also tested whether these observations could be recapitulated in PDAC cells. Live-cell TIRF imaging of clathrin in migrating PDAC cells revealed a very strong preponderance of highly dynamic clathrin. As described in our previous work, when imaged by TIRF microscopy, clathrin can either be static, laterally mobile or disappear vertically into the cell (12,39). Furthermore, it has previously been suggested that movement of clathrin along microtubules can occur prior or subsequent to the endocytosis event (35,39). Thus, we quantified the 'dynamic' population of clathrin in migrating PDAC cells, combining those that disappeared vertically as well as those that moved laterally in the plane of the plasma membrane. As it has previously been demonstrated that individual microtubule tracks near the adherent cell surface can curve axially, potentially out of the TIRF field (40), we followed each clathrin spot present in the first image of a 1 min TIRF video. As previously described, we divided the cell into front, middle and back regions. Within each region we counted the number of dynamic clathrin spots. Similar to our results obtained in MDA-MB-231 cells, there were significant differences between the clathrin in the front of the cell, relative to the middle or back. When analysed as a fraction of the total number of spots per region, the front was significantly more dynamic (Figure 9A). Similarly, when we normalised to the area of each region, we found the front contained more dynamic clathrin than the middle or back (Figure 9B). Additionally, we found that EGFR and clathrin colocalised in PDACs, including within spots disappearing from the cell surface (Figure 9C). Thus, we have shown in both MDA-MB-231 and PDAC cells that (1) EGF-directed chemotaxis is dynamin dependant, (2) clathrin dynamics are polarised to the front of the migrating cell, and (3) that clathrin and EGFR can colocalise including during internalisation.

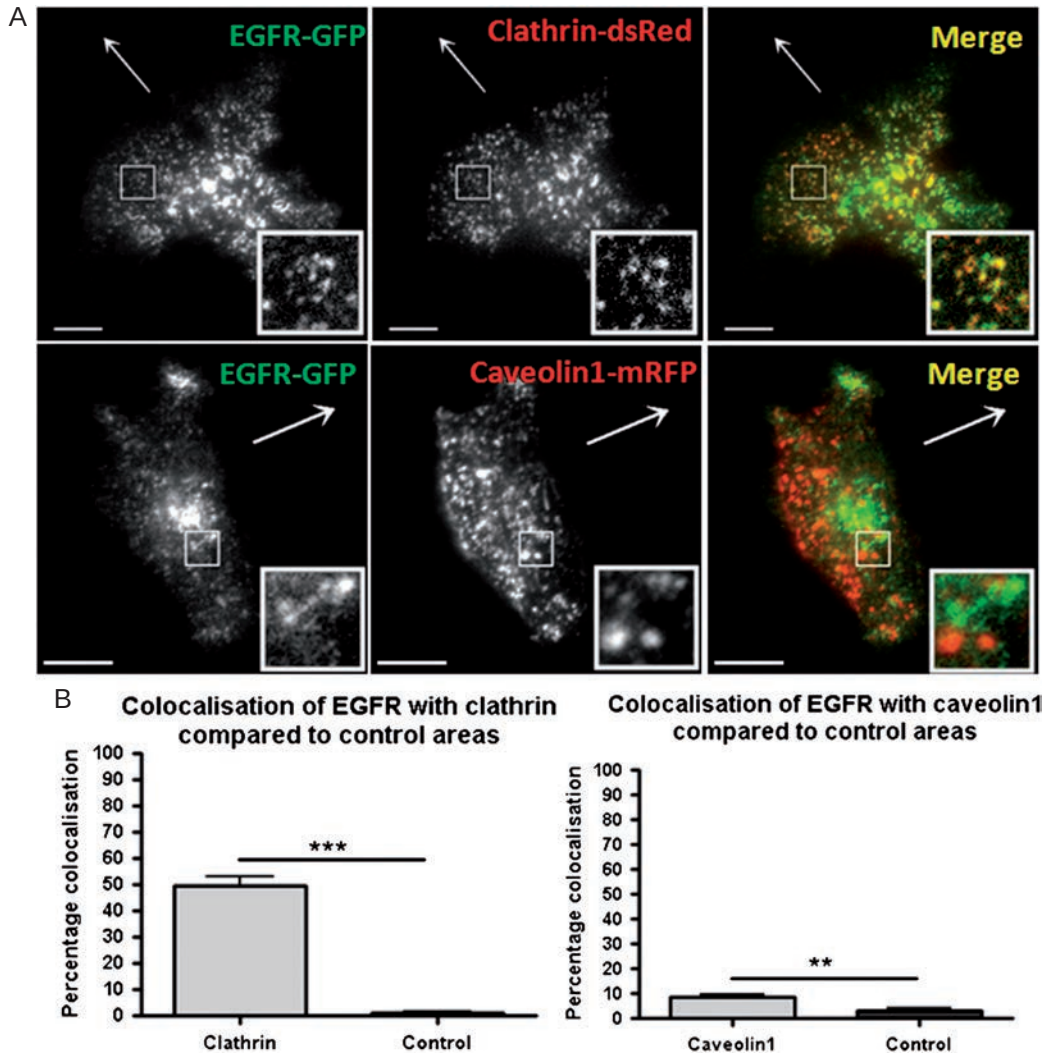

Figure 6: Colocalisation between clathrin-dsRed and EGFR-GFP. A) Representative images of EGFR-GFP with clathrin-dsRed or caveolin1-mRFP in cells migrating towards EGF. Scale bars 10 μm. B) Quantification of colocalisation of EGFR-GFP with clathrin-dsRed and caveolin1-mRFP. $n = 14$ cells for each experiment.

Clathrin-mediated endocytosis is not involved in focal adhesion disassembly

The inability of Dynasore treatment to cause redistribution of focal adhesions in migrating cells suggests that endocytosis is not required for focal adhesion disassembly in this model. To further test this hypothesis we investigated whether there was a role for clathrin-mediated endocytosis in focal adhesion disassembly in migrating MDA-MB-231 cells. Thus, we investigated the potential colocalisation between clathrin and a previously validated focal adhesion marker GFP-β3-integrin in cells migrating towards EGF in the agarose spot assay (37,41).

As depicted in Figure 10, colocalisation of clathrin and GFP-β3-integrin was not evident. Only approximately 7% of focal adhesions were positive for clathrin. In addition, as shown in Figure 9B, a previously published technique for assessing colocalisation by analysing the effect on Pearson's correlation coefficient of shifting one channel relative to another one pixel at a time confirms the lack of colocalisation of clathrin and focal adhesions (39,42). Finally, we performed two colour live-cell TIRF imaging to specifically determine if clathrin was transiently recruited to disassembling focal adhesions and as depicted in Figure 10C, this was not observed.

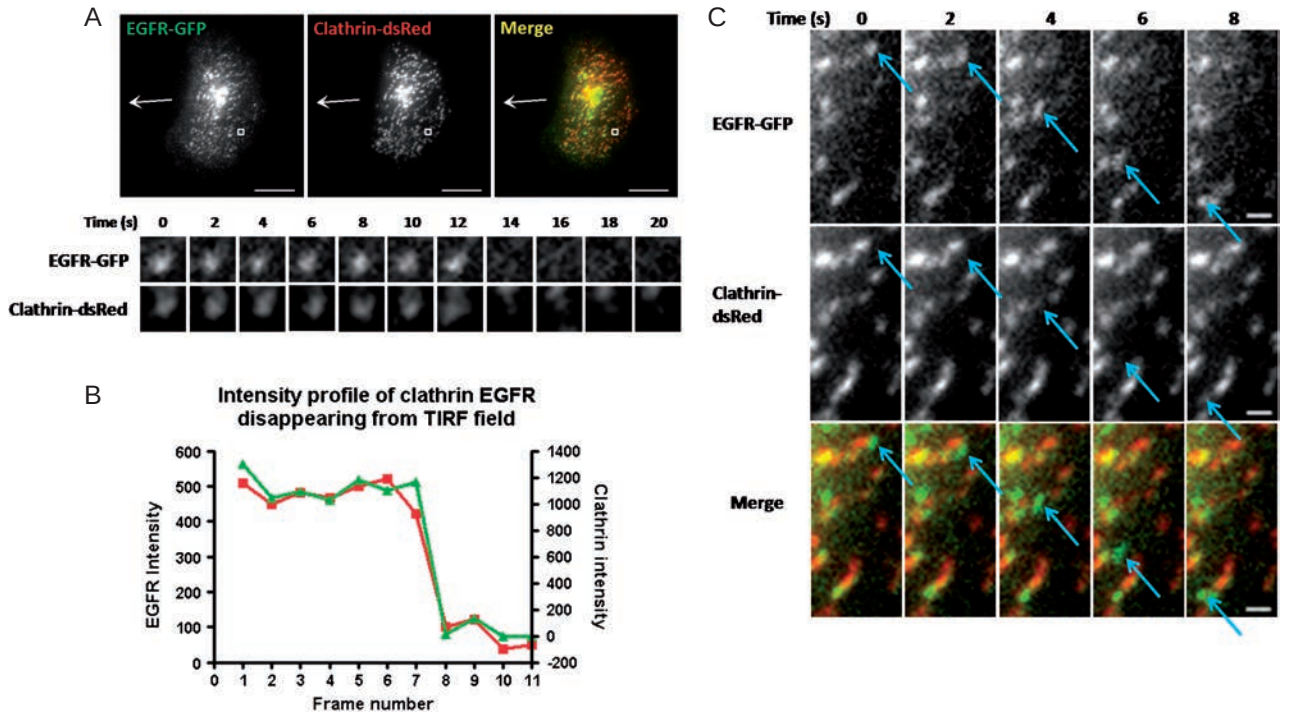

Figure 7: Live-cell TIRF imaging of clathrin-dsRed and EGFR-GFP. A) Representative image to show an instance of both markers leaving the TIRF field at the same time. Scale bars are 10 μm. B) Quantification of the disappearance event depicted in (A). C) Directed motility of an EGFR cluster devoid of clathrin. Scale bars are 1 μm.

We chose to use a fluorescent tagged integrin (in this case GFP-β3-integrin) as our focal adhesion marker as it represents a potential endocytic cargo localised to the sites of focal adhesions, and therefore has the potential to colocalise with clathrin during endocytosis. However β3-integrin might not be present in all focal adhesions, thus we performed similar analyses with paxillin-mRFP. Importantly in control studies we assessed the colocalisation of GFP-β3-integrin and paxillin-mRFP. As can be seen in Figure S4, all regions of paxillin-mRFP also contain GFP-β3-integrin.

As with GFP-β3-integrin, no colocalisation was observed between paxillin-mRFP and clathrin-GFP in either static images of migrating cells or by analysing whether clathrin was recruited to regions of disassembling focal adhesions, as in the previous analysis (Figure S5A). Thus, these results confirm that clathrin-mediated endocytosis does not contribute directly to focal adhesion disassembly in this system. Similarly, although siRNA silencing of caveolin1 did not inhibit EGF-directed chemotactic invasion of MDA-MB-231 cells we also verified that caveolin1 also did not colocalise with GFP-β3-integrin (Figure S5B).

As a final means to investigate a potential role for clathrin-mediated endocytosis in focal adhesion disassembly we assessed whether inhibition of clathrin-mediated endocytosis with siRNA against α-adaptin altered the rate of focal adhesion disassembly measured by timelapse TIRF microscopy of mRFP-paxillin, a previously employed assay strategy (7). However, as cells treated with α-adaptin siRNA do not readily migrate into EGF-containing agarose spots these experiments were performed with MDA-MB-231 cells migrating in a wound healing assay. Consistent with our colocalisation analysis (Figure 9), we found no differences in the time taken for focal adhesions to disassemble in knock-down cells compared to control (Figure 11A and B), indicating that clathrin is not required for disassembly of focal adhesions in migrating cells. Furthermore, as α-adaptin siRNA did not reduce the rate of wound healing (Figure 11C and D) it may be that EGFR trafficking is the

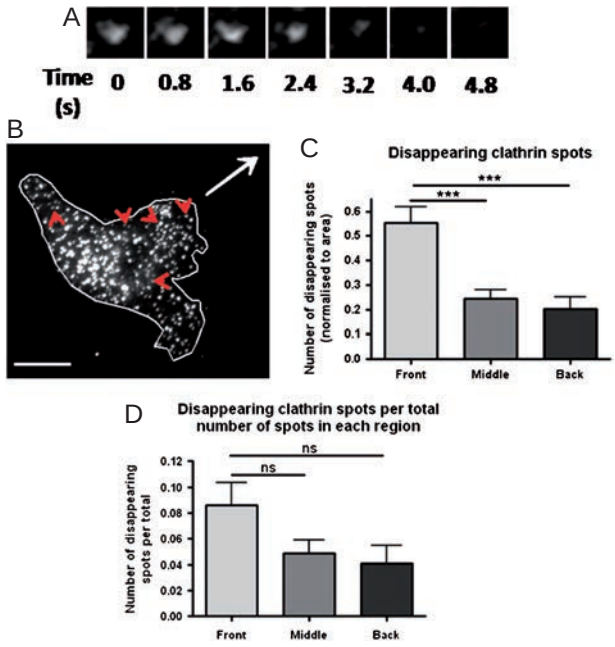

Figure 8: Clathrin spot disappearance is polarised to the front of migrating cells. A) Representative images of a clathrin spot disappearing from the TIRF imaging field. B) Representative image of a clathrin-dsRed expressing migrating cell with instances of clathrin disappearance circled. Scale bars are 10 μm. C) Quantification of clathrin disappearance by cell region. D) Quantification of clathrin disappearance compared to total number of spots in each region. $n = 18$ cells.

main role of clathrin-mediated endocytosis during chemotactic invasion and during wound healing this pathway is not required.

Discussion

The role of endocytosis in chemotactic invasion has not been adequately investigated. It has been suggested in some models that endocytosis is involved in focal adhesion disassembly (10,11,16,17). Furthermore, endocytosis can play a role in the modulation of receptor signalling (5,43–45). Therefore we conducted a series of studies to determine the role(s) of endocytosis in driving chemotactic invasion of breast cancer-derived cells. Increased understanding of how endocytosis regulates chemotactic invasion may assist in developing therapeutic interventions that might target tumour cell invasion and metastasis.

We firstly sought to establish whether endocytosis was important for chemotactic invasion of MDA-MB-231 cells towards EGF. Using Dynasore to inhibit dynamin-dependent endocytosis we found that far fewer cells were able to migrate, and that the migration of those which could still migrate was significantly impaired (Figure 1). In addition, we obtained identical results using an unrelated pancreatic cancer-derived cell line, further emphasising the reproducibility of the assay used and the necessity for dynamin-dependent endocytosis in chemotactic invasion (Figure 2). Because Dynasore had such a profound effect on migration we next investigated whether this might be as a result of a role involving endocytosis of receptors (noteably EGFR) or focal adhesion components (e.g. integrins). We found that Dynasore caused an accumulation of EGFR towards the front of migrating cells, however did not affect the localisation of focal adhesion components (Figures 3 and 4).

Because multiple endocytosis pathways are dynamin-dependent (46–48) we employed an RNAi approach to inhibit specific routes of endocytosis and further narrow down the role of endocytosis in chemotactic invasion. Upon inhibition of clathrin-mediated endocytosis by siRNA against α-adaptin we again saw a significant reduction in the number of cells able to migrate, demonstrating this to be a pathway necessary for migration towards EGF (Figure 5). Conversely, using siRNA against caveolin1 to inhibit caveolar endocytosis, we saw no alteration in cell migration.

Aspects of these results are in contrast to those reported by other groups. In 2012 Urra et al. inhibited caveolin1 in MDA-MB-231 cells and found this inhibition to decrease migration of cells in a wound healing model (49). The authors therefore suggested a role for caveolin1 in enhancing the metastatic potential of cancer cells. However, another study found that expression of caveolin1 led to an inhibition of chemotaxis and chemoinvasion in melanoma cells and suggested a role for the protein in inhibiting cell migration (50). Thus controversy remains, with different groups pointing to a role for caveolin1 in either promoting or inhibiting migration in some way (49–53). In order to verify our results we also undertook TIRF imaging of caveolin1-mRFP in conjunction with GFP-β3-integrin in cells migrating towards EGF and found no notable

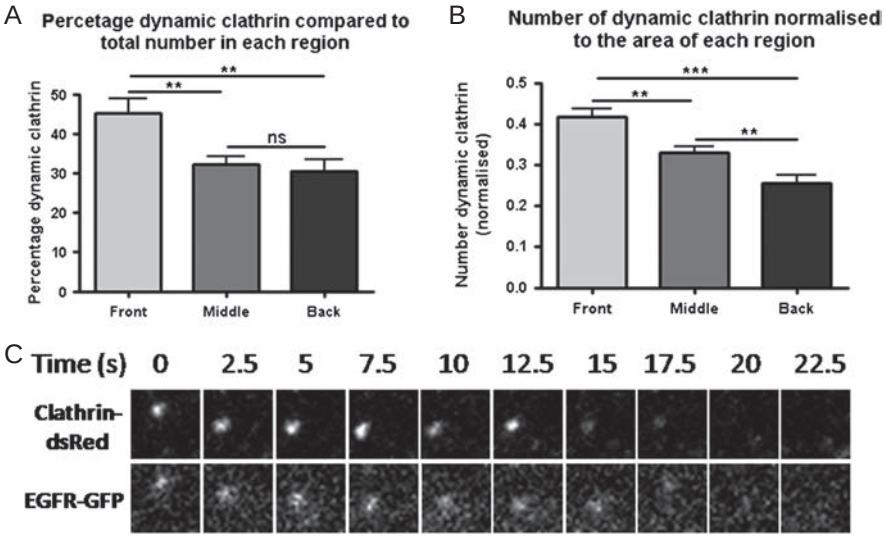

Figure 9: Active clathrin in migrating PDAC cells. A) Graph to show that there is a higher proportion of active or internalising clathrin compared to total clathrin at the front of migrating PDAC cells compared to the middle or the back. B) Graph to show that there is more active or internalising clathrin at the front of migrating PDAC cells when normalised to the area of each region. $n = 12$ cells. C) An instance to show clathrin-dsRed and EGFR-GFP internalising from the TIRF field together.

colocalisation between the two (Figure S5B). We therefore conclude that caveolar endocytosis is unnecessary for EGF-directed chemotactic invasion of MDA-MB-231 cells. However, it may be necessary for other modes of migration.

As clathrin-mediated endocytosis was required for chemotactic invasion towards EGF we tested for colocalisation between clathrin and EGFR and found a high degree of colocalisation between the two (Figure 6). When we tested colocalisation of EGFR with caveolin1 we found that this was negligible compared to the colocalisation with clathrin. This indicates a clathrin-dependent internalisation route for the EGFR in cells migrating in an EGF-dependent manner. In the literature there is much support for a clathrin-dependent route of EGFR endocytosis (20,21,54,55) but also contrary evidence supporting a clathrin-independent route in certain situations (22,22,23,56,57). In support of our findings, previous work by Huang et al. and Rappoport and Simon demonstrated that in non-migrating cells the EGFR enters primarily through clathrin-coated pits and not through caveolae (20,21). In addition to assessing colocalisation of clathrin and EGFR we were able to image instances of both simultaneously disappearing from the TIRF field (Figure 7A and B). During this live-cell imaging we also saw instances of EGFR clusters devoid of clathrin moving laterally adjacent to the plasma membrane, likely to be post-endocytic structures or post-Golgi vesicles (Figure 7C). This observation suggests that some EGFR in our analysis in Figure 6 may be EGFR of this category and therefore the colocalisation of EGFR clusters with clathrin-coated pits/vesicles on the plasma membrane could be even higher than originally thought.

An emerging idea is that polarised vesicle trafficking is involved in the regulation of directed cell migration (6). A link between polarised trafficking of cell adhesion components has been shown in a number of cell types (11,58–60). The occurrence of polarised trafficking of chemoattractant receptors is less well studied than that of focal adhesions, but may play a role in regulation of directed cell migration (61). A recent study by Assaker et al. found that particular endocytic proteins were necessary to control the trafficking, and hence spatial polarisation, of receptor tyrosine kinases during Drosophila boarder cell migration (62). Another study by Belleudi et al. found endocytosis and polarised recycling of the keratinocyte growth factor receptor regulated receptor polarisation at the plasma membrane, and that this was necessary for keratinocyte migration (63). Upon inhibition of dynamin-dependent endocytosis we have already shown a redistribution of EGFR localisation towards the front of migrating cells (Figure 3). This implies that EGFR internalisation is polarised to the front of migrating cells, as inhibition of endocytosis caused a build up endocytosis cargo in this region. This led us to test whether clathrin-mediated endocytosis is polarised in MDA-MB-231 cells during EGF-directed chemotactic invasion. As expected, we saw an increased number of internalisation events at the

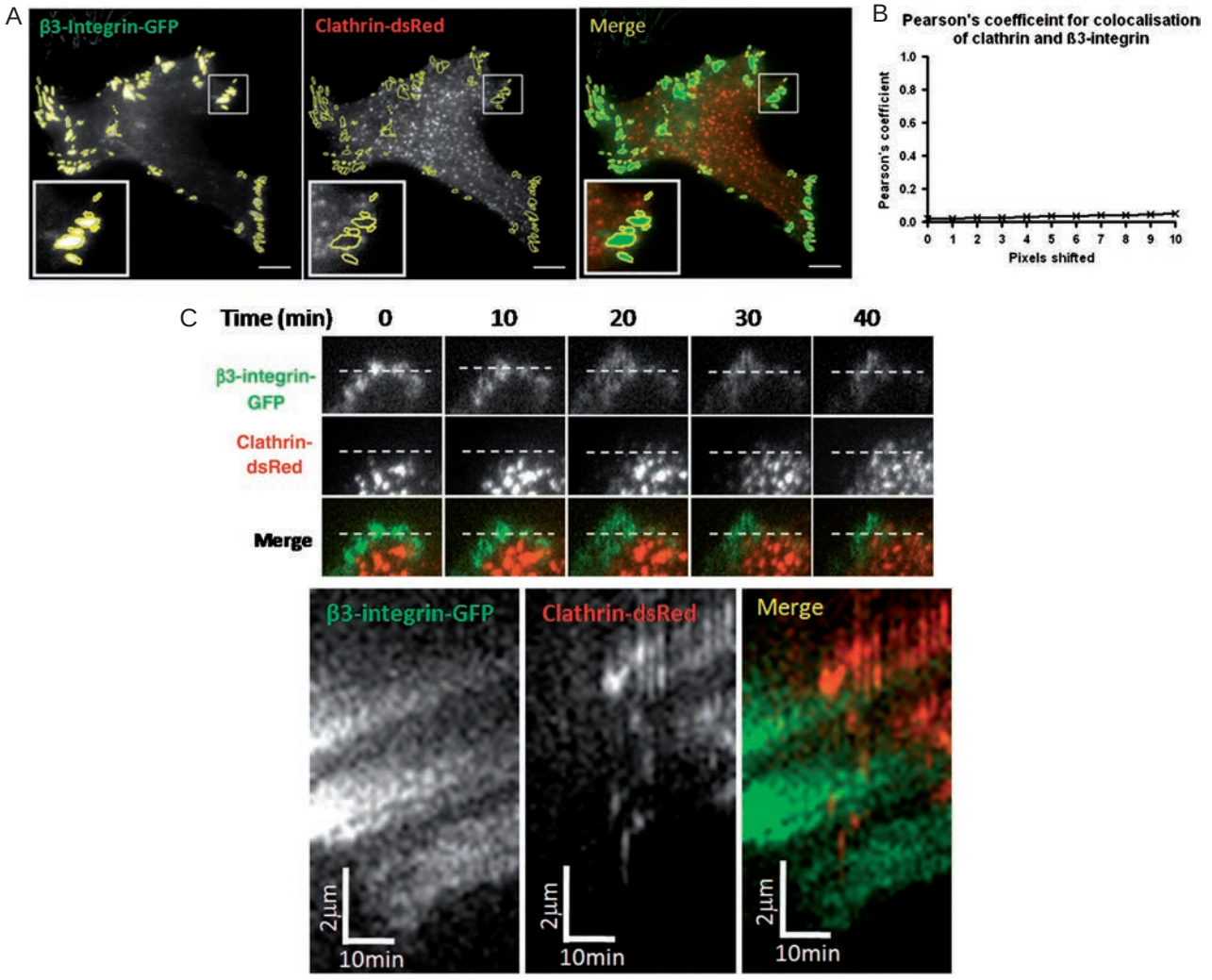

Figure 10: Clathrin-dsRed does not co-localise with focal adhesions using GFP-β3-integrin as the focal adhesion marker. A) Representative images with focal adhesions circled from the GFP-β3-integrin image to assess colocalisation with clathrin. Scale bars are 10 μm. B) Pearson's coefficient of GFP-β3-integrin with clathrin-dsRed. $n = 30$ cells. C) Kymograph to show lack of co-localisation between clathrin-dsRed and GFP-β3-integrin labelled focal adhesions. A 10 μm line was drawn across two disassembling focal adhesions and a kymograph across this region demonstrated no co-localisation of clathrin during focal adhesion disassembly.

front of cells migrating towards EGF rather than at the middle or back (Figure 8). In addition to the necessity for clathrin-mediated endocytosis for migration in this model, these results suggest that polarised endocytosis of the EGFR is important for migration in this breast cancer cell line.

There has been data reported suggesting a role for clathrin-mediated endocytosis of integrins from disassembling focal adhesions (34,35). However, in other studies this has not been observed (7,36). As inhibition of endocytosis significantly decreased chemotactic invasion, we tested whether there is a role for clathrin-mediated endocytosis in focal adhesion disassembly. However, we found no significant colocalisation between clathrin and the focal adhesion markers β3-integrin and paxillin, including specifically during focal adhesion disassembly (Figure 10 and Figure S5A). In addition to chemotactic invasion studies we also undertook wound healing studies using MDA-MB-231 cells where we found knock-down of α-adaptin had no

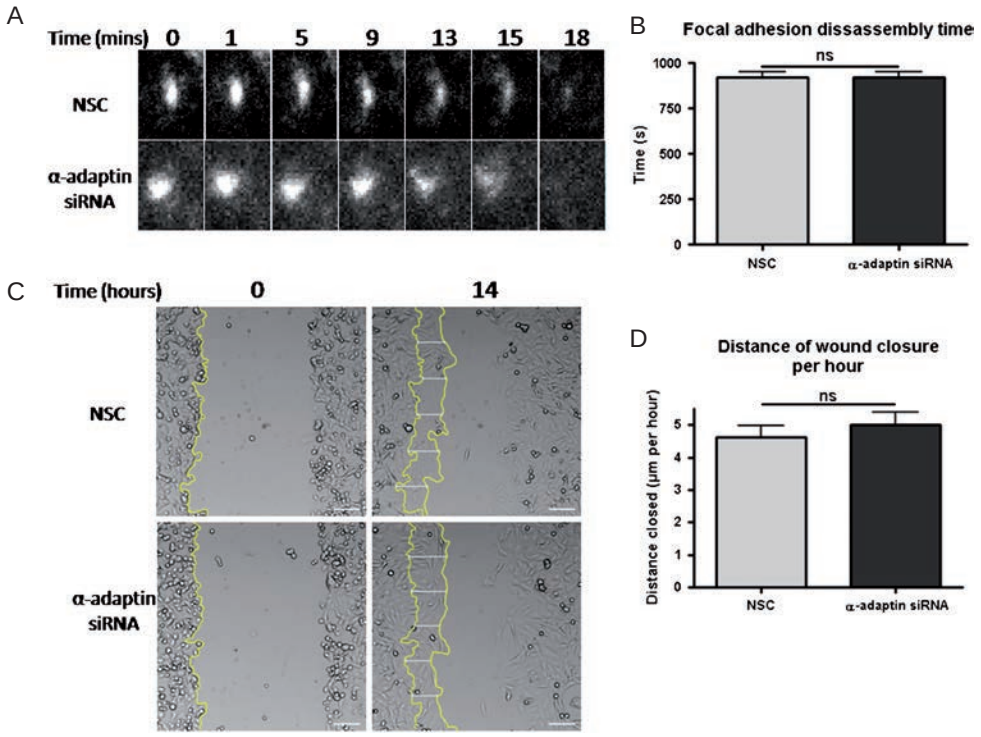

Figure 11: siRNA silencing of α-adaptin does not inhibit focal adhesion disassembly during wound healing. A) Disappearance of paxillin-mRFP over time using NSC and α-adaptin siRNA. B) Graph showing mean focal adhesion disassembly time for cells treated with NSC and α-adaptin siRNA. $n \geq 100$ focal adhesions from 20 cells per treatment. C) Wound healing assay with α-adaptin knock-down. Representative images of wounds at time 0 and after 14 h. Lines denote edge of wound at both time points. Distances between cells at time 0 and 14 h were measured at various points in each image to give an average distance migrated in NSC and α-adaptin siRNA treated cells. D) Quantification of distance moved by siRNA treated cells. $n = 22$ fields of view per treatment.

effect on focal adhesion disassembly time. Wound healing was assessed here because silencing of α-adaptin had such a profound effect on chemotactic invasion that we could not perform these analyses in that model.

Our data in MDA-MB-231 wound healing corroborates with wound healing results from other studies, including those from Fletcher et al. in MDCK cells where they also found no role for endocytosis during focal adhesion disassembly (7). The contrast in these results compared to some studies performed in fibroblasts indicates that effects seen on focal adhesions may be cell type and/or migratory stimulus specific and that while there may be a requirement for clathrin in focal adhesion disassembly in fibroblasts, this is not the case during chemotactic invasion of MDA-MB-231 breast cancer cells (34,35).

In addition we found that knocking down α-adaptin had no effect on the wound closure rate of MDA-MB-231. This indicated that while some pathways may be necessary for one process they may be dispensable for other, otherwise similar, phenotypes. Furthermore, this suggests that EGFR trafficking might be a critical role of clathrin-mediated endocytosis during chemotactic invasion towards EGF in MDA-MB-231 cells, but not necessary for wound healing.

Taken together these results suggest a model where dynamin and clathrin are necessary for chemotactic invasion in MDA-MB-231 cells, but caveolin1 is not. We also establish that clathrin-mediated endocytosis is not necessary for focal adhesion disassembly in this cell line. We propose that the main route of EGFR internalisation is clathrin-mediated endocytosis, which is polarised towards the front of migrating cells. Comparison of these results with other studies provides significant evidence for

differences between cell types, as well as migratory models. Thus, there results suggest that a more systematic and empirical approach is required before broad conclusions can be suggested to describe the role(s) of endocytosis in directed cell motility.

Materials and methods

Cell culture

MDA-MB-231 (ATCC), PDAC and PDACs cells (gift from Kurt Anderson, Beatson Institute) were incubated at 37°C in 5% (v/v) CO_2. Cells were maintained in Dulbecco modified Eagle medium (DMEM, Lonza) supplemented with 10% foetal calf serum (FCS) (Gibco) and 1% Pen-Strep (Gibco). PDACs cells are stably transfected versions of PDAC cells with a Src FLIM/FRET probe and, for the purpose of this manuscript, are referred to as PDACs (rather than PDAC) to denote the difference from regular PDAC cells.

Transfection and plasmid constructs

cDNA transfections of MDA-MB-231 cells were achieved using Lipofectamine 2000 (Life Technologies). Cells were plated to approximately 80% confluency 24 h prior to transfection. Assays with these cells were performed 24 or 48 h post transfection (depending on the cDNA construct and assay being performed).

cDNA transfection of PDAC cells was achieved using electroporation. Cells were plated 24 h prior to transfection and on the day of transfection were trypsinised and counted. Per transfection we used 2.5×10^5 cells with 4 µg cDNA, 100 µL electroporation solution (Ingenio) and programme X-01 on the Lonza Nucleofector 2b device.

The construct encoding clathrin-dsRed was a gift from Thomas Kirchhausen (Harvard Medical School), GFP-β3-integrin was a gift from Jonathan Jones (Northwestern University Medical School), paxillin-mRFP was a gift from Maddy Parsons (King's Collage London), Cav1–mRFP was a gift from Ari Helenius (Swiss Federal Institute of Technology Zurich) and EGFR-GFP was a gift from Alexander Sorkin (University of Pittsburgh).

siRNA transfections were achieved using DharmaFECT 1 (Thermo Scientific). siRNA constructs were obtained from Thermo Scientific. Cells were plated to approximately 40% confluency 24 h prior to transfection. Assays with these cells were performed 72 h post transfection.

Endocytosis assays

Uptake assays were used to assess the effect of Dynasore treatment, α-adaptin knock-down and caveolin1 knock-down on endocytosis. 24 h prior to the assay cells were plated onto sterilised glass cover slips. For assays with Dynasore each well was rinsed with serum free media (SFM) before incubation with SFM containing 80 µM Dynasore (Sigma), or the equivalent volume of dimethyl sulphoxide (DMSO), for 30 min. A 10 min incubation with just SFM was used for assays utilising siRNA transfected cells. After this initial incubation cells were then further incubated for 5 min with either transferrin (Alexa Fluor 568 conjugate, 10 µg/mL, Life Technologies) or cholera toxin B subunit (CTxB, Alexa Fluor 555 conjugate, 1 µg/mL, Life Technologies) diluted in SFM. After incubation cells incubated with transferrin were washed with acid PBS twice followed by a PBS wash; cells incubated with CTxB were washed twice with SFM followed by a PBS wash. Cover slips were fixed in 4% paraformaldehyde (PFA, Electron Microscopy Sciences) for 5 min. Cover slips were fixed to slides using ProLong Gold (Life Technologies) and imaged using a Nikon TE300 Inverted Epi-fluorescence microscope with a 60× oil objective lens. Random fields of view from each slide were recorded and the light intensity of 20 random cells per slide was analysed.

Transwell assays

Chemotaxis assays were carried out using Transwell plates (24 mm diameter polycarbonate inserts with 8 µm pores, Corning Life Sciences). EGF was used as the chemoattractant at a concentration of 1 µg/mL EGF. The Dynasore group was treated with 80 µM, and 5×10^5 cells were plated into each insert and Transwells were incubated at 37°C, 5% CO_2 for 5 h. After incubation, inserts were washed in PBS and fixed in 4% PFA for 5 min. After fixing, membranes were treated with Vectashield mounting medium with DAPI (4′,6-diamidino-2-phenylindole) (Vector Laboratories) to stain cell nuclei and fixed to slides. Imaging was done using a Nikon TE300 Inverted Epi-fluorescence microscope with a 40× oil objective lens. Random fields of view from each slide were recorded and numbers of migrated cells in each field were counted.

Western blot

Cells were lysed in 1% Triton X-100 (Sigma) in PBS with protease inhibitors (complete mini EDTA-free protease inhibitor cocktail, Roche). Proteins were separated by SDS–PAGE and transferred from the gel onto Immobilon-FL membrane (Millipore). The membrane was blotted with primary antibody overnight at 4°C and then with secondary antibody for 2 h at room temperature. Primary antibodies used were polyclonal rabbit anti-α-adaptin (Life Technologies), polyclonal rabbit anti-caveolin1 (BD Biosciences) and monoclonal mouse anti-tubulin (Sigma). Secondary antibodies used were anti-rabbit IRDye 800 and anti-mouse 680 (Li-cor) for use in Odyssey. Quantification of knock-downs was performed using Odyssey relative to control tubulin.

Agarose spot assay

A recently developed agarose spot assay was utilised to investigate chemotactic invasion as described in Wiggins and Rappoport (24). For TIRF imaging or overnight timelapses cell imaging media [10 mM Hepes (Sigma), 9.7 g Hank's Balanced Salt Solution (Life Technologies) in 1 L dH_2O, pH 7.4] with low serum content (0.1% FCS) was used. For the

Dynasore treatment assays the low serum media contained Dynasore at 80 μM and the control group was given the same volume of DMSO (Sigma).

Imaging and image analysis

Overnight timelapses (for agarose spot assays) were performed on a Nikon eclipse Ti inverted microscope using a 10× air objective lens (Nikon Instruments). TIRF imaging was carried out using a Nikon A1-R Ti TIRF system with a 60× oil objective lens (CFI TIRF Apo 60× oil NA 1.49, Nikon) (Nikon Instruments).

For quantification of fluorescence for the endocytosis assays IMAGEJ was used. For all other image analysis NIS elements (version 3.1) was used. For cell tracking analysis the manual tracking software in NIS elements was used.

For colocalisation analysis of clathrin-dsRed or caveolin1-mRFP with EGFR-GFP 50 clusters of EGFR in the green channel were circled, the number of these corresponding to a cluster of clathrin/caveolin1 in the red channel was then recorded. To assess colocalisation by chance, the same 50 circled regions were moved slightly so that they corresponded to regions where EGFR-GFP was not present; the number of these control regions which corresponded to a clathrin/caveolin1 cluster was recorded as the control value. For assessing colocalisation of clathrin with β3-integrin or paxillin-mRFP a 10 μm line was drawn across two disassembling focal adhesions and a kymograph across this region over 40 min was made.

For analysis involving splitting the cell into front, middle and back regions of migrating cells control timelapses (i.e. no inhibition of migration) were used to establish the overall direction taken by cells within agarose spots. We calculated the angle of cells from the last point on the timelapses with respect to a line perpendicular to the edge of the agarose spot. From this analysis it was found that on average cells migrate to within 2.80° (±2.3°) to the perpendicular, effectively meaning that the line perpendicular to the agarose spot edge can be used to estimate the direction of migration. For analysis involving establishing the front, middle and back of migrating cells we therefore used a line perpendicular to the edge of the agarose spot and divided this into three equal lengths. All analyses were normalised to the area of each region to account for their different sizes (unless stated otherwise).

Wound healing assay

For focal adhesion disassembly experiments, cells transfected with α-adaptin siRNA and paxillin-mRFP were plated onto 35-mm glass-bottomed dishes (MatTek Corporation) 24 h prior to wounding to give a confluent layer of cells. Cells were wounded using a 200 μL pipette tip. Cells at the edge of the wound were imaged using a Nikon A1-R Ti TIRF system with a 60× oil objective lens.

For experiments on the effect of α-adaptin knock-down on wound closure rate, cells were plated onto 35-mm glass-bottomed dishes and transfected with siRNA 72 h prior to wounding with a 200 μL pipette tip. Wounds were imaged every 15 min for 14 h with a Nikon eclipse Ti inverted microscope using a 10× air objective lens. Images were analysed using NIS elements (version 3.1) and average distance of migration was recorded.

Acknowledgements

The TIRF microscope used in this research was obtained through Birmingham Science City Translational Medicine Clinical Research and Infrastructure Trials Platform with support from Advantage West Midlands. This work was funded by the Biotechnology and Biosciences Research Council (J. Z. R. and L. J. M.). Abstract figure courtesy of Robert Lees.

Supporting Information

Additional Supporting Information may be found in the online version of this article:

Figure S1 Endocytosis controls for Dynasore treatment. A) Representative images of transferrin uptake (left panels) and cholera toxin B subunit uptake (right panels) with DMSO (as control) or Dynasore. B) Quantification of inhibition of transferrin and cholera toxin B subunit uptake by Dynasore treatment. Dynasore inhibited transferrin uptake by 60% and inhibited cholera toxin uptake by 52%. $n = 60$ cells per treatment.

Figure S2 Imaging of clathrin-dsRed and EGFR-GFP in cells with no EGF stimulation. Scale bars are 10 μm.

Figure S3 Controls for α-adaptin and caveolin1 siRNA. A) Western blot analysis of α-adaptin and caveolin1 knock-down in siRNA treated cells. B) Representative images and quantification of transferrin uptake and cholera toxin B subunit uptake inhibition in siRNA treated cells. Inhibition of transferrin uptake in α-adaptin siRNA treated cells (45%) and inhibition of cholera toxin B subunit uptake in caveolin1 siRNA treated cells (50%). $n = 3$ for knock-down analysis, $n = 60$ cells per treatment for transferring and cholera toxin uptake assays.

Figure S4 Colocalisation analysis of focal adhesion markers in migrating cells. Representative image showing a high degree of colocalisation between paxillin-mRFP and GFP-β3-integrin.

Figure S5 Lack of colocalisation between endocytosis markers and focal adhesions. A) Representative images of paxillin-mRFP and clathrin-GFP in migrating cells. Scale bars are 10 μm. Kymograph to show lack of colocalisation between paxillin-mRFP labelled focal adhesions and clathrin-GFP over time. A 10 μm line was drawn across two disassembling focal adhesions and a kymograph across this region demonstrated no colocalisation of clathrin during focal adhesion disassembly. B) Representative image showing a lack of colocalisation between caveolin1-mRFP and GFP-β3-integrin. Scale bars are 10 μm. Arrows show direction of migration.

References

1. Sporn MB. The war on cancer. Lancet 1996;347:1377–1381.

2. Condeelis J, Jones J, Segall JE. Chemotaxis of metastatic tumor cells: clues to mechanisms from the *Dictyostelium* paradigm. Cancer Metastasis Rev 1992;11:55–68.
3. Bagorda A, Mihaylov VA, Parent CA. Chemotaxis: moving forward and holding on to the past. Thromb Haemost 2006;95:12–21.
4. Bagorda A, Parent CA. Eukaryotic chemotaxis at a glance. J Cell Sci 2008;121:2621–2624.
5. Doherty GJ, McMahon HT. Mechanisms of endocytosis. Annu Rev Biochem 2009;78:857–902.
6. Fletcher SJ, Rappoport JZ. Moving forward: polarised trafficking in cell migration. Trends Cell Biol 2010;20:71–78.
7. Fletcher SJ, Poulter NS, Haining EJ, Rappoport JZ. Clathrin-mediated endocytosis regulates occludin, and not focal adhesion, distribution during epithelial wound healing. Biol Cell 2012;104:238–256.
8. Kawada K, Upadhyay G, Ferandon S, Janarthanan S, Hall M, Vilardaga J, Yajnik V. Cell migration is regulated by platelet-derived growth factor receptor endocytosis. Mol Cell Biol 2009;29:4508–4518.
9. Ridley AJ, Schwartz MA, Burridge K, Firtel RA, Ginsberg MH, Borisy G, Parsons JT, Horwitz AR. Cell migration: integrating signals from front to back. Science 2003;302:1704–1709.
10. Caswell P, Norman J. Endocytic transport of integrins during cell migration and invasion. Trends Cell Biol 2008;18:257–263.
11. Nishimura T, Kaibuchi K. Numb controls integrin endocytosis for directional cell migration with aPKC and PAR-3. Dev Cell 2007;13:15–28.
12. Rappoport JZ, Simon SM. Real-time analysis of clathrin-mediated endocytosis during cell migration. J Cell Sci 2003;116:847–855.
13. Sheetz MP, Felsenfeld DP, Galbraith CG. Cell migration: regulation of force on extracellular-matrix-integrin complexes. Trends Cell Biol 1998;8:51–54.
14. Lauffenburger DA, Horwitz AF. Cell migration: a physically integrated molecular process. Cell 1996;84:359–369.
15. Beningo KA, Dembo M, Kaverina I, Small JV, Wanga YL. Nascent focal adhesions are responsible for the generation of strong propulsive forces in migrating fibroblasts. J Cell Biol 2001;153:881–888.
16. Panicker AK, Buhusi M, Erickson A, Maness PF. Endocytosis of beta1 integrins is an early event in migration promoted by the cell adhesion molecule L1. Exp Cell Res 2006;312:299–307.
17. Fabbri M, Di Meglio S, Gagliani MC, Consonni E, Molteni R, Bender JR, Tacchetti C, Pardi R. Dynamic partitioning into lipid rafts controls the endo-exocytic cycle of the alphaL/beta2 integrin, LFA-1, during leukocyte chemotaxis. Mol Biol Cell 2005;16:5793–5803.
18. Yarden Y, Sliwkowski MX. Untangling the ErbB signalling network. Nat Rev Mol Cell Biol 2001;2:127–137.
19. Seshadri R, Matthews C, Dobrovic A, Horsfall DJ. The significance of oncogene amplification in primary breast cancer. Int J Cancer 1989;43:270–272.
20. Huang F, Khvorova A, Marshall W, Sorkin A. Analysis of clathrin-mediated endocytosis of epidermal growth factor receptor by RNA interference. J Biol Chem 2004;279:16657–16661.
21. Rappoport JZ, Simon SM. Endocytic trafficking of activated EGFR is AP-2 dependent and occurs through preformed clathrin spots. J Cell Sci 2009;122:1301–1305.
22. Sigismund S, Woelk T, Puri C, Maspero E, Tacchetti C, Transidico P, Di Fiore PP, Polo S. Clathrin-independent endocytosis of ubiquitinated cargos. Proc Natl Acad Sci U S A 2005;102:2760–2765.
23. Orlichenko L, Huang B, Krueger E, McNiven MA. Epithelial growth factor-induced phosphorylation of caveolin 1 at tyrosine 14 stimulates caveolae formation in epithelial cells. J Biol Chem 2006;281:4570–4579.
24. Wiggins H, Rappoport JZ. An agarose spot assay for chemotactic invasion. Biotechniques 2010;48:121–124.
25. Warnock DE, Schmid SL. Dynamin GTPase, a force-generating molecular switch. Bioessays 1996;18:885–893.
26. Hinshaw JE. Dynamin and its role in membrane fission. Annu Rev Cell Dev Biol 2000;16:483–519.
27. Macia E, Ehrlich M, Massol R, Boucrot E, Brunner C, Kirchhausen T. Dynasore, a cell-permeable inhibitor of dynamin. Dev Cell 2006;10:839–850.
28. Timpson P, McGhee EJ, Morton JP, von Kriegsheim A, Schwarz JP, Karim SA, Doyle B, Quinn JA, Carragher NO, Edward M, Olson MF, Frame MC, Brunton VG, Sansom OJ, Anderson KI. Spatial regulation of RhoA activity during pancreatic cancer cell invasion driven by mutant p53. Cancer Res 2011;71:747–757.
29. Dozynkiewicz MA, Jamieson NB, Macpherson I, Grindlay J, van den Berghe PV, von Thun A, Morton JP, Gourley C, Timpson P, Nixon C, McKay CJ, Carter R, Strachan D, Anderson K, Sansom OJ, et al. Rab25 and CLIC3 collaborate to promote integrin recycling from late endosomes/lysosomes and drive cancer progression. Dev Cell 2012;22:131–145.
30. Eppinga RD, Krueger EW, Weller SG, Zhang L, Cao H, McNiven MA. Increased expression of the large GTPase dynamin 2 potentiates metastatic migration and invasion of pancreatic ductal carcinoma. Oncogene 2012;31:1228–1241.
31. Auciello G, Cunningham DL, Tatar T, Heath JK, Rappoport JZ. Regulation of fibroblast growth factor receptor signalling and trafficking by Src and Eps8. J Cell Sci 2013;126:613–624.
32. Mattheyses AL, Simon SM, Rappoport JZ. Imaging with total internal reflection fluorescence microscopy for the cell biologist. J Cell Sci 2010;123:3621–3628.
33. Carter RE, Sorkin A. Endocytosis of functional epidermal growth factor receptor-green fluorescent protein chimera. J Biol Chem 1998;273:35000–35007.
34. Chao WT, Kunz J. Focal adhesion disassembly requires clathrin-dependent endocytosis of integrins. FEBS Lett 2009;583:1337–1343.
35. Ezratty EJ, Bertaux C, Marcantonio EE, Gundersen GG. Clathrin mediates integrin endocytosis for focal adhesion disassembly in migrating cells. J Cell Biol 2009;178:733–747.
36. Gu Z, Noss EH, Hsu VW, Brenner MB. Integrins traffic rapidly via circular dorsal ruffles and macropinocytosis during stimulated cell migration. J Cell Biol 2011;193:61–70.
37. Deakin NO, Turner CE. Paxillin comes of age. J Cell Sci 2008;121:2435–2444.
38. Kruchten AE, McNiven MA. Dynamin as a mover and pincher during cell migration and invasion. J Cell Sci 2006;119:1683–1690.

39. Rappoport JZ, Taha BW, Simon SM. Movement of plasma-membrane-associated clathrin spots along the microtubule cytoskeleton. Traffic 2003;4:460–467.
40. Yang Q, Karpikov A, Toomre D, Duncan JS. 3-D reconstruction of microtubules from multi-angle total internal reflection fluorescence microscopy using Bayesian framework. IEEE Trans Image Process 2011;20:2248–2259.
41. Tsuruta D, Gonzales M, Hopkinson SB, Otey C, Khuon S, Goldman RD, Jones JC. Microfilament-dependent movement of the beta3 integrin subunit within focal contacts of endothelial cells. FASEB J 2002;16:866–868.
42. Rappoport JZ, Taha BW, Lemeer S, Benmerah A, Simon SM. The AP-2 complex is excluded from the dynamic population of plasma membrane-associated clathrin. J Biol Chem 2003;278:47357–47360.
43. Nakayama M, Nakayama A, van Lessen M, Yamamoto H, Hoffmann S, Drexler HC, Itoh N, Hirose T, Breier G, Vestweber D, Cooper JA, Ohno S, Kaibuchi K, Adams RH. Spatial regulation of VEGF receptor endocytosis in angiogenesis. Nat Cell Biol 2013;15:249–260.
44. Sadowski L, Jastrzębski K, Kalaidzidis Y, Heldin CH, Hellberg C, Miaczynska M. Dynamin inhibitors impair endocytosis and mitogenic signaling of PDGF. Traffic 2013;14:725–736.
45. Vieira AV, Lamaze C, Schmid SL. Control of EGF receptor signaling by clathrin-mediated endocytosis. Science 1996;274:2086–2089.
46. Gold ES, Underhill DM, Morrissette NS, Guo J, McNiven MA, Aderem A. Dynamin 2 is required for phagocytosis in macrophages. J Exp Med 1999;190:1849–1856.
47. Ochoa GC, Slepnev VI, Neff L, Ringstad N, Takei K, Daniell L, Kim W, Cao H, McNiven M, Baron R, De Camilli P. A functional link between dynamin and the actin cytoskeleton at podosomes. J Cell Biol 2000;150:377–389.
48. McNiven MA, Kim L, Krueger EW, Orth JD, Cao H, Wong TW. Regulated interactions between dynamin and the actin-binding protein cortactin modulate cell shape. J Cell Biol 2000;151:187–198.
49. Urra H, Torres VA, Ortiz RJ, Lobos L, Díaz MI, Díaz N, Härtel S, Leyton L, Quest AF. Caveolin-1-enhanced motility and focal adhesion turnover require tyrosine-14 but not accumulation to the rear in metastatic cancer cells. PLoS One 2012;7:e33085.
50. Trimmer C, Whitaker-Menezes D, Bonuccelli G, Milliman JN, Daumer KM, Aplin AE, Pestell RG, Sotgia F, Lisanti MP, Capozza F. CAV1 inhibits metastatic potential in melanomas through suppression of the integrin/Src/FAK signaling pathway. Cancer Res 2010;70:7489–7499.
51. Grande-García A, Echarri A, de Rooij J, Alderson NB, Waterman-Storer CM, Valdivielso JM, del Pozo MA. Caveolin-1 regulates cell polarization and directional migration through Src kinase and Rho GTPases. J Cell Biol 2001;177:683–694.
52. Arpaia E, Blaser H, Quintela-Fandino M, Duncan G, Leong HS, Ablack A, Nambiar SC, Lind EF, Silvester J, Fleming CK, Rufini A, Tusche MW, Brüstle A, Ohashi PS, Lewis JD, et al. The interaction between caveolin-1 and Rho-GTPases promotes metastasis by controlling the expression of alpha5-integrin and the activation of Src, Ras and Erk. Oncogene 2012;31:884–896.
53. Song Y, Xue L, Du S, Sun M, Hu J, Hao L, Gong L, Yeh D, Xiong H, Shao S. Caveolin-1 knockdown is associated with the metastasis and proliferation of human lung cancer cell line NCI-H460. Biomed Pharmacother 2012;66:439–447.
54. Sorkina T, Huang F, Beguinot L, Sorkin A. Effect of tyrosine kinase inhibitors on clathrin-coated pit recruitment and internalization of epidermal growth factor receptor. J Biol Chem 2002;277:27433–27441.
55. Johannessen LE, Pedersen NM, Pedersen KW, Madshus IH, Stang E. Activation of the epidermal growth factor (EGF) receptor induces formation of EGF receptor- and Grb2-containing clathrin-coated pits. Mol Cell Biol 2006;26:389–401.
56. Hinrichsen L, Harborth J, Andrees L, Weber K, Ungewickell EJ. Effect of clathrin heavy chain- and alpha-adaptin-specific small inhibitory RNAs on endocytic accessory proteinsand receptor trafficking in HeLa cells. J Biol Chem 2003;278:45160–45170.
57. Orth JD, Krueger EW, Weller SG, McNiven MA. A novel endocytic mechanism of epidermal growth factor receptor sequestration and internalization. Cancer Res 2006;66:3603–3610.
58. Caswell PT, Vadrevu S, Norman JC. Integrins: masters and slaves of endocytic transport. Nat Rev Mol Cell Biol 2009;10:843–853.
59. Ulrich F, Carl-Philipp Heisenberg C. Trafficking and cell migration. Traffic 2009;10:811–818.
60. Thapa N, Sun Y, Schramp M, Choi S, Ling K, Anderson RA. Phosphoinositide signaling regulates the exocyst complex and polarized integrin trafficking in directionally migrating cells. Dev Cell 2012;22:116–130.
61. Bailly M, Wyckoff J, Bouzahzah B, Hammerman R, Sylvestre V, Cammer M, Pestell R, Segall JE. Epidermal growth factor receptor distribution during chemotactic response. Mol Biol Cell 2000;11:3873–3883.
62. Assaker G, Ramel D, Wculek SK, González-Gaitán M, Emery G. Spatial restriction of receptor tyrosine kinase activity through a polarized endocytic cycle controls border cell migration. Proc Natl Acad Sci U S A 2010;107:22558–22563.
63. Belleudi F, Scrofani C, Torrisi MR, Mancini P. Polarized endocytosis of the keratinocyte growth factor receptor in migrating cells: role of SRC-signaling and cortactin. PLoS One 2011;6:e29159.

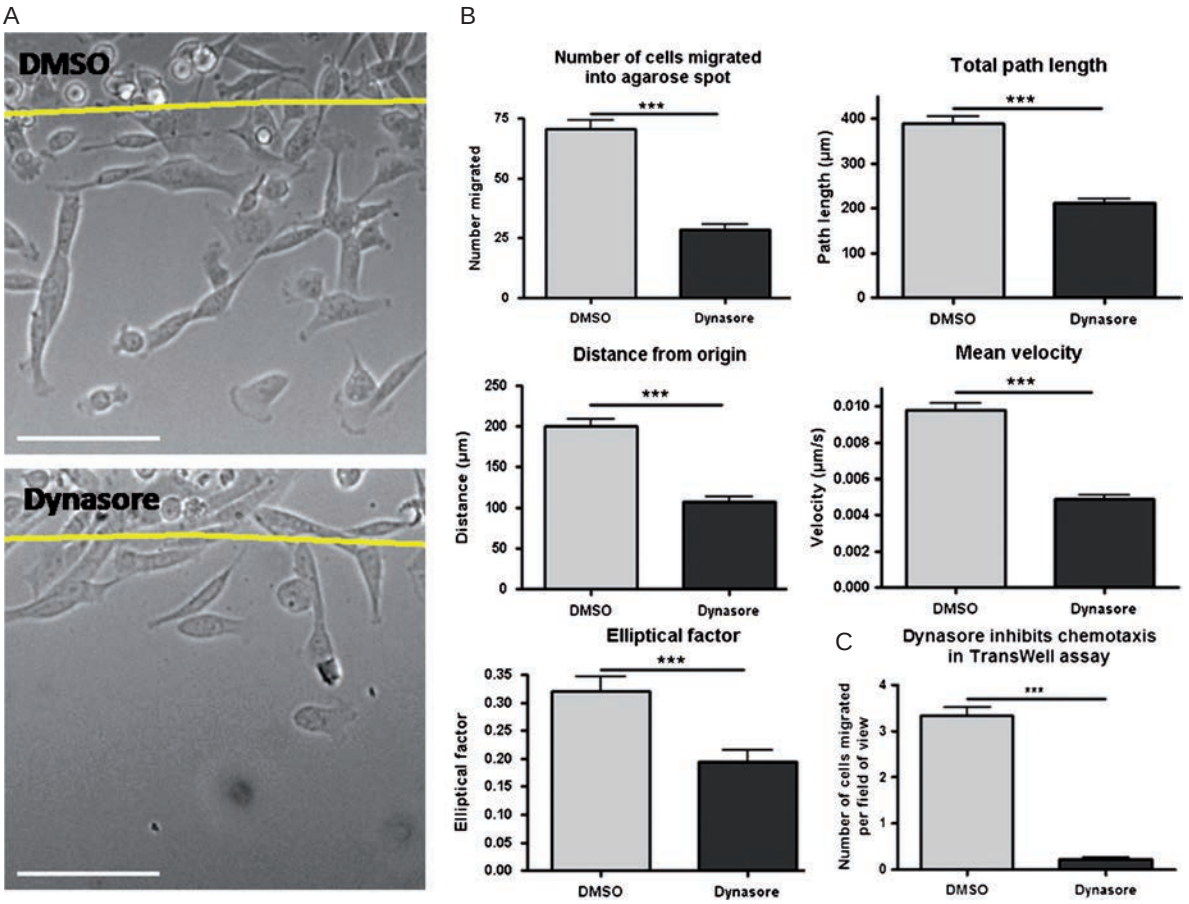

Figure 1: Dynasore inhibits MDA-MB-231 chemotactic invasion into EGF spots. A) Representative images treated with DMSO or Dynasore after 14 h migration into an agarose spot containing EGF. Line denotes edge of the agarose spot. Scale bars 100 μm. B) Results of tracking cells over the course of the timelapses. Parameters analysed include total number of cells migrated, total path length, distance from origin, average velocity and elliptical factor (found by dividing width of cell by length to give a number between 0 and 1). $n = 36$ fields of view per treatment for 'number of cell migrated' graph, $n = 100$ cells per treatment for all other analyses. C) Dynasore inhibits chemotaxis towards EGF in Transwells. Number of cells migrated per field of view following DMSO and Dynasore treatment. $n \geq 50$ fields of view per treatment.

clathrin-mediated endocytosis and fluorescent cholera toxin B (CTxB) as a marker for caveolar endocytosis we confirmed that Dynasore inhibits both these routes of internalisation (Figure S1, Supporting Information). When we treated MDA-MB-231 cells in the chemotactic invasion assay with Dynasore we saw significant differences in a number of parameters investigated, including an overall reduction in the total number of cells which migrated (60% decrease, Figure 1A and B). Investigating the 40% of cells which still migrated led us to find perturbations in the total path length travelled (45% decrease), the distance travelled from their start point (46% decrease) and their average velocity (50% decrease, Figure 1B). We next chose to validate these results with conventional Transwell-based experiments. As depicted in Figure 1C, Dynasore treatment resulted in a nearly complete inhibition of EGF-directed motility in these studies. Thus, dynamin-dependent endocytosis plays a major role in EGF-directed chemotactic invasion in MDA-MB-231 cells.

In order to further expand the applicability of our studies we analysed a second cell line. Pancreatic ductal adenocarcinoma (PDAC) cells derived from a pancreatic tumour, have been previously characterised and are chemotactic

and metastatic (28–30). As depicted in Figure 2A, as with MDA-MB-231 cells, PDACs demonstrate chemotactic invasion into agarose spots containing EGF. Both the number of migratory cells, and distance travelled were significantly greater in EGF spots compared to control spots containing PBS in place of chemoattractant. Furthermore, as with MDA-MB-231 cells, chemotactic invasion of PDACs was sensitive to Dynasore treatment (Figure 2B). Importantly these results are similar to those obtained following Dynasore treatment in PDACs cells in studies employing other cell migration models, including EGF stimulated wound healing (30), and suggest that dynamin function is required for chemotactic invasion in multiple cell platforms.

Previously we have shown that activated growth factor receptors cluster to sites of endocytosis (21,31). As depicted in Figure 3 when we visualised GFP-tagged EGFR by total internal reflection fluorescence (TIRF) microscopy performed on cells undergoing EGF-directed chemotactic invasion we observed EGFR clusters in the front, middle and back of the adherent plasma membrane (32,33). Importantly, in non-stimulated cells not exposed to EGF this construct does not form clusters in the plasma membrane of MDA-MB-231 cells (Figure S2). Thus, we next set out to determine if Dynasore treatment altered the distribution of EGFR clusters.

As depicted in Figure 3, when comparing the distribution of EGFR clusters in the adherent plasma membrane of cells migrating in EGF spots Dynasore treatment caused a decrease in the proportion of clusters in the middle of the cell, and an increase in those towards the front, although only the former was statistically significant. In further analyses we found that following Dynasore treatment, but not in untreated control cells, there were more EGFR clusters in the front of the cell relative to the middle and back of the adherent plasma membrane. Thus, Dynasore treatment causes a redistribution of EGFR clusters, potentially suggesting that endocytosis of activated EGFR is polarised during EGF-directed chemotactic invasion. Furthermore, consistent with our previous work investigating the endocytic trafficking of activated EGFR in non-motile cells, Dynasore treatment did not increase the total number of EGFR clusters in the adherent plasma membrane (Figure 3C); previously we demonstrated that inhibition

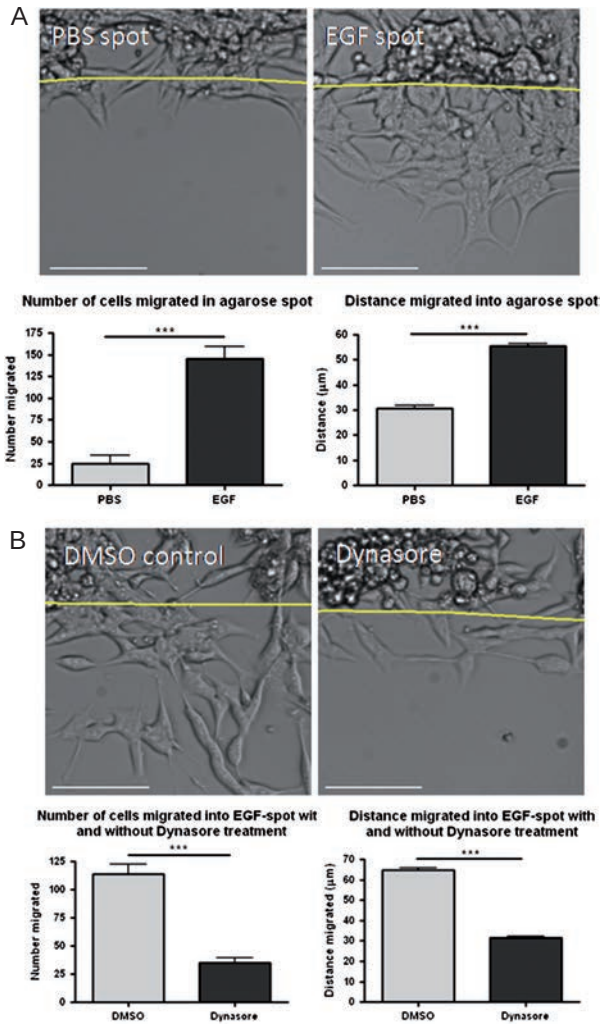

Figure 2: Dynasore inhibits PDACs chemotactic invasion into EGF spots. A) The total number of PDACs cells migrated into the spot and the distance migrated by cells was significantly higher in EGF spots compared to control PBS spots. Line denotes edge of the agarose spot. B) Dynasore treatment caused a decrease in the number of PDACs cells migrated and distance migrated into EGF spots. Scale bars are 100 µm. $n \geq 12$ fields of view per treatment.

of clathrin-mediated endocytosis with siRNA silencing of α-adaptin similarly did not increase the number of EGFR clusters in EGF stimulated cells (21).

One potential role previously suggested for endocytosis in cell migration is internalisation of integrins from disassembling focal adhesions, although this phenomenon has not been universally observed (7,34–36). Thus we

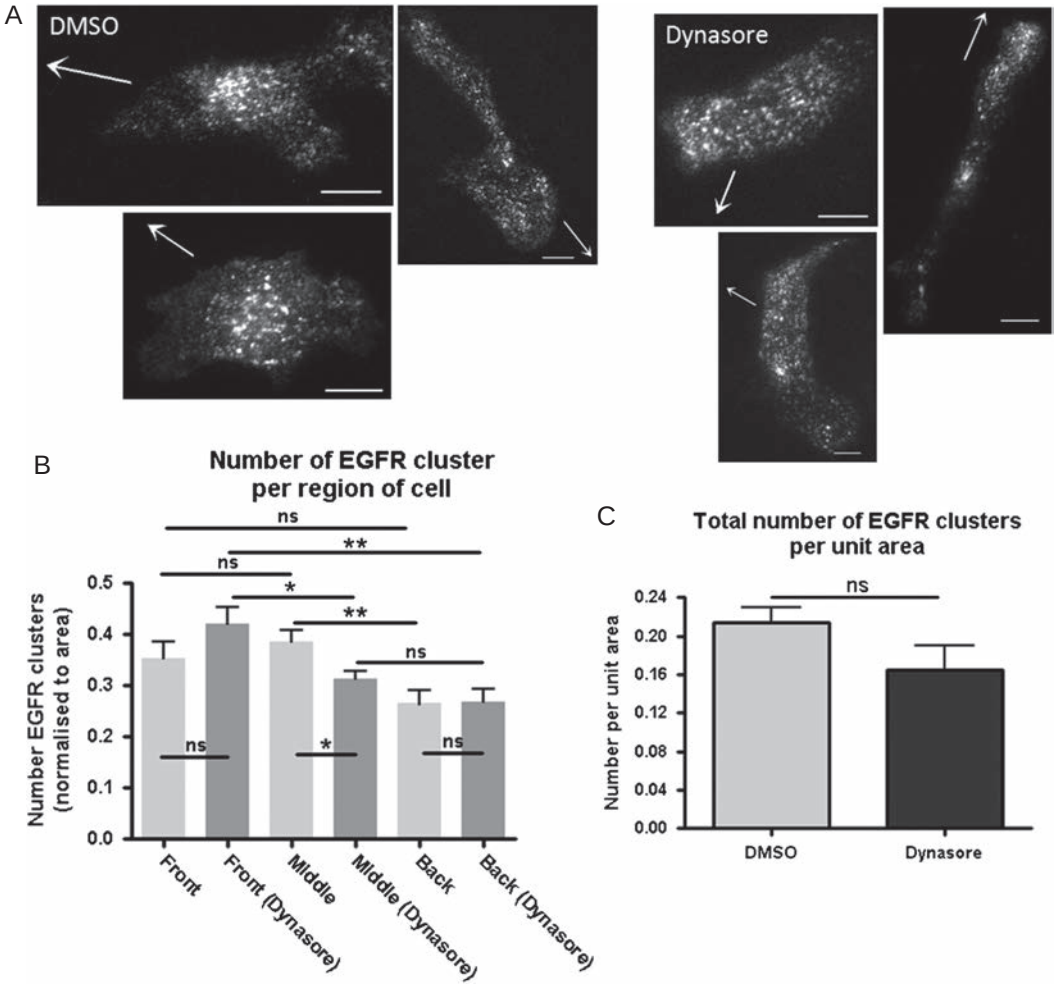

Figure 3: Dynasore causes redistribution of EGFR during chemotactic invasion. A) Representative images of cells used for EGFR cluster number counts in migrating cells treated with DMSO and Dynasore. Scale bars 10 μm. B) Quantification of EGFR clusters by cell region with and without Dynasore treatment. C) Overall there is no significant increase in the number of clusters following Dynasore treatment. $n = 12$ cells per treatment.

investigated whether Dynasore treatment causes a similar alteration in the distribution of focal adhesions in migrating MDA-MB-231 cells.

We chose to employ paxillin-mRFP for these studies, which should be present in all focal adhesions (37). As depicted in Figure 4, Dynasore treatment did not cause a redistribution of focal adhesions, within each cell region (front, middle and back), the number of focal adhesions was similar with and without Dynasore treatment. Additionally, Dynasore treatment did not increase the total number of focal adhesions per cell (Figure 4C). Thus, in contrast with EGFR, focal adhesion distribution does not seem, in this model, to depend on dynamin function.

Clathrin-mediated endocytosis of EGFR during chemotactic invasion

Dynamin functions in multiple endocytosis pathways, as well as in other cellular processes relevant to cell migration (5,25,26,38). In order to specifically determine the endocytosis pathway(s) that might be important for EGF-directed migration we performed a series of RNAi studies. We employed previously validated siRNA sequences to achieve silencing of α-adaptin, a component of the AP2 complex necessary for clathrin-medicated

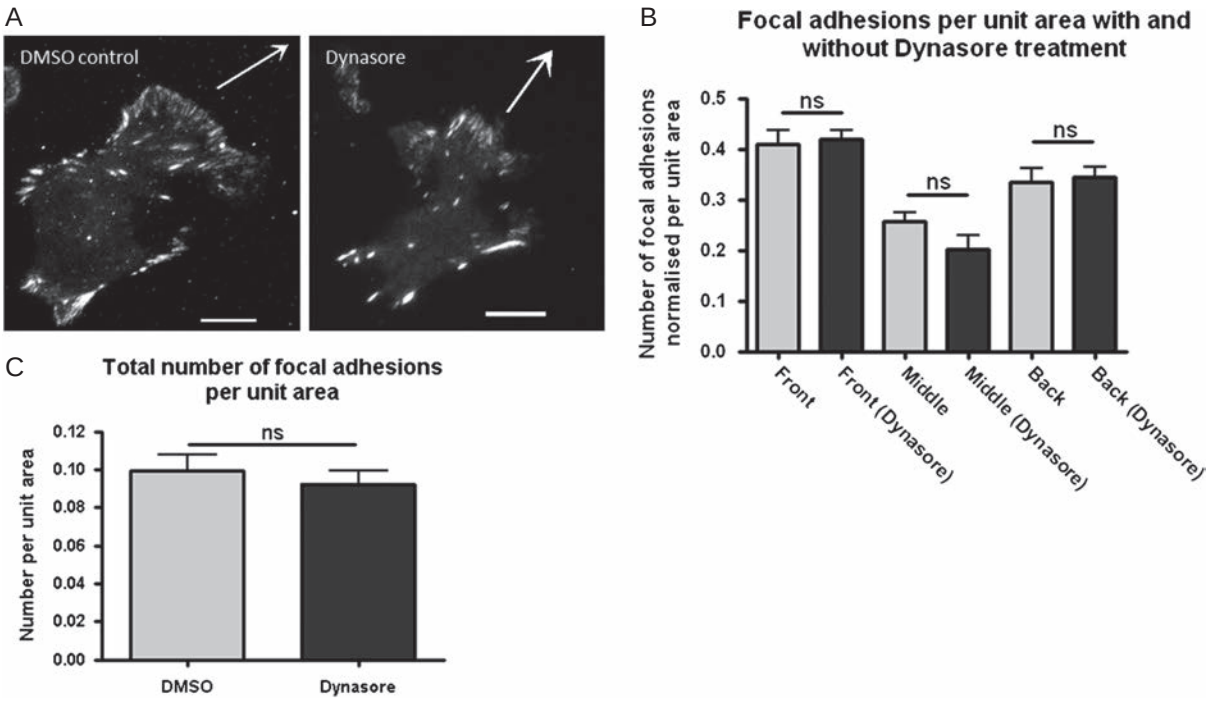

Figure 4: Dynasore does not cause redistribution of focal adhesions during chemotactic invasion. A) Representative images of paxillin-mRFP in cells migrating towards EGF. Scale bars are 10 μm. B) Quantification of number of focal adhesions in the front, middle and back regions of migrating cells. C) Overall there is no significant increase in the number of focal adhesions following Dynasore treatment. $n = 25$ cells per treatment.

endocytosis, and caveolin1, necessary for caveolar endocytosis (31). Knock-down was confirmed by western blot (Figure S3A), and inhibition of clathrin-mediated endocytosis and caveolar endocytosis were validated by inhibition of transferrin and CTxB uptake, respectively (Figure S3B). Using siRNA against α-adaptin we saw a large decrease in the total number of cells able to migrate into the agarose spot (65% decrease), conversely, knock-down of caveolin1 had no effect on cell migration (Figure 5A and B). Thus these results indicate that there is a requirement for clathrin-mediated endocytosis in the process of EGF-directed chemotactic invasion, but that caveolar endocytosis is dispensable.

Becausewe had observed a necessity for clathrin-mediated endocytosis in EGF-directed migration we predicted that this pathway might be the route of internalisation of EGFR following ligand binding in this model of migration. Thus, in the agarose spot assay migrating cells expressing GFP-tagged EGFR and clathrin-dsRed were imaged by TIRF microscopy and the degree of colocalisation between the two was quantified. As depicted in Figure 6, significant colocalisation between EGFR and clathrin was observed when compared to 'control' regions devoid of EGFR spots. As clathrin-independent endocytosis, such as caveolar endocytosis, has been suggested to play a role in EGFR internalisation in certain situations (20–23) we performed similar analyses assessing the degree of colocalisation between EGFR-GFP and caveolin1-mRFP. In stark contrast to the colocalisation observed between EGFR and clathrin, only approximately 5% of EGFR clusters colocalised with caveolin1, almost 10-fold less than the colocalisation seen with clathrin (Figure 6A and B).

Clathrin and EGFR colocalisation during endocytosis was also validated by live cell TIRF imaging and instances of both markers simultaneously disappearing from the TIRF field were observed (Figure 7A and B). However, in these live-cell studies dynamic EGFR spots devoid of clathrin were also tracked. As depicted in Figure 7C, laterally motile EGFR spots, potentially uncoated endocytic structures or post-Golgi carriers, were observed. Thus, these data

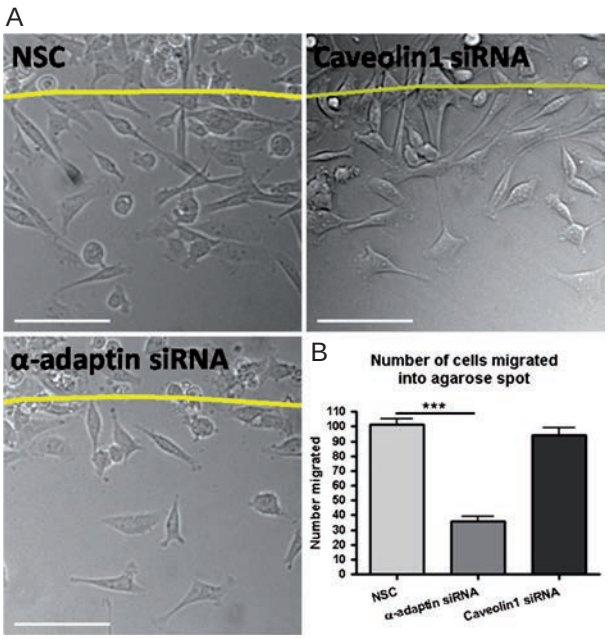

Figure 5: siRNA silencing of α-adaptin inhibits MDA-MB-231 migration into EGF spots. A) Representative images treated with control siRNA, α-adaptin siRNA and caveolin1 siRNA after 14 h migration into an agarose spot containing EGF. Scale bars are 100 μm. B) Quantification of total number of cells migrated under siRNA conditions. Line denotes edge of the agarose spot. $n = 22$ fields of view per treatment. NSC = non-silencing control siRNA.

suggest that during EGF-directed chemotactic invasion activated EGFR enters the cell via clathrin-mediated endocytosis.

Dynasore treatment caused a redistribution of EGFR spots in migrating cells (Figure 3), suggesting the possibility of polarised endocytosis in migrating cells. In order to further investigate this possibility we imaged clathrin-dsRed by live-cell TIRF microscopy in cells migrating in the agarose spot assay. We looked for instances where clathrin disappeared from the evanescent field to indicate an internalisation event. The disappearance of clathrin from the evanescent field was taken to be due to endocytosis only if it was not due to photobleaching, if it occurred rapidly (within 10 frames of imaging) and if it did not reappear in the evanescent field within 10 frames of its disappearance. It was found that over the course of these timelapses significantly more clathrin internalisation events occurred at the front of migrating cells, as opposed to the middle or the back (Figure 8A–C). Furthermore, although it seemed that clathrin-coated pits at the front of the cell are more likely to undergo endocytosis, this effect was not statistically significant (Figure 8D). Thus, taken together with the above results, during EGF-directed migration EGFR is internalised by clathrin-mediated endocytosis and that this internalisation is polarised towards the front of migrating cells.

We also tested whether these observations could be recapitulated in PDAC cells. Live-cell TIRF imaging of clathrin in migrating PDAC cells revealed a very strong preponderance of highly dynamic clathrin. As described in our previous work, when imaged by TIRF microscopy, clathrin can either be static, laterally mobile or disappear vertically into the cell (12,39). Furthermore, it has previously been suggested that movement of clathrin along microtubules can occur prior or subsequent to the endocytosis event (35,39). Thus, we quantified the 'dynamic' population of clathrin in migrating PDAC cells, combining those that disappeared vertically as well as those that moved laterally in the plane of the plasma membrane. As it has previously been demonstrated that individual microtubule tracks near the adherent cell surface can curve axially, potentially out of the TIRF field (40), we followed each clathrin spot present in the first image of a 1 min TIRF video. As previously described, we divided the cell into front, middle and back regions. Within each region we counted the number of dynamic clathrin spots. Similar to our results obtained in MDA-MB-231 cells, there were significant differences between the clathrin in the front of the cell, relative to the middle or back. When analysed as a fraction of the total number of spots per region, the front was significantly more dynamic (Figure 9A). Similarly, when we normalised to the area of each region, we found the front contained more dynamic clathrin than the middle or back (Figure 9B). Additionally, we found that EGFR and clathrin colocalised in PDACs, including within spots disappearing from the cell surface (Figure 9C). Thus, we have shown in both MDA-MB-231 and PDAC cells that (1) EGF-directed chemotaxis is dynamin dependant, (2) clathrin dynamics are polarised to the front of the migrating cell, and (3) that clathrin and EGFR can colocalise including during internalisation.

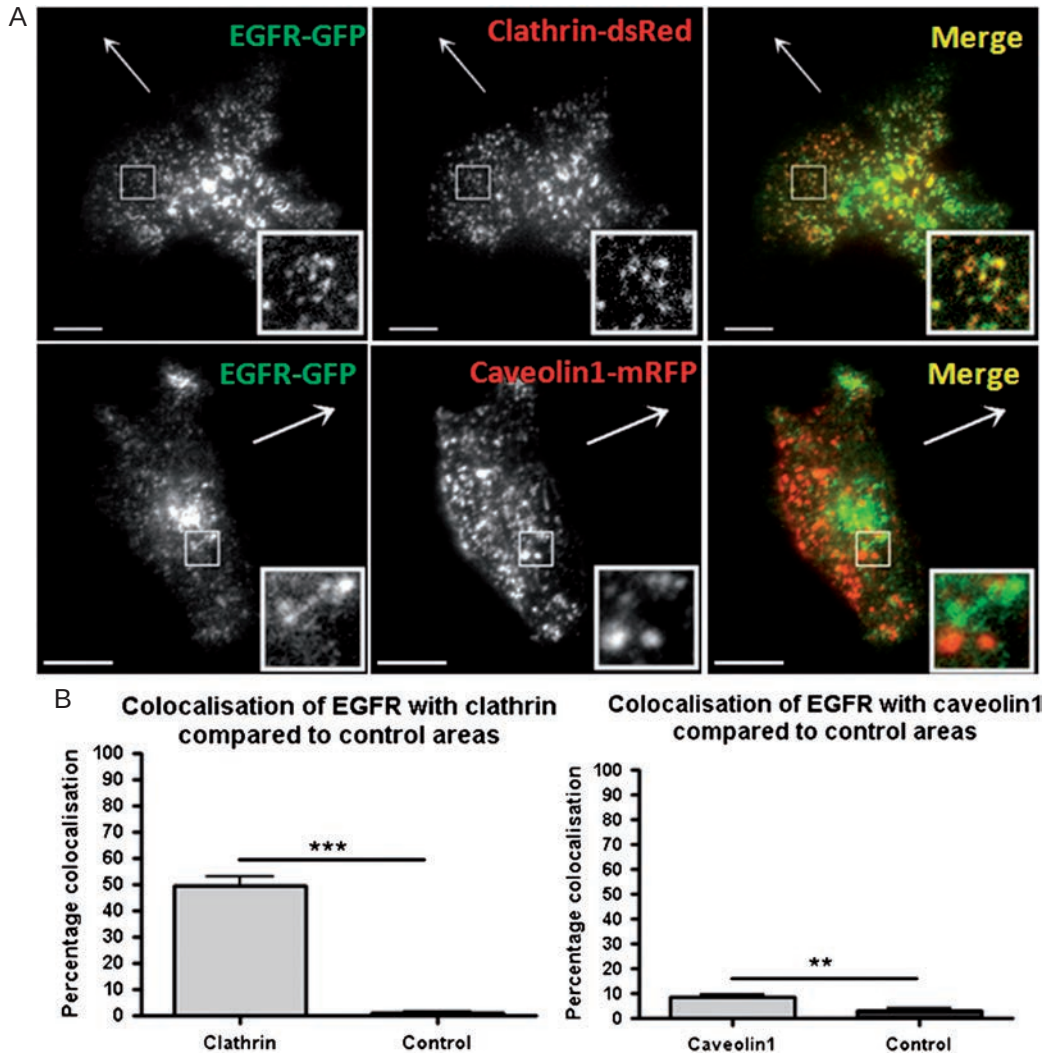

Figure 6: Colocalisation between clathrin-dsRed and EGFR-GFP. A) Representative images of EGFR-GFP with clathrin-dsRed or caveolin1-mRFP in cells migrating towards EGF. Scale bars 10 μm. B) Quantification of colocalisation of EGFR-GFP with clathrin-dsRed and caveolin1-mRFP. $n = 14$ cells for each experiment.

Clathrin-mediated endocytosis is not involved in focal adhesion disassembly

The inability of Dynasore treatment to cause redistribution of focal adhesions in migrating cells suggests that endocytosis is not required for focal adhesion disassembly in this model. To further test this hypothesis we investigated whether there was a role for clathrin-mediated endocytosis in focal adhesion disassembly in migrating MDA-MB-231 cells. Thus, we investigated the potential colocalisation between clathrin and a previously validated focal adhesion marker GFP-β3-integrin in cells migrating towards EGF in the agarose spot assay (37,41).

As depicted in Figure 10, colocalisation of clathrin and GFP-β3-integrin was not evident. Only approximately 7% of focal adhesions were positive for clathrin. In addition, as shown in Figure 9B, a previously published technique for assessing colocalisation by analysing the effect on Pearson's correlation coefficient of shifting one channel relative to another one pixel at a time confirms the lack of colocalisation of clathrin and focal adhesions (39,42). Finally, we performed two colour live-cell TIRF imaging to specifically determine if clathrin was transiently recruited to disassembling focal adhesions and as depicted in Figure 10C, this was not observed.

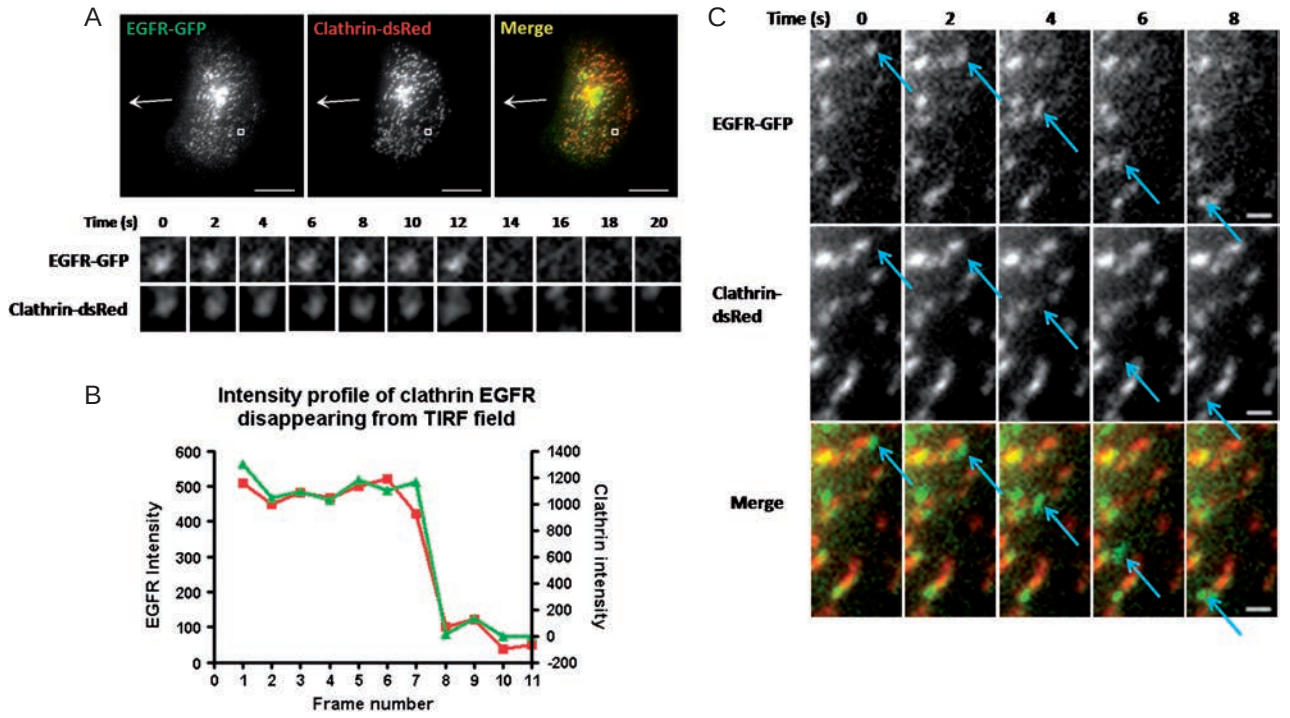

Figure 7: Live-cell TIRF imaging of clathrin-dsRed and EGFR-GFP. A) Representative image to show an instance of both markers leaving the TIRF field at the same time. Scale bars are 10 μm. B) Quantification of the disappearance event depicted in (A). C) Directed motility of an EGFR cluster devoid of clathrin. Scale bars are 1 μm.

We chose to use a fluorescent tagged integrin (in this case GFP-β3-integrin) as our focal adhesion marker as it represents a potential endocytic cargo localised to the sites of focal adhesions, and therefore has the potential to colocalise with clathrin during endocytosis. However β3-integrin might not be present in all focal adhesions, thus we performed similar analyses with paxillin-mRFP. Importantly in control studies we assessed the colocalisation of GFP-β3-integrin and paxillin-mRFP. As can be seen in Figure S4, all regions of paxillin-mRFP also contain GFP-β3-integrin.

As with GFP-β3-integrin, no colocalisation was observed between paxillin-mRFP and clathrin-GFP in either static images of migrating cells or by analysing whether clathrin was recruited to regions of disassembling focal adhesions, as in the previous analysis (Figure S5A). Thus, these results confirm that clathrin-mediated endocytosis does not contribute directly to focal adhesion disassembly in this system. Similarly, although siRNA silencing of caveolin1 did not inhibit EGF-directed chemotactic invasion of MDA-MB-231 cells we also verified that caveolin1 also did not colocalise with GFP-β3-integrin (Figure S5B).

As a final means to investigate a potential role for clathrin-mediated endocytosis in focal adhesion disassembly we assessed whether inhibition of clathrin-mediated endocytosis with siRNA against α-adaptin altered the rate of focal adhesion disassembly measured by timelapse TIRF microscopy of mRFP-paxillin, a previously employed assay strategy (7). However, as cells treated with α-adaptin siRNA do not readily migrate into EGF-containing agarose spots these experiments were performed with MDA-MB-231 cells migrating in a wound healing assay. Consistent with our colocalisation analysis (Figure 9), we found no differences in the time taken for focal adhesions to disassemble in knock-down cells compared to control (Figure 11A and B), indicating that clathrin is not required for disassembly of focal adhesions in migrating cells. Furthermore, as α-adaptin siRNA did not reduce the rate of wound healing (Figure 11C and D) it may be that EGFR trafficking is the

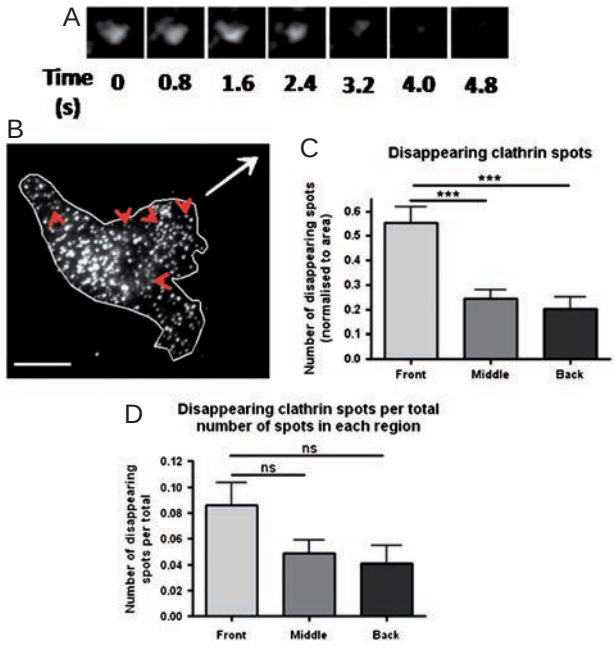

Figure 8: Clathrin spot disappearance is polarised to the front of migrating cells. A) Representative images of a clathrin spot disappearing from the TIRF imaging field. B) Representative image of a clathrin-dsRed expressing migrating cell with instances of clathrin disappearance circled. Scale bars are 10 μm. C) Quantification of clathrin disappearance by cell region. D) Quantification of clathrin disappearance compared to total number of spots in each region. $n = 18$ cells.

main role of clathrin-mediated endocytosis during chemotactic invasion and during wound healing this pathway is not required.

Discussion

The role of endocytosis in chemotactic invasion has not been adequately investigated. It has been suggested in some models that endocytosis is involved in focal adhesion disassembly (10,11,16,17). Furthermore, endocytosis can play a role in the modulation of receptor signalling (5,43–45). Therefore we conducted a series of studies to determine the role(s) of endocytosis in driving chemotactic invasion of breast cancer-derived cells. Increased understanding of how endocytosis regulates chemotactic invasion may assist in developing therapeutic interventions that might target tumour cell invasion and metastasis.

We firstly sought to establish whether endocytosis was important for chemotactic invasion of MDA-MB-231 cells towards EGF. Using Dynasore to inhibit dynamin-dependent endocytosis we found that far fewer cells were able to migrate, and that the migration of those which could still migrate was significantly impaired (Figure 1). In addition, we obtained identical results using an unrelated pancreatic cancer-derived cell line, further emphasising the reproducibility of the assay used and the necessity for dynamin-dependent endocytosis in chemotactic invasion (Figure 2). Because Dynasore had such a profound effect on migration we next investigated whether this might be as a result of a role involving endocytosis of receptors (noteably EGFR) or focal adhesion components (e.g. integrins). We found that Dynasore caused an accumulation of EGFR towards the front of migrating cells, however did not affect the localisation of focal adhesion components (Figures 3 and 4).

Because multiple endocytosis pathways are dynamin-dependent (46–48) we employed an RNAi approach to inhibit specific routes of endocytosis and further narrow down the role of endocytosis in chemotactic invasion. Upon inhibition of clathrin-mediated endocytosis by siRNA against α-adaptin we again saw a significant reduction in the number of cells able to migrate, demonstrating this to be a pathway necessary for migration towards EGF (Figure 5). Conversely, using siRNA against caveolin1 to inhibit caveolar endocytosis, we saw no alteration in cell migration.

Aspects of these results are in contrast to those reported by other groups. In 2012 Urra et al. inhibited caveolin1 in MDA-MB-231 cells and found this inhibition to decrease migration of cells in a wound healing model (49). The authors therefore suggested a role for caveolin1 in enhancing the metastatic potential of cancer cells. However, another study found that expression of caveolin1 led to an inhibition of chemotaxis and chemoinvasion in melanoma cells and suggested a role for the protein in inhibiting cell migration (50). Thus controversy remains, with different groups pointing to a role for caveolin1 in either promoting or inhibiting migration in some way (49–53). In order to verify our results we also undertook TIRF imaging of caveolin1-mRFP in conjunction with GFP-β3-integrin in cells migrating towards EGF and found no notable

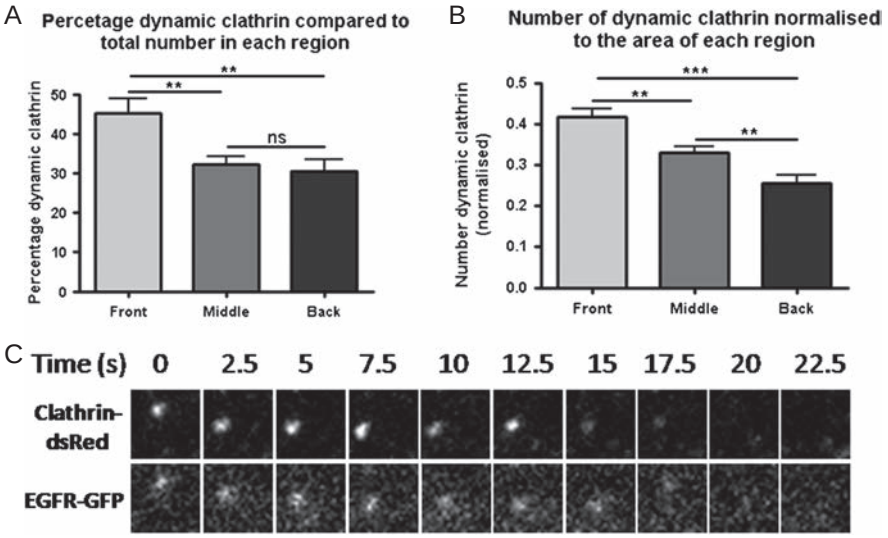

Figure 9: Active clathrin in migrating PDAC cells. A) Graph to show that there is a higher proportion of active or internalising clathrin compared to total clathrin at the front of migrating PDAC cells compared to the middle or the back. B) Graph to show that there is more active or internalising clathrin at the front of migrating PDAC cells when normalised to the area of each region. $n = 12$ cells. C) An instance to show clathrin-dsRed and EGFR-GFP internalising from the TIRF field together.

colocalisation between the two (Figure S5B). We therefore conclude that caveolar endocytosis is unnecessary for EGF-directed chemotactic invasion of MDA-MB-231 cells. However, it may be necessary for other modes of migration.

As clathrin-mediated endocytosis was required for chemotactic invasion towards EGF we tested for colocalisation between clathrin and EGFR and found a high degree of colocalisation between the two (Figure 6). When we tested colocalisation of EGFR with caveolin1 we found that this was negligible compared to the colocalisation with clathrin. This indicates a clathrin-dependent internalisation route for the EGFR in cells migrating in an EGF-dependent manner. In the literature there is much support for a clathrin-dependent route of EGFR endocytosis (20,21,54,55) but also contrary evidence supporting a clathrin-independent route in certain situations (22,22,23,56,57). In support of our findings, previous work by Huang et al. and Rappoport and Simon demonstrated that in non-migrating cells the EGFR enters primarily through clathrin-coated pits and not through caveolae (20,21). In addition to assessing colocalisation of clathrin and EGFR we were able to image instances of both simultaneously disappearing from the TIRF field (Figure 7A and B). During this live-cell imaging we also saw instances of EGFR clusters devoid of clathrin moving laterally adjacent to the plasma membrane, likely to be post-endocytic structures or post-Golgi vesicles (Figure 7C). This observation suggests that some EGFR in our analysis in Figure 6 may be EGFR of this category and therefore the colocalisation of EGFR clusters with clathrin-coated pits/vesicles on the plasma membrane could be even higher than originally thought.

An emerging idea is that polarised vesicle trafficking is involved in the regulation of directed cell migration (6). A link between polarised trafficking of cell adhesion components has been shown in a number of cell types (11,58–60). The occurrence of polarised trafficking of chemoattractant receptors is less well studied than that of focal adhesions, but may play a role in regulation of directed cell migration (61). A recent study by Assaker et al. found that particular endocytic proteins were necessary to control the trafficking, and hence spatial polarisation, of receptor tyrosine kinases during Drosophila boarder cell migration (62). Another study by Belleudi et al. found endocytosis and polarised recycling of the keratinocyte growth factor receptor regulated receptor polarisation at the plasma membrane, and that this was necessary for keratinocyte migration (63). Upon inhibition of dynamin-dependent endocytosis we have already shown a redistribution of EGFR localisation towards the front of migrating cells (Figure 3). This implies that EGFR internalisation is polarised to the front of migrating cells, as inhibition of endocytosis caused a build up endocytosis cargo in this region. This led us to test whether clathrin-mediated endocytosis is polarised in MDA-MB-231 cells during EGF-directed chemotactic invasion. As expected, we saw an increased number of internalisation events at the

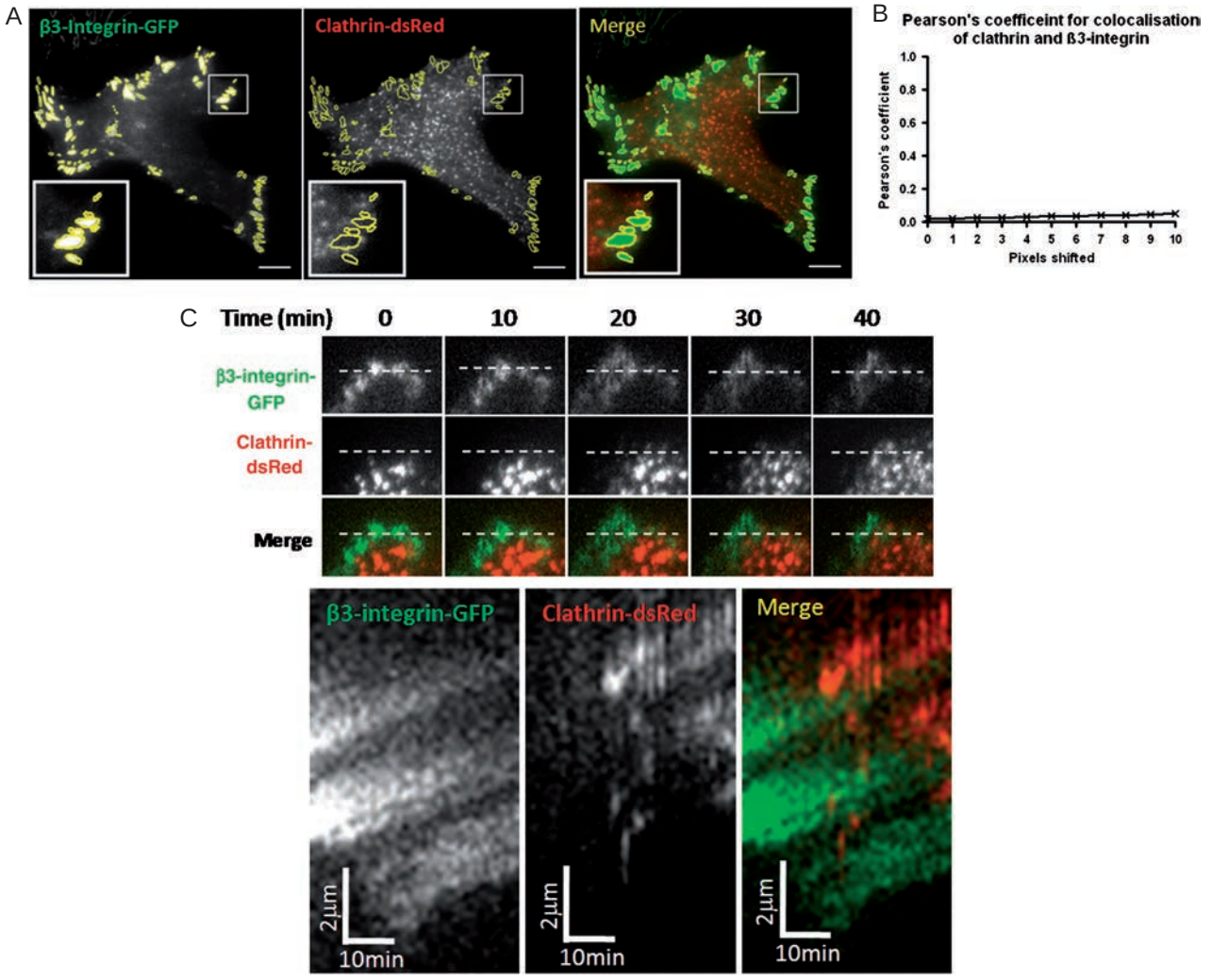

Figure 10: Clathrin-dsRed does not co-localise with focal adhesions using GFP-β3-integrin as the focal adhesion marker. A) Representative images with focal adhesions circled from the GFP-β3-integrin image to assess colocalisation with clathrin. Scale bars are 10 μm. B) Pearson's coefficient of GFP-β3-integrin with clathrin-dsRed. $n = 30$ cells. C) Kymograph to show lack of co-localisation between clathrin-dsRed and GFP-β3-integrin labelled focal adhesions. A 10 μm line was drawn across two disassembling focal adhesions and a kymograph across this region demonstrated no co-localisation of clathrin during focal adhesion disassembly.

front of cells migrating towards EGF rather than at the middle or back (Figure 8). In addition to the necessity for clathrin-mediated endocytosis for migration in this model, these results suggest that polarised endocytosis of the EGFR is important for migration in this breast cancer cell line.

There has been data reported suggesting a role for clathrin-mediated endocytosis of integrins from disassembling focal adhesions (34,35). However, in other studies this has not been observed (7,36). As inhibition of endocytosis significantly decreased chemotactic invasion, we tested whether there is a role for clathrin-mediated endocytosis in focal adhesion disassembly. However, we found no significant colocalisation between clathrin and the focal adhesion markers β3-integrin and paxillin, including specifically during focal adhesion disassembly (Figure 10 and Figure S5A). In addition to chemotactic invasion studies we also undertook wound healing studies using MDA-MB-231 cells where we found knock-down of α-adaptin had no

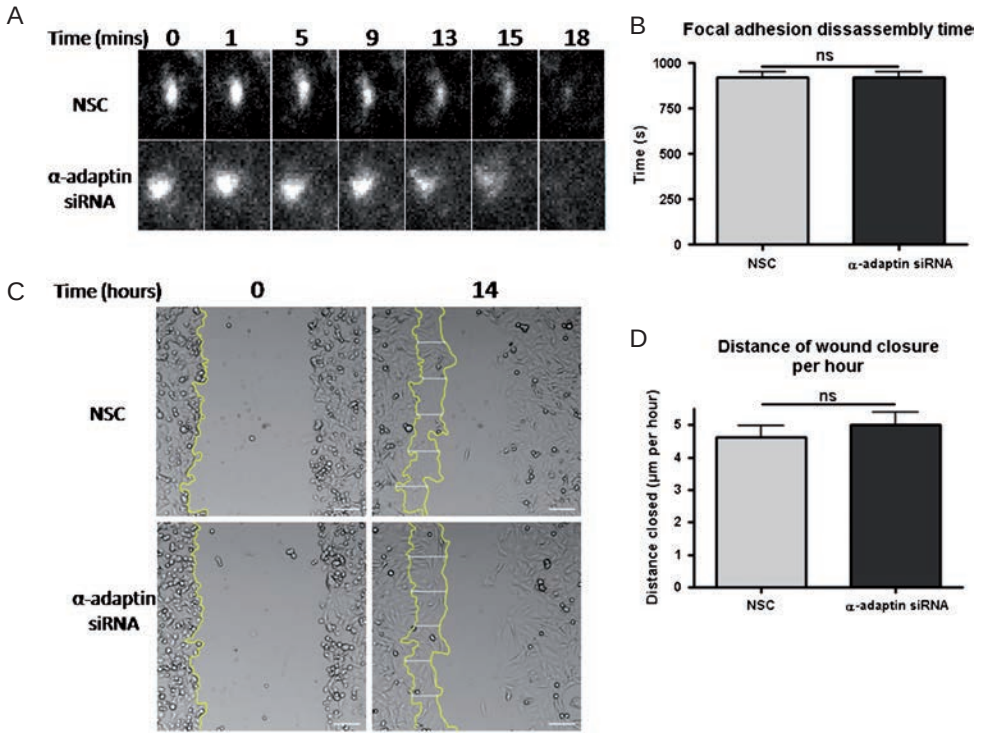

Figure 11: siRNA silencing of α-adaptin does not inhibit focal adhesion disassembly during wound healing. A) Disappearance of paxillin-mRFP over time using NSC and α-adaptin siRNA. B) Graph showing mean focal adhesion disassembly time for cells treated with NSC and α-adaptin siRNA. $n \geq 100$ focal adhesions from 20 cells per treatment. C) Wound healing assay with α-adaptin knock-down. Representative images of wounds at time 0 and after 14 h. Lines denote edge of wound at both time points. Distances between cells at time 0 and 14 h were measured at various points in each image to give an average distance migrated in NSC and α-adaptin siRNA treated cells. D) Quantification of distance moved by siRNA treated cells. $n = 22$ fields of view per treatment.

effect on focal adhesion disassembly time. Wound healing was assessed here because silencing of α-adaptin had such a profound effect on chemotactic invasion that we could not perform these analyses in that model.

Our data in MDA-MB-231 wound healing corroborates with wound healing results from other studies, including those from Fletcher et al. in MDCK cells where they also found no role for endocytosis during focal adhesion disassembly (7). The contrast in these results compared to some studies performed in fibroblasts indicates that effects seen on focal adhesions may be cell type and/or migratory stimulus specific and that while there may be a requirement for clathrin in focal adhesion disassembly in fibroblasts, this is not the case during chemotactic invasion of MDA-MB-231 breast cancer cells (34,35).

In addition we found that knocking down α-adaptin had no effect on the wound closure rate of MDA-MB-231. This indicated that while some pathways may be necessary for one process they may be dispensable for other, otherwise similar, phenotypes. Furthermore, this suggests that EGFR trafficking might be a critical role of clathrin-mediated endocytosis during chemotactic invasion towards EGF in MDA-MB-231 cells, but not necessary for wound healing.

Taken together these results suggest a model where dynamin and clathrin are necessary for chemotactic invasion in MDA-MB-231 cells, but caveolin1 is not. We also establish that clathrin-mediated endocytosis is not necessary for focal adhesion disassembly in this cell line. We propose that the main route of EGFR internalisation is clathrin-mediated endocytosis, which is polarised towards the front of migrating cells. Comparison of these results with other studies provides significant evidence for